General Disclaimer

One or more of the Following Statements may affect this Document

- This document has been reproduced from the best copy furnished by the organizational source. It is being released in the interest of making available as much information as possible.

- This document may contain data, which exceeds the sheet parameters. It was furnished in this condition by the organizational source and is the best copy available.

- This document may contain tone-on-tone or color graphs, charts and/or pictures, which have been reproduced in black and white.

- This document is paginated as submitted by the original source.

- Portions of this document are not fully legible due to the historical nature of some of the material. However, it is the best reproduction available from the original submission.

Produced by the NASA Center for Aerospace Information (CASI)

NASA CR-
144559

(NASA-CR-144559) EVALUATION OF EARLY RECOGNITION OF VIRAL INFECTIONS IN MAN Final Report (McDonnell-Douglas Astronautics Co.) 250 p HC $8.00 CSCL 06E G3/52

N76-11712

Unclas 01923

EVALUATION OF EARLY RECOGNITION OF VIRAL INFECTIONS IN MAN

FINAL REPORT

CONTRACT NAS9-13740

MCDONNELL DOUGLAS ASTRONAUTICS COMPANY

MCDONNELL DOUGLAS CORPORATION

MCDONNELL DOUGLAS ASTRONAUTICS COMPANY
5301 Bolsa Avenue, Huntington Beach, CA 92647 (714) 896 3311

OCTOBER 1975

EVALUATION OF EARLY RECOGNITION OF VIRAL INFECTIONS IN MAN

NASA Contract NAS9-13740

FINAL REPORT

Prepared by:

A. A. Kelton, PhD

M. B. Lawton

Approved by:

K. H. Houghton, M. D.
Chief Biotechnology and Space Sciences Engineer
Biotechnology and Space Sciences Department
Engineering Division

Prepared for:

National Aeronautics and Space Administration
Johnson Spacecraft Center
Houston, Texas

MCDONNELL DOUGLAS CORPORATION

TABLE OF CONTENTS

Section	Title	Page
1.0	INTRODUCTION	1
2.0	METHODS AND MATERIALS	2
2.1	PREPARATION OF THE FICOLL	3
2.2	DESCRIPTION OF THE GRADIENT FORMER AND GRADIENT FORMATION	5
2.3	COLLECTION OF BLOOD AND DEFIBRINATION	5
2.4	RECOVERY OF LYMPHOCYTES	5
2.5	EQUILIBRIUM CNETRIFUGATION	7
2.6	DISPLACEMENT, COUNTING AND PLOTTING OF THE DISTRIBUTION	7
2.7	DONOR SELECTION, VIRAL DIAGNOSIS AND IMMUNIZATION	9
2.8	ANALYSIS OF LSGDs FOR SUBPOPULATIONS	10
2.8.1	Dissection by Parabolas	10
2.8.2	Computer Program for Fitting Gaussians to Data	10
2.8.3	Sizing of Nuclei from Lymphocytes of Different Specific Gravity	11
2.9	STUDY OF GRADIENT CHARACTERISTICS	11
2.9.1	Relationship Between RI and Specific Gravity	12
2.9.2	Gradient Linearity and Similarity	12
2.9.3	LSGD Reproducibility	13
3.0	RESULTS	13
3.1	COMPARISON OF HEALTHY DONORS AND PATIENTS	13
3.2	IMMUNIZATION STUDIES	21
3.3	ANALYSIS OF DISTRIBUTIONS FOR SUBPOPULATIONS	27

TABLE OF CONTENTS

Section	Title	Page
3.3.1	Hand-fit of Parabolas	27
3.3.2	Computer-fit of Gaussians	36
3.3.3	Characterization of Subpopulations by Density and Nuclear Size	36
3.3.4	Miscellaneous LSGDs	43
3.3.4.1	Serendipitous Observations on Viral Disease	43
3.3.4.2	LSGD from Chronic Skin Cancer	43
3.3.5	Gradient Characteristics	50
3.3.5.1	Relationship Between Refractive Index and Specific Gravity	50
3.3.5.2	Gradient Linearity and Similarity	50
3.3.5.3	LSGD Reproducibility of Simultaneous Gradients	58
4.0	Discussion	61
	APPENDIX A	
	APPENDIX B	
	APPENDIX C	
	APPENDIX D	
	BIBLIOGRAPHY	

FIGURES

Number	Title	Page
1	Apparatus for Continuous Dialysis of Ficoll	4
2	Density Gradient Former	6
3	Schematic of Apparatus for Determination of Specific Gravity Distribution	8
4	Healthy Donors	14
5	Patient V10	15
6	Patient V11	16
7	Patient V12	17
8	Patient V14	18
9	Patient V15	19
10	Patient V16	20
11	Temporal Changes in LSGD Following Immunization	25
12	LSGDs for Subject	26
13	Temporal Changes in the 1.05 to 1.07 g/cc Region	28
14	Control N6	29
15	Control N8	30
16	Control N10	31
17	Patient V11 - Varicella	32
18	Patient V12 - Varicella	33
19	Patient V15 - Varicella	34
20	Frequency Distribution of Peaks at Density Intervals	35
21	Normalized Cell Number of Component Gaussians vs Density at Peak Count - Normal	37
22	Normalized Cell Number of Component Gaussians vs Density at Peak Count - Varicella	38

FIGURES

Number	Title	Page
23	Normalized Cell Number of Component Gaussians vs Density at Peak Count - Measles	39
24	Normalized Cell Number of Component Gaussians vs Density at Peak Count - Mumps	40
25	Normalized Cell Number of Component Gaussians vs Density at Peak Count - Herpes	41
26	Specific Gravity Distribution of Peripheral Lymphocytes from Patient with Varicella Relative Size of Nuclei of Lymphocytes Separated on a Ficoll Density Gradient	42
27	Three Days Before Symptoms of Viral Illness	44
28	Same Donor as in Figure 27, Twelve Days Later	45
29	Same Donor as in Figure 27, 19 Days Later	46
30	Same Donor as in Figure 27, 31 Days Later	47
31	One Day After "24-Hour Flu"	48
32	Chronic Skin Cancer	49
33	Refractive Index versus Specific Gravity	51
34a	Refractive Index versus Fraction Number	52
34b	Refractive Index versus Fraction Number	53
34c	Refractive Index versus Fraction Number	54
34d	Refractive Index versus Fraction Number	55
35	Composite RI versus Fraction Number	57
36	LSGD Reproducibility of Simultaneously Formed Gradients	59
37	Correlation of Distributions from Simultaneously Formed Gradients	60
38.	Tentative Model for Identity of Subpopulations of Peripheral Blood Lymphocytes in the Normal LSGD	69

TABLES

Number	Title	Page
I	Statistical Analysis of LSGD Parameters for Healthy Donors	22
II	Statistical Analysis of LSGD Parameters for Patients with Viral Disease	23
III	Serology of Viral Disease	24
IV	Serology of Viral Immunization	56

1.0 INTRODUCTION

This research project investigated the potential of the lymphocyte specific gravity distribution (LSGD) as a nonspecific procedure for early diagnosis of viral disease in astronauts. A general diagnostic test is needed to screen astronauts and scientific investigators prior to space travel. Extensive medical background data and long quarantines will become impractical as the frequency of space flight, the variety and versatility of investigations, and the assorted backgrounds of flight scientists culminate during the era of Shuttle. Also, such a procedure would offer additional benefits. Since viral infections can interfere with human performance during any critical situation, individuals could be screened prior to an extensive travel assignment, underwater expeditions, isolation duty, etc. In elective surgery, diagnosis of early or subclinical virus infections could reduce postoperative complications. Such a procedure might be useful for general screening of blood donations since recipients should not be subjected to a virus insult in their weakened condition.

Virus infections invoke the host immune mechanisms. Of the two major immune mechanisms, humoral and cellular, the cell mediated immune response (CMIR) conducted by the circulating peripheral blood lymphocytes may present the earliest and most indicative evidence of viral infection. The CMIR has been shown to be the major specific immunological defense against virus infection and to precede the appearance of circulating antibody[1]. Lymphoid cells disseminate the immune response: obscure morphological changes in circulating lymphocytes have been noted in most virus diseases as early as 2-3 days following infection[2]. Indeed, several hematologists have stated that the appearance of atypical lymphoid cells in the blood appears to be an almost universal consequence of infection if sensitive methods for detection are used[2].

An extremely sensitive method for detection of subpopulations of lymphocytes involves the analysis of their specific gravity distribution. Recently, investigators have reported that normal, differentiated cells possess narrow

specific gravity distributions that are independent of cell size or stage of cell cycle and that a change in differentiation frequently produces quantum changes in specific gravity[3]. Quantum-like changes in narrow specific gravity distributions have been observed for lymph node lymphocytes in response to antigenic stimulation[4]. Early investigations by Kelton showed that circulating lymphocytes from a healthy donor had an extremely narrow specific gravity distribution that was radically altered prior to clinical manifestation of a virus infection[5]. Further, a recent publication by Shortman reports an altered specific gravity distribution for a case of influenza[6]. A recent study by us showed abnormal specific gravity distributions for patients with multiple sclerosis and other neurological diseases[7]. In our hands, subpopulations constituting only about 0.1% of the total population can be readily identified if isolated by the density gradient technique. Thus, the specific gravity spectrum of lymphocytes may embody the sensitivity necessary to recognize activity of the CMIR related to early virus infections.

In our study, virus infections are shown to result in significant differences between the specific gravity distribution of peripheral blood lymphocytes from patients and those from healthy volunteers. Additionally, new subpopulations of lymphocytes and changes in the distribution of those subpopulations usually present in healthy donors were identified as a result of analysis of the specific gravity distributions of lymphocytes from patients with viral disease. Alterations in the LSGD were also noted following immunization against viral disease. A computer program was developed to aid in quantitative characterization of the distributions and important improvements in technique are reported. Although much additional research is required, there should be little doubt as a result of this study that characterization of lymphocytes by physical parameters is an important contribution to the diagnosis and study of human disease.

2.0 METHODS AND MATERIALS

The procedures are related in order of temporal sequence. More detail is furnished where significant improvements in technique were accomplished.

2.1 PREPARATION OF THE FICOLL

In these experiments, Ficoll (Pharmacia, Uppsala, Sweden) was used as the gradient material. There has been some discussion in the literature that the low molecular weight molecules in the Ficoll cause a loss of resolution, so the Ficoll was dialyzed to circumvent this problem. The dialysis was carried out using a Dow HFD-15 Mini-Plant Dialyzer (cellulose hollow fibers) with a nominal molecular weight cut-off of 5000 (Dow Chemical Company). Ficoll was dissolved in deionized, distilled water (30g to 70 ml) and filtered through a 5μ, 142 mm filter (Millipore Corporation, Bedford, Mass.). The apparatus for dialysis is shown in Figure 1. Essentially, the Ficoll was drawn from a flask and pumped into the fibers of the dialysis cartridge by a peristaltic pump. The resultant pressure on the fibers was monitored by a gauge on the line between the pump and the fibers. On the output side of the fibers, a micrometer needle valve (Gilmont) was placed to provide sufficient back pressure to lessen osmotic dilution during dialysis. After passing the needle valve, the Ficoll flowed into the recovery flask. Distilled water bathed the outside of the fibers in the dialysis cartridge. The water was drawn from a distilled water bottle by vacuum past a needle valve and ball flowmeter in order to measure and regulate flow through the cartridge and establish counter-current flow. The water was drawn out by a Vanton flex-i-liner vacuum pump, capable of pumping both air and water. The vacuum was controlled by an air bleed and monitored by a vacuum gauge between the pump and the dialysis cartridge. Conditions used during dialysis were: counter current flow with a ratio of eight water to one Ficoll solution, 6.5" Hg vacuum on the water, and 25 psi on the Ficoll. These conditions resulted in a Ficoll flow rate of about 9 ml/min. After dialysis, the osmolarity of the Ficoll was increased to human osmolarity (289 MOsm/Kg, Reference 8) by addition of 10X Hank's Balanced Salt, Ca and Mg free. Osmolarity was measured by freezing point depression (Advanced Digimatic Osmometer, Advanced Instruments, Needham, Mass.). Finally, Ficoll was filtered sterilized through a 0.22 micron, 142 mm Millipore plate filter and a FMI lab pump (Model RRP-SY, Fluid Metering, Inc., Oyster Bay, N.Y.

Figure 1. APPARATUS FOR CONTINUOUS DIALYSIS OF FICOLL

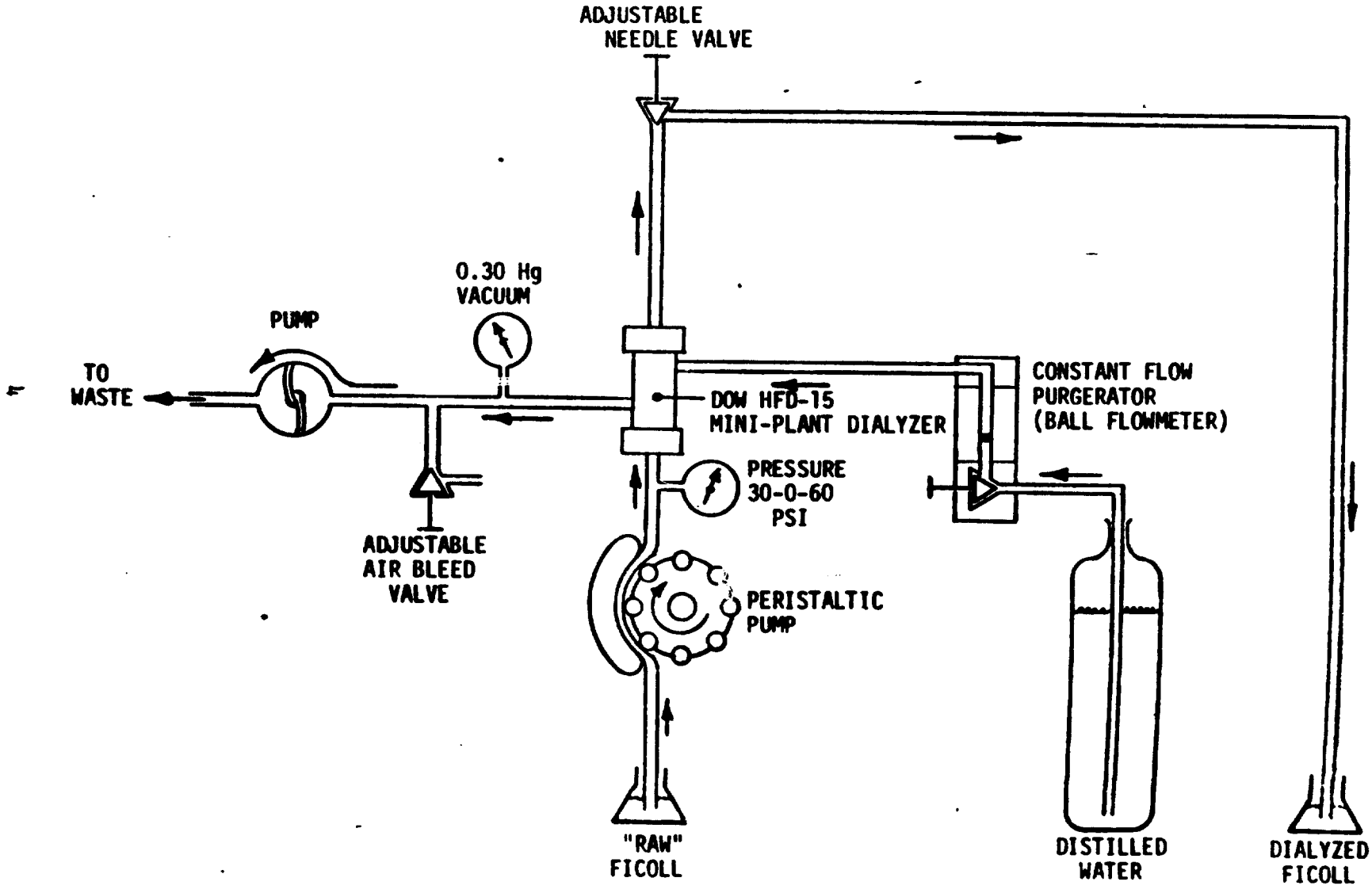

2.2 DESCRIPTION OF THE GRADIENT FORMER AND GRADIENT FORMATION

A highly precise gradient former was developed by our laboratory and is shown in Figure 2. The gradient former used a mixing chamber containing the high density, Ficoll-HBSS mixture. HBSS, Ca + Mg free, was introduced continuously into the chamber, while the Ficoll-HBSS mixture was removed at twice the rate of HBSS infusion. These inflow and outflow rates resulted in the formation of a linear gradient. The exact outflow to inflow ratio is very critical to the formation of truly linear gradients. Other devices commonly used for forming gradients employ peristaltic pumps which have been found to vary excessively in the pumping rate and constancy of each channel, so it was necessary to design and develop a new gradient former. Our device employs three syringes, one for inflow and two for outflow. The two outflow syringes remove a dense fluorocarbon liquid (FC-80, Medical Products Division, Minnesota Mining and Manufacturing Company) from a centrifuge tube. The use of a cone and fluorocarbon liquid help insure the deposition of a smooth, linear gradient.

2.3 COLLECTION OF BLOOD AND DEFIBRINATION

Blood was obtained by venipuncture using a 20 gauge needle and 30 cc syringe. Defibrination was accomplished in 16 x 150 mm siliconized glass tubes containing six 5 mm diameter siliconized glass beads. The tubes were vigorously rocked for five to ten minutes to complete the defibrination.

2.4 RECOVERY OF LYMPHOCYTES

The defibrinated blood was mixed with Plasma Gel (Roger Bellon Laboratories, France) in a ratio of three parts blood to one part plasma gel. After mixing by gentle rocking, the tubes were allowed to stand at room temperature. As the red blood cells sedimented due to aggregation into rouleaux, the supernatant containing the lymphocytes was removed by successive pipettings. Sedimentation was complete in 20 to 40 minutes. PMNs and monocytes were eliminated by passing the supernatant through a column of scrubbed nylon fiber (Fenwall Laboratories, Division of Travenol Laboratories). The column consisted of 0.3 grams of nylon fiber inserted into a 200 mm long, 27 cc condenser with a water jacket heated to 37°C by a water bath. Flow

Figure 2. DENSITY GRADIENT FORMER

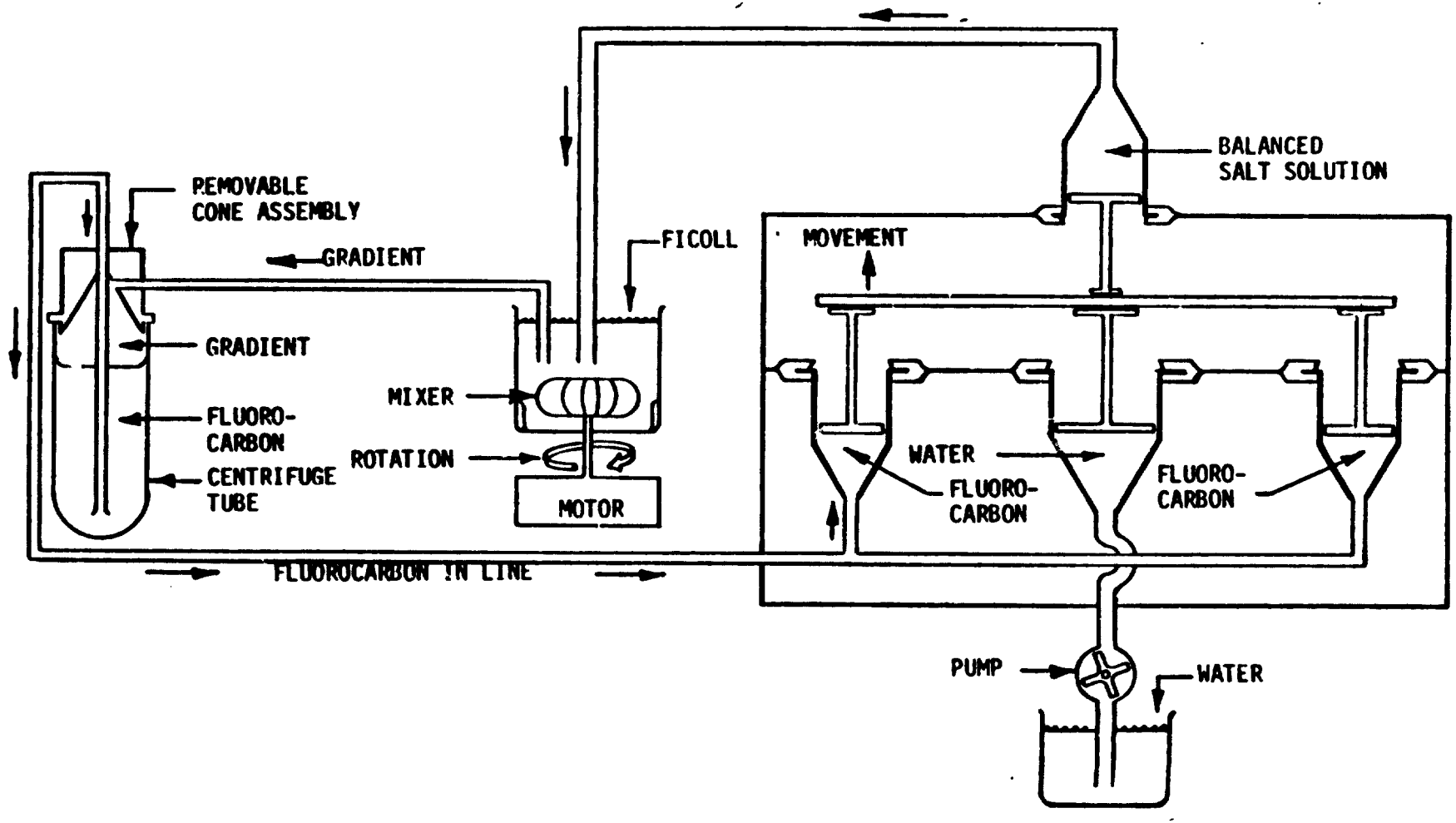

rate of the supernatant through the column was 25 ml/hr. The column was rinsed with about three ml of tris buffered saline (North American Biologicals, Inc.). The column effluent was centrifuged for 5 min at 200 g and resuspended in 0.87% NH_4Cl at 37°C for three minutes to lyse the remaining red blood cells. Next, the cells were centrifuged and resuspended in Hank's Balanced Salt Solution (HBSS) containing 1.0 mg/ml fibrinolysin, counted in a hemocytometer, and finally about 2×10^6 lymphocytes were resuspended in a 0.5 ml HBSS-fibrinolysin. This final suspension was passed through a 37 micron nylon mesh to eliminate any remaining clumps and layered on the gradient.

2.5 EQUILIBRIUM CENTRIFUGATION

The cells were centrifuged to buoyant equilibrium in a swinging bucket rotor and high speed centrifuge (Sorvall, RC2-B with HB-4 rotor) at 10,500 rpm for 60 minutes. Previous studies have established the conditions for equilibrium and acceptability of the spin-down technique[5].

2.6 DISPLACEMENT, COUNTING AND PLOTTING OF THE DISTRIBUTION

Apparatus for displacement and characterization of the distribution is shown in Figure 3. The gradient was displaced by infusing fluorocarbon into the bottom of the centrifuge tube. The displacement was effected by a Harvard syringe pump (Harvard Apparatus Mills, Mass.), modified to be capable of producing 100 psi. The gradient was displaced through a cone, through a continuous refractometer (Anacon Model 47 modified to accommodate a 1/16" flow-through cell), and into a continuous dilution system where the incoming sample was diluted 1:12 with filtered BSS and vigorous mixing. The cells were then counted by a continuous particle counter (HIAC Model PC-302 SSTA High Accuracy Products Corp., Claremont, CA). Channel settings for the counter were 2-15μ for the cell counting channel, and >15μ for the upper channel which was used to monitor any clumping of cells.

The dilution system consisted of a FMI pump (Model RRPG150), several 0.2 micron pleated membrane filter capsules (Gelman #12016 Gelman Instrument Company, Ann Arbor, Michigan), a ball-type flowmeter (Gilmont), a Millipore 47 mm membrane filter, a 500 ml reservoir, mixing chamber, and the cell

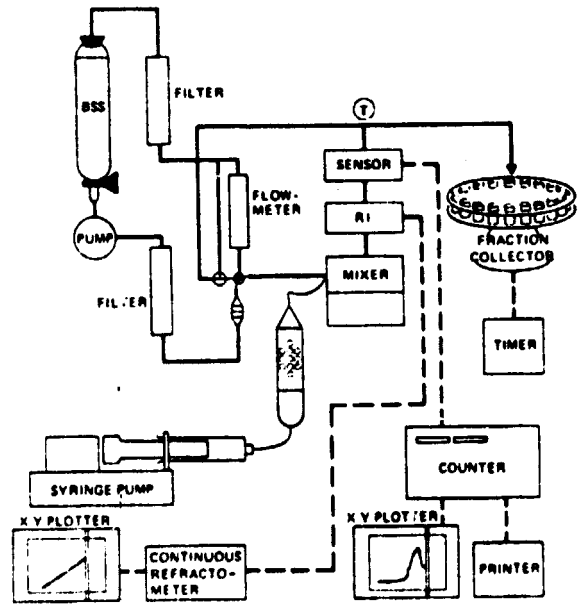

Figure 3. SCHEMATIC OF APPARATUS FOR DETERMINATION OF SPECIFIC GRAVITY DISTRIBUTION

counting sensor. These components were connected in a recirculating system. Isotonic balanced salt solution was used as the dilution fluid, and the fluid in the reservoir was replaced after the displacement of two gradients. The mixing chamber consisted of a glass tube containing two loose-fitting,cylindrical, stirring magnets positioned in line with like poles in repulsion. An Alnico V horseshoe magnet mounted on a stirring motor was positioned under the mixing chamber. The rotation of the horseshoe magnet caused the stirring bar magnets in the mixing chamber to wobble and mix the solution. This design was an effective mixer and had a low dead volume (about 0.3 cc), thus keeping loss of resolution to a minimum during the dilution and mixing. The continuous refractometer verified the continuity and linearity of the gradient. The continuous cell counter printed the number of cells counted at each one-minute interval. The data, along with the refractive index of samples (Bausch and Lomb Precision Refractometer) taken at the start and end of the gradient were entered into a Hewlett-Packard HP 9810 desk top calculator with plotter which, using a program we developed, normalized the data to peak count, converted refractive index to density, subtracted background, and plotted the cell number as a function of cell density.

2.7 DONOR SELECTION, VIRAL DIAGNOSIS AND IMMUNIZATION

Peripheral blood samples (5-20 ml) were obtained from donors in subjective good health and from patients selected by T. Yamauchi, M. D., at Harbor General Hospital, Torrance, California, under a subcontract. Due to difficulty in establishing positive serological diagnosis of any particular viral disease, patients with disease of certain clinical diagnosis were selected and serological diagnosis was thereafter used to support the clinical diagnosis.

In addition to the selection of patients with viral disease, characterization of changes in the specific gravity distribution of lymphocytes following immunization against viral disease was attempted. A total of ten volunteers were each immunized with one of the following vaccines: influenza, mumps, rubella, or smallpox. Blood samples were obtained and analyzed before

immunization and at 1, 2, 3, 7, 9, 14, 17, 21 and 30 days postimmunization.

This study sought to safeguard the rights and safety of subjects. Donors were given a full explanation of the procedure and the intended use of the blood sample prior to obtaining freely given consent. The risk was minimal since only a small amount of blood was drawn. The research was justified by prior studies that established need for further research and was accomplished by scientifically trained personnel.

2.8 ANALYSIS OF LSGDs FOR SUBPOPULATIONS

2.8.1 Dissection by Parabolas

To investigate the presence of subpopulations in the obviously heterogenous LSGDs, the distributions were plotted semilogarithmically with cell number on the ordinate and density on the abscissa. Each distribution was dissected into a sum of parabolas, corresponding to the components of the heterogenous distribution, by standard mathematical technique[9]. Essentially, parabolas were fitted by hand to each major component characterized by a peak or shoulder and that portion of the associated descending limb that was least influenced by other components. The parabola was plotted about the axis of symmetry at the peak or shoulder. Smaller components were identified by subtraction of the major parabolas from the heterogenous distributions.

2.8.2 Computer Program for Fitting Gaussians to Data

In order to develop parameters for analysis of the distributions, a computer program was written using published subroutines[10]. This program fits Gaussians to the data, computes chi-square, and iteratively adjusts the Gaussians until chi-square is minimized. The program is delineated in Appendix A.

Input to the program is: each peak's estimated central density, σ, and maximum count; starting and ending densities (X); and cell counts (Y). Output from the program consists of: the input data; the best fit peak center, σ, and max count for each peak; the sum of the best fit Gaussians (for comparison with the original data); the component Gaussians; and a

plot of the original data, the composite fit, and each Gaussian. Appendix A contains the computer program and a representative data printout. Program MAIN is essentially a driving program for CHIFIT and other subroutines. Data are input up to line 43, and lines 44-48 set up the X values. The increment sizes used by CHIFIT are then set up, and CHIFIT called in line 57. In lines 61 to 74, the process is repeated until CSQ (the sum of the squares of the differences between input and output Y values) reaches a minimum. The rest of the program prints and plots the results.

2.8.3 Sizing of Nuclei from Lymphocytes of Different Specific Gravity

In order to further investigate the presence of subpopulations of lymphocytes within the heterogenous LSGD, another physical parameter, the size of the nucleus, was measured for lymphocytes isolated in different density regions of the gradient. Thus, a purified suspension of lymphocytes was split and each sample simultaneously centrifuged to buoyant equilibrium on identical gradients. One gradient was displaced and counted by the usual procedure to characterize the LSGD. The second gradient was displaced through the continuous refractometer and fractions collected in centrifuge tubes. Based upon the LSGD from the first gradient and the refractive index of fractions from the second gradient, fractions were collected for each selected region of the LSGD. Each density fraction was diluted and the lymphocytes concentrated by centrifugation. The lymphocytes were resuspended in BSS containing 5 mg/ml of hexadecyltrimethyl ammonium bromide (Matheson) in order to strip the nuclei of outer membrane and cytoplasm. The isolated nuclei were counted and sized by a Cytofluorograf (Biophysics Model 4802A). Relative size was measured by small angle scattering at 4800 Å and the distribution of number at each size stored in a 100 channel analyzer. The size distributions for each selected density region were hand plotted from printout of the data.

2.9 STUDY OF GRADIENT CHARACTERISTICS

Since the results of this study were very dependent upon the characteristics of the linear density gradient, studies were conducted on the relationship between refractive index (RI) and specific gravity, the linearity and

similarity of simultaneously formed gradients, and the reproducibility of LSGD.

2.9.1 Relationship Between RI and Specific Gravity

The stock solutions of Ficoll-HBSS used in formation of linear gradients were used to make up several calibration solutions. Solutions from about 1.0070 g/cc to 1.0973 g/cc were made by mixing the Ficoll-HBSS with HBSS. Densities were determined using a specific gravity balance (Troemner: Philadelphia, Pa.) Temperature of the solutions while being measured for density was kept at 20°C±0.02°C by circulating water through a jacket on the balance's fluid reservoir and through a bucking heating and chilling system. RIs corresponding to the density measurements were determined using the temperature controlled high precision refractometer which gave RI to the fifth decimal place by interpolation (Bausch and Lomb Precision Refractometer).

A plot of RI vs density was made with RI on the ordinate and density on the abscissa. A Hewlett-Packard 9810 calculator with statistics pack was used to do a linear regression on the data.

2.9.2 Gradient Linearity and Similarity

Any work involving linear gradients must show that the gradients are indeed linear. Any significant deviation from linearity or discontinuity in the gradient would distort the LSGD and could produce artifacts. Further, gradients simultaneously formed by the same apparatus must be highly similar if the conditions of linearity and uniformity are to be met. In this work, linearity and similarity were demonstrated by displacing four simultaneously formed gradients, as described, and fractionating each into thirty equal fractions. The refractive index of each fraction was measured using the high precision refractometer. The correlation coefficient was determined for the least squares, linear fit of the useful portion of each gradient, and the composite of the four gradients as a measure of the similarity of the gradients.

2.9.3 LSGD Reproducibility

Reproducibility was investigated by dividing a sample of purified lymphocytes, layering onto each of two simultaneously formed gradients, centrifuging to buoyant equilibrium, and characterizing each LSGD as usual. Comparison was made by difference in density of prominent features of the peak and calculation of the correlation coefficient.

3.0 RESULTS

The results are presented in five parts: comparison of healthy donors and patients, studies of immunization, analysis of distributions for subpopulations, miscellaneous studies of disease, and inspection of gradient characteristics. Throughout these studies, monitoring of over 150 gradients by the continuous refractometer did not show any discontinuities in the gradients and did not reveal any significant departure from linearity over the region of the gradient used to characterize the specific gravity distribution of lymphocytes.

3.1 COMPARISON OF HEALTHY DONORS AND PATIENTS

Peripheral blood samples were analyzed for 25 healthy donors and 20 patients with positively diagnosed viral disease. Figure 4 shows a superpositon of distributions from the first 15 healthy donors, while Figures 5-10 show example, individual distributions for six patients with viral disease. The computer plot, with original data points for each healthy donor and patient with virus disease, is shown in Appendix B. Note the similarity of the distributions for the controls in contrast to distributions from disease states. The typical distribution for a healthy person, when plotted on a linear scale, shows few cells at low densities, rises quickly to the peak, and tapers off at high densities.

The most striking differences between distributions from control and from patients are the density position of the main peak, the width of the main peak, and the relative percentage of cells contained by the main peak. Therefore, the parameters chosen for statistical comparison were: density,

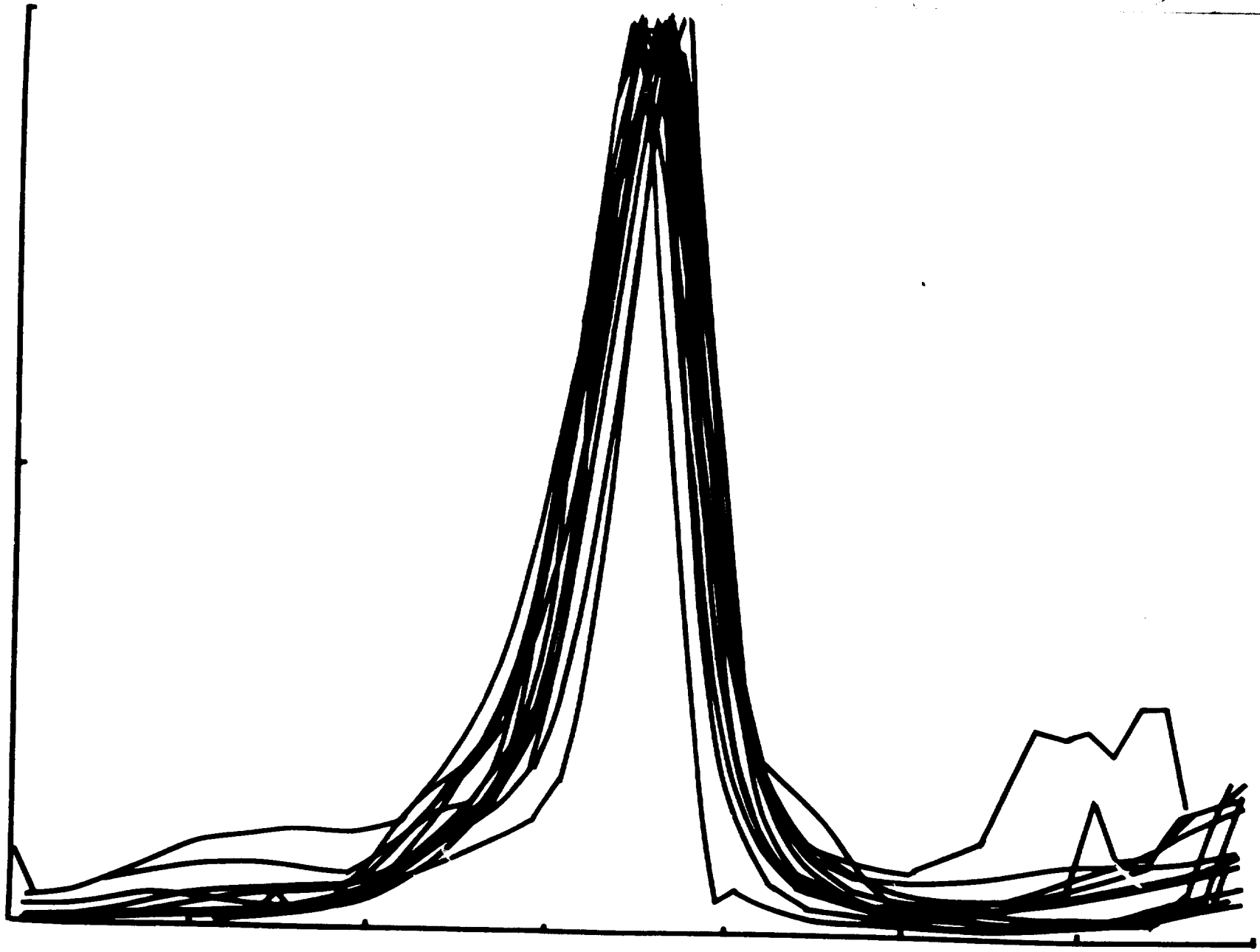

Figure 4. Healthy Donors

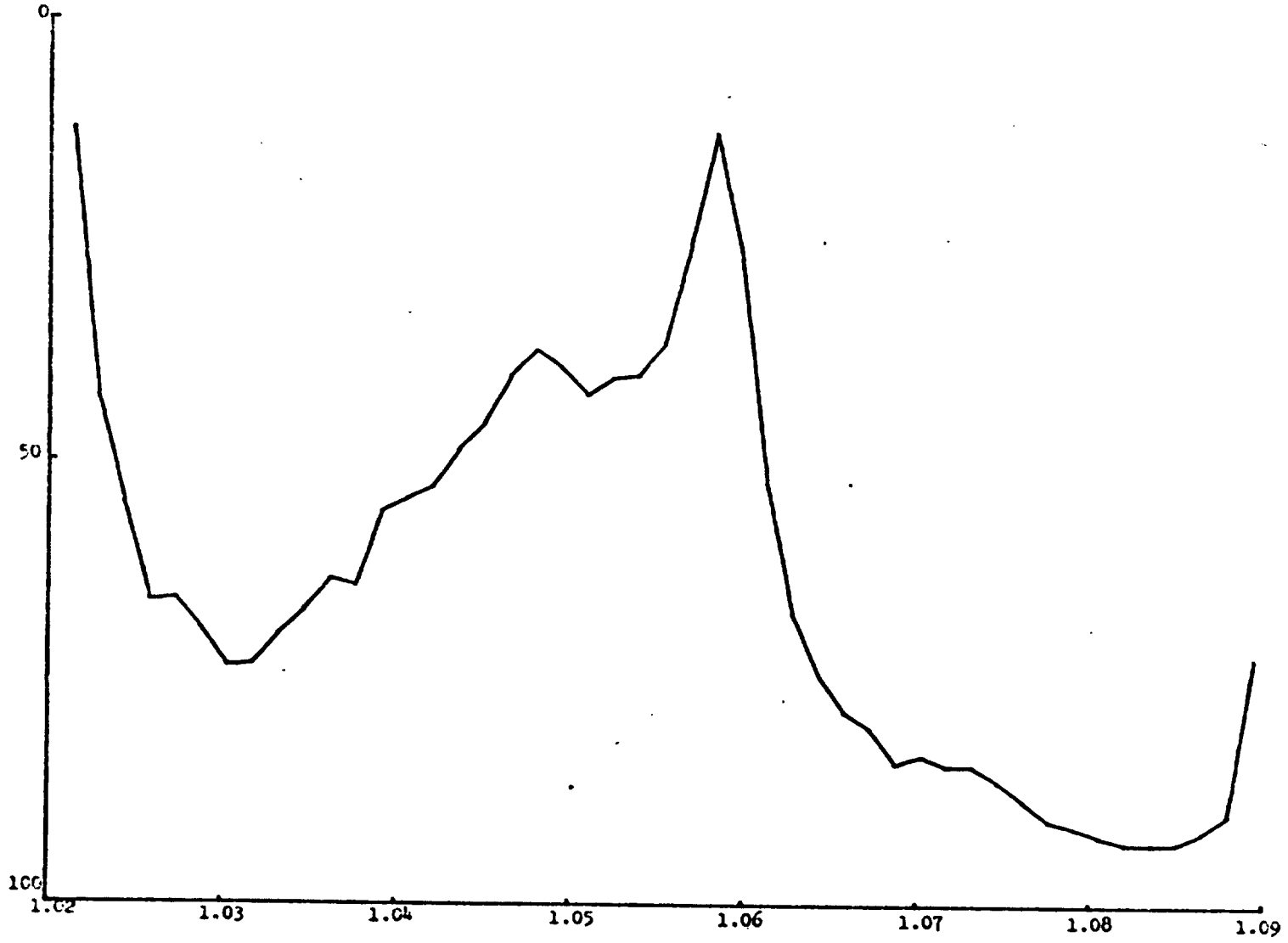

Figure 5. PATIENT V10

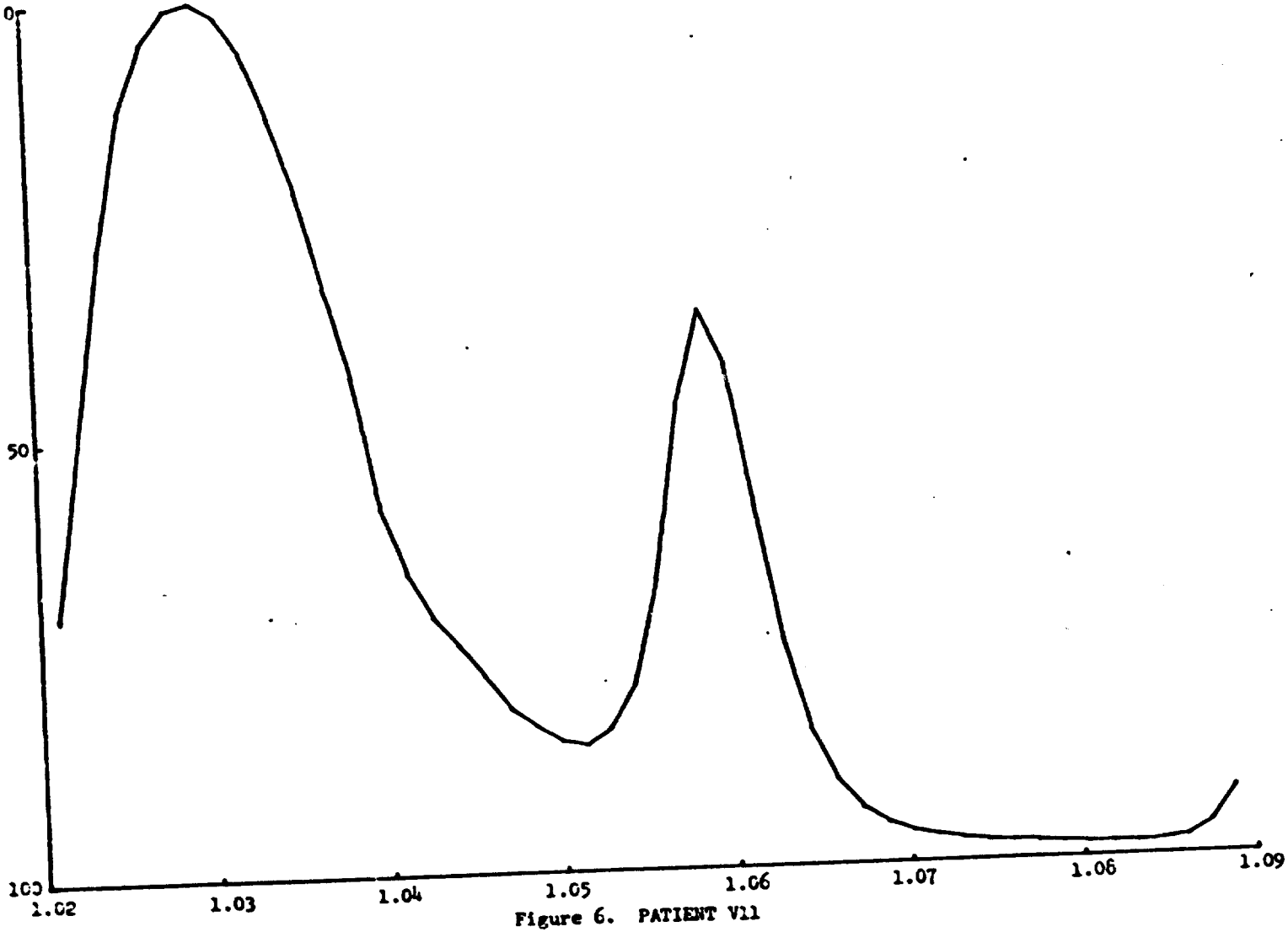

Figure 6. PATIENT V11

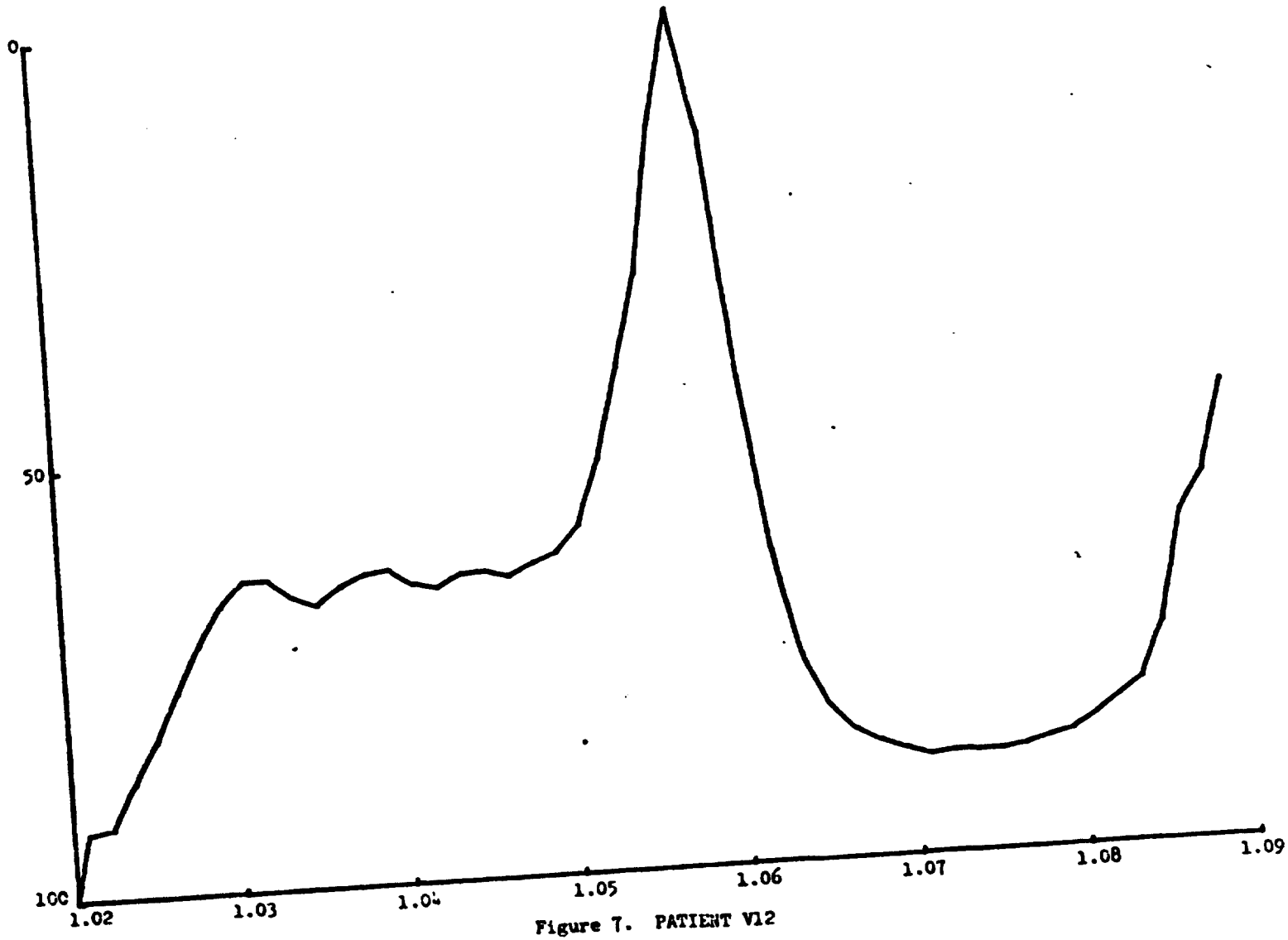

Figure 7. PATIENT V12

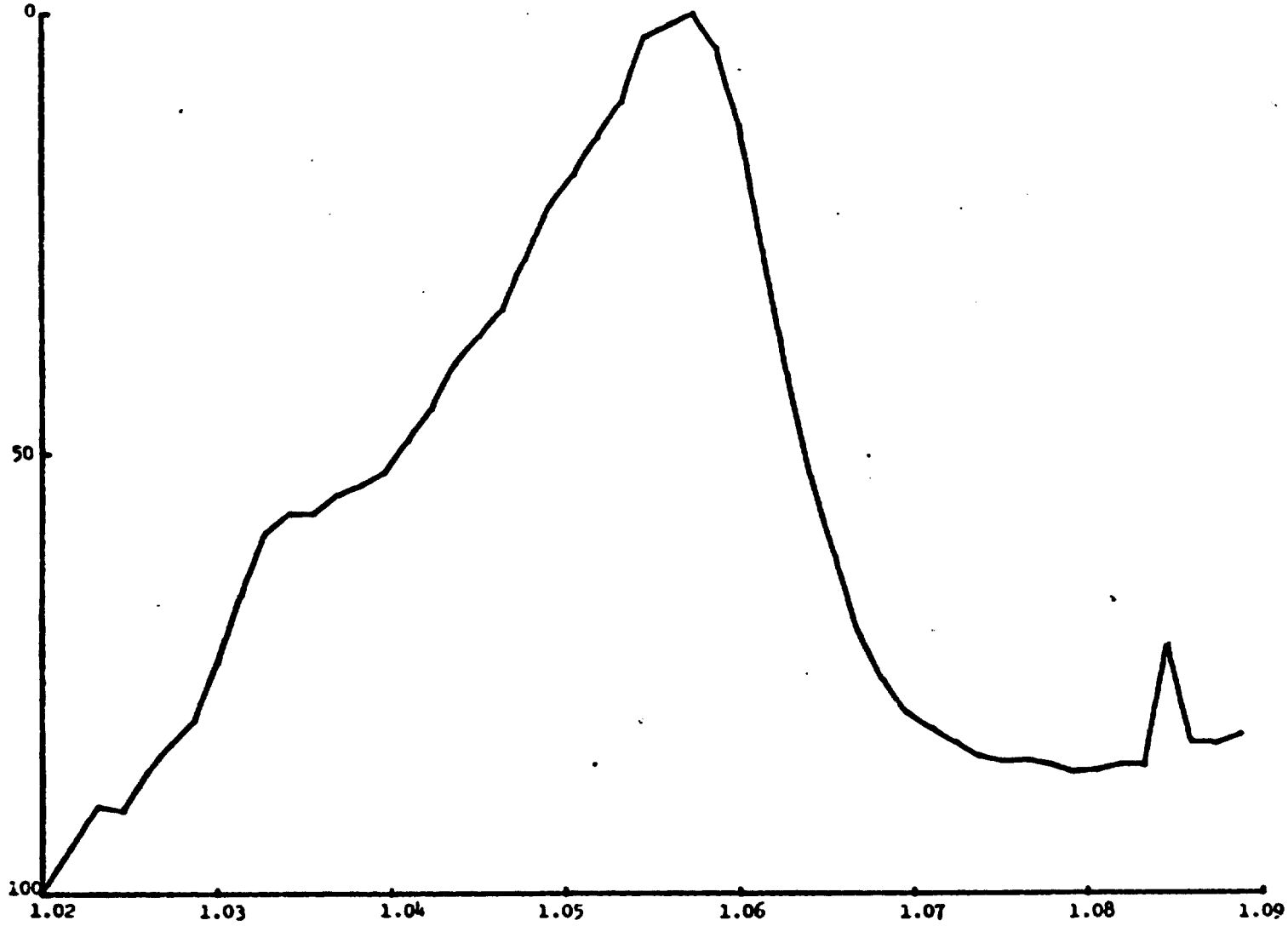

Figure 8. PATIENT V14

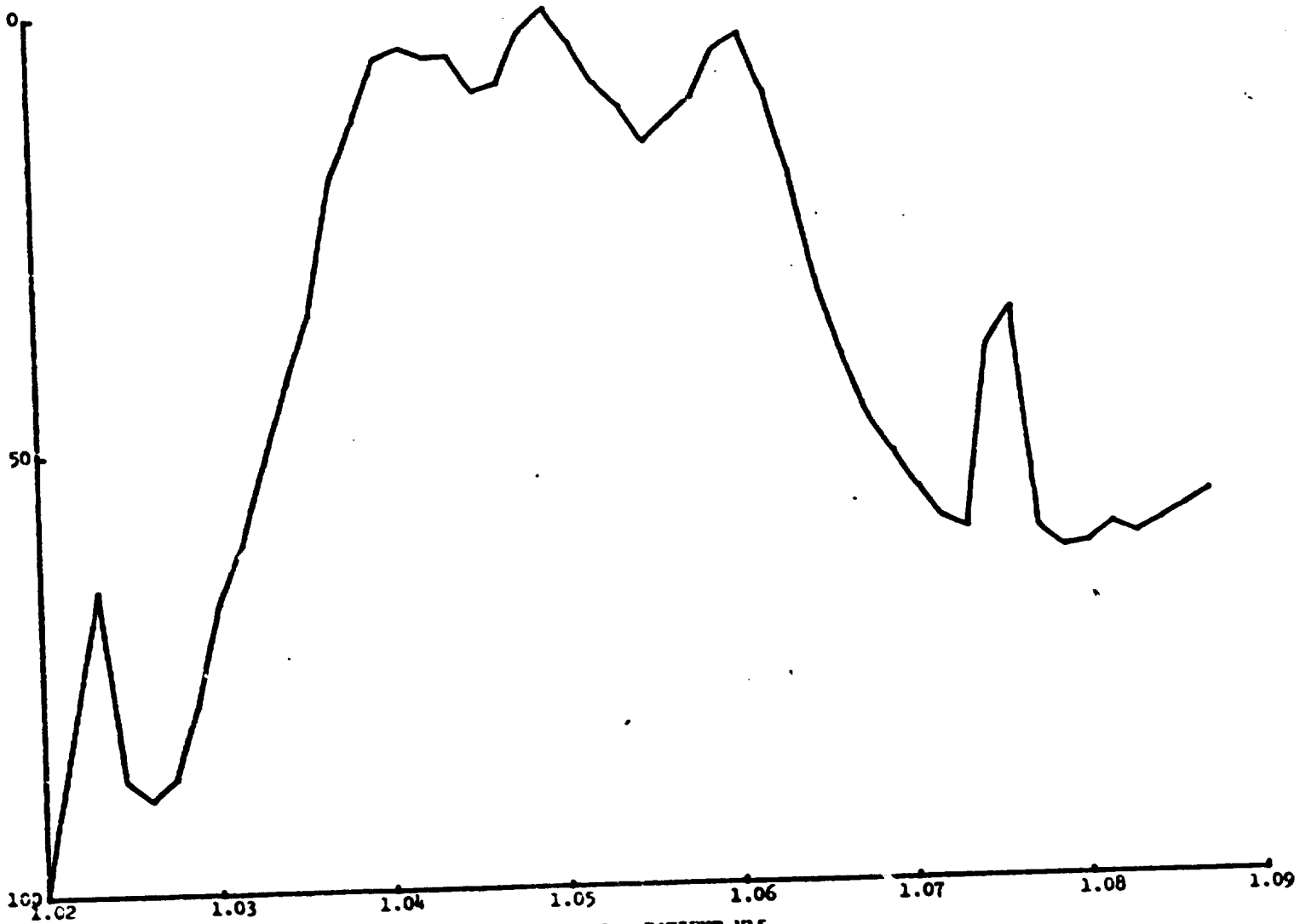

Figure 9. PATIENT V15

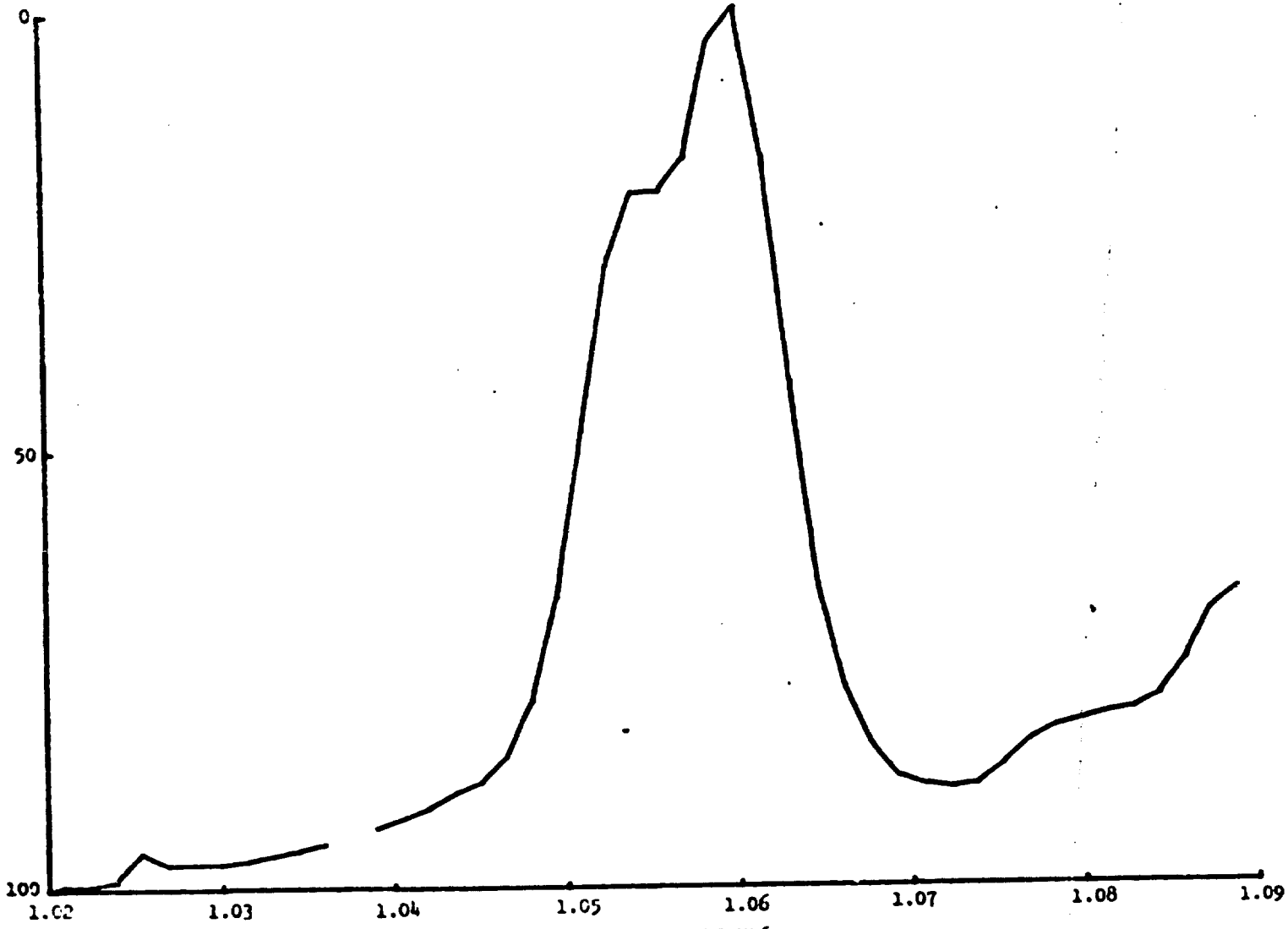

Figure 10. PATIENT V16

of the main peak at its highest count, full width at half maximum (FWHM) of the main peak, and area encompassed by the FWHM. In order to obtain these measurements, the distributions were normalized to the highest cell count and plotted with a linear scale using the HP 9810 with plotter. The density position of the main peak and FWHM were measured directly from these plots. The fraction of the total area encompassed by the FWHM was measured by planimetry.

Table I gives the values for the main peak density, area fraction, and FWHM for healthy donors, along with the upper and lower confidence limits at the 90, 95 and 98 percent levels. The values which fall outside these limits are indicated with an asterisk. Table II contains the same information for donors with viral disease. As can be seen from the two tables, by requiring all measures to be inside the confidence limits for normals and at least one measure to be outside for subjects with viral disease, only 3 false negatives of 20 patients would have been diagnosed. In order to minimize false negatives and false positives using all three criteria, the 95% level of confidence would yield 3 false negatives and one false positive.

The serology results are given in Table III. Although the serology eliminated 2 additional false negatives, no additional insight was provided regarding the analysis of the specific gravity distributions.

3.2 IMMUNIZATION STUDIES

The temporal changes in LSGD following immunization are illustrated in Figure 11. for subjects 3 and 5. The changes can be generally characterized by a shift in density of the main peak to somewhat lower densities after day 1 or 2, and the appearance of more cells in the low density region (1.02 - 1.04 g/cc) after about day 9 following immunization. The LSGDs for subject 5 are shown superimposed in Figure 12. The presence of at least 3 major subpopulations of lymphocytes during immunological response can be easily identified.

TAULE I. STATISTICAL ANALYSIS OF LSGD PARAMETERS FOR HEALTHY DONORS

SUBJECT NO.	MAIN PEAK DENSITY				MAIN PEAK AREA FRACTION				MAIN PEAK FWHM			
	VALUE	Confidence Limits 90%	95%	98%	VALUE	Confidence Limits 90%	95%	98%	VALUE	CONFIDENCE LIMITS 90%	95%	98%
		1.0603 1.0535	1.0610 1.0528	1.0617 1.0521		.69990 .48026	.72319 .45697	.74516 .43500		.009091 .005599	.009461 .005229	.009810 .004880
N1	1.0541				.575				.00636			
N2	1.0564				.477	*			.00530	*		
N3	1.0544				.588				.00712			
N4	1.0547				.487				.00833			
N5	1.0565				.595				.009242	*		
N6	1.0562				.520				.00712			
N7	1.0544				.565				.00758			
N8	1.0547				.576				.00788			
N9	1.0559				.544				.00727			
N10	1.0572				.509				.00667			
N11	1.0571				.541				.00667			
N12	1.0548				.606				.00727			
N13	1.0541				.549				.00591			
N14	1.0555				.590				.00727			
N15	1.0565				.513				.00773			
N16	1.0595				.640				.0083			
N17	1.0608	*			.599				.0092	*		
N18	1.0592				.626				.0087			
N19	1.0571				.740	*	*		.0062			
N20	1.0583				.672				.0075			
N21	1.0590				.605				.0093	*		
N22	1.0565				.662				.0066			
N23	1.0593				.619				.0068			
N24	1.0595				.635				.0071			
N25	1.0599				.719	*			.0062			

* Outside of Confidence Limits

ORIGINAL PAGE IS
OF POOR QUALITY

TABLE II. STATISTICAL ANALYSIS OF LSGD PARAMETERS FOR PATIENTS WITH VIRAL DISEASES

SUBJECT NO.	VIRAL DISEASE	MAIN PEAK DENSITY				MAIN PEAK AREA FRACTION				MAIN PEAK FWHM			
			Confidence Limitss				Confidence Limits				Confidence Limits		
		Value	90%	95%	98%	Value	90%	95%	98%	Value	90%	95%	98%
			1.0603 1.0535	1.0610 1.0528	1.0617 1.0521		.69990 .48026	.72319 .45697	.74516 .43500		.009091 .005599	.009461 .005229	.009810 .004880
V1	SSPE	1.0634	*	*	*	.3696	*	*	*	.00856			
V2	MEASLES	1.0612	*	*		.5359				.008788			
V3	MUMPS	1.0646	*	*	*	.6071				.015672	*	*	*
V4	H. SIMPLEX	1.0640	*	*	*	.6204				.009850	*	*	*
V5	CHICKEN POX	1.0634	*	*	*	.6497				.014179	*	*	*
V6	MUMPS	1.0609	*			.5011				.006364			
V7	MEASLES	1.0543				.6586				.012239	*	*	*
V8	VIRAL EXANTHEMA	1.0670	*	*	*	.2908	*	*	*	.00500			
V9	VARICELLA	1.0571				.3758	*	*	*	.015758	*	*	*
V10	VARICELLA	1.0589				.4614	*			.018333	*	*	*
V11	VARICELLA	1.0298	*	*	*	.5905				.016818	*	*	*
V12	VARICELLA	1.0579				.2969	*	*	*	.008657			
V13	VARICELLA	1.0580				.5018				.006800			
V14	VARICELLA	1.0577				.6368				.023636	*	*	*
V15	VARICELLA	1.0500	*	*	*	.6272				.035757	*	*	*
V16	VARICELLA	1.0606	*			.5844				.012879	*	*	*
V17	MUMPS	1.0608	*			.5637				.007727			
V18	HERPES ZOSTER	1.0599				.8058				.0092	*		
V19	HERPES ZOSTER	1.0602				.8513				.0041	*	*	*
V20	HERPES ZOSTER	1.0603				.4281	*	*	*	.0105	*	*	*

* Outside of Confidence Limits

Table III. SEROLOGY OF VIRAL DISEASE

PATIENT #	CLINICAL DIAGNOSIS OF DISEASE	VIRAL RESULTS		
		ISOLATION	SEROLOGY ACUTE	CONT.
V1	SSPE	Not Done	Not Done	
V2	Measles	No Isolation	+	0
V3	Mumps	No Isolation	+	0
V4	H. Simplex	H. Simplex	1/64	1/64
V5	Chicken Pox	No Isolation	+	0
V6	Mumps	No Isolation	1/64	1/64
V7	Measles	No Isolation	+	0
V8	Viral Exanthema	No Isolation	+	+
V9	Varicella	No Isolation		
V10	Varicella	Not done	Not done	
V11	Varicella	Varicella		
V12	Varicella	No isolation		
V13	Varicella	Not done	Not done	
V14	Varicella	Not done	Not done	
V15	Varicella	Not done	Not done	
V16	Varicella-Reyes	No isolation		
V17	Mumps	Mumps virus		
V18	Herpes Simplex	Herpes Simplex		
V19	Herpes Zoster	No isolation	<1/8	≥1/64
V20	Herpes Zoster	No isolation		

+ = serum available
0 = serum not available

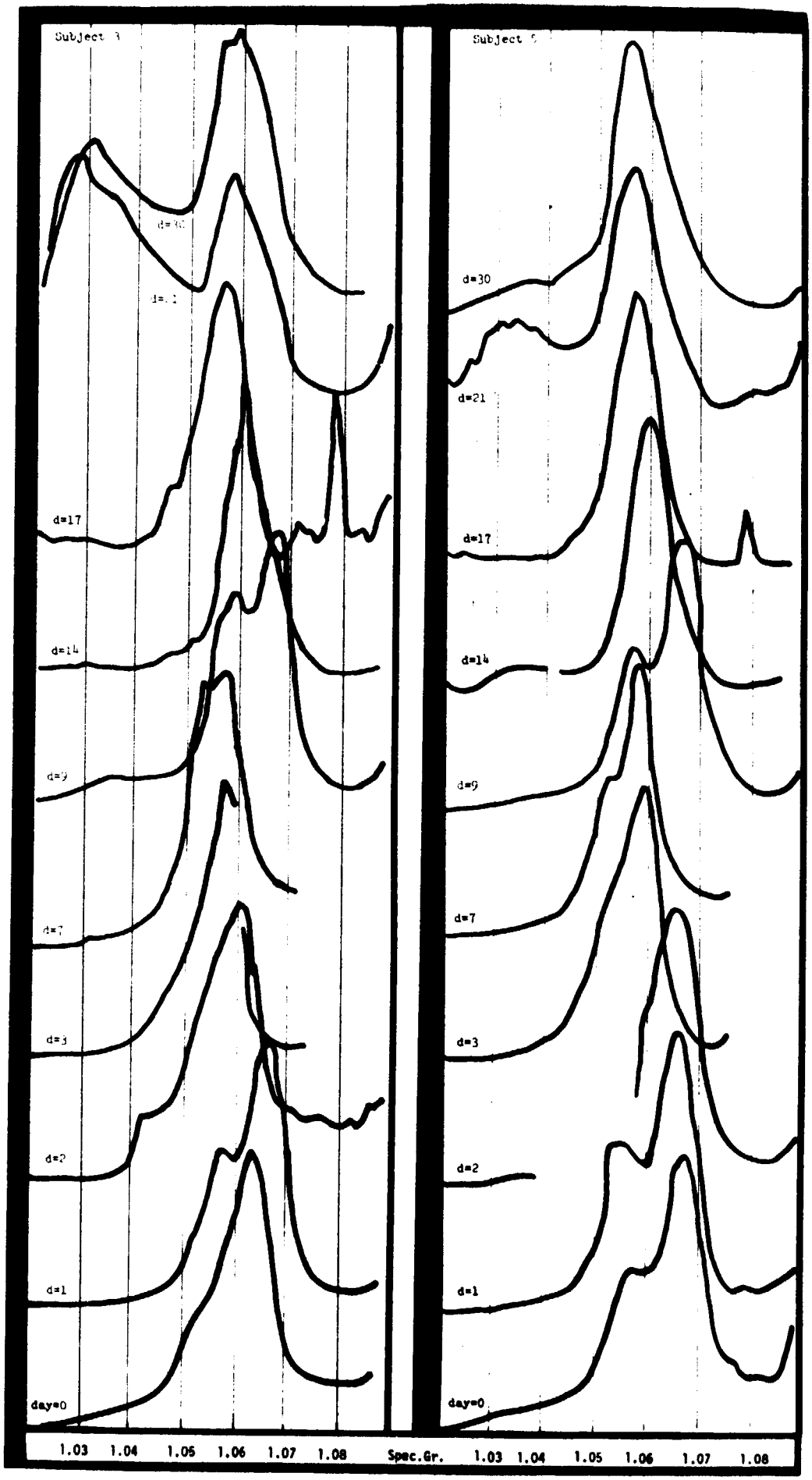

Figure 11. TEMPORAL CHANGES IN LSGD FOLLOWING IMMUNIZATION

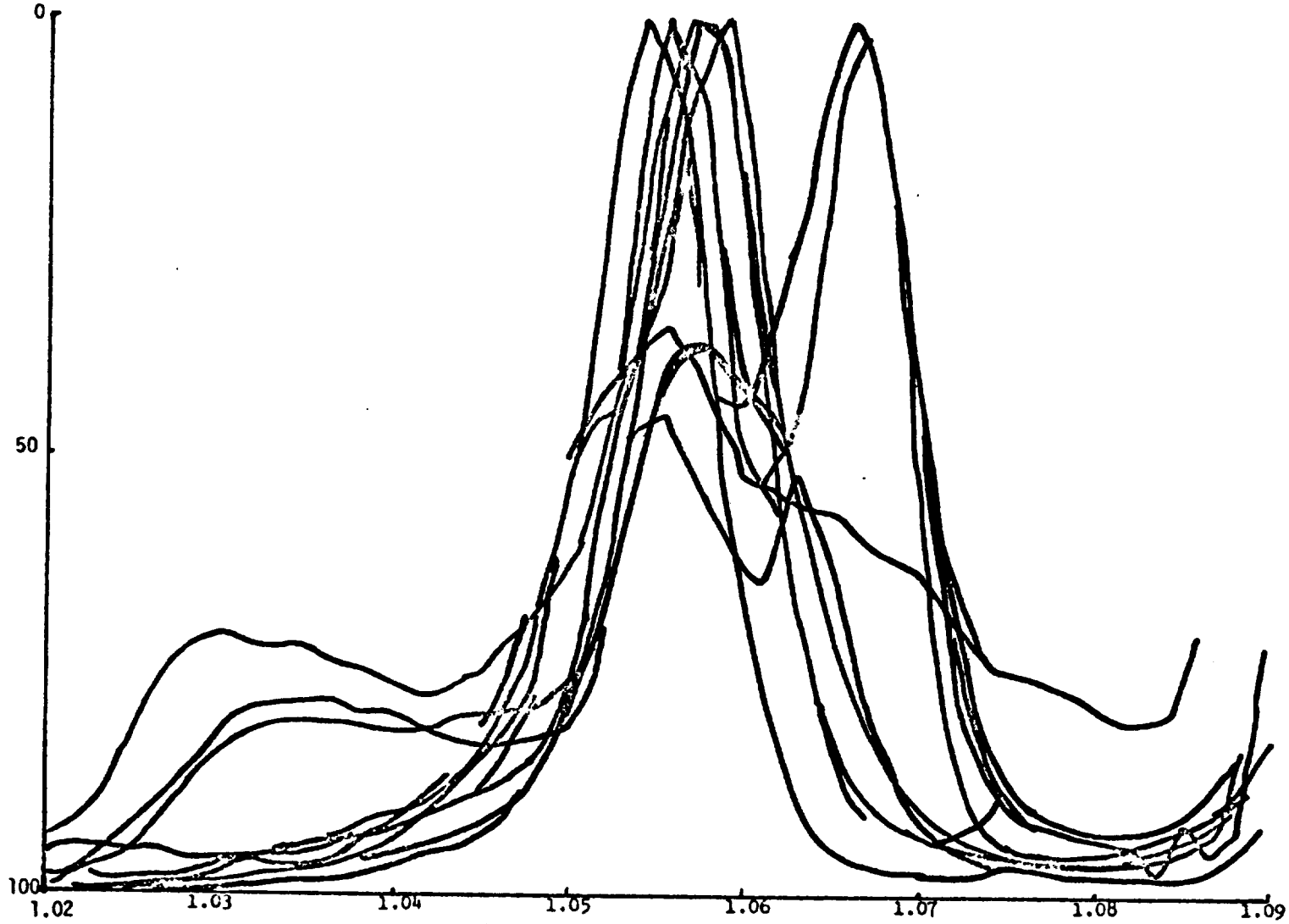

Figure 12. LSGDs FOR SUBJECT 5

The temporal changes for all 10 subjects are shown in Appendix B. Their features cannot be conveniently characterized, but certain common features did emerge. Thus, in the low density region (1.02 - 1.04 g/cc), the subpopulations shifted to slightly higher densities during the interval between 2 and 6 days postimmunization in 7 out of 9 cases, and tended to lower densities during 7 to 10 days in 8 of 9 cases. In the density region above, 1.05 g/cc (see Figure 13), there was a general shift to a position of lower density for the major peak at 7-10 days postimmunization, disappearance of subpopulations at 11-20 days, and indication of reappearnce of subpopulations at 21-34 days.

3.3 ANALYSIS OF DISTRIBUTIONS FOR SUBPOPULATIONS

Potential subpopulations of lymphocytes were dissected from the LSGDs by a standard method of fitting parabolas to the distribution by hand, by fitting Gaussian distributions with a computer program, and by determining the size of nuclei of cells separated on a density gradient.

3.3.1 Hand-fit of Parabolas

All of the LSGDs for healthy donors and patients with viral disease were hand-fit with parabolas for each likely subpopulation. Representative plots are shown in Figures 14 to 16 for healthy donors and in Figures 17 to 19 for patients with varicella.

The method usually revealed the presence of 3 subpopulations in the healthy donors and 2 to 4 subpopulations in the viral cases. The three subpopulations from healthy donors clustered at 1.035, 1.048, and 1.056 g/cc, while the subpopulations of lymphocytes from viral cases were diffusely scattered; although, some clustering could be detected at 1.062 g/cc. This clustering is illustrated by Figure 20, the frequency distribution of modal densities of subpopulations at density intervals of 0.005 g/cc. This represents the number of subpopulations at each interval of density without regard to the number of cells in each subpopulation. The major difference between health and viral disease was the existence of additional subpopulations of lymphocytes during disease.

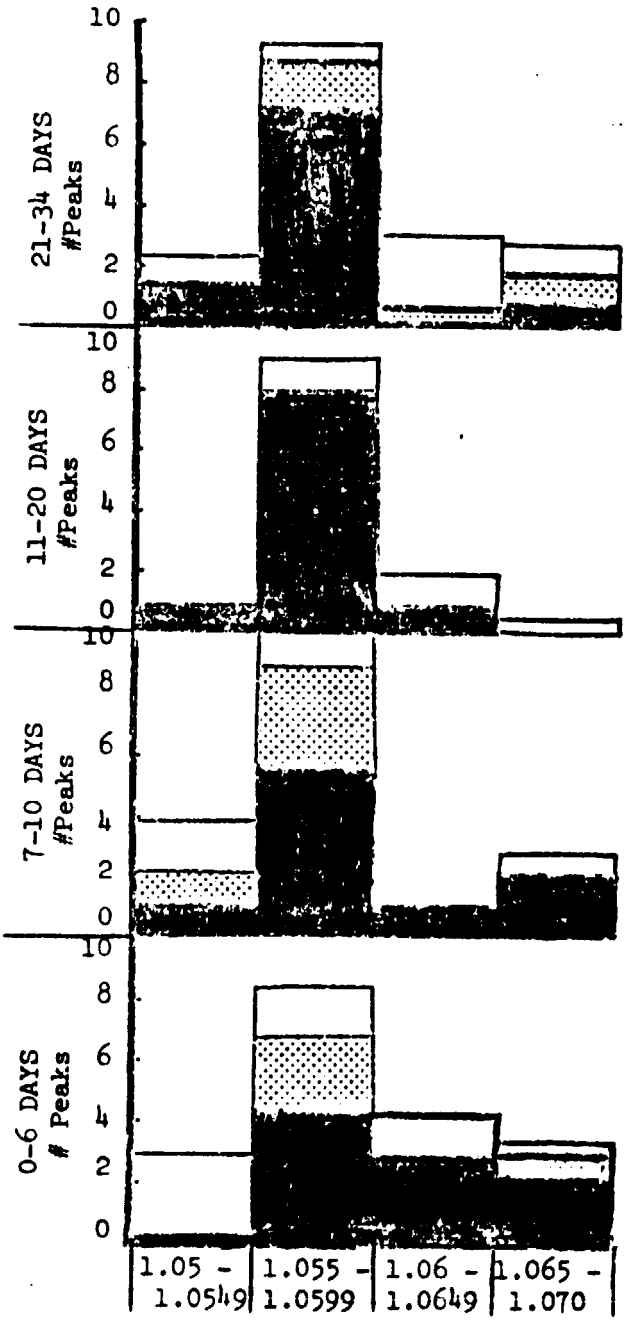

Figure 13. TEMPORAL CHANGES IN THE 1.05 TO 1.07 G/CC REGION

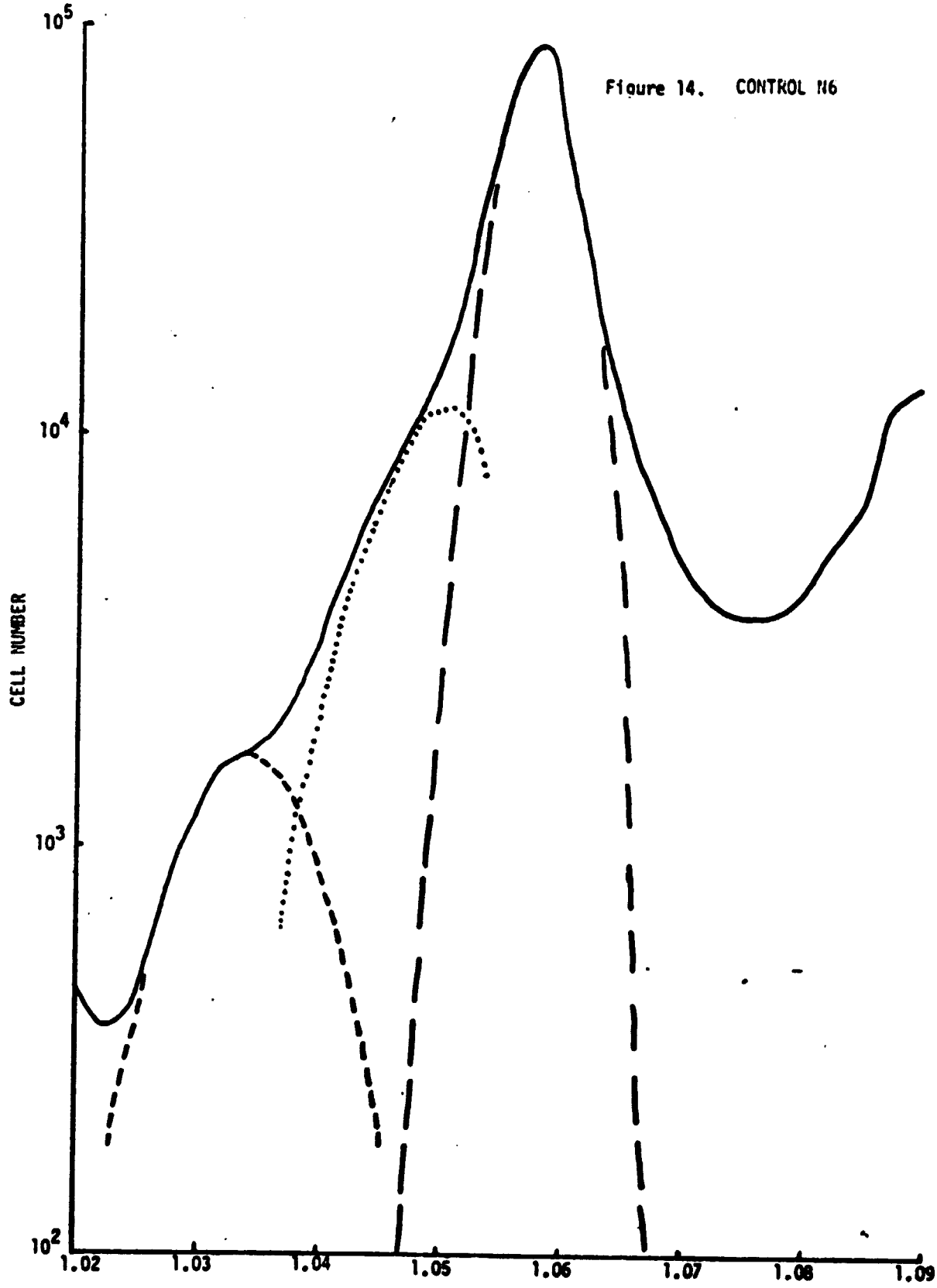

Figure 14. CONTROL N6

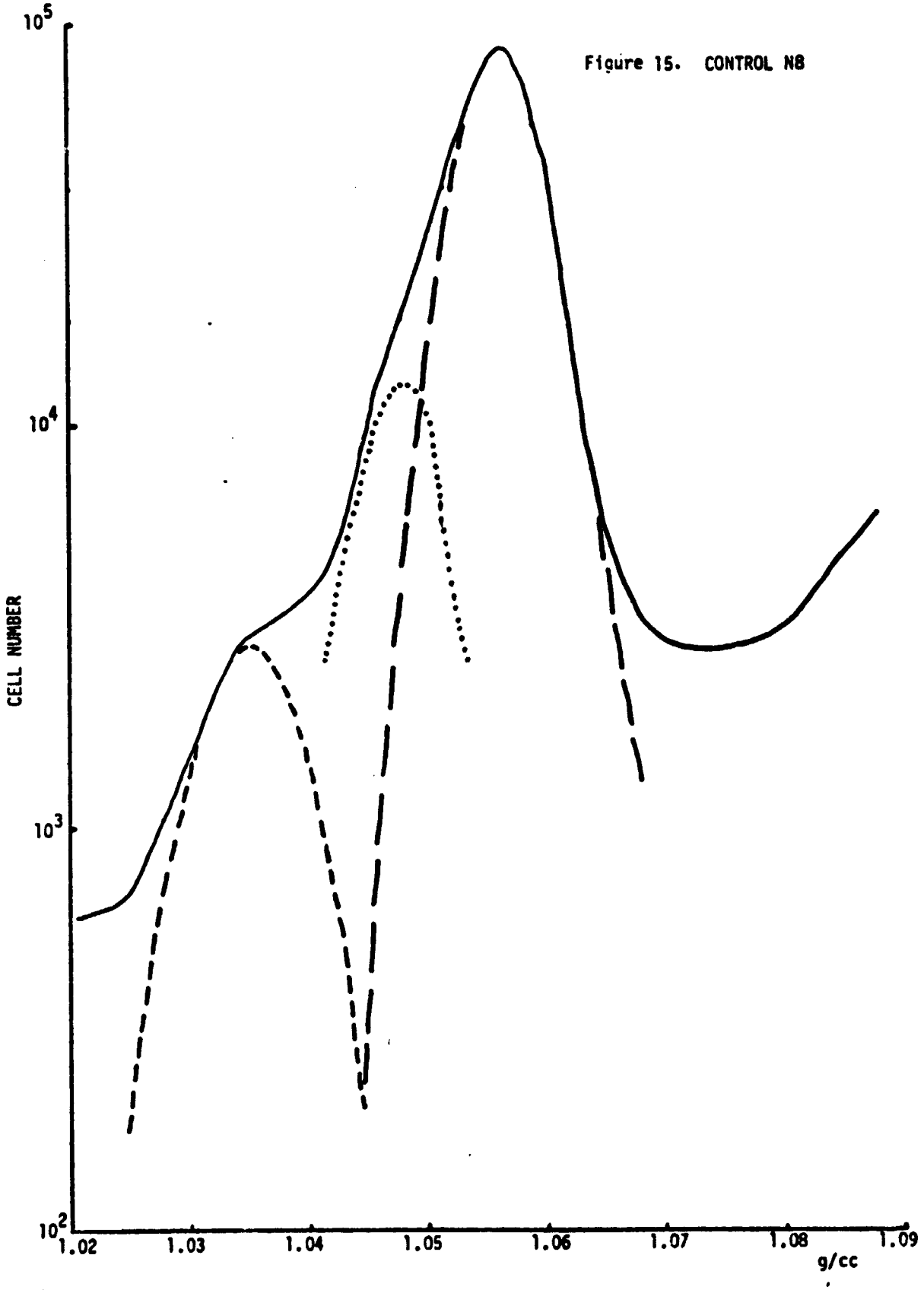

Figure 15. CONTROL N8

Figure 16. CONTROL N10

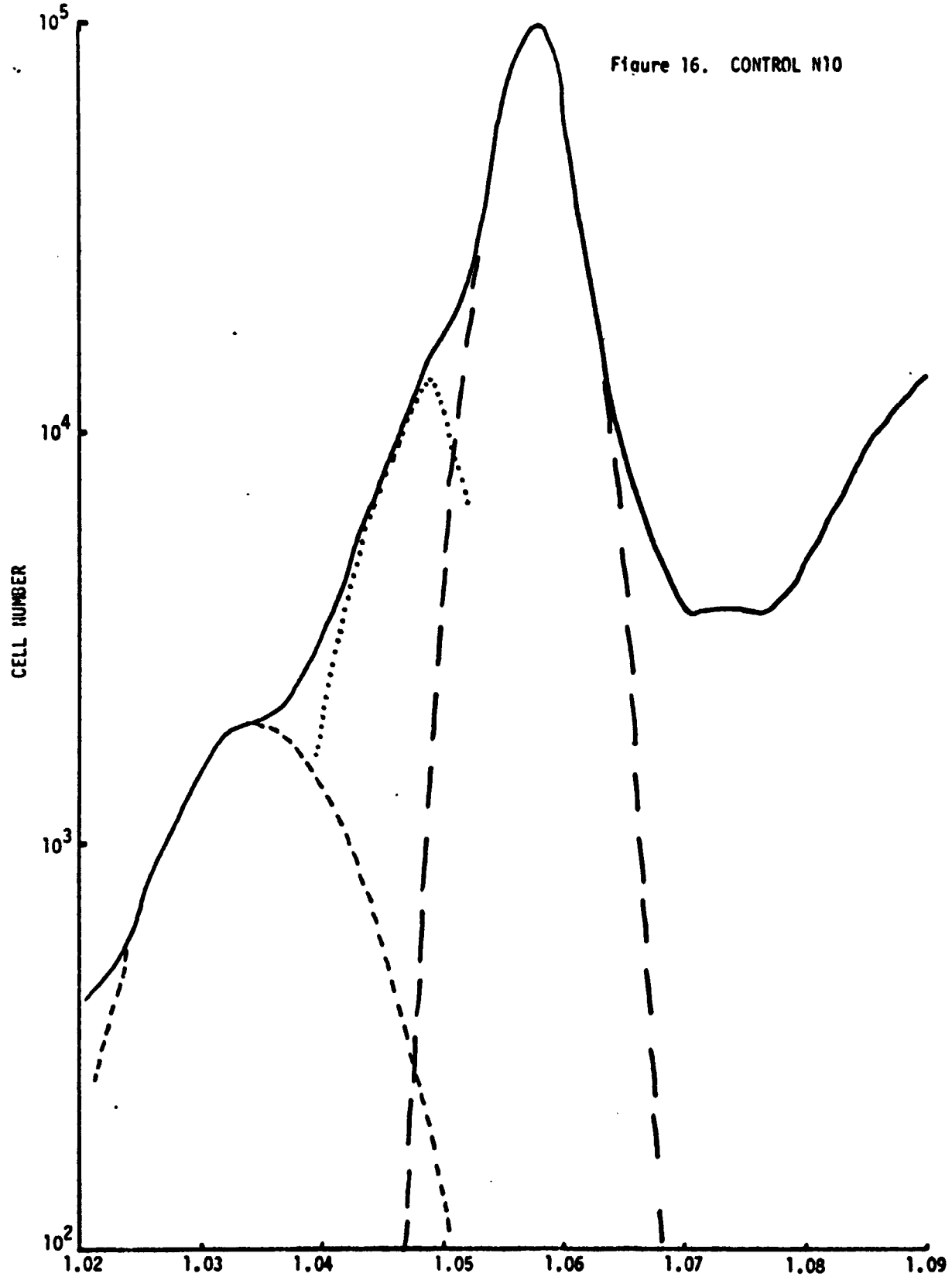

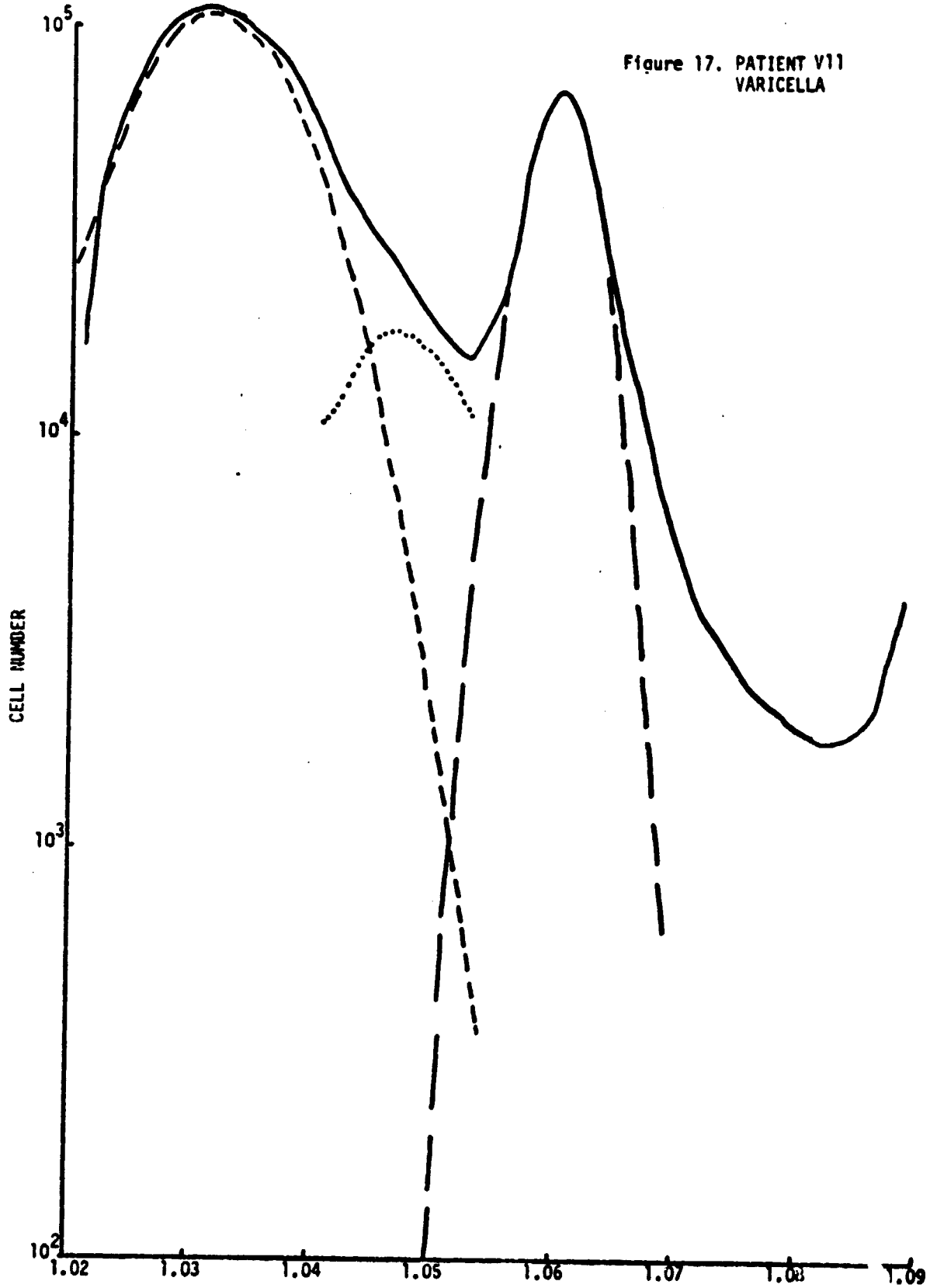

Figure 17. PATIENT V11
VARICELLA

Figure 18. PATIENT V12
VARICELLA

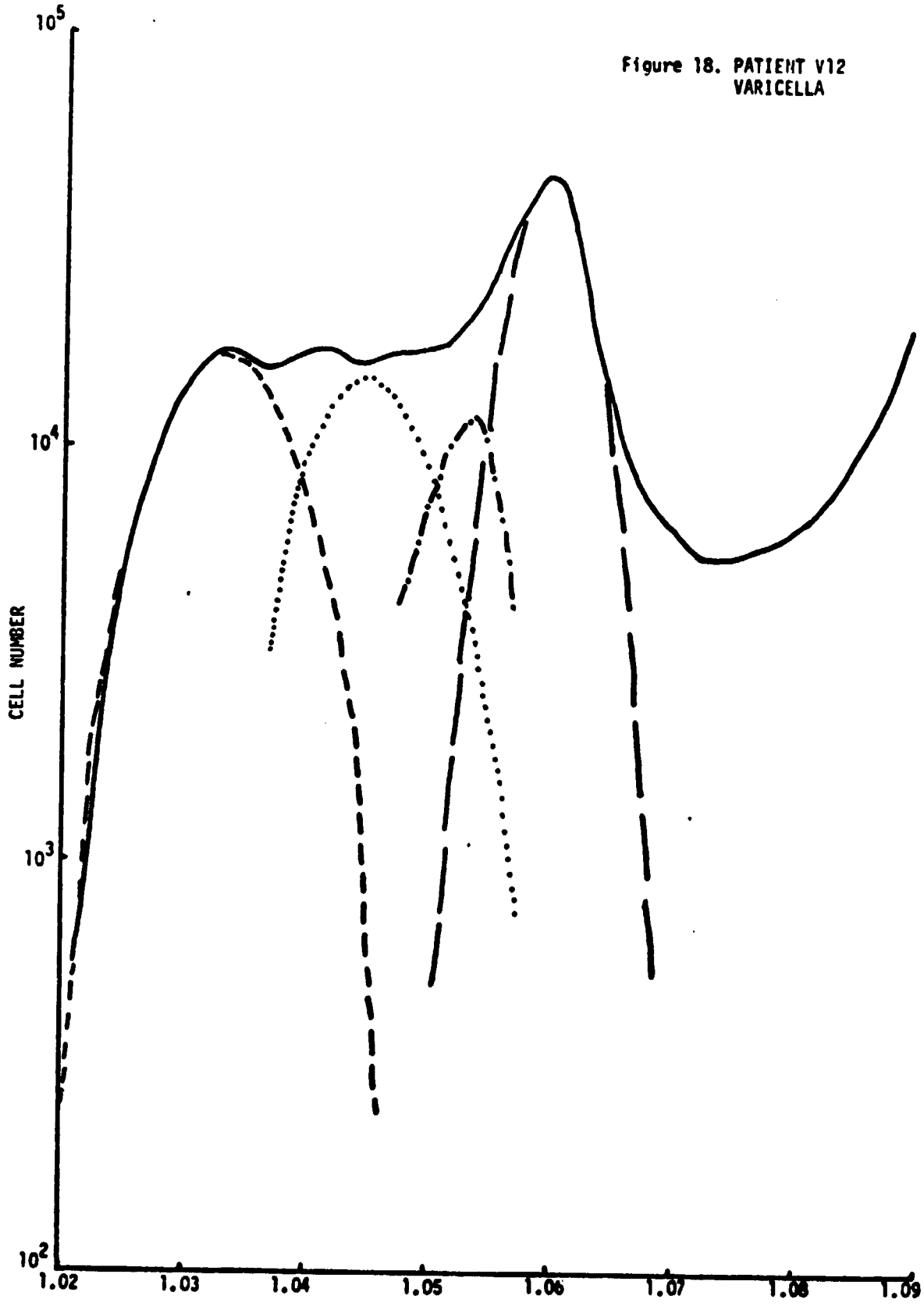

Figure 19. PATIENT V15
VARICELLA

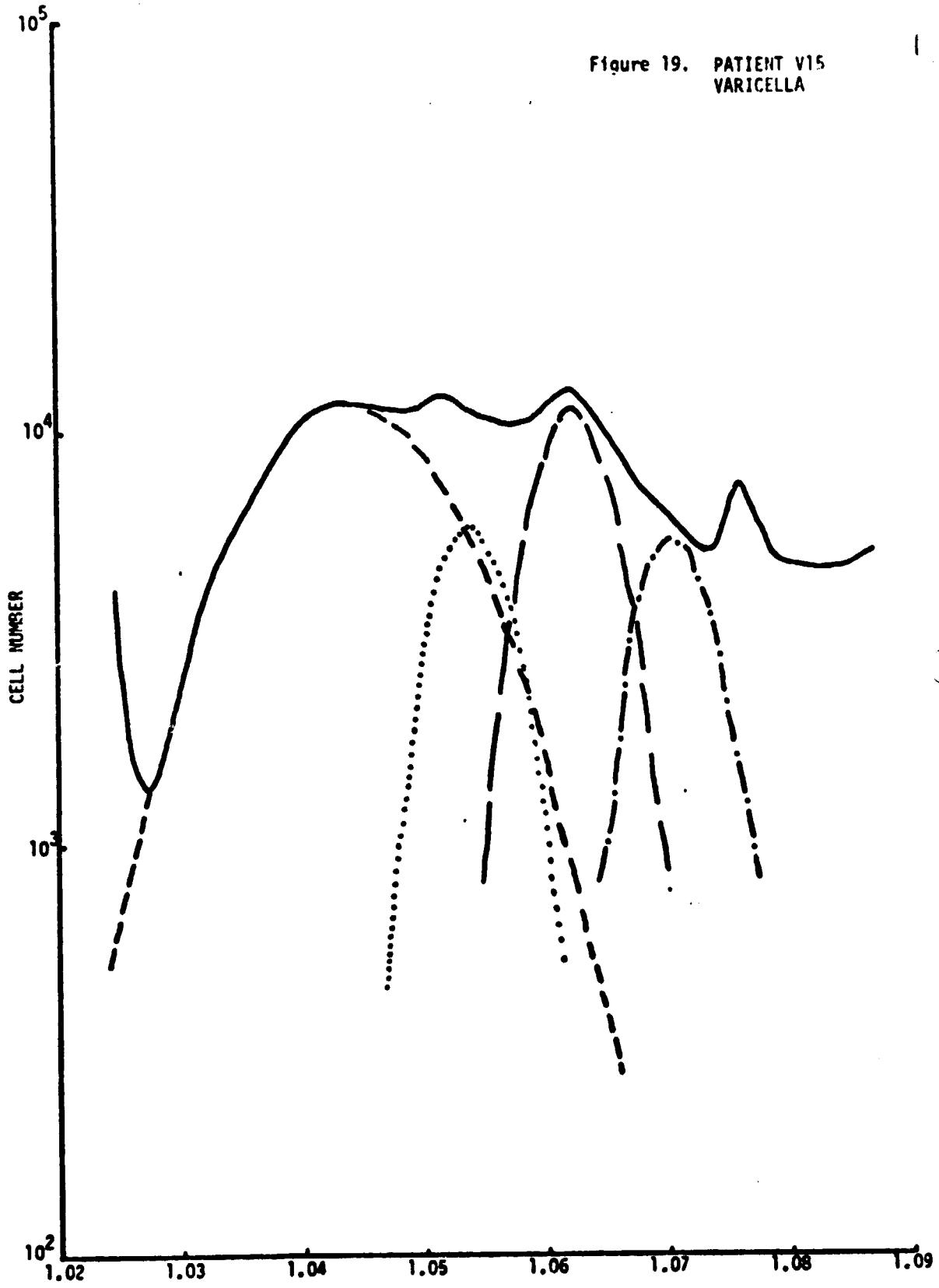

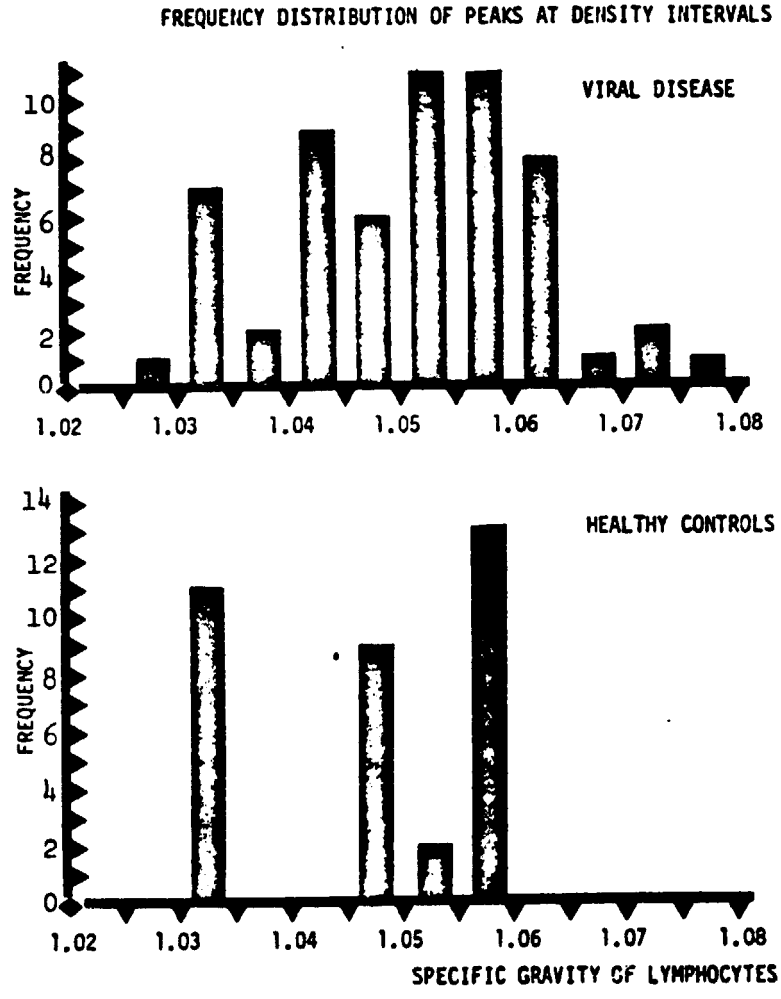
FREQUENCY DISTRIBUTION OF PEAKS AT DENSITY INTERVALS
VIRAL DISEASE
FREQUENCY
0
2
4
6
8
10
1.02
1.03
1.04
1.05
1.06
1.07
1.08
HEALTHY CONTROLS
FREQUENCY
0
2
4
6
8
10
12
14
1.02
1.03
1.04
1.05
1.06
1.07
1.08
SPECIFIC GRAVITY OF LYMPHOCYTES

Figure 20

3.3.2 Computer-fit of Gaussians

Results of the computer-fit of Gaussians to the LSGDs are shown in Appendix C, Figures N1 to N25 and V1 to V20, which are detailed in Tables I, II, and III. These correlated well with the results of the handfitting method, provided information on the relative number of cells in each subpopulations, and gave a goodness-of-fit criterion.

Computer analysis alloved comparison of normalized cell numbers of component Gaussians at their modal densities for health and disease. The computer analysis gave cell number normalized to a total count of 1,000 for each distribution. For comparison, all distributions for each category, disease or health, were summed, normalized to 1,000 and plotted on a semilogarithmic scale to emphasize the subpopulations in each density interval. Figures 21, 22, 23, 24, and 25 show the modal densities for subpopulations of lymphocytes from healthy donors, varicella, measles, mumps, and herpes, respectively.

Comparison of the subpopulations identified for healthy donors with the subpopulations identified for each disease category clearly shows the presence of new or additional subpopulations of lymphocytes during disease. Further, there is some indication of different subpopulations for different viral diseases; although many additional cases remain to be characterized before any conclusions may be drawn.

3.3.3 Characterization of Subpopulations by Density and Nuclear Size

Figure 26 shows the nuclear size distributions of lymphocytes separated on a density gradient. The lymphocytes were obtained from a patient with aricella. At least three subpopulations are clearly demonstrated by this technique: a low density, 1.02 - 1.045 g/cc, subpopulation with a large nucleus (~channel 35); a population with a small nucleus (~channel 23) at density region 1.045-1.058 g/cc and predominant on the low density, ascending half of the major peak; and a subpopulation with a large nucleus (~channel 30) which appears in the density region 1.058 - 1.064 g/cc and predominates at higher densities. In addition, the analysis provides strong evidence for a distinct, fourth subpopulation of lymphocytes with a small nucleus

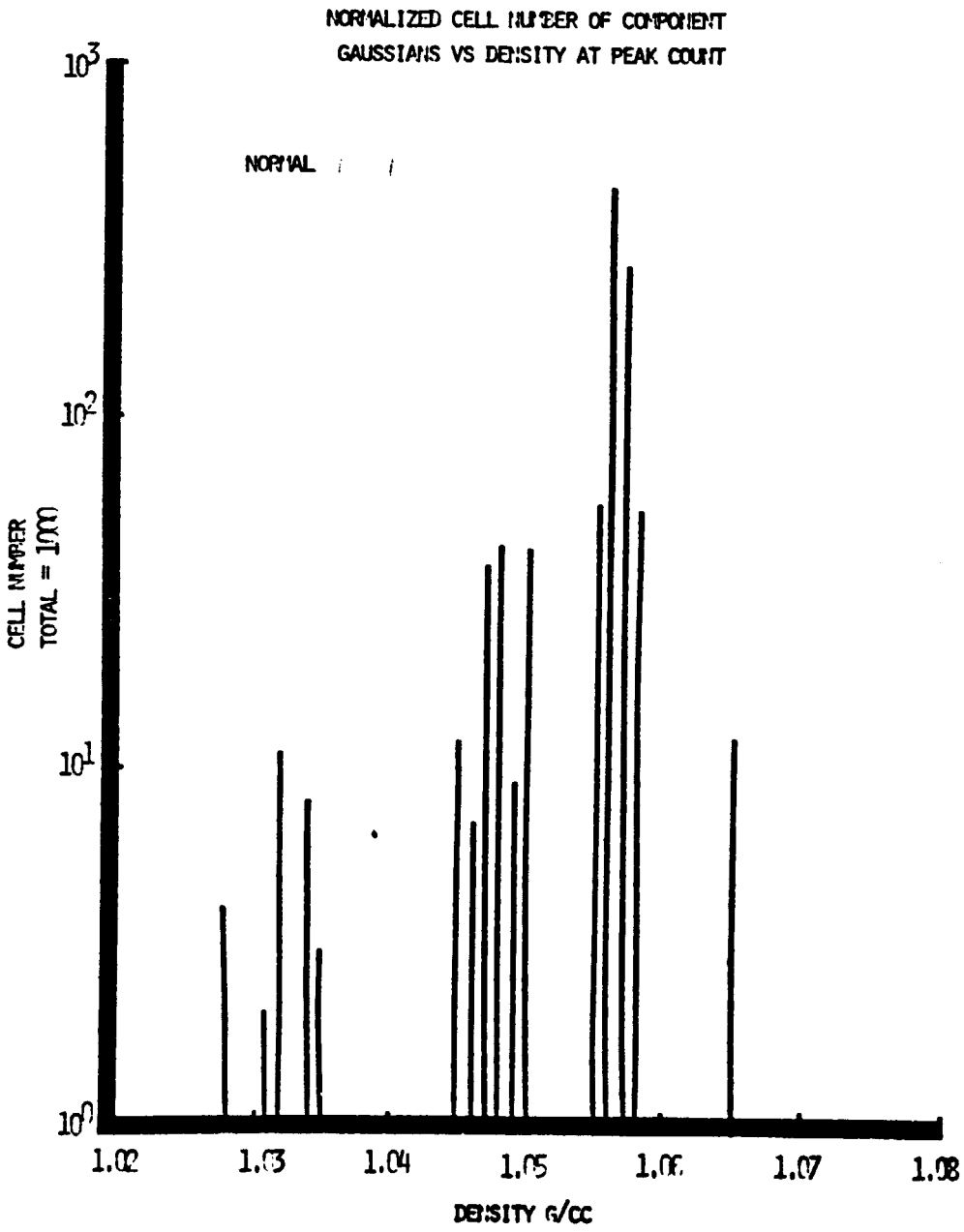
NORMALIZED CELL NUMBER OF COMPONENT
GAUSSIANS VS DENSITY AT PEAK COUNT
NORMAL
CELL NUMBER
TOTAL = 1000
10^3
10^2
10^1
10^0
1.02
1.03
1.04
1.05
1.06
1.07
1.08
DENSITY G/CC

Figure 21

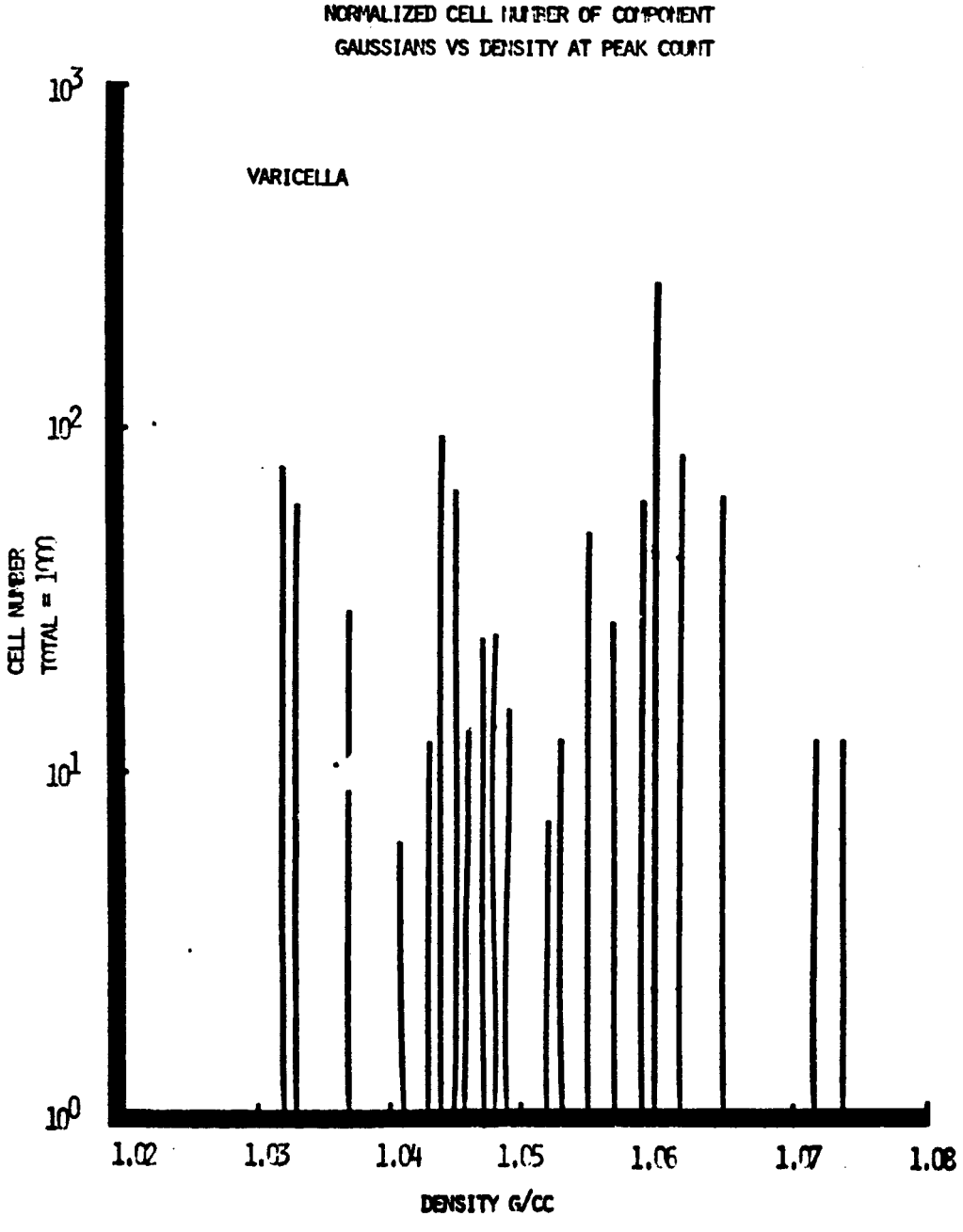
NORMALIZED CELL NUMBER OF COMPONENT
GAUSSIANS VS DENSITY AT PEAK COUNT
VARICELLA
CELL NUMBER
TOTAL = 1000
10^3
10^2
10^1
10^0
1.02
1.03
1.04
1.05
1.06
1.07
1.08
DENSITY G/CC

Figure 22

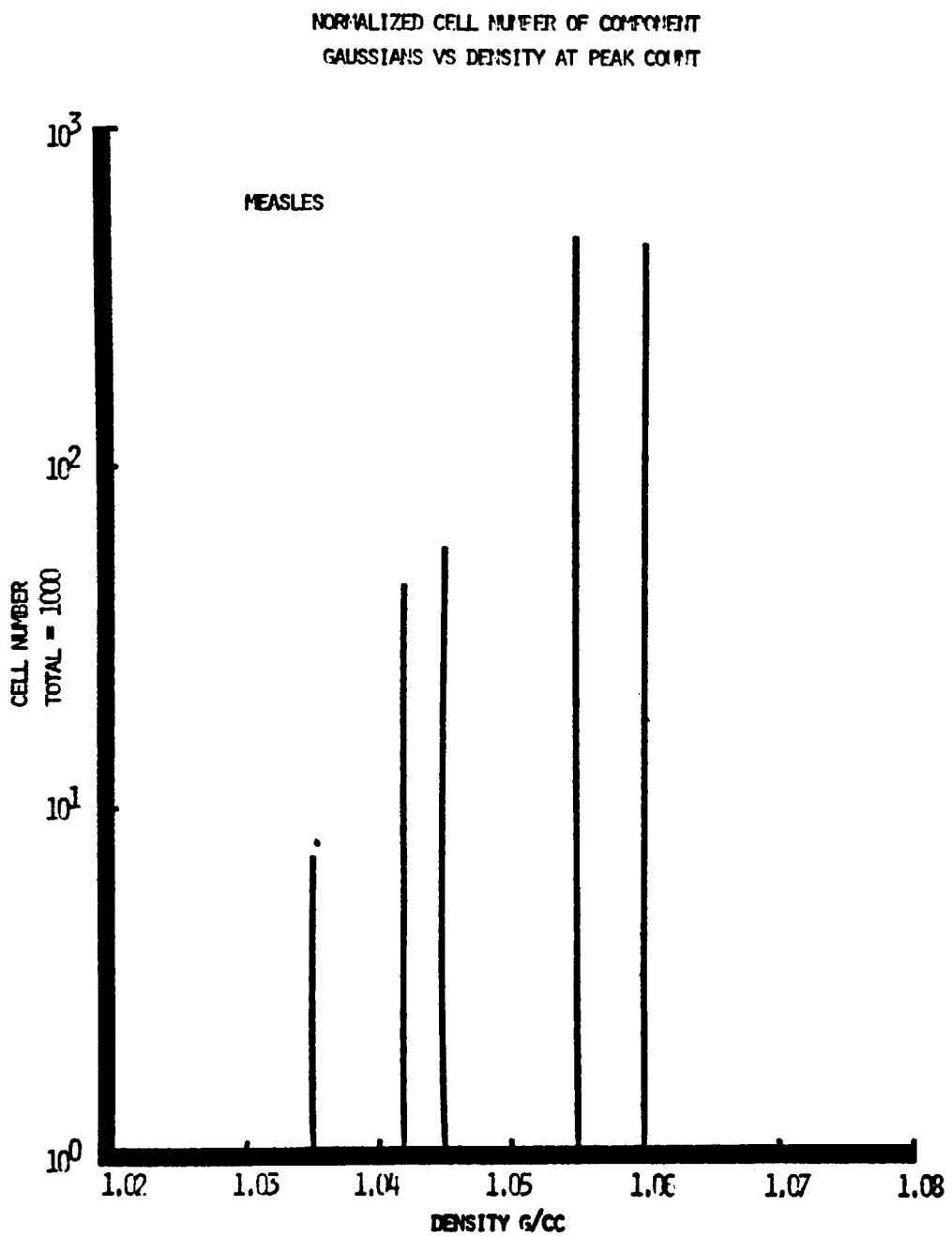
NORMALIZED CELL NUMBER OF COMPONENT
GAUSSIANS VS DENSITY AT PEAK COUNT
MEASLES
10^3
10^2
10^1
10^0
CELL NUMBER
TOTAL = 1000
1.02
1.03
1.04
1.05
1.06
1.07
1.08
DENSITY G/CC

Figure 23

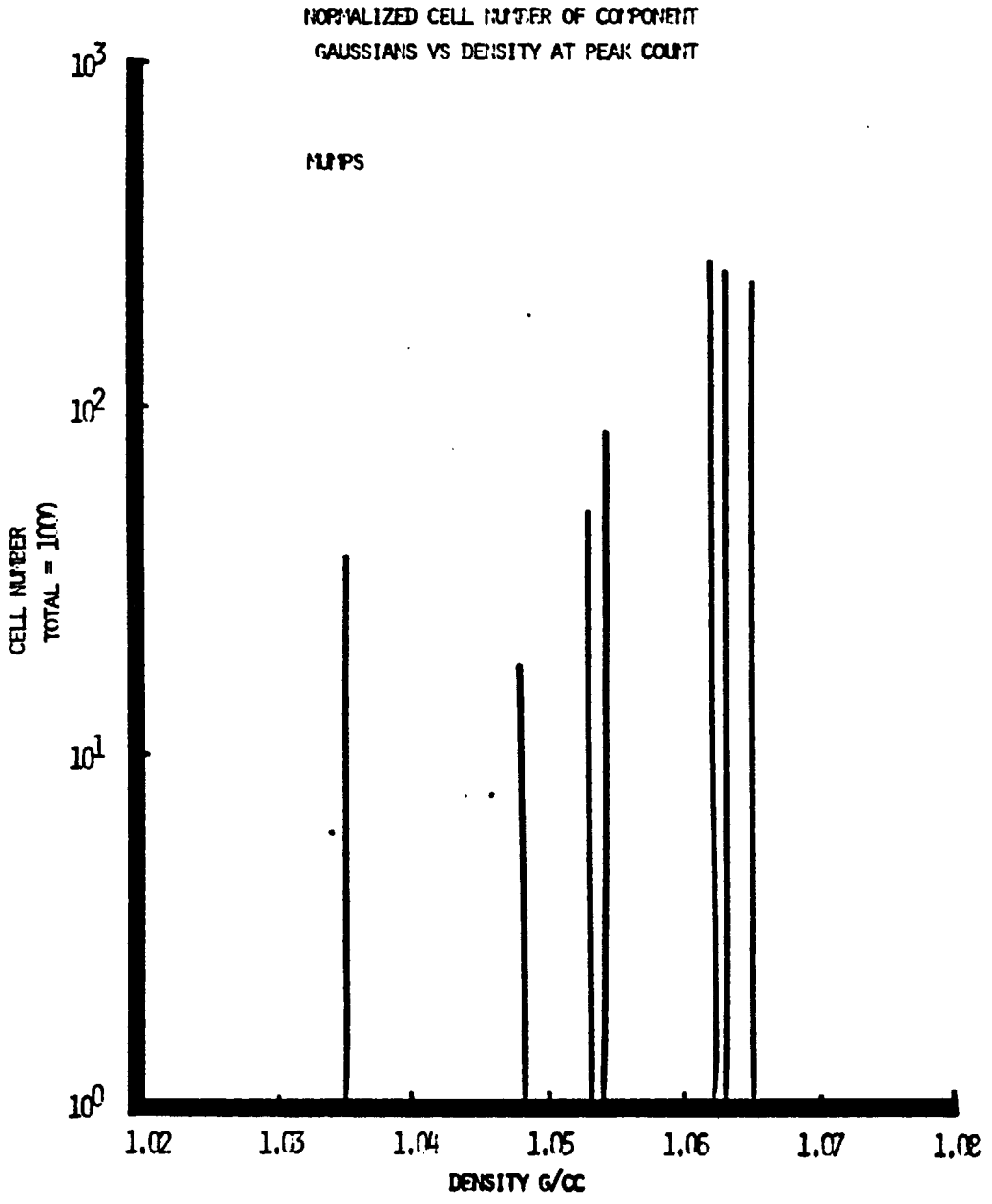
NORMALIZED CELL NUMBER OF COMPONENT
GAUSSIANS VS DENSITY AT PEAK COUNT
MLMPS
CELL NUMBER
TOTAL = 1000
10^3
10^2
10^1
10^0
1.02
1.03
1.04
1.05
1.06
1.07
1.08
DENSITY G/CC

Figure 24

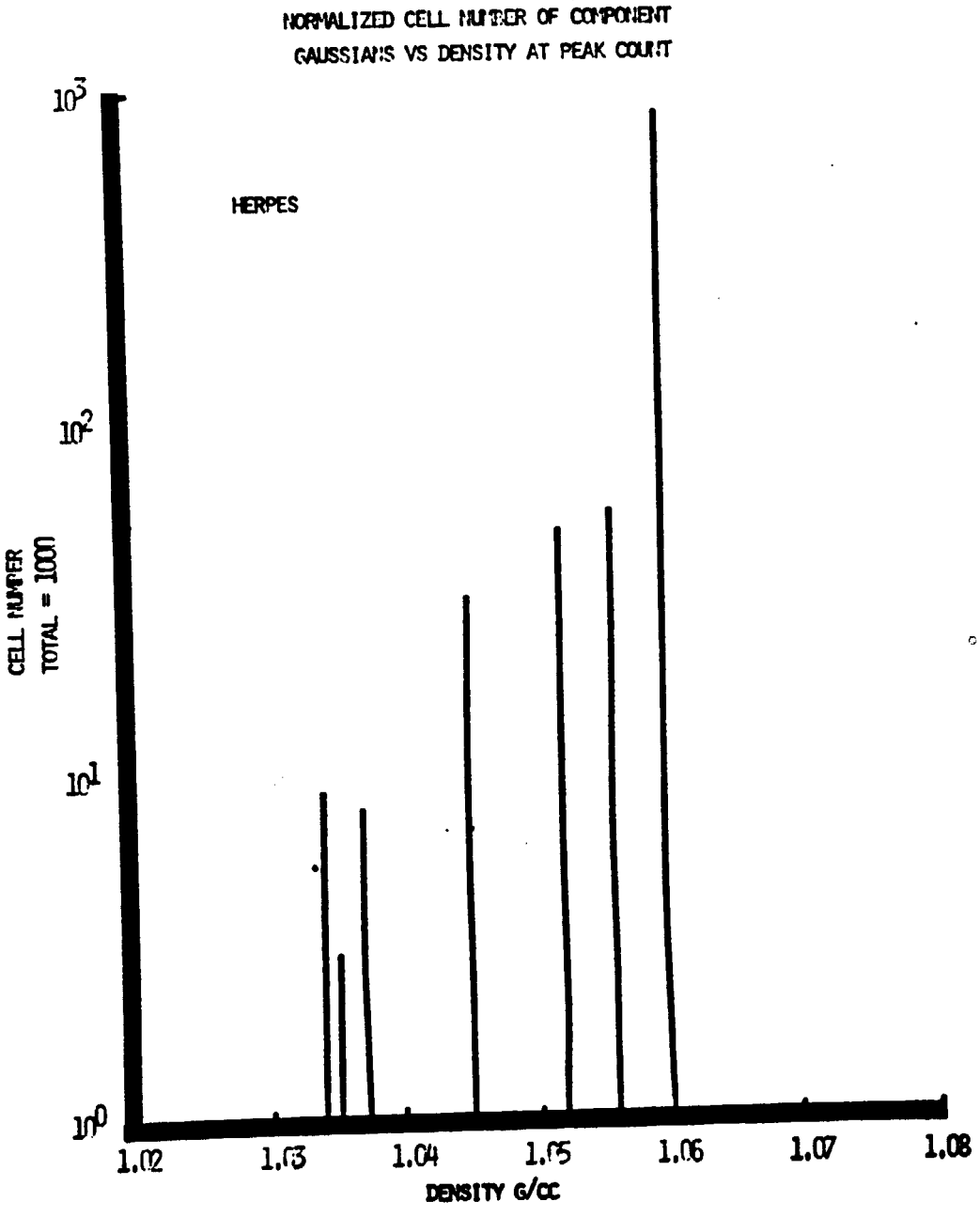
NORMALIZED CELL NUMBER OF COMPONENT
GAUSSIANS VS DENSITY AT PEAK COUNT
HERPES
CELL NUMBER
TOTAL = 1000
10^3
10^2
10^1
10^0
1.02
1.03
1.04
1.05
1.06
1.07
1.08
DENSITY G/CC

Figure 25

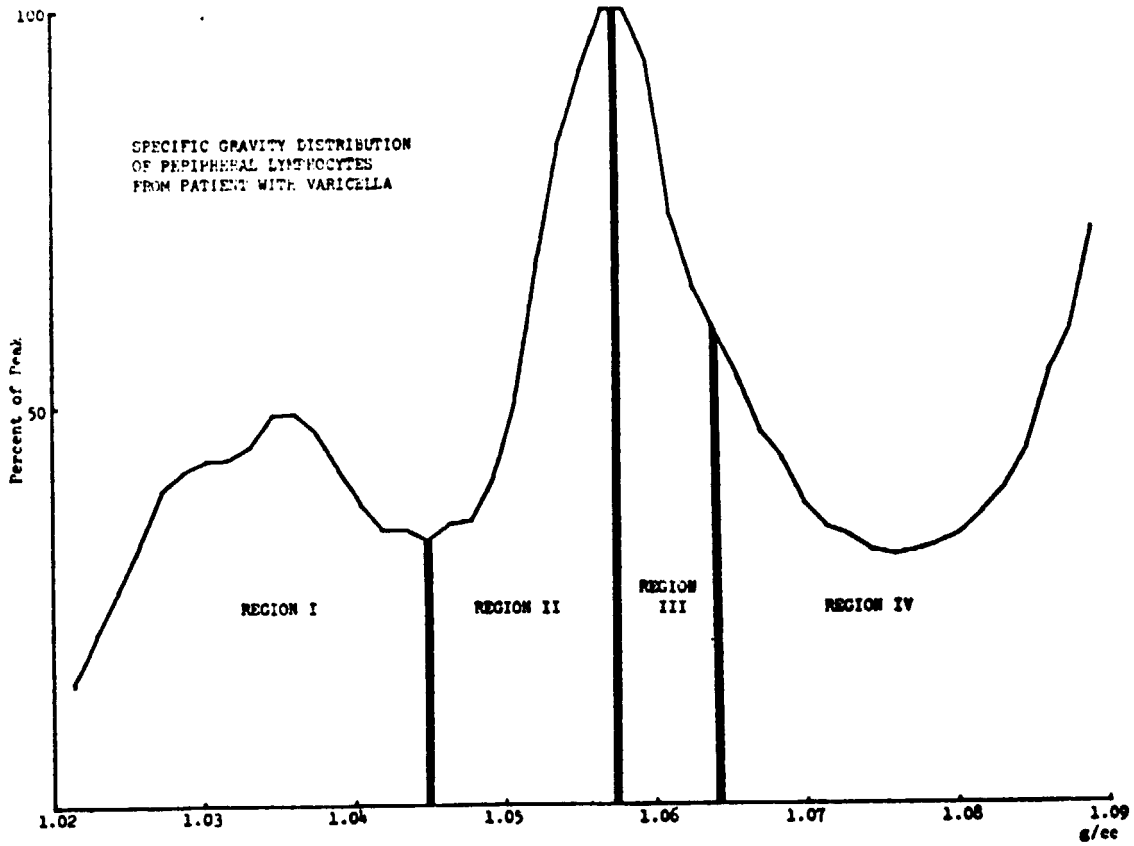
SPECIFIC GRAVITY DISTRIBUTION
OF PERIPHERAL LYMPHOCYTES
FROM PATIENT WITH VARICELLA
Percent of Peak
100
50
REGION I
REGION II
REGION III
REGION IV
1.02
1.03
1.04
1.05
1.06
1.07
1.08
1.09
g/cc

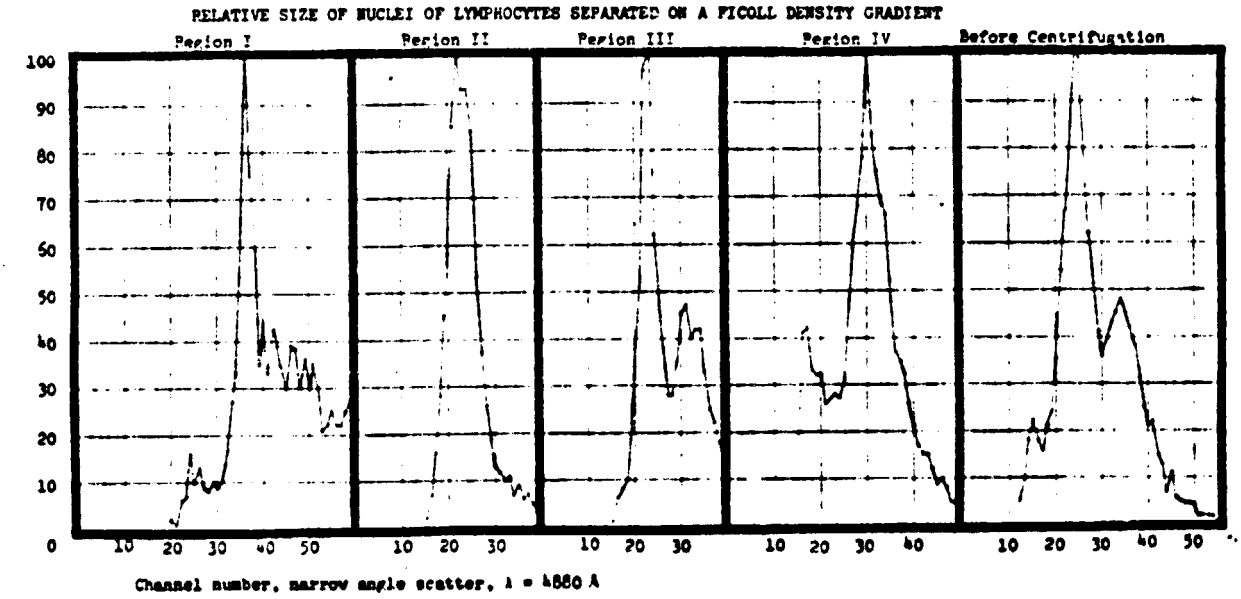
RELATIVE SIZE OF NUCLEI OF LYMPHOCYTES SEPARATED ON A FICOLL DENSITY GRADIENT
Region I
Region II
Region III
Region IV
Before Centrifugation
100
90
80
70
60
50
40
30
20
10
0
10 20 30 40 50
10 20 30
10 20 30
10 20 30 40
10 20 30 40 50
Channel number, narrow angle scatter, λ = 4880 A

Figure 26

(>channel 16) in the region of densities >1.064 g/cc.

3.3.4 Miscellaneous LSGDs

During the course of this study, LSGDs were occasionally obtained by chance from donors that had or subsequently developed disease thought to involve cell-mediated immunity.

3.3.4.1 Serendipitous Observations on Viral Disease

Figures 27 to 30 show the temporal sequence of changes in the LSGD during a probable virus infection encountered by chance in a donor who was initially presumed to be healthy. Figure 27 shows the LSGD three days before debilitating symptoms. The LSGD contains an overwhelming number of cells in the low density region 1.02-1.05 g/cc, and a peak in the region 1.05 - 1.07 g/cc that is shifted from the normal position for healthy donors to a peak density of about 1.062 g/cc. Figure 28 shows the LSGD at 9 days after first clinical symptoms and following recovery from debilitating symptoms. The LSGD is split into 2 distinct peaks at about 1.058 and 1.065 g/cc. A subpopulation at about 1.048 g/cc is also evident. Figure 29 shows the LSGD at 16 days after clinical symptoms. This LSGD is also bimodal with peaks at about the same density locations as the previous LSGD, but with the peak at 1.065 g/cc greatly reduced in size compared with the peak at about 1.058 g/cc. Finally, the LSGD at 27 days after clinical symptoms (Figure 30) has the appearance of the usual LSGD from healthy donors.

Figure 31 shows the LSGD from a donor on the day after significant debilitation as a result of the "24-hour flu". This LSGD is shown superimposed over a LSGD from the same individual when healthy. Obviously, the main peak was shifted from about 1.056 to a position of slightly higher density, about 1.059, and the subpopulation at approximately 1.047 g/cc became conspicuous.

3.3.4.2 LSGD from Chronic Skin Cancer

Figure 32 shows the LSGD from a donor with chronic skin cancer. This LSGD has an unusually prominent subpopulation at about 1.046 g/cc and the shoulder at about 1.052 g/cc suggests a prominent subpopulation. Both

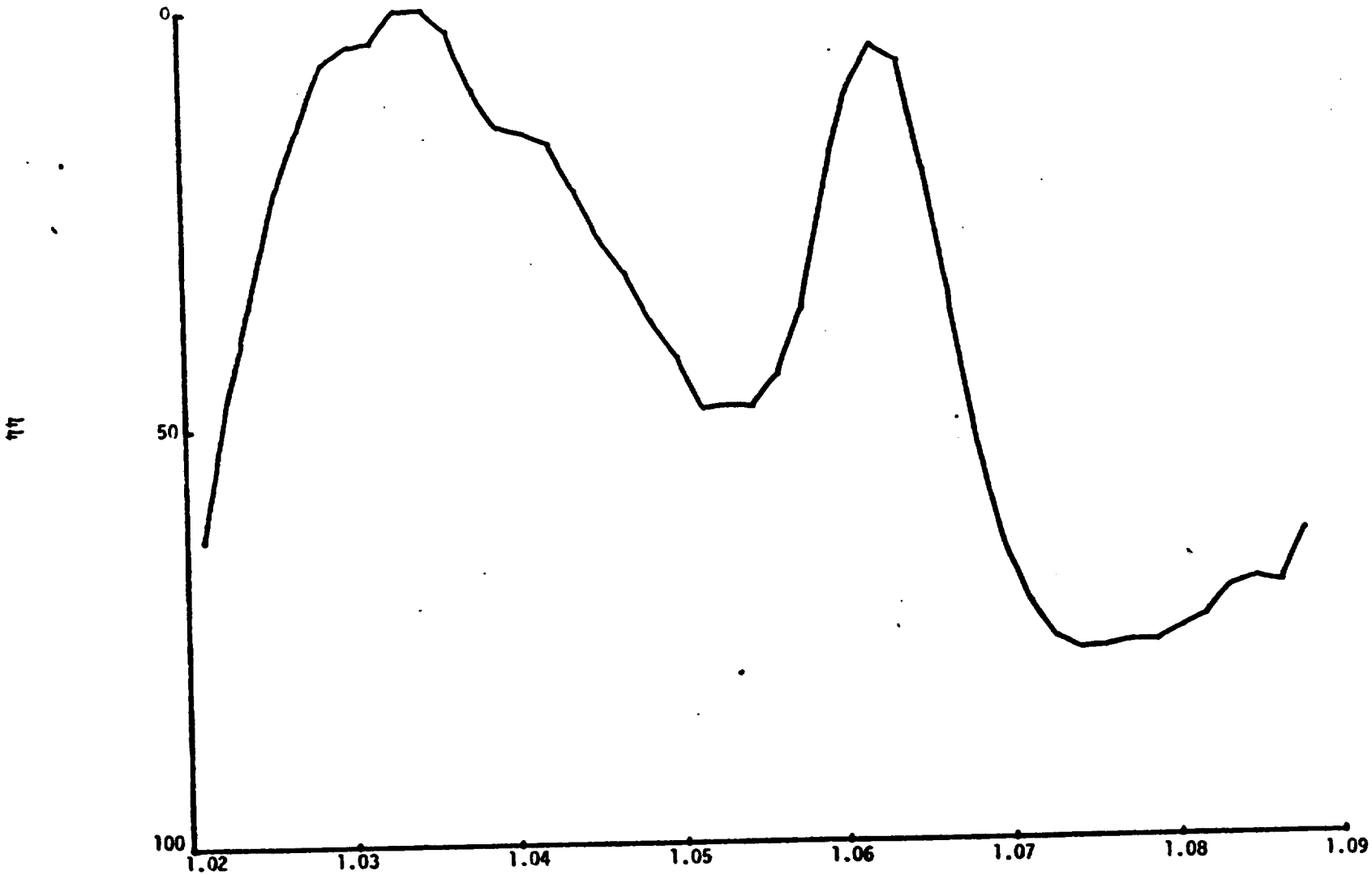

Figure 27. 3 DAYS BEFORE SYMPTOMS OF VIRAL ILLNESS

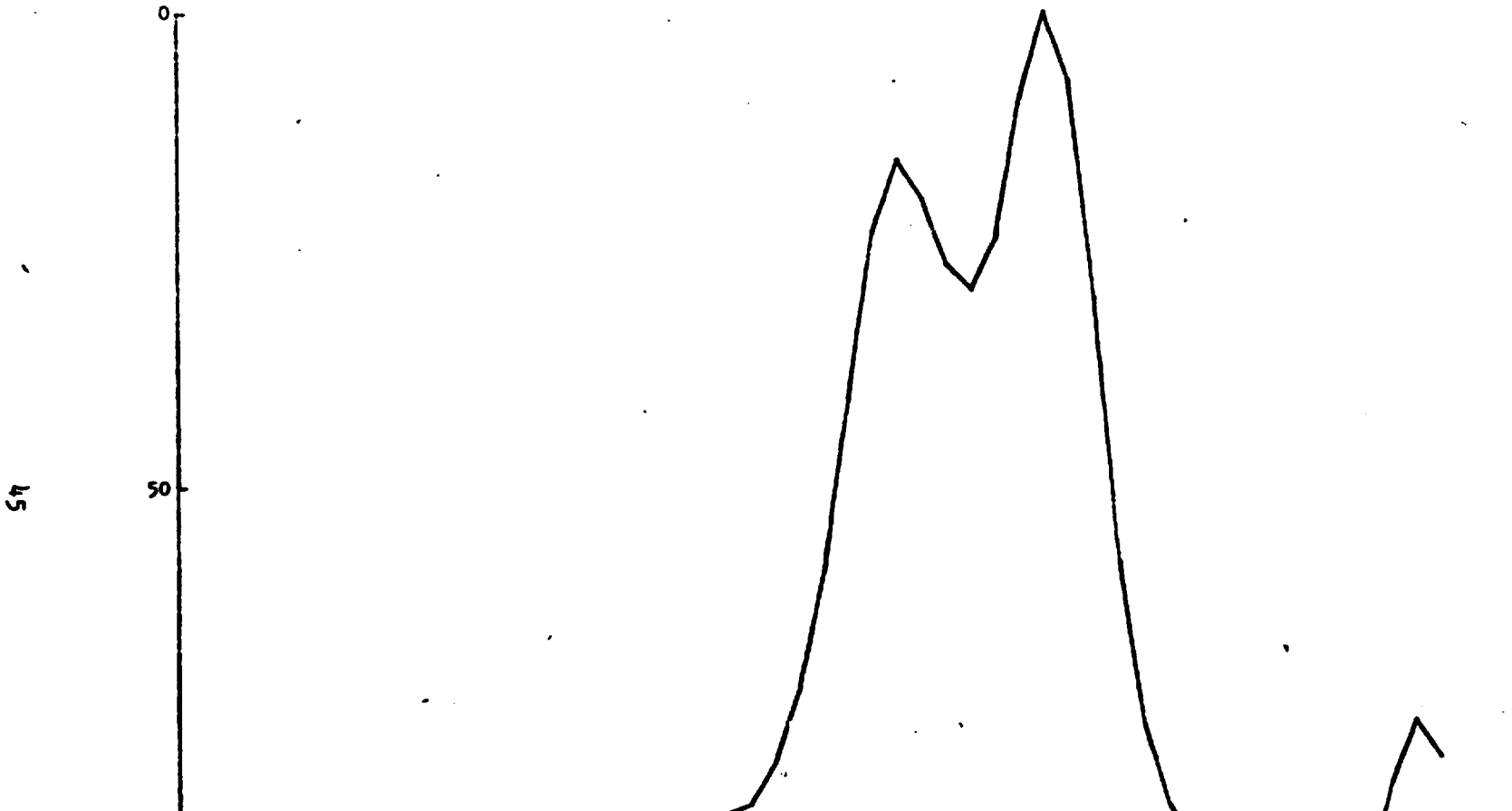

Figure 28. SAME DONOR AS IN FIGURE 27, TWELVE DAYS LATER

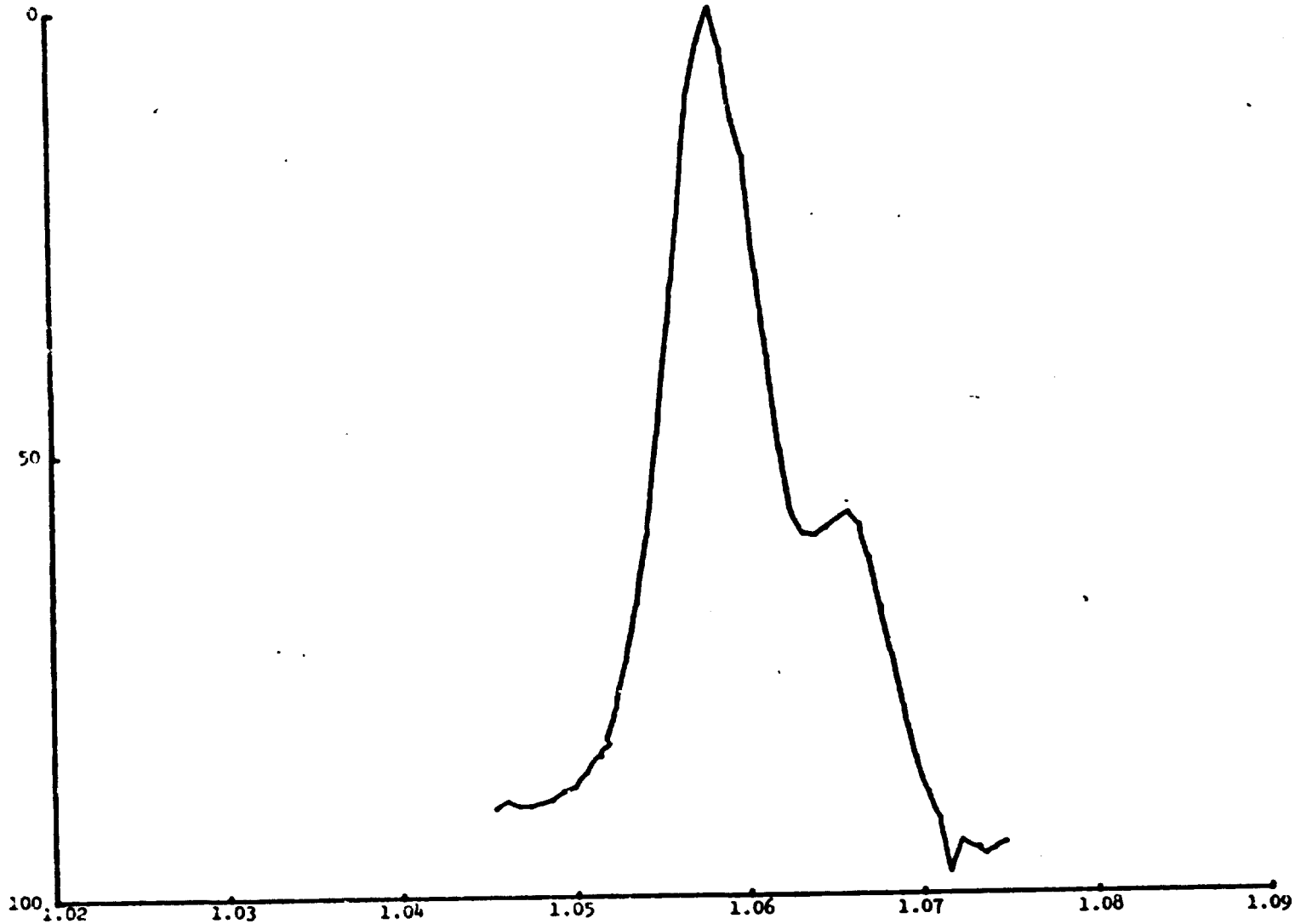

Figure 29. SAME DONOR AS IN FIGURE 27, 19 DAYS LATER

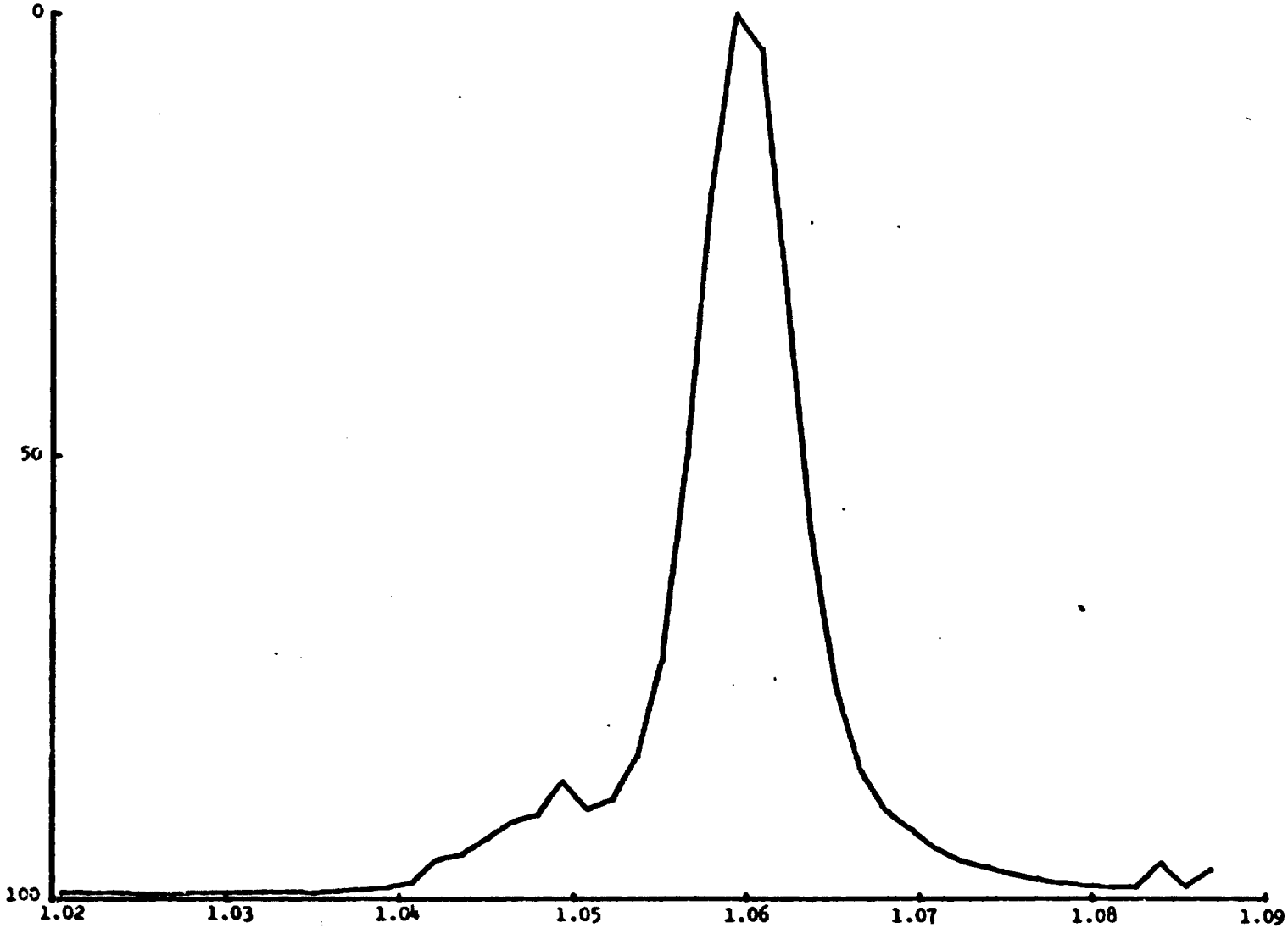

Figure 30. SAME DONOR AS IN FIGURE 27, 31 DAYS LATER

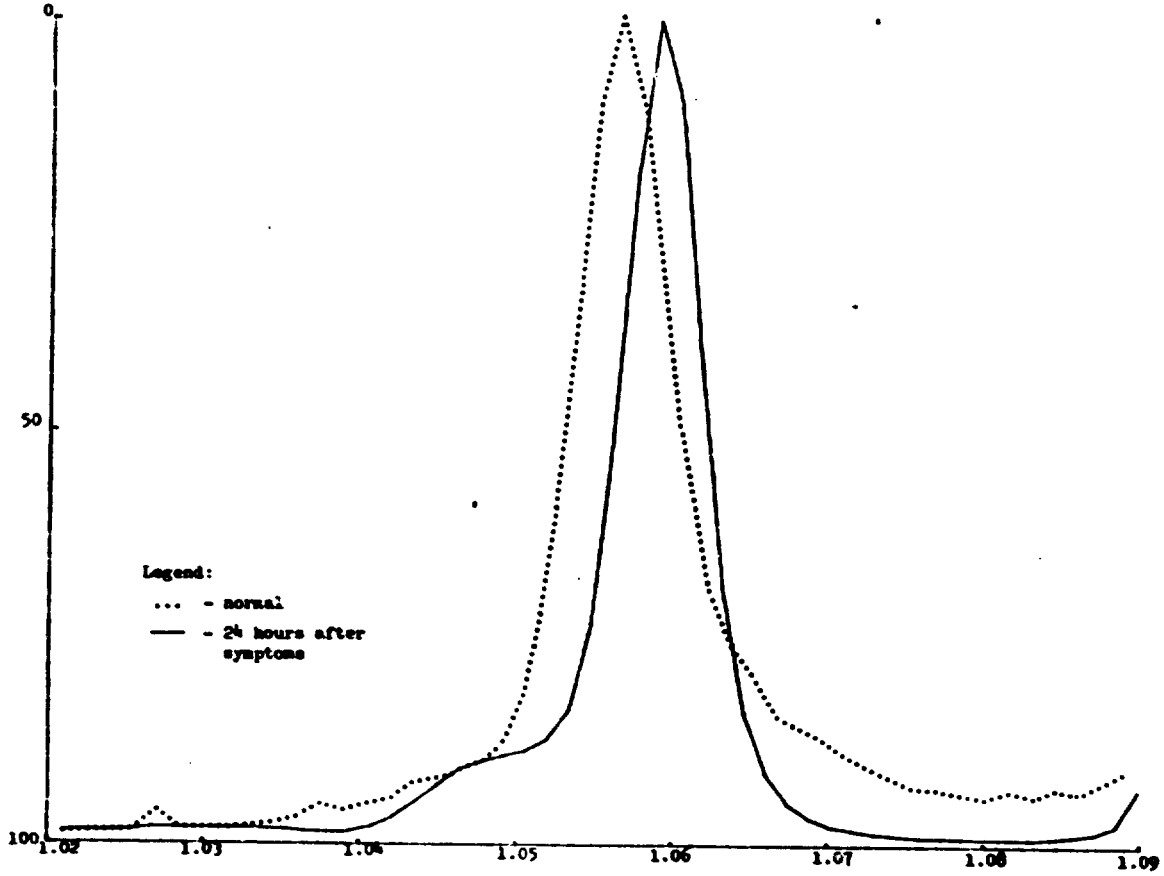

Figure 31. ONE DAY AFTER "24-HOUR FLU"

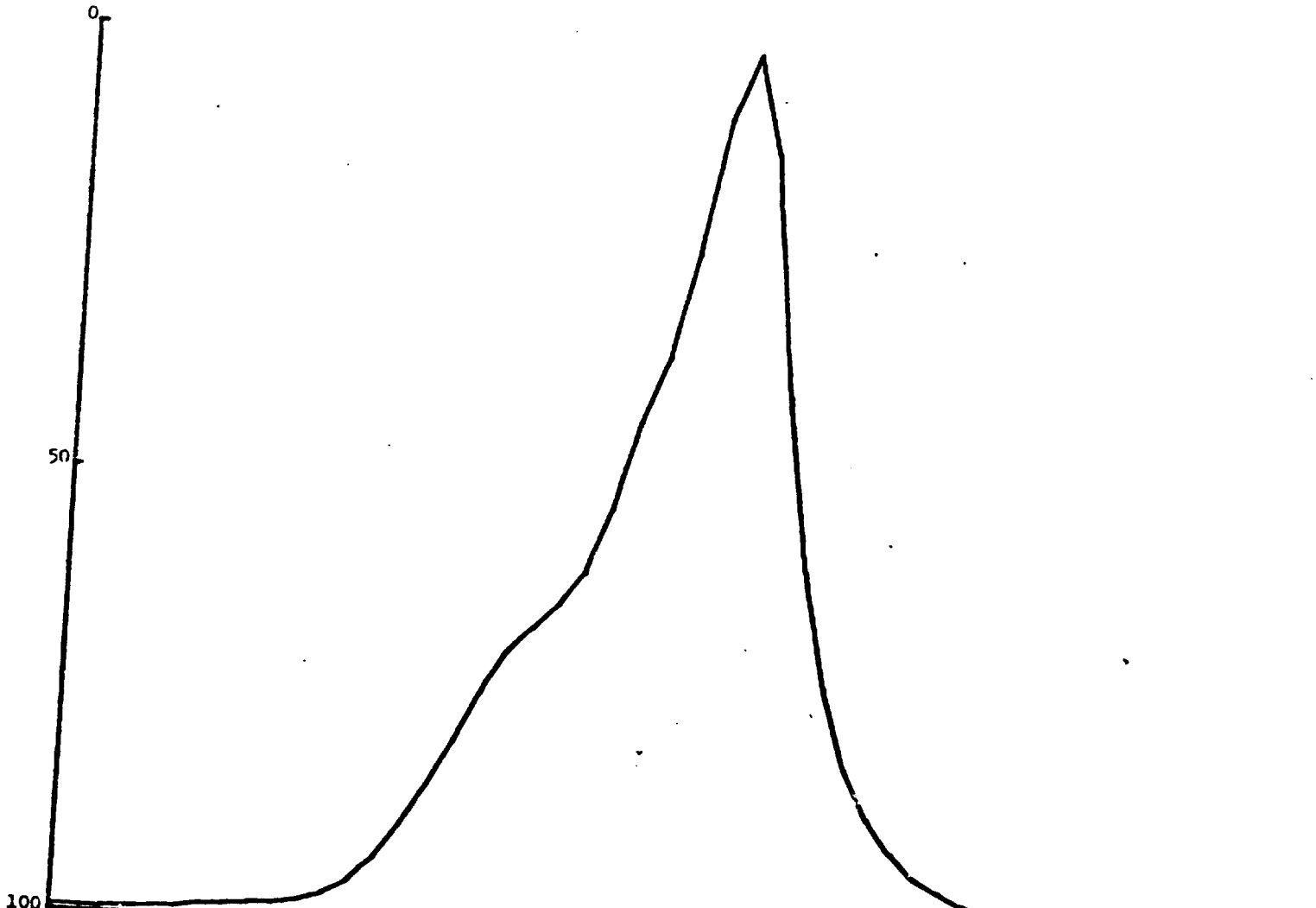

Figure 32. CHRONIC SKIN CANCER

of these subpopulations are seldom discernible in distributions from healthy donors, but are frequently prominent in viral diseases.

3.3.5 Gradient Characteristics

3.3.5.1 Relationship Between Refractive Index and Specific Gravity

A plot of refractive index (RI), versus specific gravity, for the batch of Ficoll in HBSS that was used for most of the procedures is shown in Figure 33. The linear regression, $y = mx + b$, where RI = x and sp. gr. = y, was calculated and the constants were found to be $m = 0.90044$ and $b = 0.4323$. The linear relationship is also plotted (solid line) in Figure 33. The correlation coefficient, ρ, was 0.99974. With df=4, the null hypothesis, $H_o: \rho=0$ is rejected at $P<0.001$.

3.3.5.2 Gradient Linearity and Similarity

Figures 34a, b, c & d show the RI versus fraction number of four gradients formed simultaneously using the special gradient former. Due to slight non-linearity at the beginning and end of each gradient, fractions equivalent to about 1/10 of the total fractions at the beginning and end of each gradient were discarded and the LSGD characterized only over the most linear midrange portion. Agreement with linearity over the midrange of the four fractionated gradients shown in Figure 34 is very precise as indicated by calculated correlation coefficients of 0.99992, 0.99982, 0.99972 and 0.99987. With df=20, $H_o: \rho=0$ is rejected at $P<0.001$.

Table IV shows the agreement of the RI for each fraction of the four simultaneously formed gradients. Statistical comparison results in a $\sigma = 0.0004$ g/cc between identical fractions of simultaneously formed gradients. A composite graph of all four gradients is shown in Figure 35 where the correlation coefficient was calculated to be 0.9996. With df = 86, $H_o: \rho=0$ is rejected at $P<0.001$.

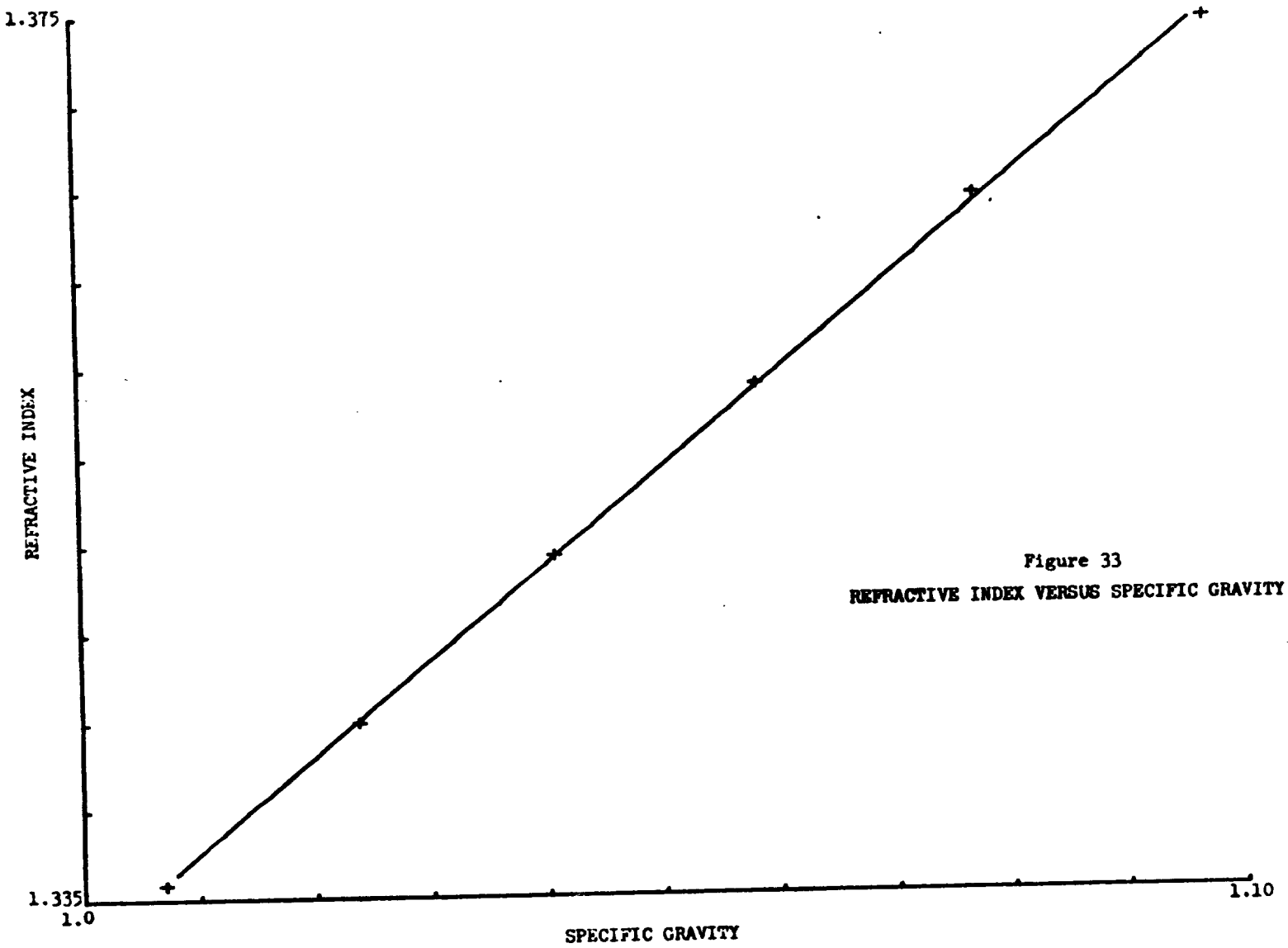

Figure 33

REFRACTIVE INDEX VERSUS SPECIFIC GRAVITY

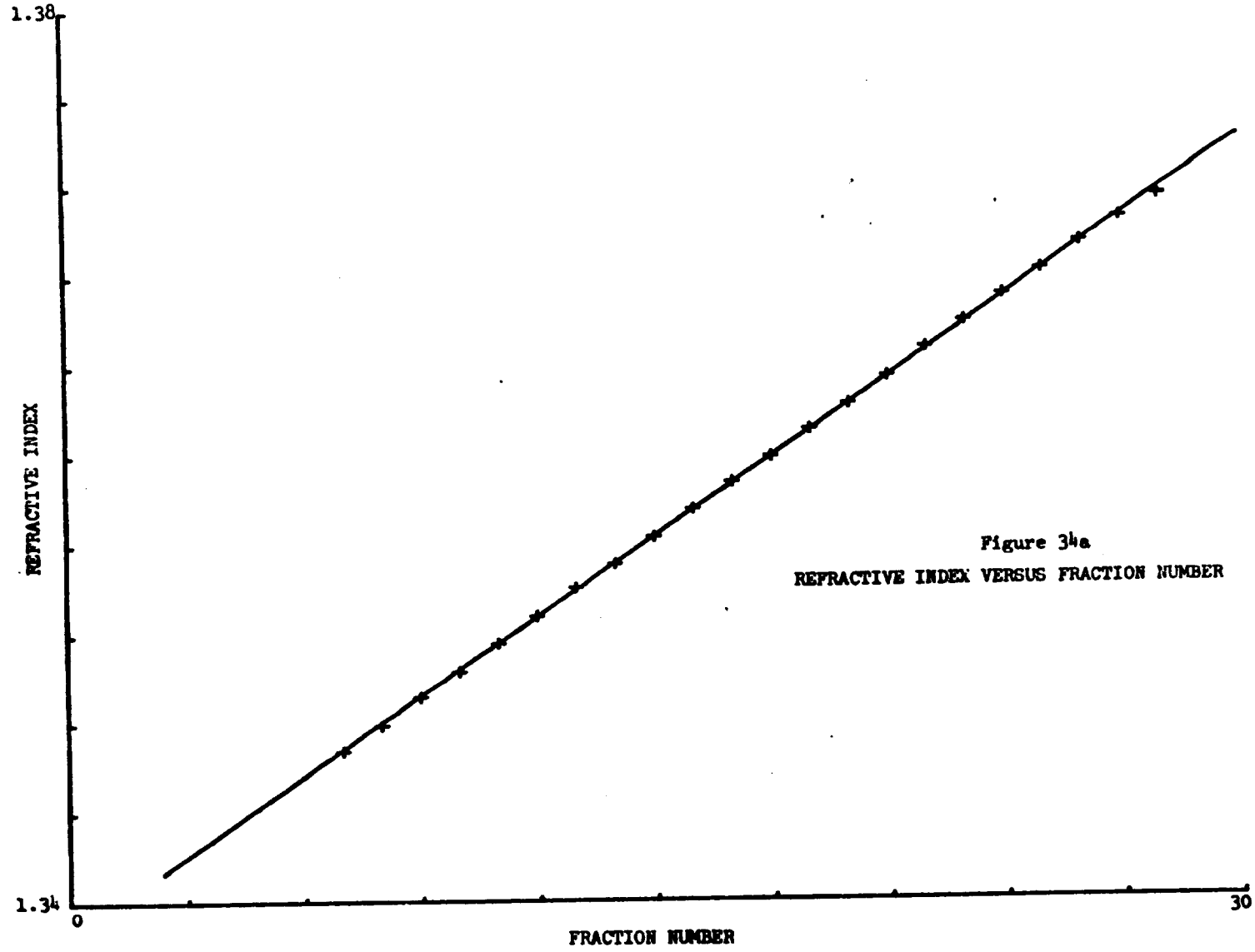

Figure 34a
REFRACTIVE INDEX VERSUS FRACTION NUMBER

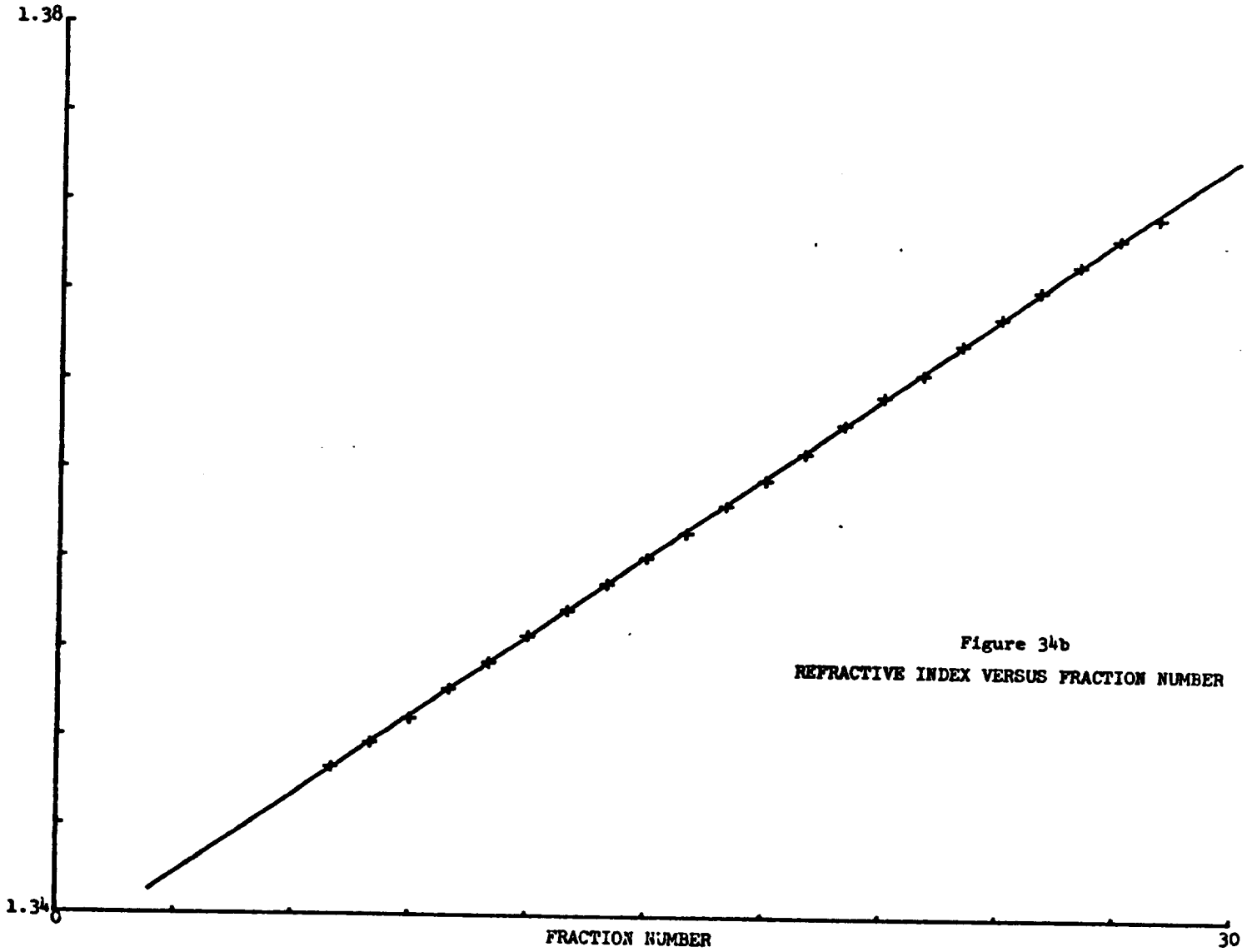

Figure 34b
REFRACTIVE INDEX VERSUS FRACTION NUMBER

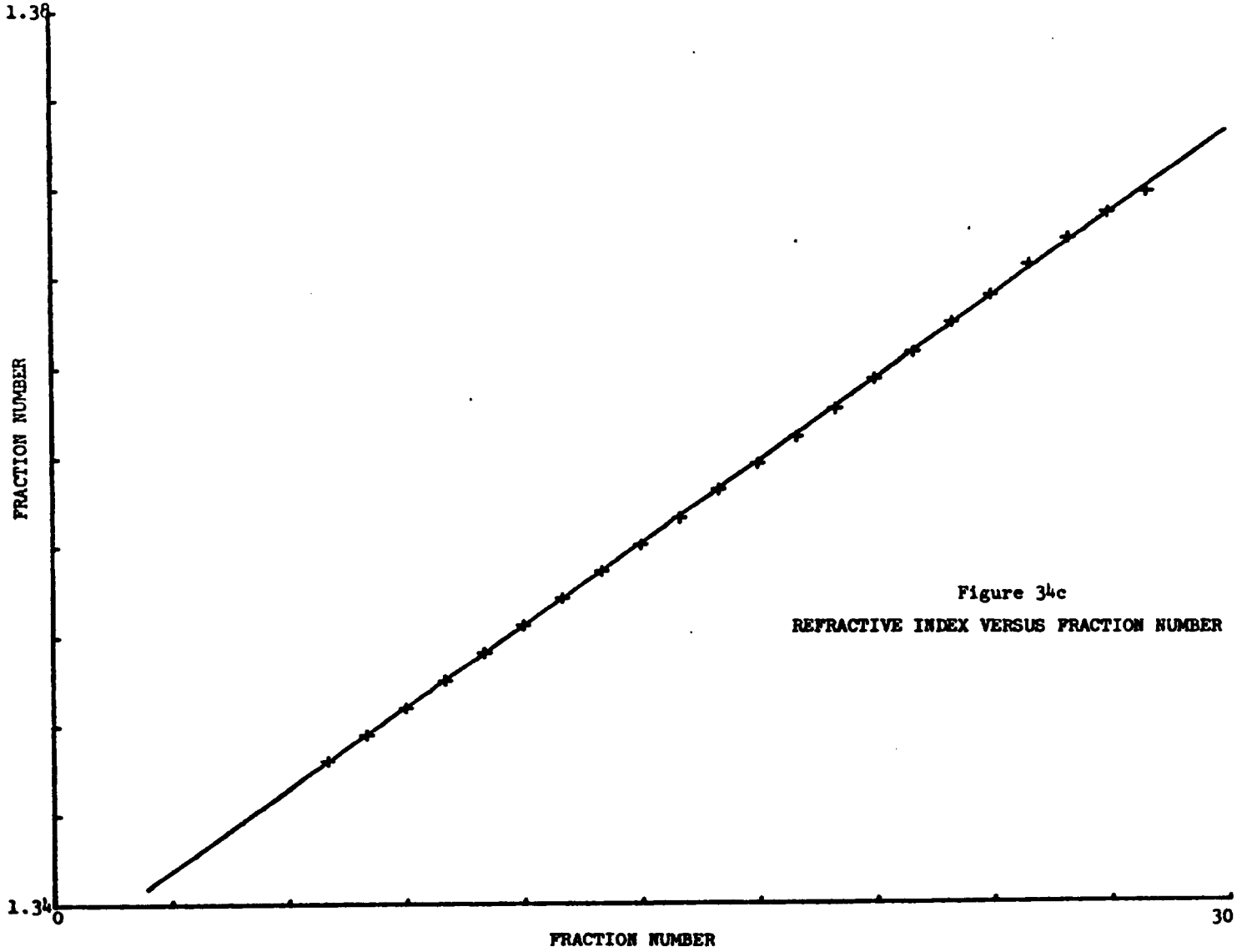

Figure 34c
REFRACTIVE INDEX VERSUS FRACTION NUMBER

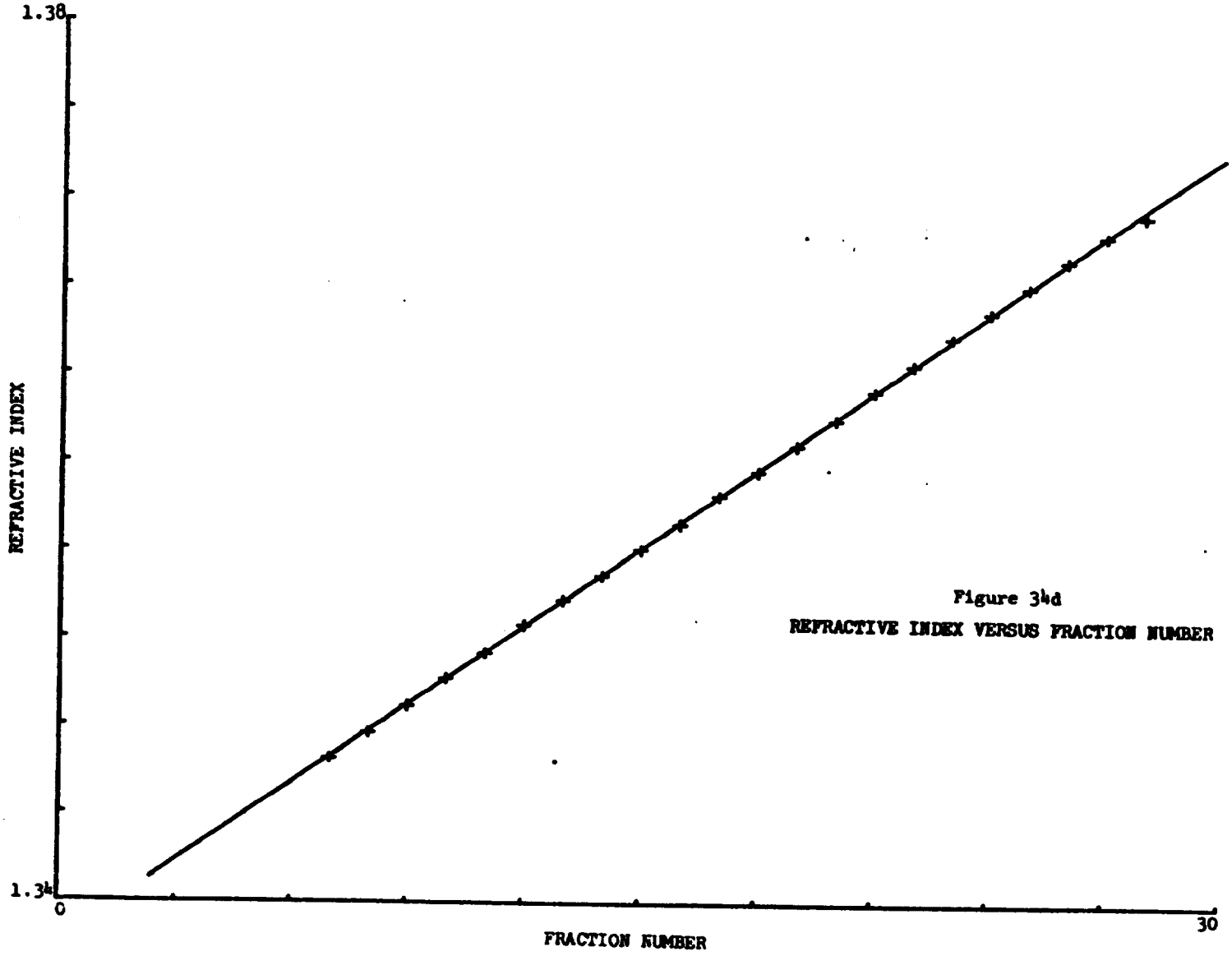

Figure 34d
REFRACTIVE INDEX VERSUS FRACTION NUMBER

Table IV

SEROLOGY OF VIRAL IMMUNIZATION

DONOR	IMMUNIZATION	VACCINE	SEROLOGY ACUTE	SEROLOGY CONVALESCENT
I-1	6-6-74	Influenza	1/8	1/16
I-2	6-6-74	Mumps	1/32	1/32
I-3	7-9-74	Rubella	<1/10	<1/10
I-4	7-9-74	Mumps	<1/10	<1/10
I-5	7-9-74	Mumps	1/16	1/32
I-6	7-9-74	Mumps	1/32	1/32
I-7	9-24-74	Mumps	1/8	1/8
I-8	9-24-74	Mumps	1/4	1/4
I-9	9-24-74	Rubella	<1/10	<1/10
I-10	9-24-74	Smallpox	+	+

+ = Serum available, not analyzed

Note: Serology conducted by Dr. David Imagawa, Harbor General Hospital, under subcontract.

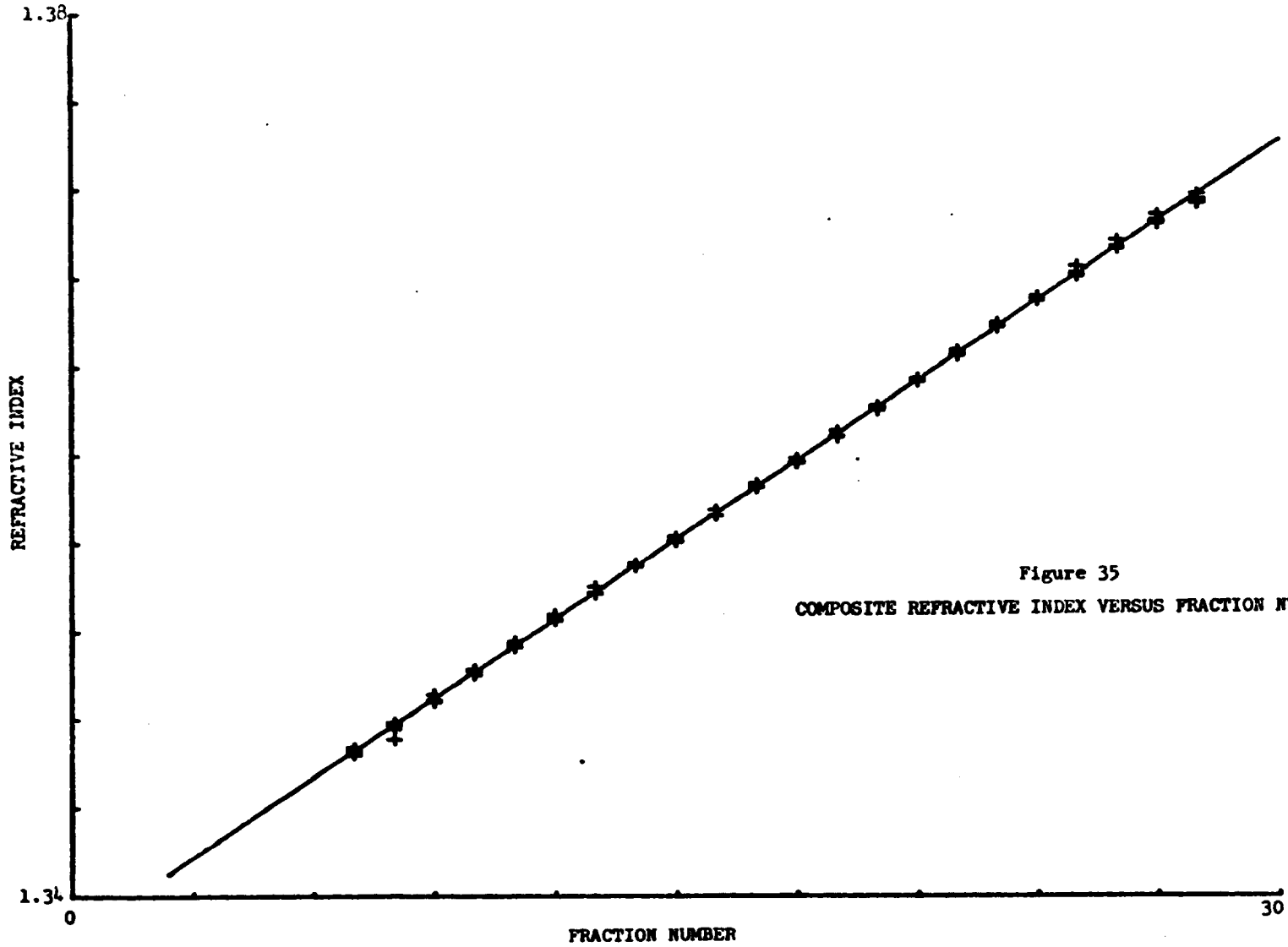

Figure 35

COMPOSITE REFRACTIVE INDEX VERSUS FRACTION NUMBER

3.3.5.3 LSGD Reproducibility of Simultaneous Gradients

Figure 36 shows the results of equilibrium centrifugation of lymphocytes from a split sample on simultaneously formed gradients. The LSGDs were reproducible to within ±0.001 g/cc of each other for identical, prominent characteristics of the distributions. The scatter diagram for correlation of these distributions is shown in Figure 37 and the correlation coefficient was calculated to be .953523. With df = 16, $H_o:\rho=0$ is rejected at $P<0.001$.

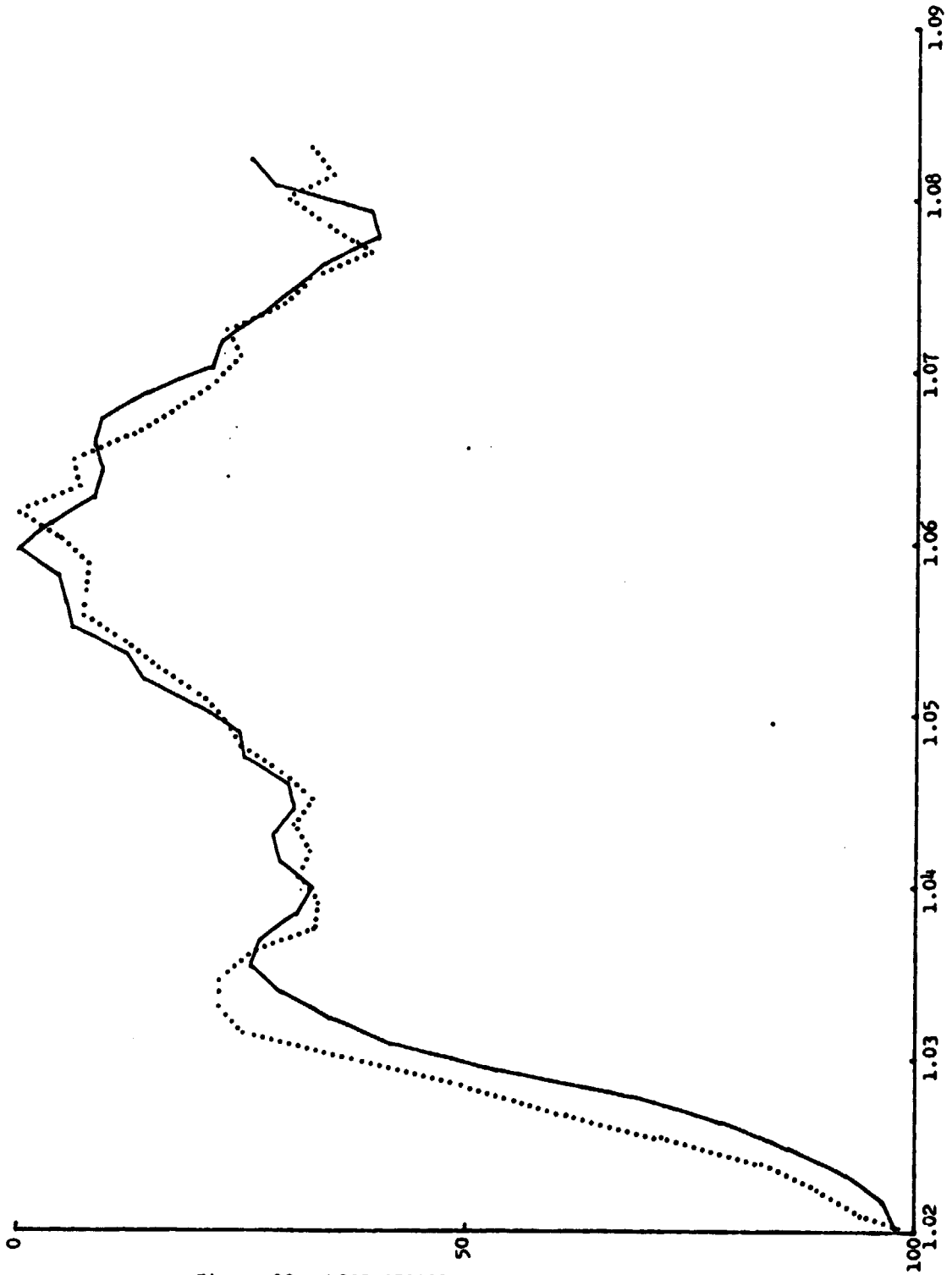

Figure 36. LSGD REPRODUCIBILITY OF SIMULTANEOUSLY FORMED GRADIENTS

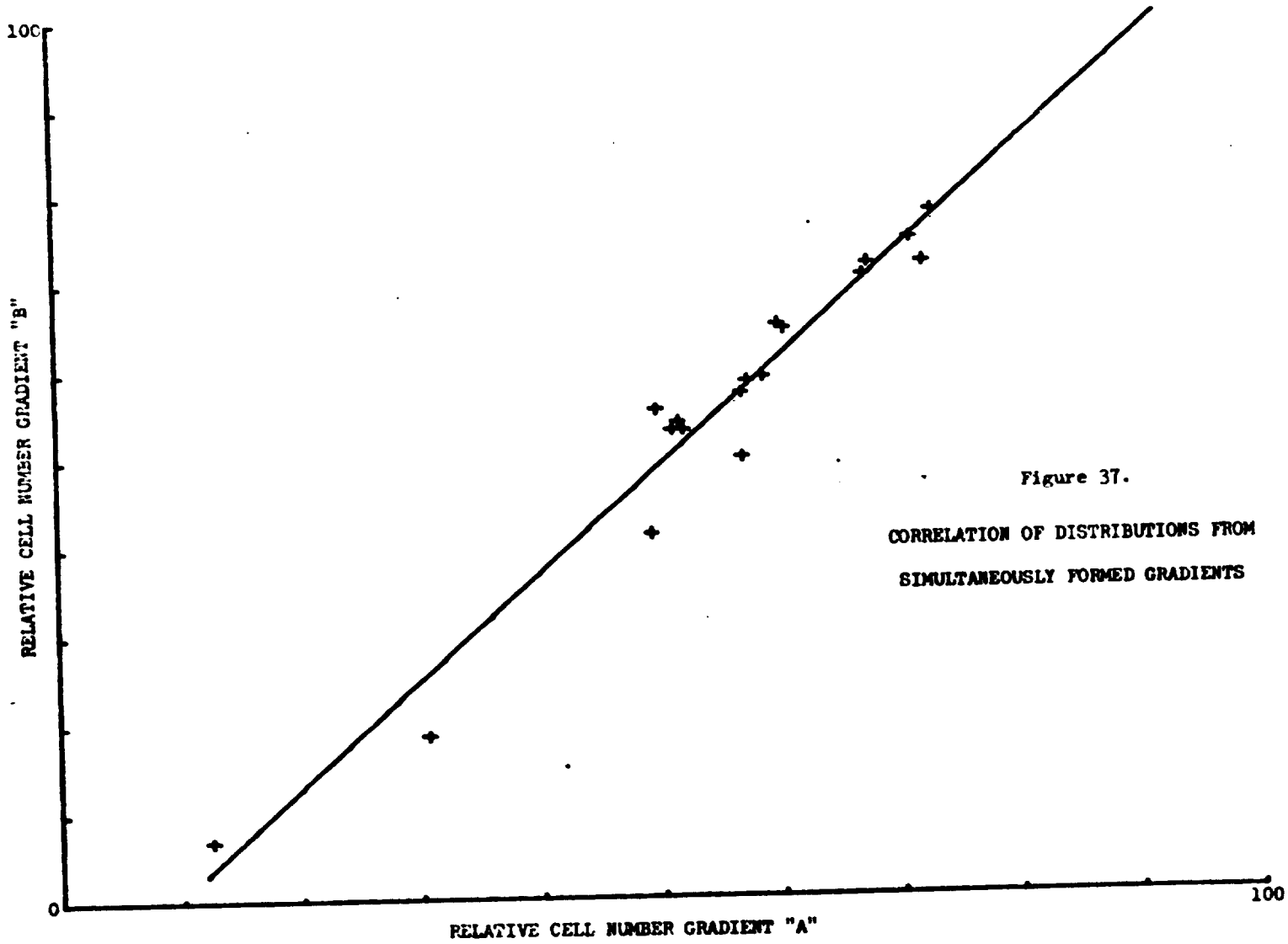

Figure 37.

CORRELATION OF DISTRIBUTIONS FROM SIMULTANEOUSLY FORMED GRADIENTS

4.0 DISCUSSION

This study clearly demonstrates significant differences between patients with viral infections and healthy donors based on comparison of the specific gravity distributions of peripheral lymphocytes. Attempts to interpret the differences in specific gravity distributions of lymphocytes from donors in health and disease must reconcile the data with known relationship between lymphocytes and virus infection and the temporal sequence of these relationships. Currently, such considerations include: a) observed changes in physical parameters of lymphocytes as a result of viral disease; b) changes in relative magnitude of the subpopulations of lymphocytes during viral infection; c) participation of lymphocytes in viral disease as host cells for acute infections of man; d) the role of peripheral lymphocytes as mediators of the immune response against viral infection. Although each of these considerations individually contributes to an understanding of the results, their commonalities present impelling evidence for a unifying interpretation and indicate several avenues for further research.

In order to attempt to fully understand the complex implications of changes in the subpopulations of peripheral lymphocytes with diseases, an exhaustive search of the literature was conducted. This effort is documented in Appendix D, Summary of Literary Review of Density Gradient Studies. Although all of the summarized reports were not directly applicable to this study, they form a foundation for an understanding of the potential and difficulties in the application of density gradient techniques.

Reports are scattered and incomplete regarding changes in physical parameters of lymphocytes as a result of viral disease. Thus, changes in morphology, size, and specific gravity have been reported. Changes in morphology were observed as early as 1898 by Turk, who reported atypical, mononuclear cells, considered to be of lymphoid origin, in the peripheral blood of patients suffering from a variety of infectious diseases[11]. In 1951, Litwins and Leibowitz summarized 30 years of observations in a report on abnormal lymphocytes in virus diseases[12]. They noted that the percentages of abnormal lymphocytes seldom exceeded 10%, except for infectious mononucleosis, and that the Type III atypical lymphocytes, the largest of Type I, II, or III

according to Downey and McKinley[13], was observed only in the very early days of illness. In 1967, Wood and Frenkel presented a comprehensive review of atypical lymphocytes in a variety of clinical circumstances[14]. They described five morphologies of atypical lymphocytes that were most commonly associated with viral illnesses and hypersensitivities. These usually constituted less than 20% of the total lymphocyte population[14]. They also reported that atypical lymphocytes were prominent during the incubation period and/or during convalescense [14,15]. They concluded that the significance and function of the atypical lymphocyte were unknown, although the scanty evidence indicated a nonspecific lymphocyte response to antigenic stimulus and a function in areas of local inflammation since they have been observed to accumulate in inflammatory areas[14,16]. In relation to this investigation, information clearly shows the association of atypical populations of lymphocytes with virus diseases and changes in the populations during the course of illness.

Changes in percentages of subpopulations of lymphocytes during virus diseases has also been reported in studies of nucleoli of peripheral blood lymphocytes. Thus, a marked increase of activated lymphocytes, blood lymphocytes that actively synthesize RNA, was found in the great majority of infectious diseases, particularly for measles, varicella, and rubella[17]. Another study demonstrated changes in the relative percentages of macronucleolar and polynucleolar lymphocytes in response to viral disease[18].

Size (lymphocyte diameter) has also been related to the appearance of atypical lymphocytes in the peripheral blood of patients with viral disease[19]. That study showed an abnormal size distribution for atypical lymphocytes from patients with acute illness. Although the distributions were not similar in shape, they demonstrated a shift to larger diameters compared to the pooled size distribution of healthy donors. The reported change agrees with our investigation where major, abnormal subpopulations had unusually large nuclei.

In our literature review, only one journal publication, 1974, has reported any change in the LSGD of a donor with virus infection[6]. In that

publication, the LSGD of a donor was obtained by happenstance prior to and during a mild respiratory tract infection. It was observed that an increase occurred in the proportion of lymphocytes in the low density region, 1.06 - 1.07 g/cc, of the distribution between 1.06 - 1.08 g/cc. The only other such observation to our knowledge was the research by Kelton in 1969 showing a large subpopulation of lymphocytes in the low density region, 1.05 - 1.075 g/cc, 3 days prior to severe influenza, as compared with the LSGD, 1.070 - 1.085 g/cc, of the same individual when healthy[6,21].

Again, our literature review revealed only one study on the effect of virus infection on the relative proportion of the two major subpopulations of human, peripheral blood lymphocytes that are designated T- and B-lymphocytes. It was found that the percentage of T-lymphocytes was depressed in most patients in the early stage of disease, while the B-lymphocyte proportion was elevated compared with convalescence and controls[21]. That observation greatly strenghtened interpretation of the LSGD data.

Careful analysis of the literature that relates to the relative location of T- and B-lymphocytes within the LSGD shows apparently disparate results. However, the methods and materials, as well as interpretation of data, varied greatly in the reports. Thus, differences can be attributed by differences in material used to form the gradients, pH, osmolarity, health status of the donor, centrifugation parameters, etc. Nevertheless, the changes in LSGD during viral illness correlate with the indicated location of T- and B-lymphocytes within the LSGD. In our data, the B-cells were believed to be located in the high density region of the LSGD because of the size of the nuclei in that region and previous experimentation showing concentration of PHA-responding cells, a major T-cell subpopulation, in the low density region of the major component of the LSGD[5]. Other investigators have also provided evidence for enrichment of PHA-reacting lymphocytes within the ascending, low density region of the LSGD of human peripheral blood lymphocytes[22,23]. However, the reverse locations for T- and B-cells within the LSGD, B-cells in the low density region and T-cells in the high

density region, have also been reported under different conditions of centrifugation; but the LSGD of the major component shifts toward lower densities during virus disease to reflect the expected increase in the proportion of B-cells[6,24] . Thus, the shift in specific gravity of the major component of the LSGD is believed to change in accordance with the relative increase in the proportion of B-cells regardless of conditions of centrifugation.

Another possible influence on the pattern of the LSGD is posed by the observed participation of lymphocytes in the disease process. Thus, studies of the atypical lymphocytes that are associated with many viral diseases have shown that their metabolism and initial depression of RNA synthesis in response to PHA suggests that they may contain a latent virus[25]. Further a herpeslike virus has been associated with diseases such as infectious mononucleosis that have a large number of atypical lymphocytes[25]. Also, rubella virus, measles virus, and mumps virus have been recovered from washed leukocytes of the buffy coat of the infected individuals[25,26,27,28]. All these diseases demonstrate high percentages of atypical lymphocytes[14]. Further, Papp in 1937 was able to transmit measles virus infections to healthy human volunteers with washed leukocytes from the buffy coats of infected individuals[25,29]. Additional evidence for lymphocytes acting as host cells for acute infections in man is the known replication of different viruses in cultures of activated, human lymphocytes. Thus, herpes simplex virus, vesicular stomatitis virus, and yellow fever virus have been observed to replicate in PHA-stimulated lymphocytes and, occasionally, in unstimulated lymphocytes[30]

Lymphocytes engaged in delayed hypersensitivity response <u>in vivo</u> have also been shown to support replication of viruses[31]. It should be noted that patients with measles, varicella, and rubella demonstrate numbers of activated lymphocytes that are several times higher than in healthy subjects of correspond' g age[17].

A few observations on viral infected lymphocytes suggest that these cells, if present, would be found in the very low density region of the LSGD.

First, the activated lymphocytes necessary for viral replication are characteristically large in diameter and are associated with very early infection, as are the Type III atypical lymphocytes[14,17]. The large, atypical lymphocytes or "virocytes" found in preclinical infection of severe influenza were located in the low density region of the LSGD[5]. During the course of most acute viral infections, some infected cells undergo morphological alterations resembling PHA-transformed cells and have increased size and cytoplasmic/nuclear volume ratio[25]. PHA-transformed cells have been observed to be present in the very low density region of the LSGD corresponding closely to the population observed in this study to be in the region of about 1.035 g/cc[20].

Probably the most significant changes in the LSGD due to acute viral disease occur as a result of the role of peripheral lymphocytes as mediators of the immune response against virus infection. Thus, peripheral lymphocytes are known to produce interferon, participate in cytotoxicity, elaborate antibody, and to have other immunologic functions such as memory, helper activity and viral inactivation. Such functions could reside in individual subpopulations which could fluctuate in relative proportion in response to variations in antigenic challenge.

Interferon is believed to be an important part of the host immune response to virus infection and is elaborated within hours of exposure[25]. Only one publication related interferon-producing lymphocytes to LSGD. Capacity for interferon elaboration was found in the high density, descending region of the major component of the LSGD and was separate from the capacity to synthesize DNA in response to stimulation by mitogens[32]. The data also suggested that capacity for interferon elaboration is not inherent in the T-lymphocyte subpopulation[22].

Cell mediated immunity is conducted by the peripheral lymphocytes and is believed to be the primary immune defense against virus infected cells[33]. The most significant study of the relationship of cytotoxic subpopulations of lymphocytes to the LSGD was conducted by Shortman, et al.[34] The

study indicated that cytotoxic lymphocytes first appear in the low density region[34]. Similar results were observed in studies of lymphocytes separated by velocity sedimentation. The lymphoblast was characterized as the important cytotoxic cell in the early immune response (day 3), while both lymphoblasts and small lymphocytes were cytotoxic by days 5 and 8, mostly small lymphocytes were cytotoxic by day 14, and by day 22 all cytotoxicity resided in small lymphocytes[35]. Several studies have established that cytotoxic lymphocytes are T-cells[35,36]. Evidence from the same laboratories established that cytotoxic lymphocytes are mainly in the low density region in the early phase of the immune response[37]. Thus, the low density cells observed in this study (1.035 g/cc) in the early viral disease may be cytotoxic lymphoclasts responding to the virus infection. LSGD subpopulations corresponding to the cytotoxic small lymphocytes after day 5 may be present in the density region about 1.045 to, perhaps, 1.055 g/cc based upon increased percentages of lymphocytes within these regions during manifest viral illness and a similar subpopulation in chronic skin cancer. However, this supposal is speculative and additional investigation is necessary.

Of the two major subpopulations, T-cells and B-cells, the B-cells constitute about 30% of the peripheral lymphocytes and are characterized by their capacity for antibody elaboration. That the B-cells may disseminate an immune response in a manner similar to the dissemination of cytotoxic effector cells by the T-cell compartment is implied by the literature. Thus, lymphocytes from the peripheral blood have been shown to synthesize specific antibody in an immune response[38]. Further, the kinetics of the response indicated to the investigators that antibody forming cells in the blood are probably a meaningful facet of the host's response to antigen[38]. From a teleological standpoint, plasma cells constitute part of the inflammatory response in local inflammation associated with specific cellular immunity which would seem to require purposeful dissemination of effector B-cells[39]. It has been established that plasma cells develop by differentiation from small lymphocytes of the peripheral circulation[40]. Antibody elaborating lymphocytes have been identified in the low density region of the LSGD[41]. Another study of the

density profile of antibody forming cells showed that these cells were located in the ascending, low density side of the major component of the LSGD[42]. This position would correspond to the approximate density region of 1.055 g/cc for the conditions of our investigation.

Other functional characteristics of lymphocytes have been studied that might reside in identifiable subpopulations within the LSGD. Lymphocytes that elaborate macrophage migration inhibitory factor have been described as large to intermediate sized T-cells that are associated with the lowest density region of the LSGD[43]. Also, a high density T-cell subpopulation has been identified that inhibits mitogenic response to PHA and Con A in purified T-cells[44]. One study has shown that a nonspecific cytotoxicity can be induced in lymphocytes by mitogens that reside in a subpopulation separate from the cells that respond by mitogenesis, but not separate from B-cells[45]. Another study has shown that the function of cell mediated lympholysis is separate from functions characterized by the mixed lymphocyte response and the T-cell mitogen response[46]. Other studies indicate that cooperation between different subpopulations of lymphocytes may be necessary for a complete immune response, thereby implying the possibility of yet other subpopulations[47,48]. Still other studies show that direct inactivation by lymphocytes may be one form of host defense in infection by some viruses[30,49]. Lymphocytes responsible for inactivation of myxovirus were characterized as large and medium-sized cells[49].

The relative proportion of various subpopulations and the shape of the LSGD might also be affected by drugs and by serum factors that may be immunoregulatory. Thus, steroids have been found to preferentially deplete the recirculating portion of the intravascular lymphocyte pool[50]. Further, hydrocortisone decreased the transforming activity of lymphocytes in response to mitogens, particularly the transforming activity following stimulation by pokeweed mitogen[51]. Non-steroidal anti-inflammatory drugs were found to induce swelling in various types of lymphocytes, thereby, perhaps, affecting the permeability of the cell membrane to various ions[52]. The chemotherapeutic drug Cyclophosphamide has been observed to affect subpopulations of peripheral

blood lymphocytes[53]. The proportion of lymphocytes stimulable to synthesis of RNA was reversibly decreased, while the nonstimulable proportion was increased[53]. An example of serum factors that might regulate proportions of lymphocyte subpopulations is the lymphocytotoxin that has been identified in association with viral disease, vaccination, and a few possibly autoimmune disorders[54,55]. Such lymphocytotoxic factors may preferentially deplete T-cells[56].

From the results of the experiment and the foregoing discussion of the literature, a tentative model can be proposed which attempts to relate the shape of the LSGD to the identity of subpopulations of peripheral lymphocytes. The tentative model is illustrated in Figure 38. Using this model, pre-clinical viral disease would be indicated by a large proportion of cells in the low density region corresponding to virus infected lymphocytes and/or large, cytotoxic cells. This population would be expected to be very transient and to disappear with the onset of manifest clinical symptoms. During manifest symptoms, the major component of the LSGD which is thought to consist of T- and B-cells would be expected to shift slightly to higher density to reflect the decreased proportion of T-cells compared to B-cells. Further, we would expect the appearance of cytotoxic lymphocytes in the region of about 1.045 g/cc; and, later, the appearance of antibody elaborating cells in the region of about 1.052 g/cc. During recovery, the LSGD would be expected to gradually return to normal with distinct subpopulations of T- and B-cells when their proportion is approximately equal. It must be recognized that this model is drawn from few observations, subject to change, and, therefore, only tentative. However, the model serves as a convenient point of departure for interpretation of ongoing research, and, also, as a stimulus for establishing objectives in further research.

Further research opportunities are numerous. As indicated in this investigation, inclusion of size of the cell nucleus would greatly enhance the definition of subpopulations separated by density. Zucker and Cassen have noted that combined cell volume analysis and density gradient separation were necessary to observe the populations of small lymphocytes in their studies[57]. Size

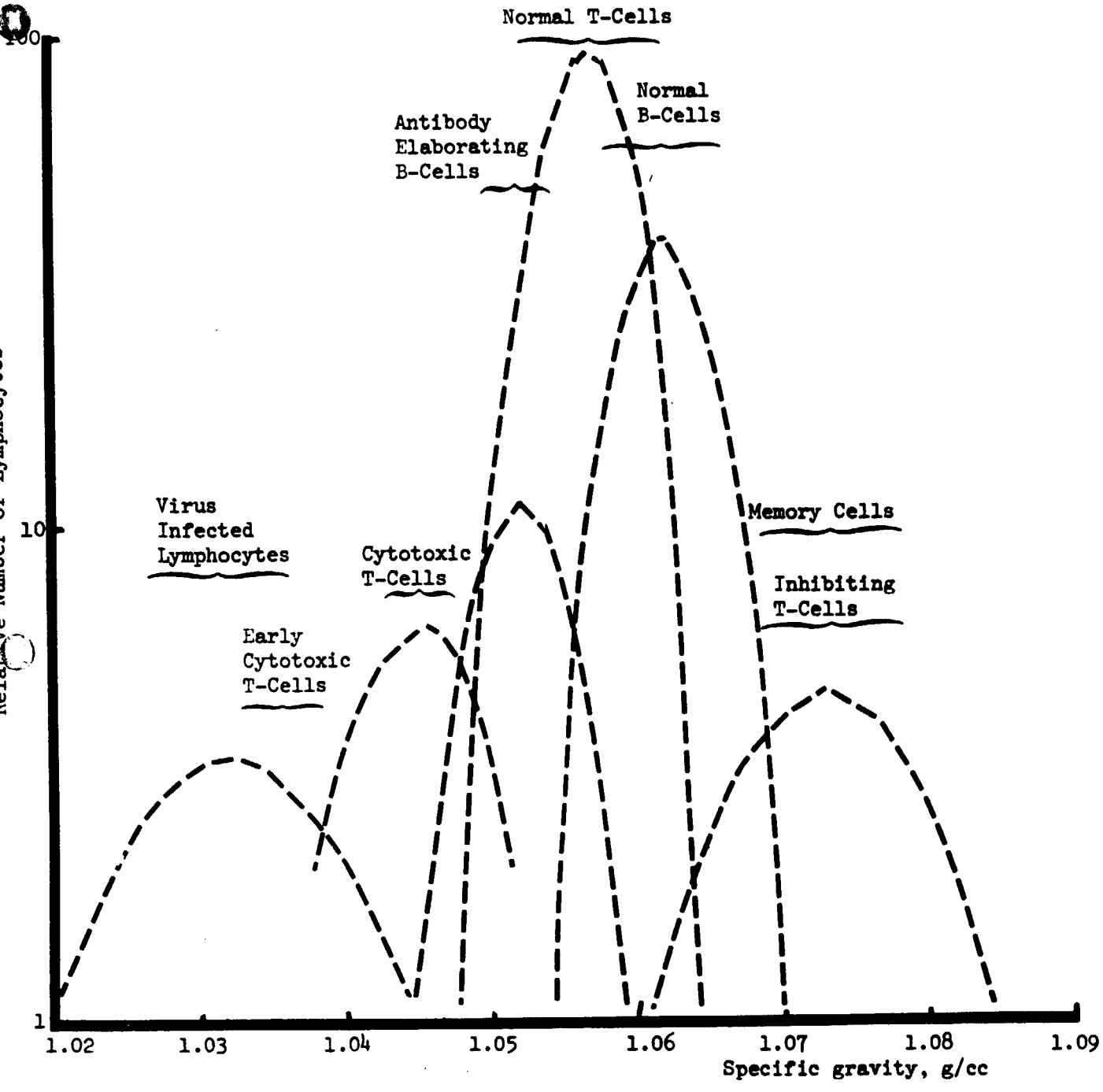

Figure 38. TENTATIVE MODEL FOR IDENTITY OF SUBPOPULATIONS OF PERIPHERAL BLOOD LYMPHOCYTES IN THE NORMAL LSGD

distributions of the nucleus would obviate the adverse effect of the variable ratio of cytoplasm to nuclear volume and could enhance the identification of subpopulations. The studies of the changes in the nucleoli of peripheral lymphocytes during disease indicate that the subpopulations might be further characterized by nucleolar morphology; and, additionally, that RNA synthesis and $\frac{RNA}{DNA}$ distribution might be useful parameters. Certainly, studies should be conducted to correlate such physical parameters with the known immunological functions. Moreover, the changes in LSGD need to be correlated with the kinetics of the immune response in order to best utilize the spectrum of physical measurements for description of the temporal profile of cellular immunity.

In conclusion, this investigation has shown that several virus diseases result in distinctive changes in the specific gravity distribution of peripheral blood lymphocytes. These changes can be interpreted to indicate the appearance of new subpopulations and/or different proportions of subpopulations of peripheral lymphocytes as a result of the disease process and the associated immune response. In view of the high degree of similarity of the LSGDs for healthy individuals, the pattern of the LSGD in conjunction with one or more other measurements may be extremely useful in studies of the immune system and may be applicable to the diagnosis of disease and monitoring the effects of immunotherapy.

```
      PROGRAM MAIN(INPUT, OUTPUT, TAPE5=INPUT,TAPE6=OUTPUT,
     *FILMPL,TAPE48=FILMPL,TAPE16)
      DIMENSION X(100),Y(100),A(21),DELTAA(21),SIGMAA(21),YFIT(100)
      DIMENSION T(6), TX(9), TY(9),Q(100), L(100), V(100), M(2), B(21)
      DATA T/3*6H      ,6H   CHI,6HSQR = ,3*6H      /
      DATA TX/3*6H      ,6H     D,6HENSITY,4*6H      /
      DATA TY/4*6H      ,6HCOUNTS,4*6H      /
      CALL CAMRAV(35)
   99 CONTINUE
C
C  INPUT(100)!  NO. GAUSSIANS, FITTING INCREMENT, X(1), X(NPTS), NAME
C
      READ 100, NGAUSS      , DELA, XI, XF, T(2), T(3)
      NTERMS = 3 * NGAUSS
      IF(NTERMS, LT,1) STOP
      IT = NTERMS
      MODE = -1
      CSI = 1.E9
      KT = 1
      K1 = 0
C
C  INPUT(101)!  Y VALUES (LAST ONE = 99999999)
C
    1 READ 101, (L(J), J = 1,10)
      DO 21 I = 1, 10
      IF(L(I),GT,1000000) GO TO 11
      K1 = K1 + 1
      Y(K1) = L(I)
   21 CONTINUE
      GO TO 1
   11 NPTS = K1
      PRINT 106
      DO 2 I = 1, IT, 9
      K1 = I + 5
      K2 = MIN0(K1, NTERMS)
C
C  INPUT(105)!  FIRST GUESSES OF GAUSSIAN PARAMETERS * *
C               ORDER!  A1, A2, A3 FOR EACH OF (NGAUSS) GAUSSIANS,
C               WHERE Y = A3 * EXP(-((X-A1)/A2)**2)
C
      READ 105, (A(J), J = I, K2)
      PRINT105, (A(J), J = I, K2)
    2 CONTINUE
      PTS = NPTS - 1
      DX = (XF - XI)/PTS
      X(1) = XI
      DO 3 I = 2, NPTS
    3 X(I) = X(I-1) + DX
C
C  ADJUST DELTAA SIZES TO INSURE FAST CONVERGENCE
C
      DO 4 I = 1, NTERMS, 3
      DELTAA(I+1) = DELA/10.
      DELTAA(I+2) = DELA*1000.
    4 DELTAA(I) = DELA
   12 CONTINUE
      CALL CHIFIT(X,Y,SIGMAY,NPTS,NTERMS,MODE,A,DELTAA,SIGMAA,YFIT,CSQ)
```

APPENDIX A

```
C
C  REPEAT IF CSQ (CHI SQUARE) IS STILL DECREASING
C
      IF(CSQ.LT.0.00001) GO TO 99
      IF((CSI-CSQ).LT.(CSQ*0.00001).OR.KT.GT.20) GO TO 13
      PRINT 102, NPTS, NTERMS, DELA, XI, XF, CSQ, T(2), T(3)
      K = NTERMS
      PRINT 103, (I, A(I), SIGMAA(I), I = 1, K)
      PRINT 101
      PRINT 104, (I, X(I), Y(I), YFIT(I), I = 1, NPTS)
      KT = KT + 1
      DO 14 I = 1, NPTS
   14 Q(I) = YFIT(I)
      CSI = CSQ
      DO 15 I = 1, NTERMS
   15 B(I) = A(I)
      GO TO 12
   13 CONTINUE
C
C  SET YMIN
C
      NPTG = NPTS + 1
      X(NPTG) = XF + DX
      Y(NPTG) = Y(1)/10.
C
C  SET UP PLOT TITLE
C
      ENCODE(12,89,R) CSI
   89 FORMAT(F6.0)
      DECODE(6,88,R  ) T(6)
   88 FORMAT(A6)
C
C  PLOT INPUT DATA (X, Y)
C
      CALL AICRT3(0,1,X,Y   ,NPTG,1,1,1,38,T,TX,TY,1,1,50,16,1,XL,XR,
     *1,YB,YT)
C
C  PLOT OUTPUT (X, YFIT)
C
      CALL AICRT3(0,1,X,Q   ,NPTS,1,2,1,42,T,TX,TY,2,1,50,16,1,XL,XR,
     *1,YB,YT)
C
C  CALCULATE Y VALUES FOR EACH GAUSSIAN
C
      DO 20 J = 1, NTERMS, 3
      A1 = B(J)
      A2 = B(J+1)
      A3 = B(J+2)
      NPTH = 0
      PRINT 101
      DO 22 I = 1, NPTS
      IF(X(I).LT.(A1-3.*A2).OR.X(I).GT.(A1+3.*A2))GO TO 22
      Z = (X(I) - A1)/A2
      Q(I) = A3*EXP(-(Z**2)/2.)
      IF(Q(I).LT.Y(NPTG))GO TO 22
      NPTH = NPTH + 1
      U(NPTH) = X(I)
```

```
      Q(NPTH) = Q(I)
C
C  PRINT AND PLOT EACH GAUSSIAN
C
      PRINT 104, I, U(NPTH), Q(NPTH)
   22 CONTINUE
      CALL AICRT3(0.1,0.0   ,NPTH,1.2,1.42,T,TX,TY,2,1.50,.16,.1,XL,XR,
     *1,YB,YT)
   20 CONTINUE
      GO TO 99
  100 FORMAT(13X,I10,F10.2,2F12.8,6X,2A6)
  101 FORMAT(15I8)
  102 FORMAT(1H0,2I10,F10.2,2F12.6,F12.2,20X,2A6//)
  103 FORMAT(    3(I10,2E12.6) )
  104 FORMAT(I5,F12.4,F10.2,F12.4)
  105 FORMAT(6F12.4)
  106 FORMAT(1H1)
      END
```

```
      FUNCTION FUNCTN(X,I,A,NTERMS)
      DIMENSION X(1), A(1)
      XI = X(I)
      PF = 0.
      K = NTERMS/3
    5 DO 10 J = 1, K
      IZ = 3*(J-1)
      PF = PF + PGAUSS(XI,A(IZ+1),A(IZ+2),A(IZ+3))
   10 CONTINUE
   10 FUNCTN = PF
      RETURN
      END
```

```
      FUNCTION PGAUSS (X, AVERAG, SIGMA, CONST)
C     FUNCTION PGAUSS
C
C     PURPOSE
C       EVALUATE GAUSSIAN PROBABILITY FUNCTION
C
C     USAGE
C       RESULT = PGAUSS (X, AVERAG, SIGMA)
C
C     DESCRIPTION OF PARAMETERS
C       X       - VALUE FOR WHICH PROBABILITY IS TO BE EVALUATED
C       AVERAG  - MEAN OF DISTRIBUTION
C     SIGMA   - STANDARD DEVIATION OF DISTRIBUTION
C
      DOUBLE PRECISION Z
    1 Z= (X-AVERAG)/SIGMA
    2 PGAUSS = CONST                * DEXP(-(Z**2)/2.)
      RETURN
      END
```

```
      FUNCTION FCHISQ(Y, SIGMAY, NPTS, NFREE, MODE, YFIT)
      DOUBLE PRECISION CHISQ, WEIGHT
      DIMENSION Y(1), SIGMAY(1), YFIT(1)
   11 CHISQ = 0.
 5 12 IF(NFREE) 13, 13, 20
   13 FCHISQ = 0.
      GO TO 40
   20 DO 30 I = 1, NPTS
   21 IF(MODE) 22, 27, 29
10 22 IF(Y(I)) 25, 27, 23
   23 WEIGHT = 1. / Y(I)
      GO TO 30
   25 WEIGHT = 1. / (-Y(I))
      GO TO 30
15 27 WEIGHT = 1.
      GO TO 30
   29 WEIGHT = 1. / SIGMAY(I)**2
   30 CHISQ = CHISQ + WEIGHT * (Y(I) - YFIT(I))**2
   31 FREE = NFREE
20 32 FCHISQ = CHISQ / FREE
   40 RETURN
      END
```

```
      SUBROUTINE CHIFIT (X, Y, SIGMAY, NPTS, NTERMS, MODE, A, DELTAA,
     1 SIGMAA, YFIT, CHISQR)
C     SUBROUTINE CHIFIT
C
C     PURPOSE
C       MAKE A LEAST-SQUARES FIT TO A NON-LINEAR FUNCTION
C          WITH A PARABOLIC EXPANSION OF CHI SQUARE
C
C     USAGE
C       CALL CHIFIT (X, Y, SIGMAY, NPTS, NTERMS, MODE, A, DELTAA,
C          SIGMAA, YFIT, CHISQR)
C
C     DESCRIPTION OF PARAMETERS
C       X      - ARRAY OF DATA POINTS FOR INDEPENDENT VARIABLE
C       Y      - ARRAY OF DATA POINTS FOR DEPENDENT VARIABLE
C       SIGMAY - ARRAY OF STANDARD DEVIATIONS FOR Y DATA POINTS
C       NPTS   - NUMBER OF PAIRS OF DATA POINTS
C       NTERMS - NUMBER OF PARAMETERS
C       MODE   - DETERMINES MODE OF WEIGHTING LEAST-SQUARES FIT
C                  +1 (INSTRUMENTAL) WEIGHT(I) = 1./SIGMAY(I)**2
C                   0 (NO WEIGHTING) WEIGHT(I) = 1.
C                  -1 (STATISTICAL)  WEIGHT(I) 1./Y(I)
C       A      - ARRAY OF PARAMETERS
C       DELTAA - ARRAY OF INCREMENTS FOR PARAMETERS A
C       SIGMAA - ARRAY OF STANDARD DEVIATIONS FOR PARAMETERS A
C       YFIT   - ARRAY OF CALCULATED VALUES OF Y
C       CHISQR - REDUCED CHI SQUARE FOR FIT
C
C
C     COMMENTS
C       DIMENSION STATEMENT VALID FOR NTERMS UP TO 10
C
      DOUBLE PRECISION ALPHA
      DIMENSION X(1), Y(1), SIGMAY(1), A(1), DELTAA(1), SIGMAA(1),
     1 YFIT(1)
      DIMENSION ALPHA(10,10), BETA(10),DA(10)
   11 NFREE = NPTS - NTERMS
      FREE = NFREE
      IF (NFREE) 14, 14, 16
   14 CHISQR = 0.
      GO TO 120
   16 DO 17 I=1, NPTS
   17 YFIT(I) = FUNCTN (X, I, A, NTERMS)
      CHISQ1 = FCHISQ (Y, SIGMAY, NPTS, NFREE, MODE, YFIT)
C
C        EVALUATE ALPHA AND BETA MATRICES
C
   20 DO 60 J=1, NTERMS
C
C        A(J) = DELTAA(J)
C
      AJ = A(J)
      A(J) = AJ + DELTAA(J)
      DO 24 I=1, NPTS
   24 YFIT(I) = FUNCTN (X, I, A, NTERMS)
      CHISQ2 = FCHISQ (Y, SIGMAY, NPTS, NFREE, MODE, YFIT)
      ALPHA(J,J) = CHISQ2 = 2.*CHISQ1
```

ORIGINAL PAGE IS
OF POOR QUALITY

```
      BETA(J) = -CHISQ2
   31 DO 50 K=1, NTERMS
      IF (K-J) 33, 50, 36
   33 ALPHA(K,J) = (ALPHA(K,J) - CHISQ2) / 2.
      ALPHA(J,K) = ALPHA(K,J)
      GO TO 50
   36 ALPHA(J,K) = CHISQ1 - CHISQ2
C
C        A(J) + DELTAA(J) AND A(K) + DELTAA(K)
C
   41 AK = A(K)
      A(K) = AK + DELTAA(K)
      DO 44 I=1, NPTS
   44 YFIT(I) = FUNCTN (X, I, A, NTERMS)
      CHISQ3 = FCHISQ (Y, SIGMAY, NPTS, NFREE, MODE, YFIT)
      ALPHA(J,K) = ALPHA(J,K) * CHISQ3
      A(K) = AK
   50 CONTINUE
C
C        A(J) - DELTAA(J)
C
   51 A(J) = AJ - DELTAA(J)
      DO 53 I=1, NPTS
   53 YFIT(I) = FUNCTN (X, I, A, NTERMS)
      CHISQ3 = FCHISQ (Y, SIGMAY, NPTS, NFREE, MODE, YFIT)
      A(J) = AJ
      ALPHA(J,J) = (ALPHA(J,J) + CHISQ3) / 2.
      BETA(J) = (BETA(J) + CHISQ3) / 4.
   60 CONTINUE
C
C        ELIMINATE NEGATIVE CURVATURE
C
   61 DO 70 J=1, NTERMS
      IF (ALPHA(J,J)) 63, 65, 70
   63 ALPHA(J,J) = -ALPHA(J,J)
      GO TO 66
   65 ALPHA(J,J) = 0.01
   66 DO 69 K=1, NTERMS
      IF (K - J) 68, 69, 68
   68 ALPHA(J,K) =0.
      ALPHA(K,J) =0.
   69 CONTINUE
   70 CONTINUE
C
C        INVERT MATRIX AND EVALUATE PARAMETER INCREMENTS
C
   71 CALL MATINV (ALPHA, NTERMS, DET)
      DO 76 J=1, NTERMS
      DA(J) = 0.
   74 DO 75 K=1, NTERMS
   75 DA(J) = DA(J) + BETA(K)*ALPHA(J,K)
   76 DA(J) = 0.2 * DA(J) + DELTAA(J)
C
C        MAKE SURE CHI SQUARE DECREASES
C
   81 DO 82 J=1, NTERMS
   82 A(J) = A(J) + DA(J)
```

ORIGINAL PAGE IS OF POOR QUALITY

```
      83 DO 84 I=1, NPTS
      84    YFIT(I) = FUNCTN (X, I, A, NTERMS)
            CHISQ2 = FCHISQ (Y, SIGMAY, NPTS, NFREE, MODE, YFIT)
            IF (CHISQ1 - CHISQ2) 87, 91, 91
      87 DO 89 J=1, NTERMS
            DA(J) = DA(J)/2.
      89 A(J) = A(J) + DA(J)
         IF((CHISQ2-CHISQ1),LT,(CHISQ2*0.00001)) GO TO 91
         GO TO 83
C
C        INCREMENT PARAMETERS UNTIL CHI SQUARE STARTS TO INCREASE
C
      91 DO 92 J=1, NTERMS
      92 A(J) = A(J) + DA(J)
         DO 94 I=1, NPTS
      94    YFIT(I) = FUNCTN (X, I, A, NTERMS)
            CHISQ3 = FCHISQ (Y, SIGMAY, NPTS, NFREE, MODE, YFIT)
            IF (CHISQ3 - CHISQ2) 97, 101, 101
      97 CHISQ1 = CHISQ2
         CHISQ2 = CHISQ3
      99 GO TO 91
C
C        FIND MINIMUM OF PARABOLA DEFINED BY LAST THREE POINTS
C
     101 DELTA = 1./(1.+(CHISQ1-CHISQ2)/(CHISQ3-CHISQ2)) + 0.5
         DO 104 J=1, NTERMS
         A(J) = A(J) - DELTA*DA(J)
         ALF = FREE * ALPHA(J,J)
         ALF = ABS(ALF)
     104 SIGMAA(J) = DELTAA(J) * SQRT (ALF)
         DO 106 I=1, NPTS
     106    YFIT(I) = FUNCTN (X, I, A, NTERMS)
            CHISQR = FCHISQ (Y, SIGMAY, NPTS, NFREE, MODE, YFIT)
     111 IF(CHISQ2 - CHISQR) 112, 120, 120
     112 DO 113 J=1, NTERMS
     113 A(J) = A(J) + (DELTA-1.)*DA(J)
         DO 115 I=1, NPTS
     115    YFIT(I) = FUNCTN (X, I, A, NTERMS)
            CHISQR= CHISQ2
     120 RETURN
         END
```

SUBROUTINE MATINV 74/74 OPT=1

```
      SUBROUTINE MATINV(ALPHA,NTERMS,DET)
      DOUBLE PRECISION ALPHA(10,10),P(10)
      DIMENSION IT(10,3)
      CALL DSID(ALPHA,NTERMS,10,8,0,0,1,P,IT)
      RETURN
      END
```

APPENDIX B

I-1 Day 0

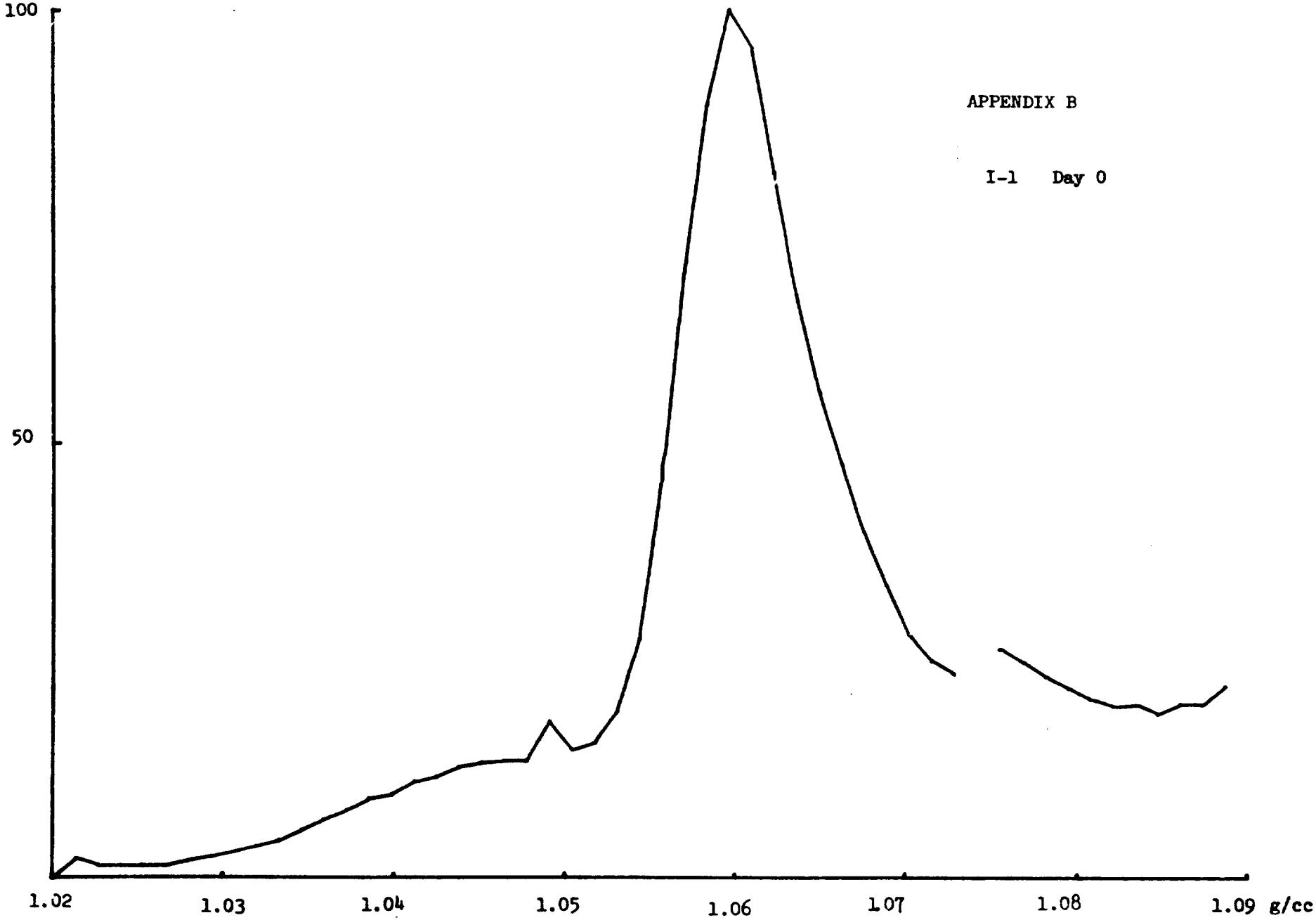

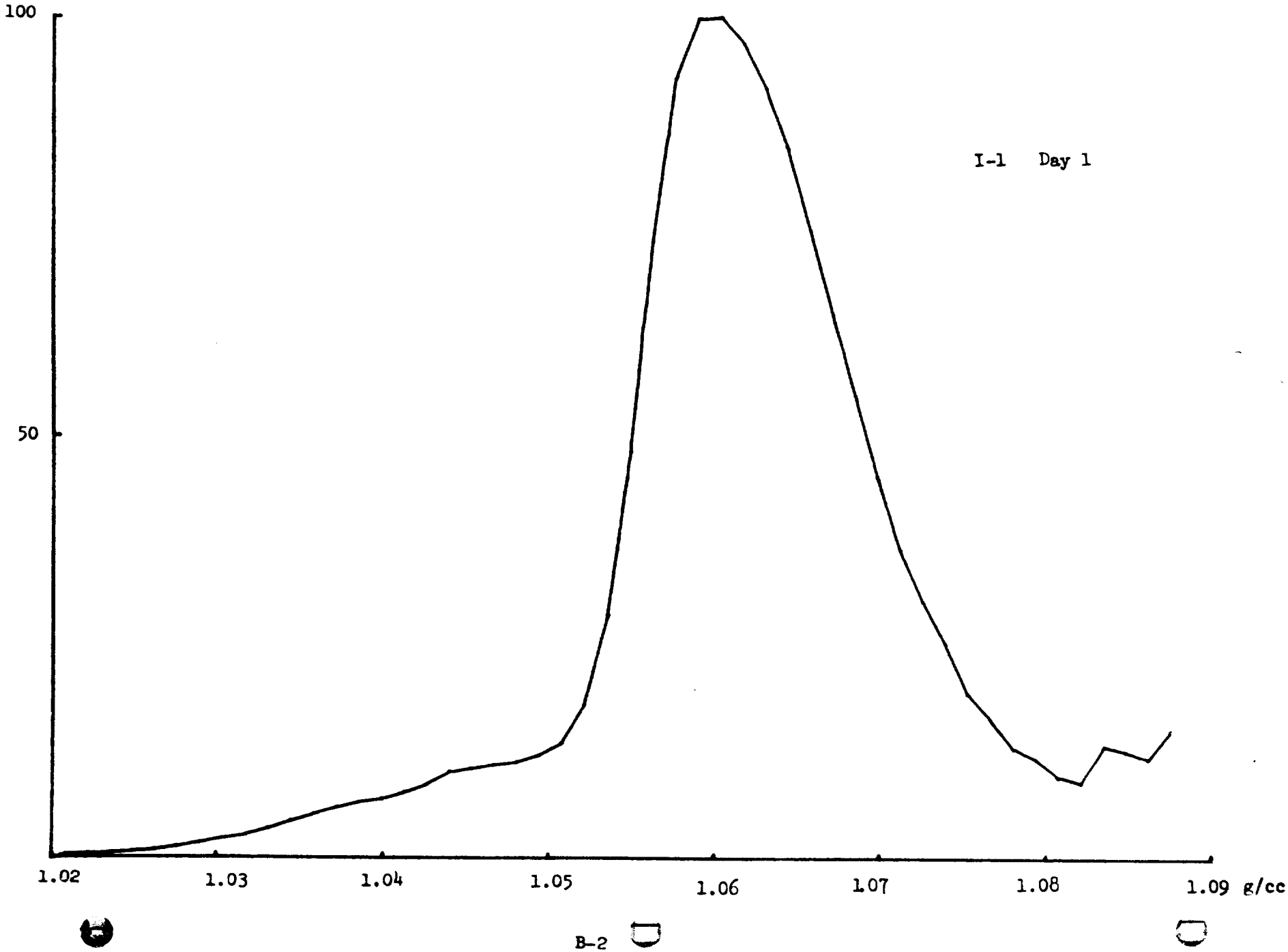
100
50
I-1 Day 1
1.02
1.03
1.04
1.05
1.06
1.07
1.08
1.09 g/cc

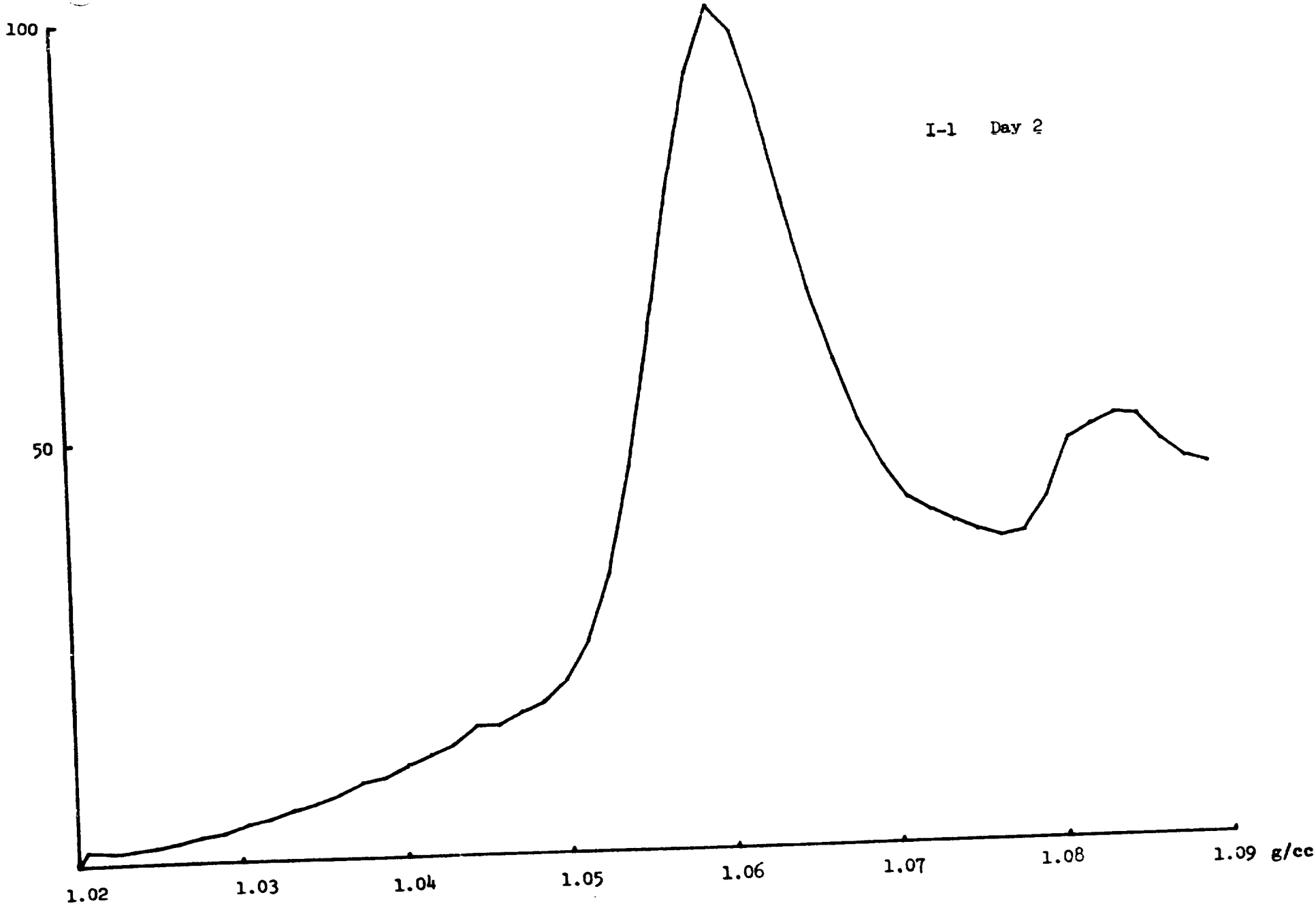
100
50
I-1 Day 2
1.02
1.03
1.04
1.05
1.06
1.07
1.08
1.09 g/cc

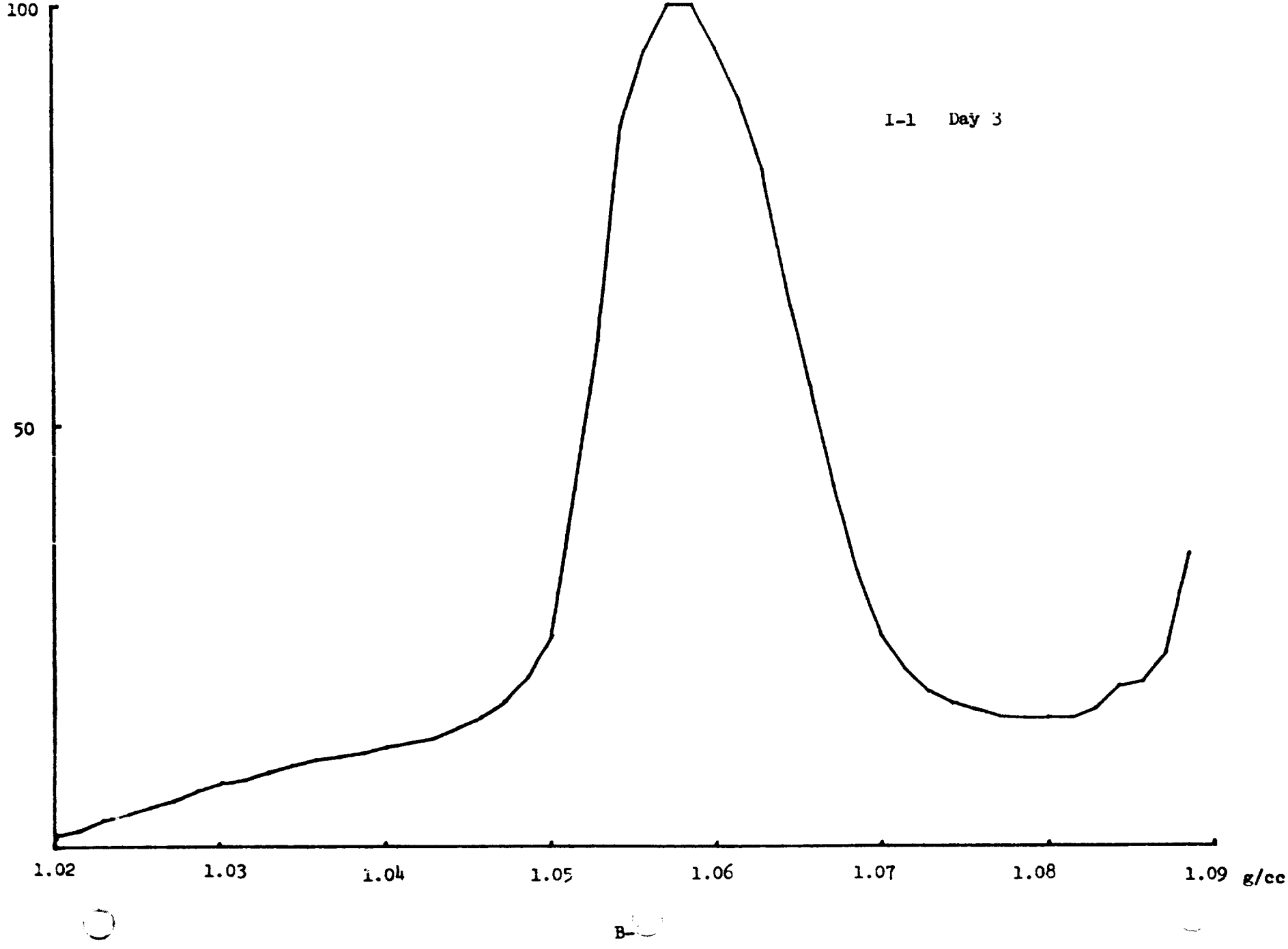
100
50
I-1 Day 3
1.02
1.03
1.04
1.05
1.06
1.07
1.08
1.09
g/cc

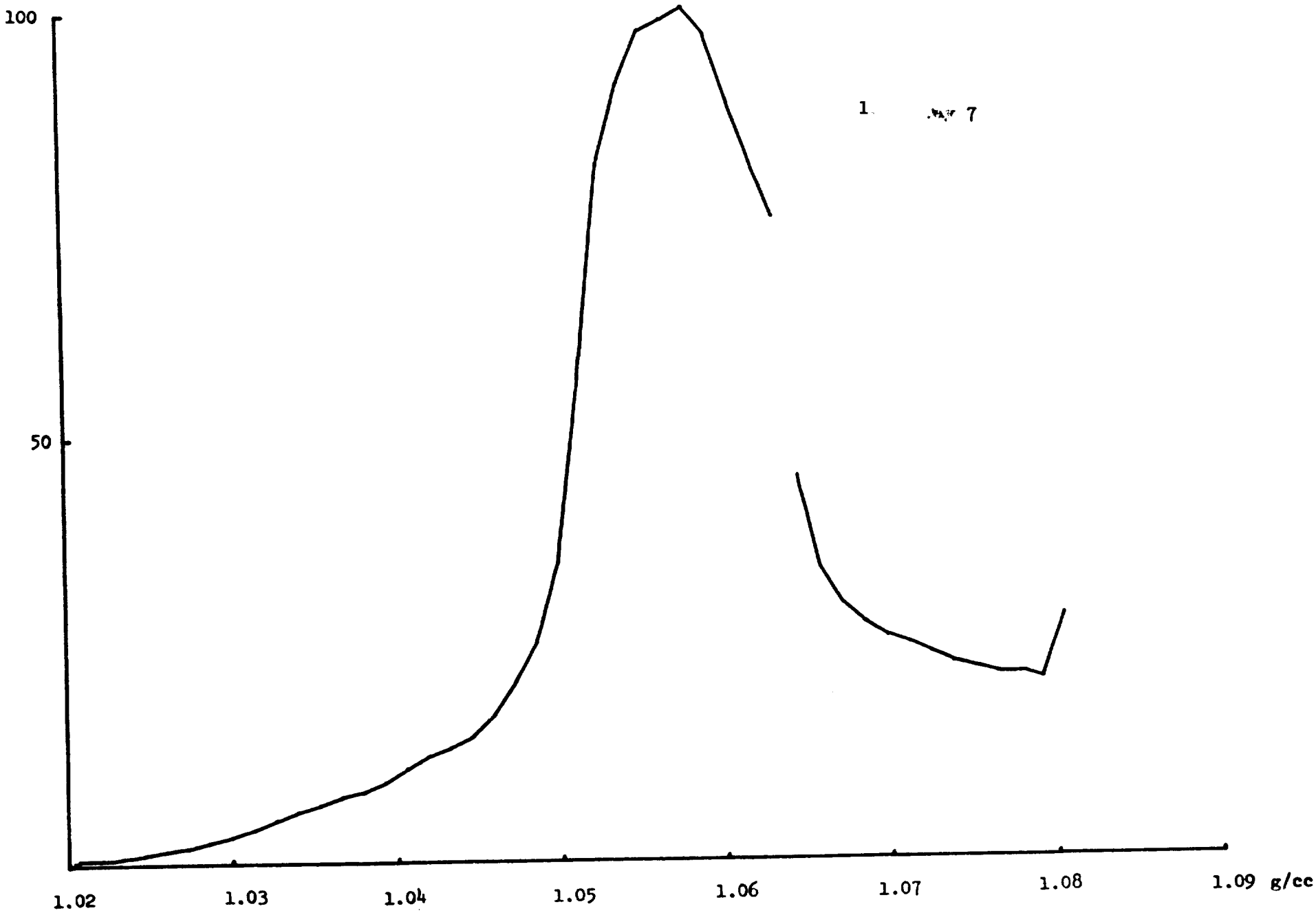
100
50
1.02
1.03
1.04
1.05
1.06
1.07
1.08
1.09 g/cc

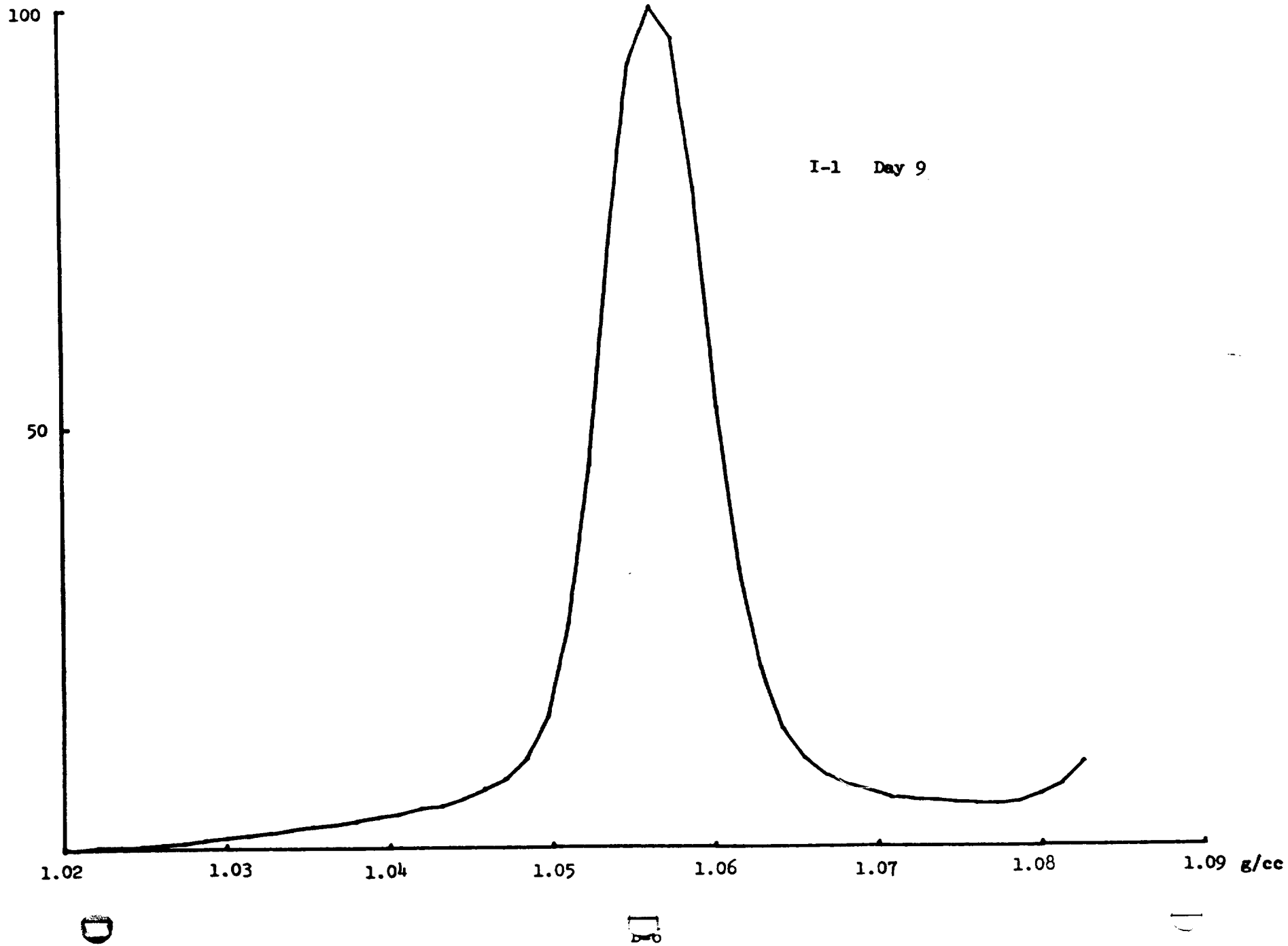
100
50
I-1 Day 9
1.02
1.03
1.04
1.05
1.06
1.07
1.08
1.09 g/cc

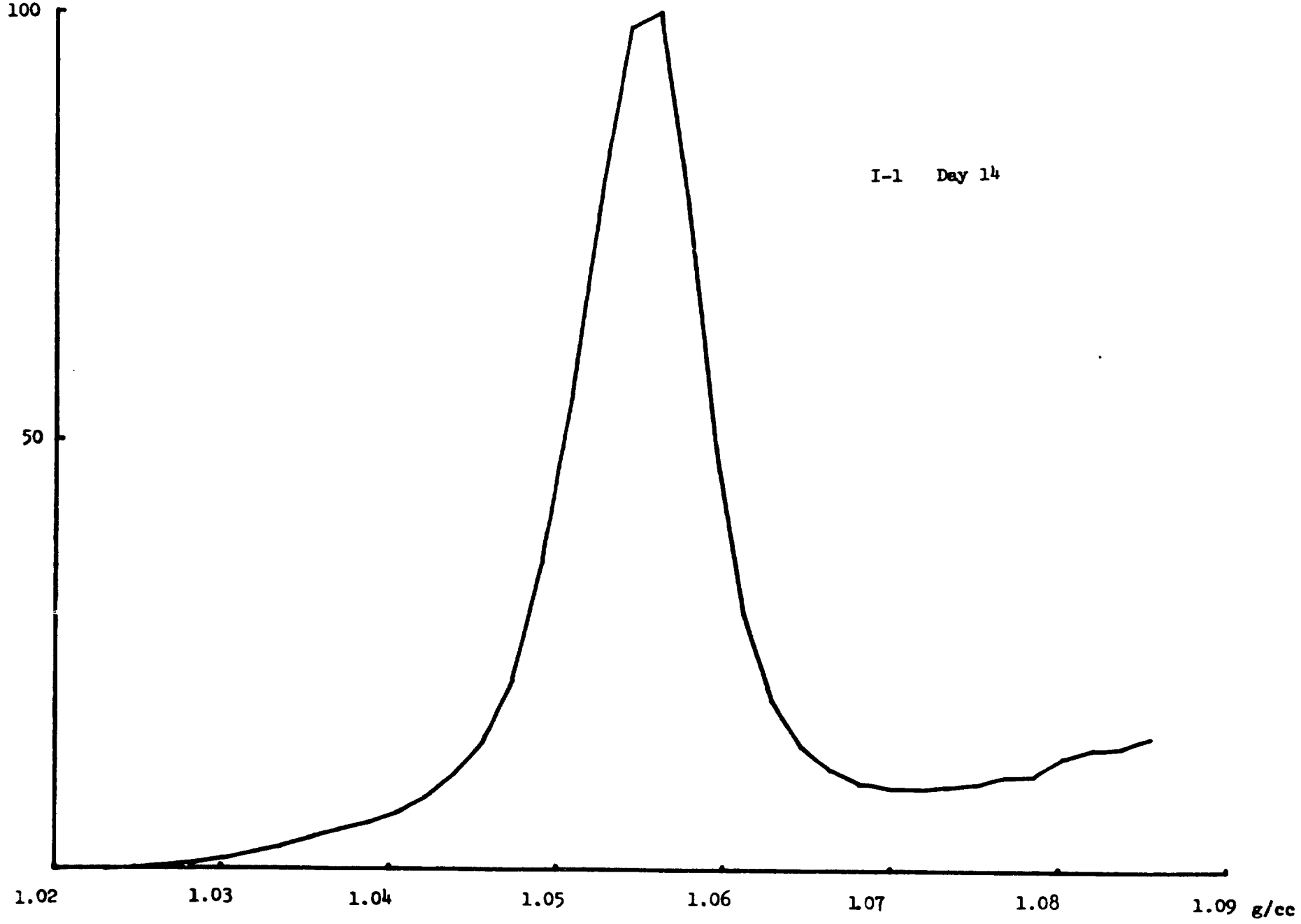
100
50
I-1 Day 14
1.02
1.03
1.04
1.05
1.06
1.07
1.08
1.09 g/cc

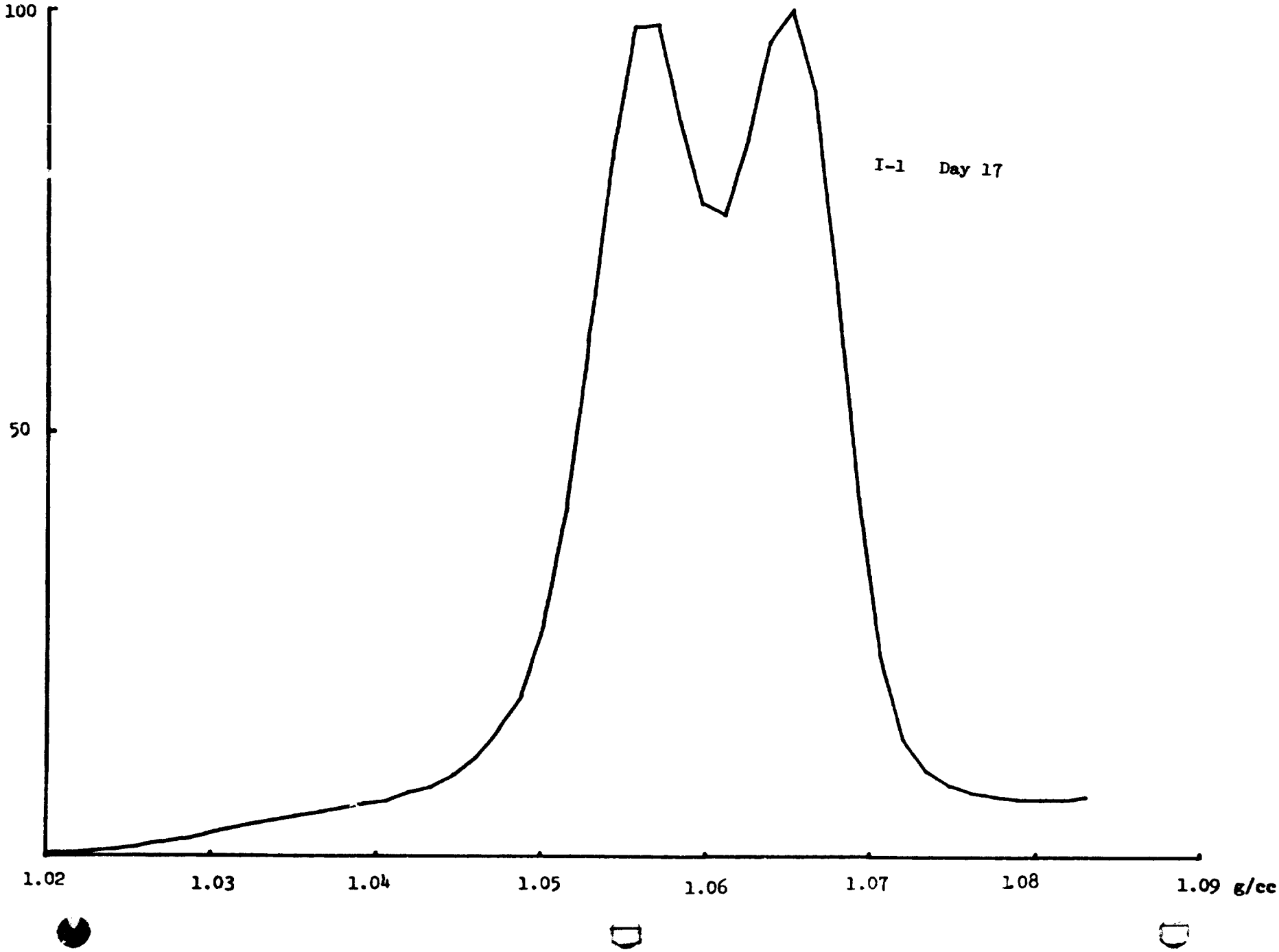
100
50
I-1 Day 17
1.02
1.03
1.04
1.05
1.06
1.07
1.08
1.09 g/cc

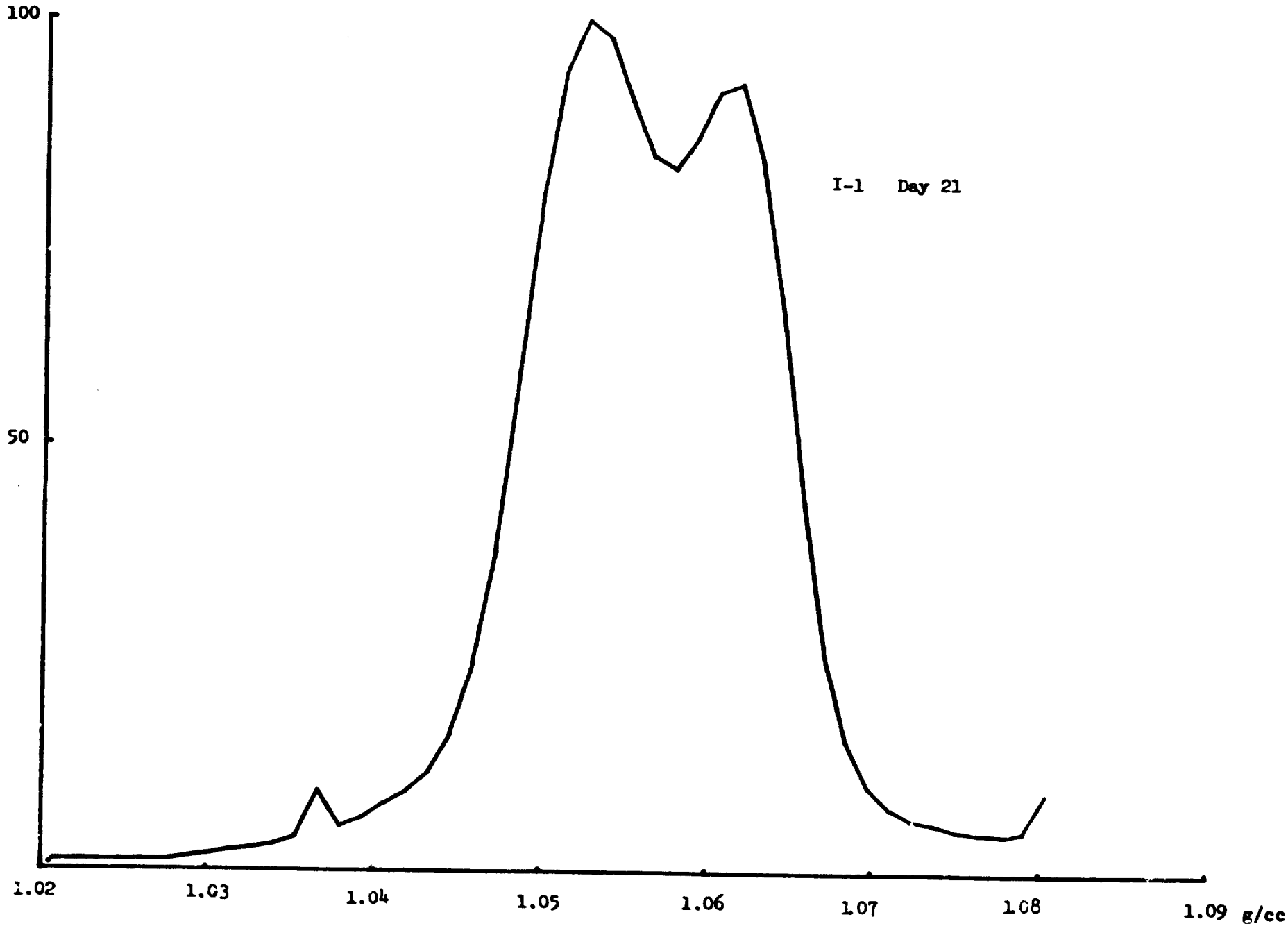
100
50
I-1 Day 21
1.02
1.03
1.04
1.05
1.06
1.07
1.08
1.09 g/cc

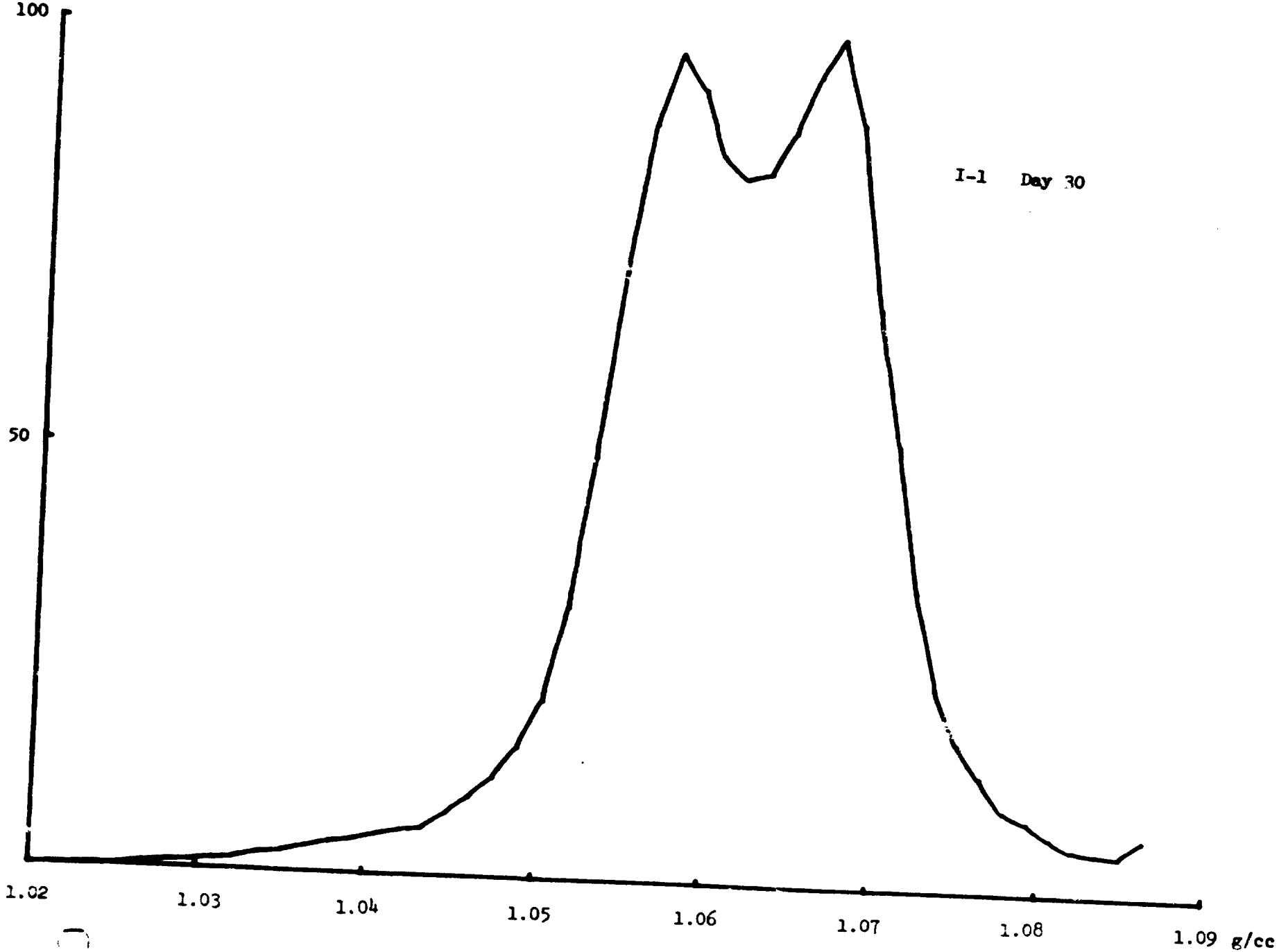
100
50
I-1 Day 30
1.02
1.03
1.04
1.05
1.06
1.07
1.08
1.09 g/cc

C-2

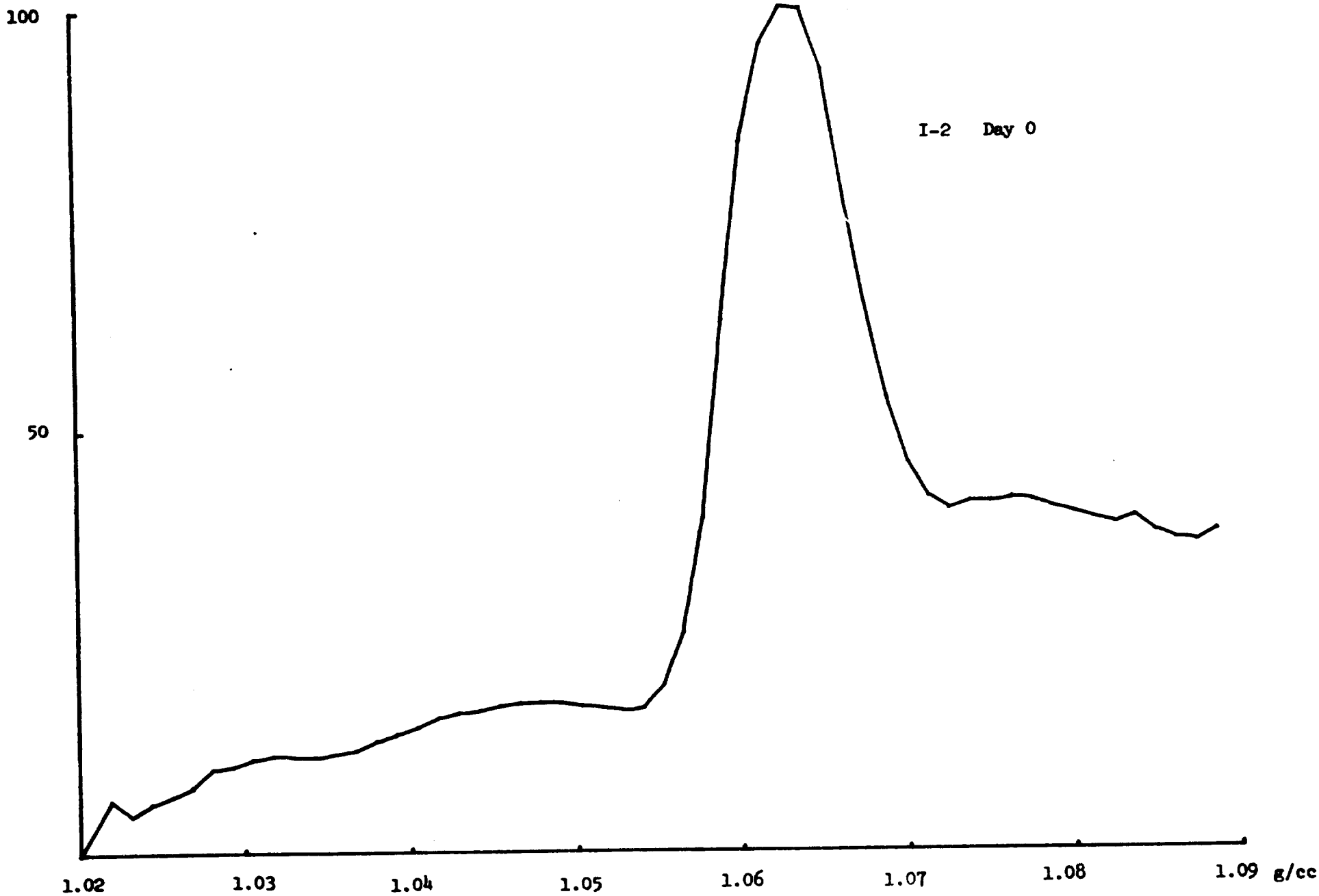

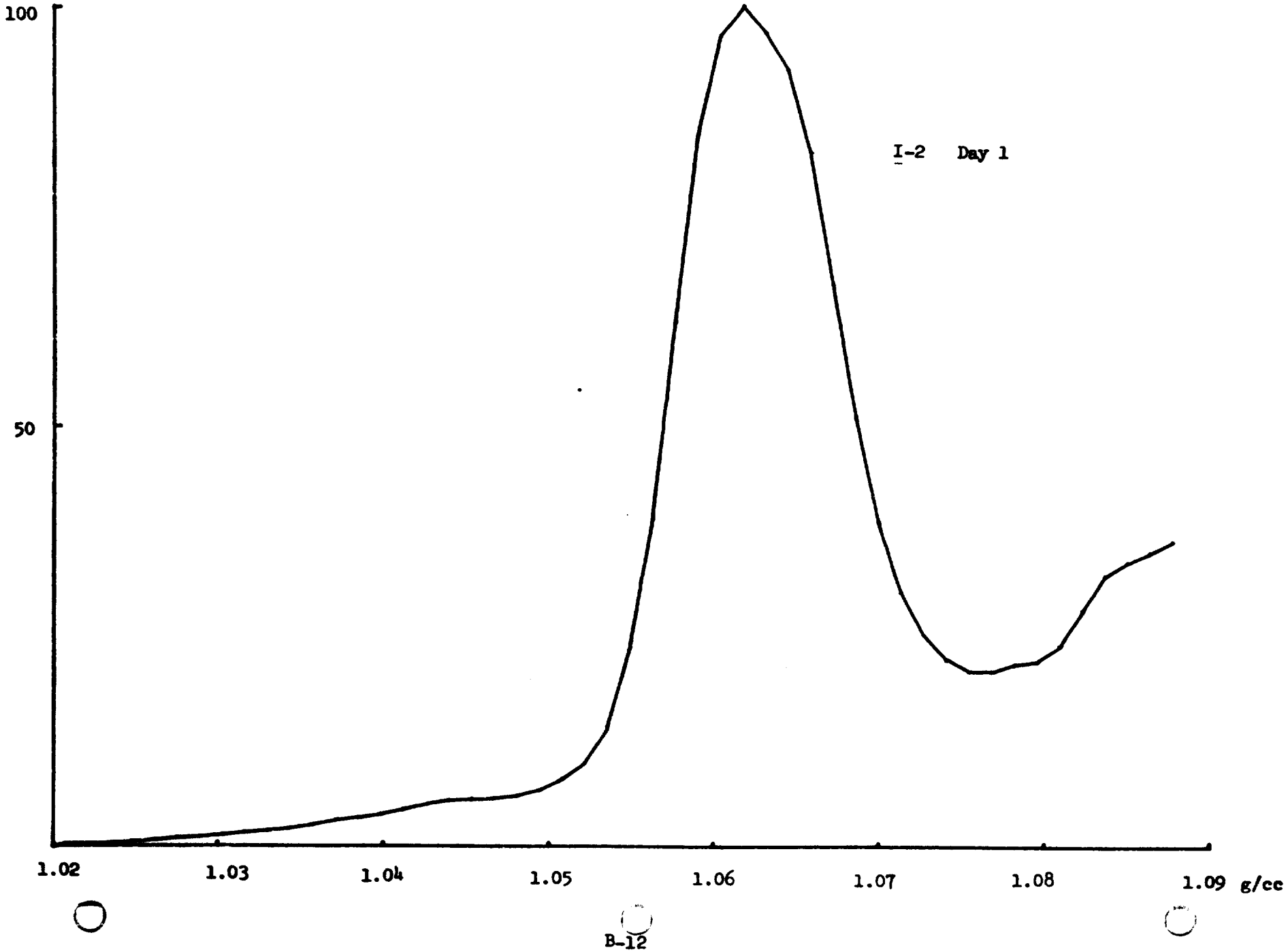
100
50
I-2 Day 1
1.02
1.03
1.04
1.05
1.06
1.07
1.08
1.09 g/cc

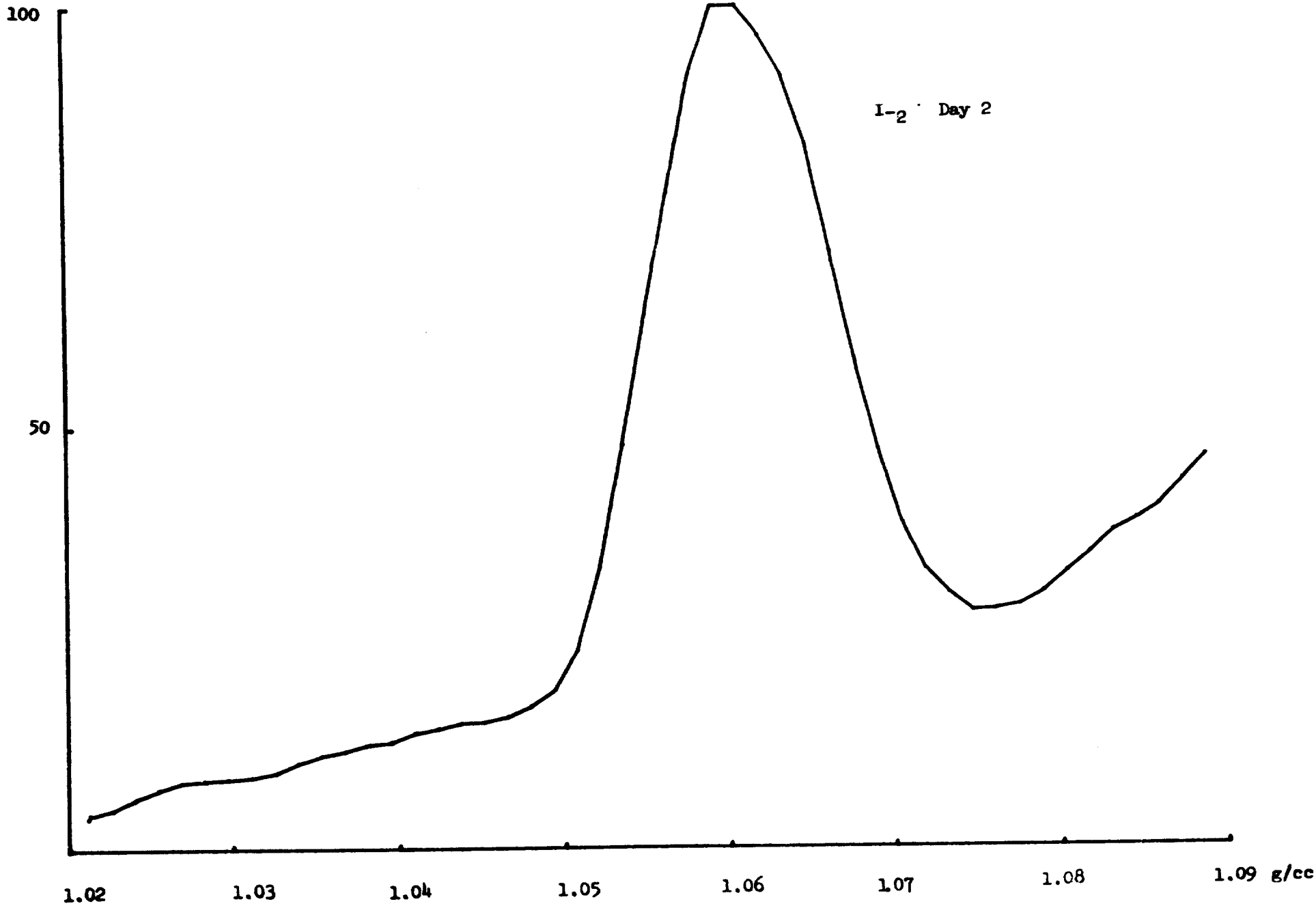
100
50
I-2 · Day 2
1.02
1.03
1.04
1.05
1.06
1.07
1.08
1.09 g/cc

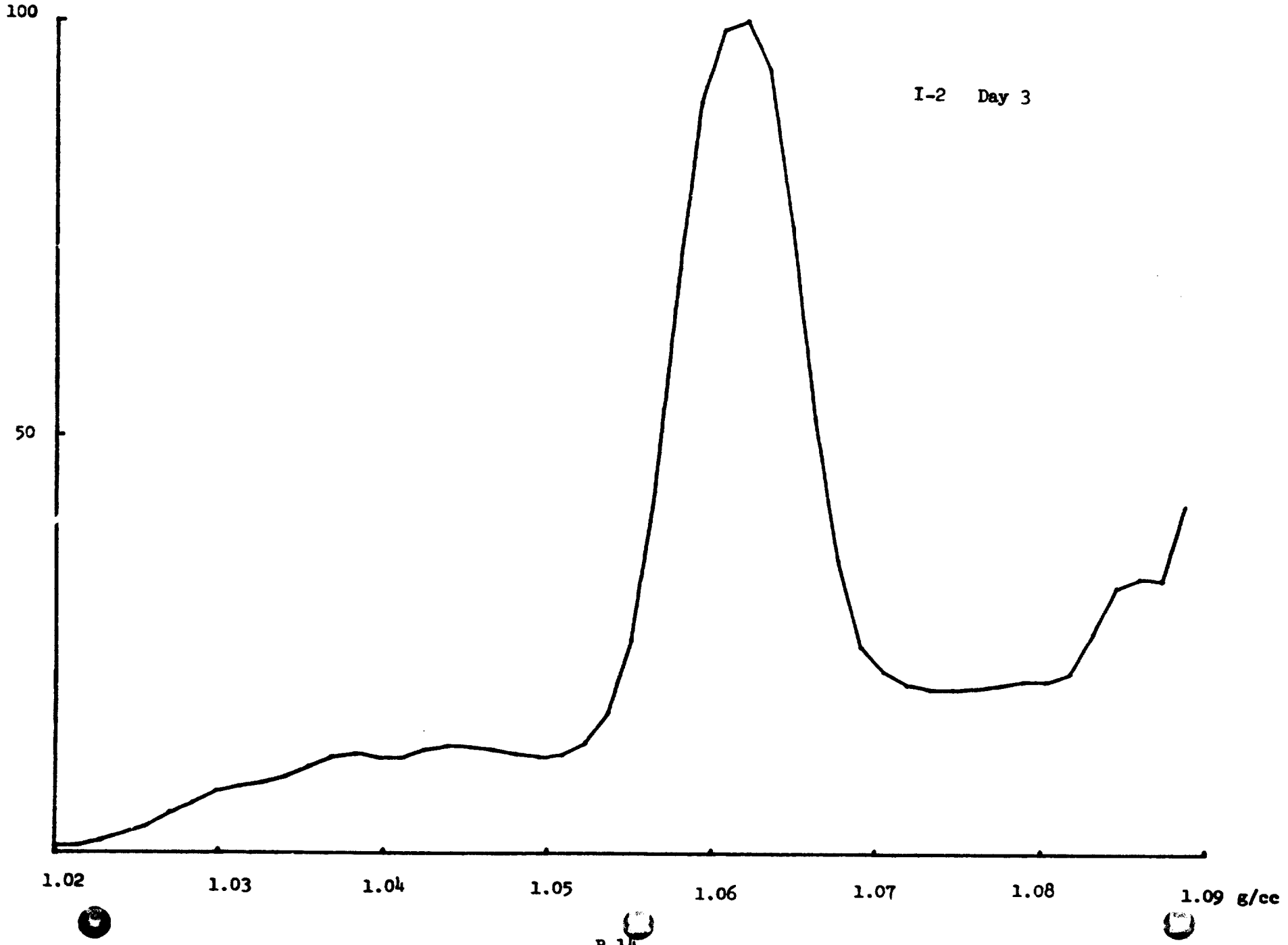
100
50
I-2 Day 3
1.02
1.03
1.04
1.05
1.06
1.07
1.08
1.09 g/cc

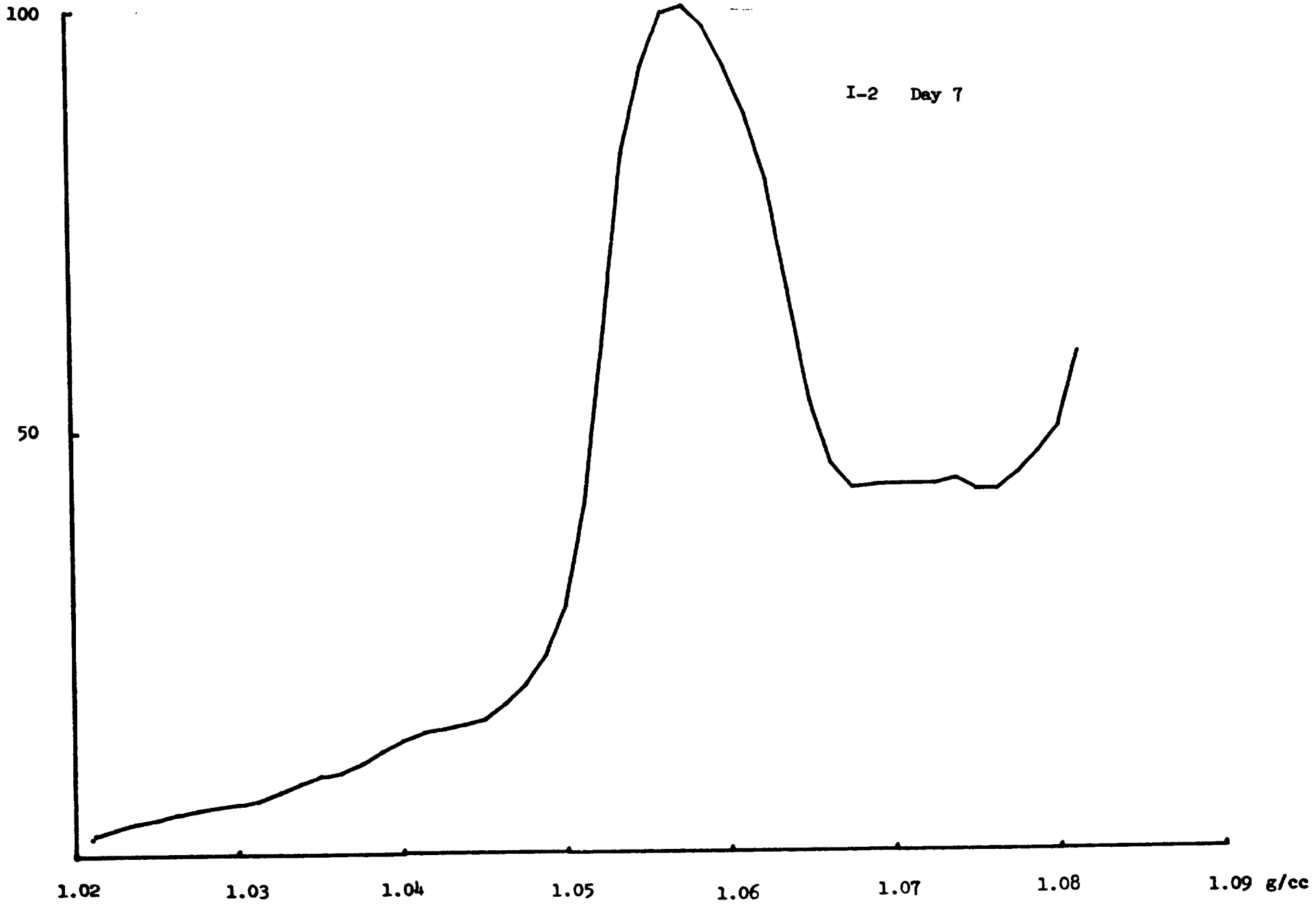
100
50
I-2 Day 7
1.02
1.03
1.04
1.05
1.06
1.07
1.08
1.09 g/cc

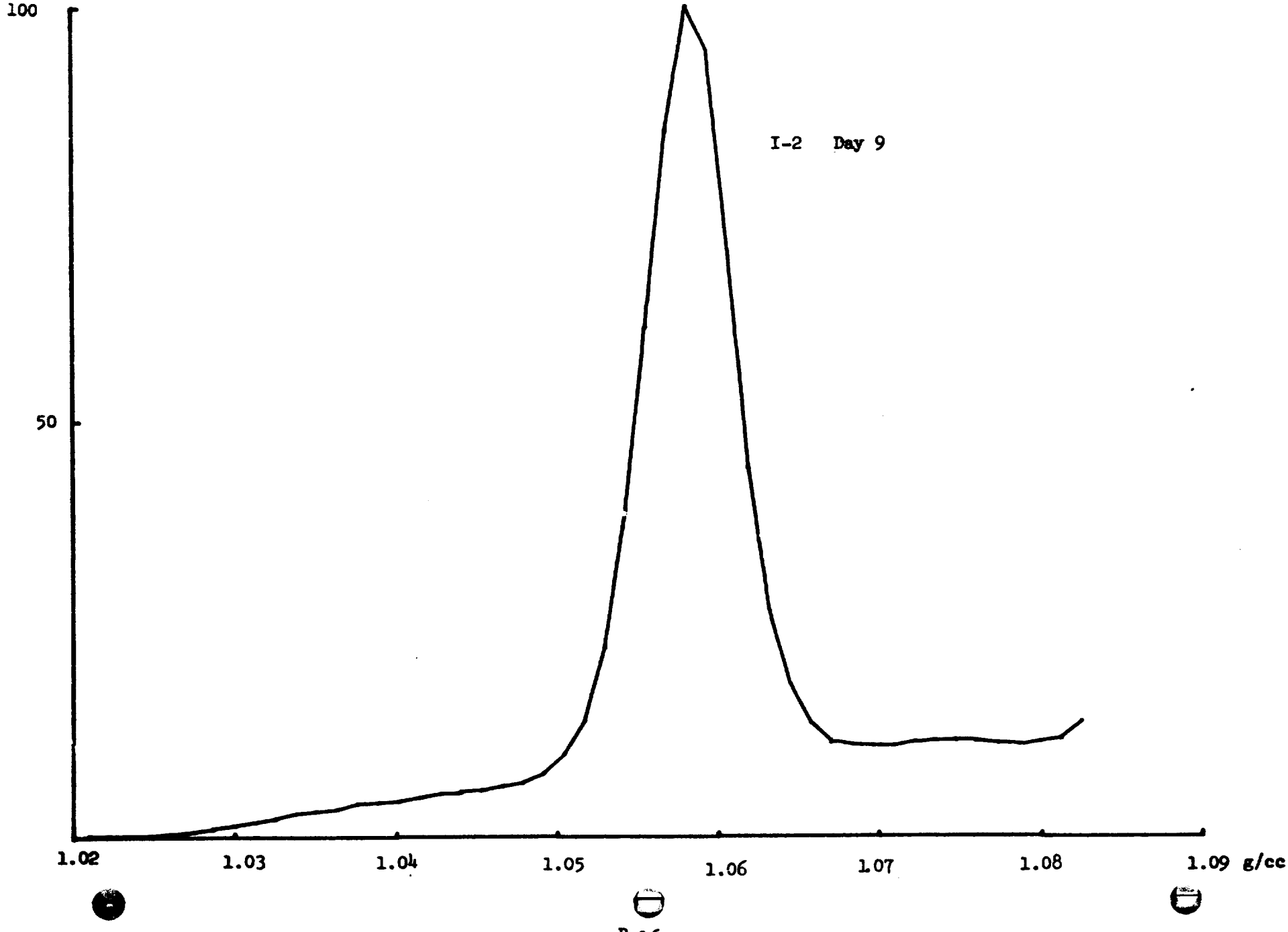
100
50
I-2 Day 9
1.02
1.03
1.04
1.05
1.06
1.07
1.08
1.09 g/cc

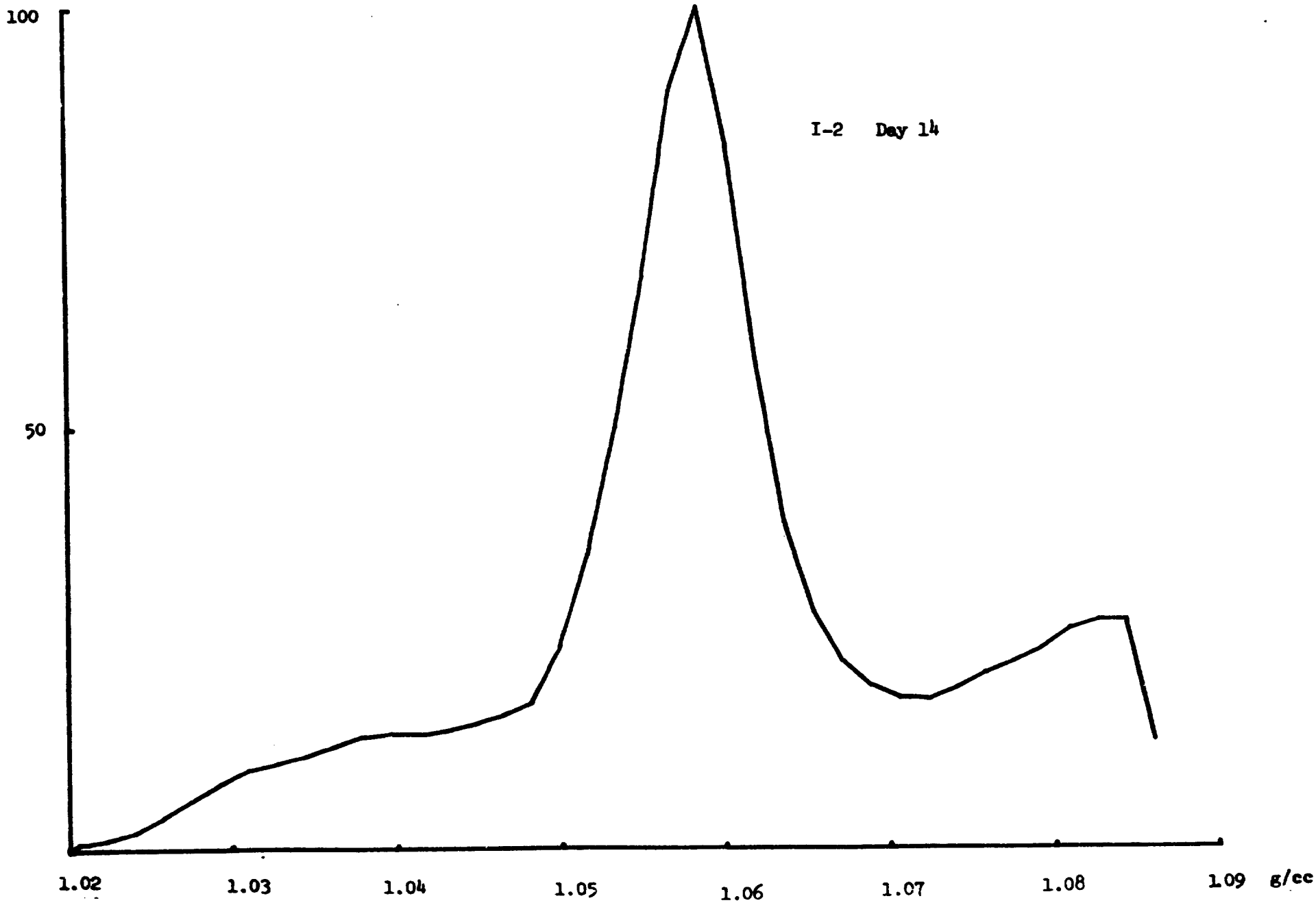
100
50
I-2 Day 14
1.02
1.03
1.04
1.05
1.06
1.07
1.08
1.09
g/cc

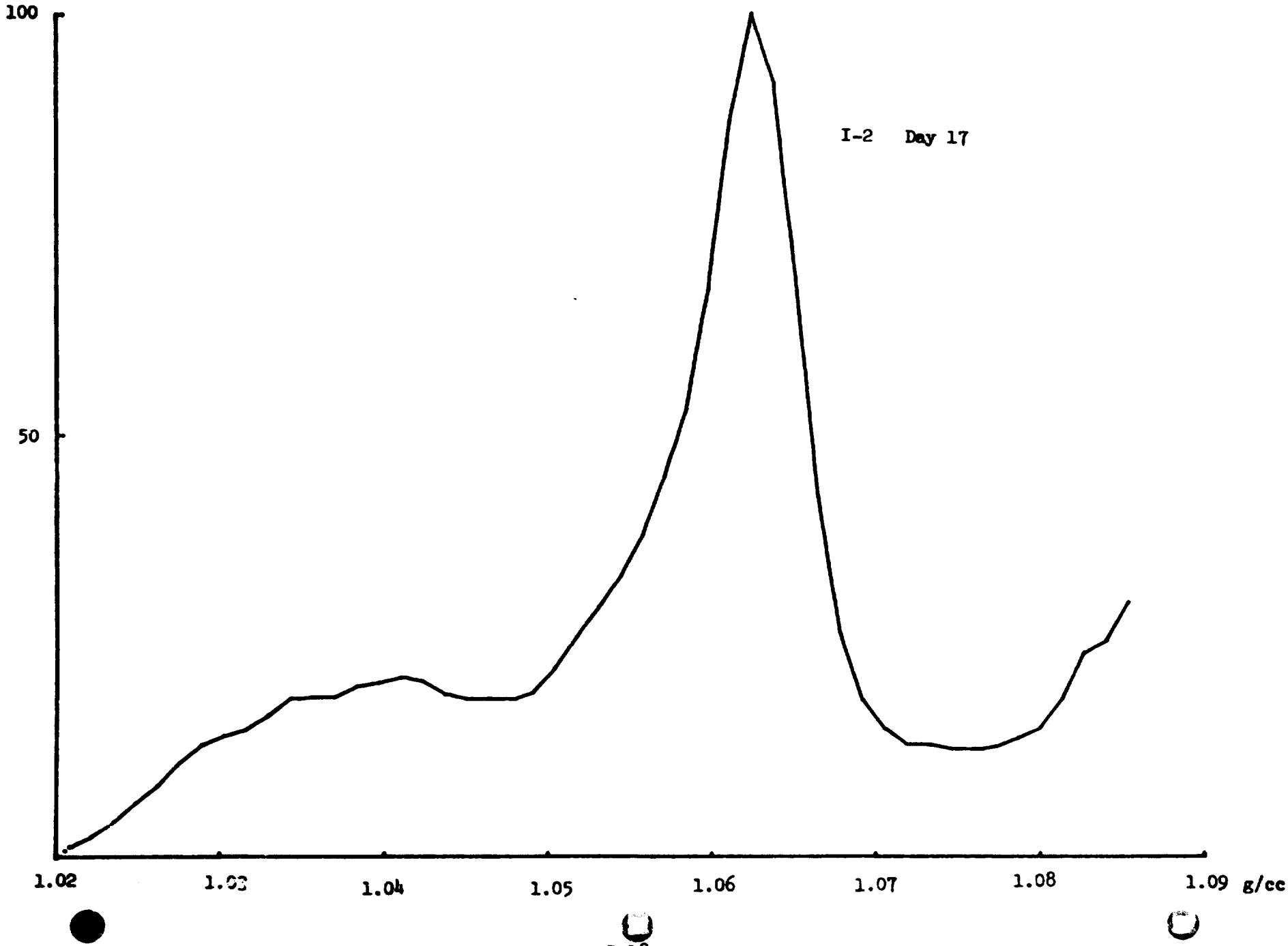
100
50
I-2 Day 17
1.02
1.03
1.04
1.05
1.06
1.07
1.08
1.09 g/cc

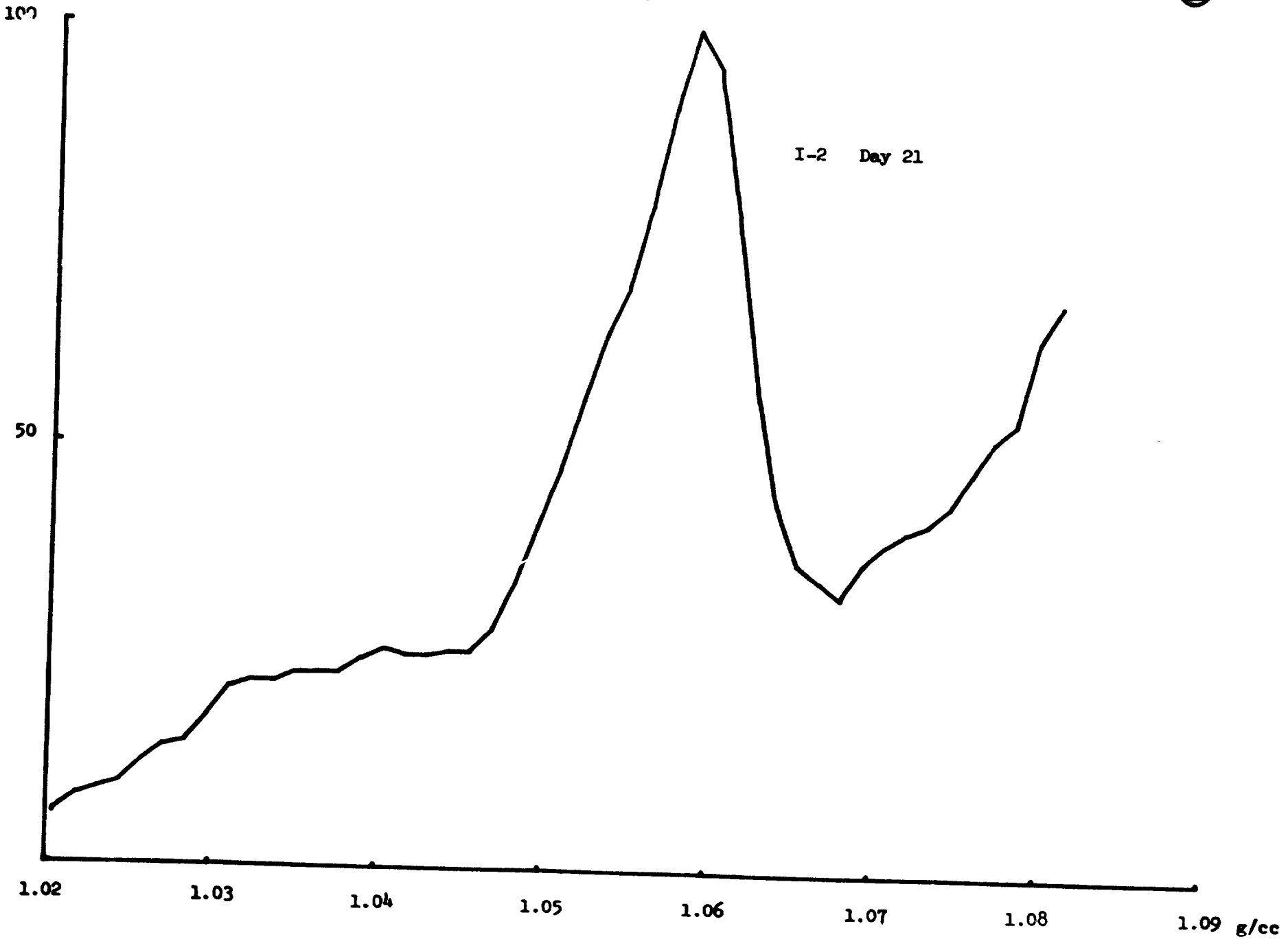
100
50
I-2 Day 21
1.02
1.03
1.04
1.05
1.06
1.07
1.08
1.09 g/cc

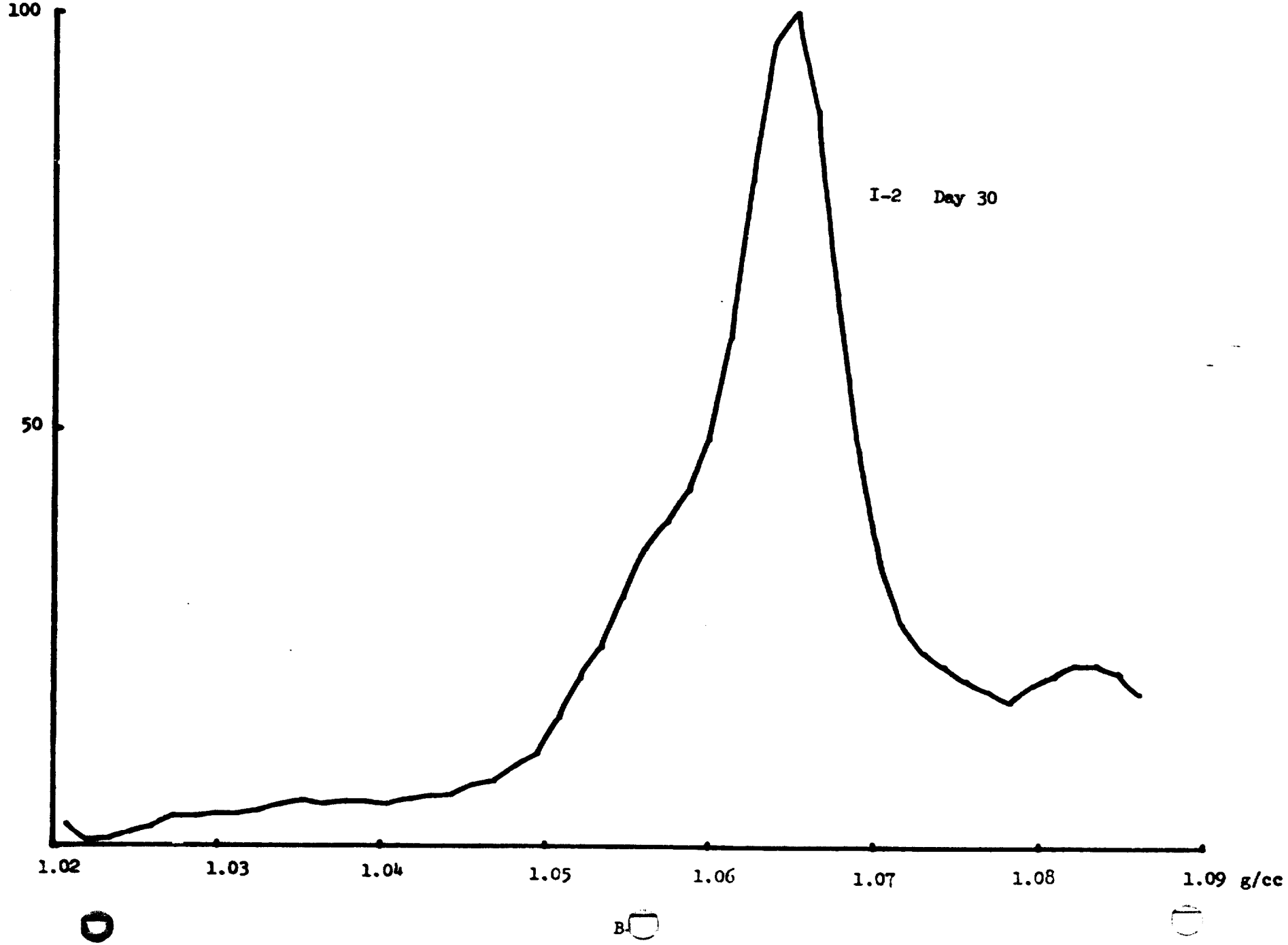
100
50
I-2 Day 30
1.02
1.03
1.04
1.05
1.06
1.07
1.08
1.09 g/cc

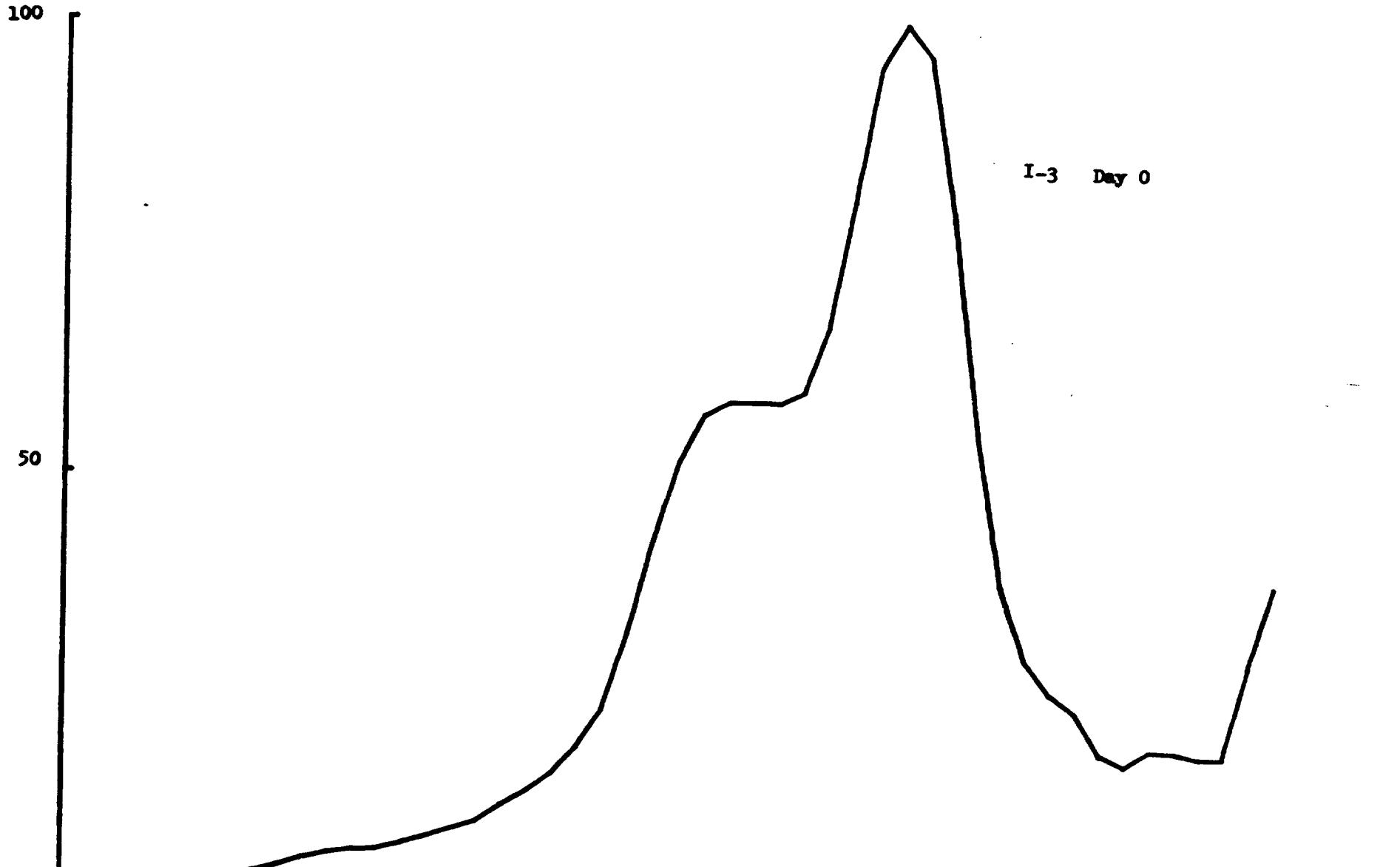
100
50
I-3 Day 0
1.02
1.03
1.04
1.05
1.06
1.07
1.08
1.09 g/cc

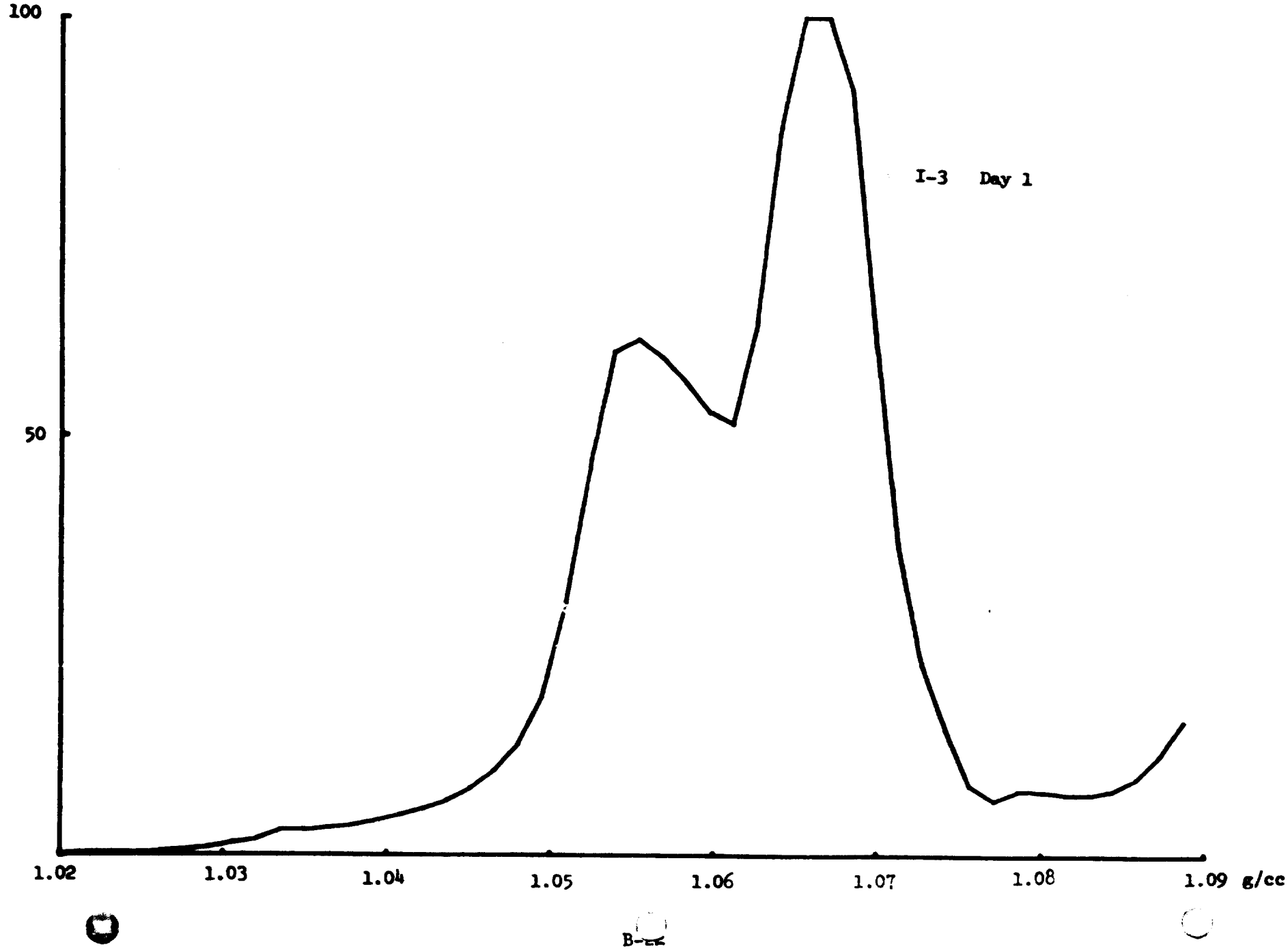
100
50
I-3 Day 1
1.02
1.03
1.04
1.05
1.06
1.07
1.08
1.09 g/cc

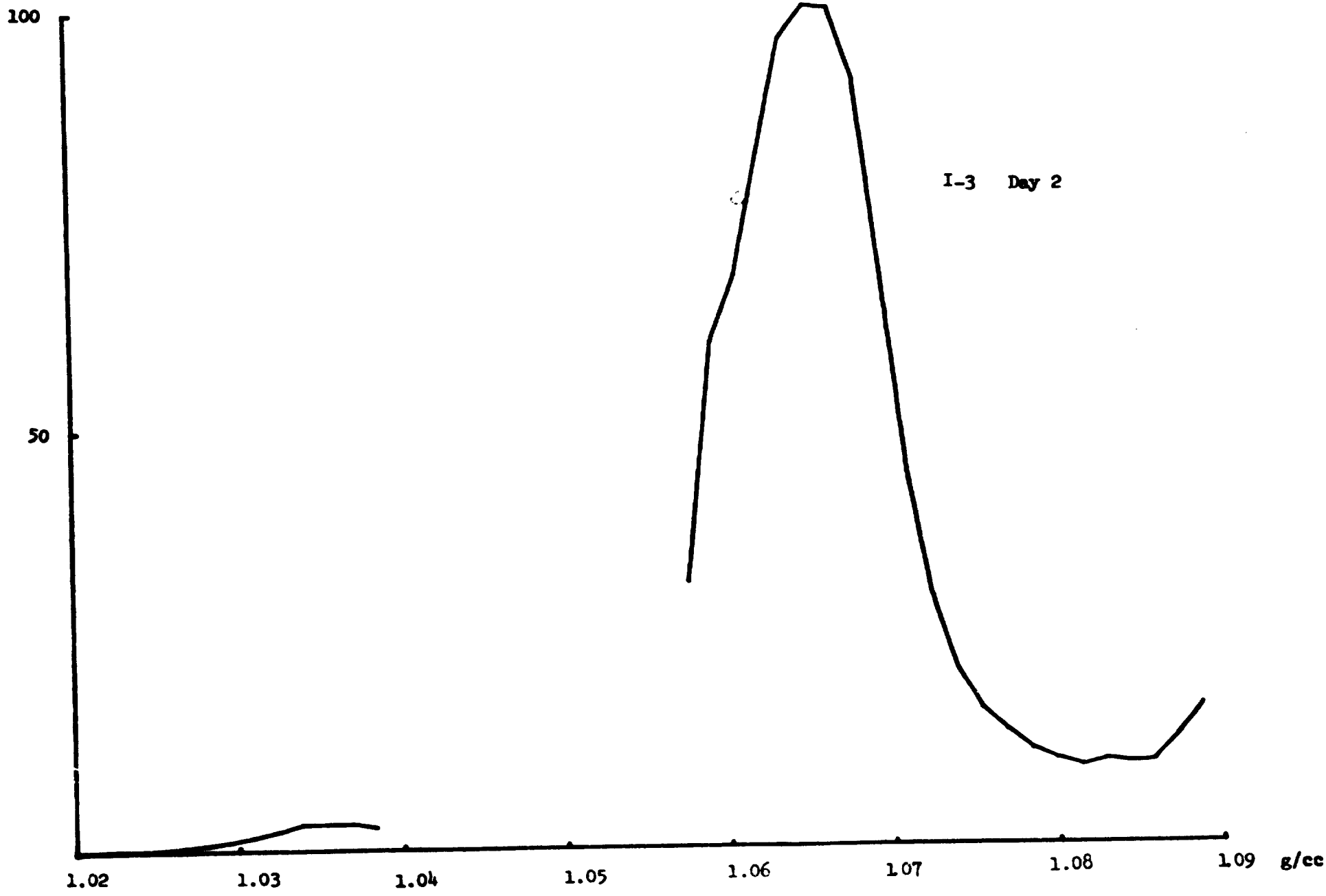
100
50
I-3 Day 2
1.02
1.03
1.04
1.05
1.06
1.07
1.08
1.09
g/cc

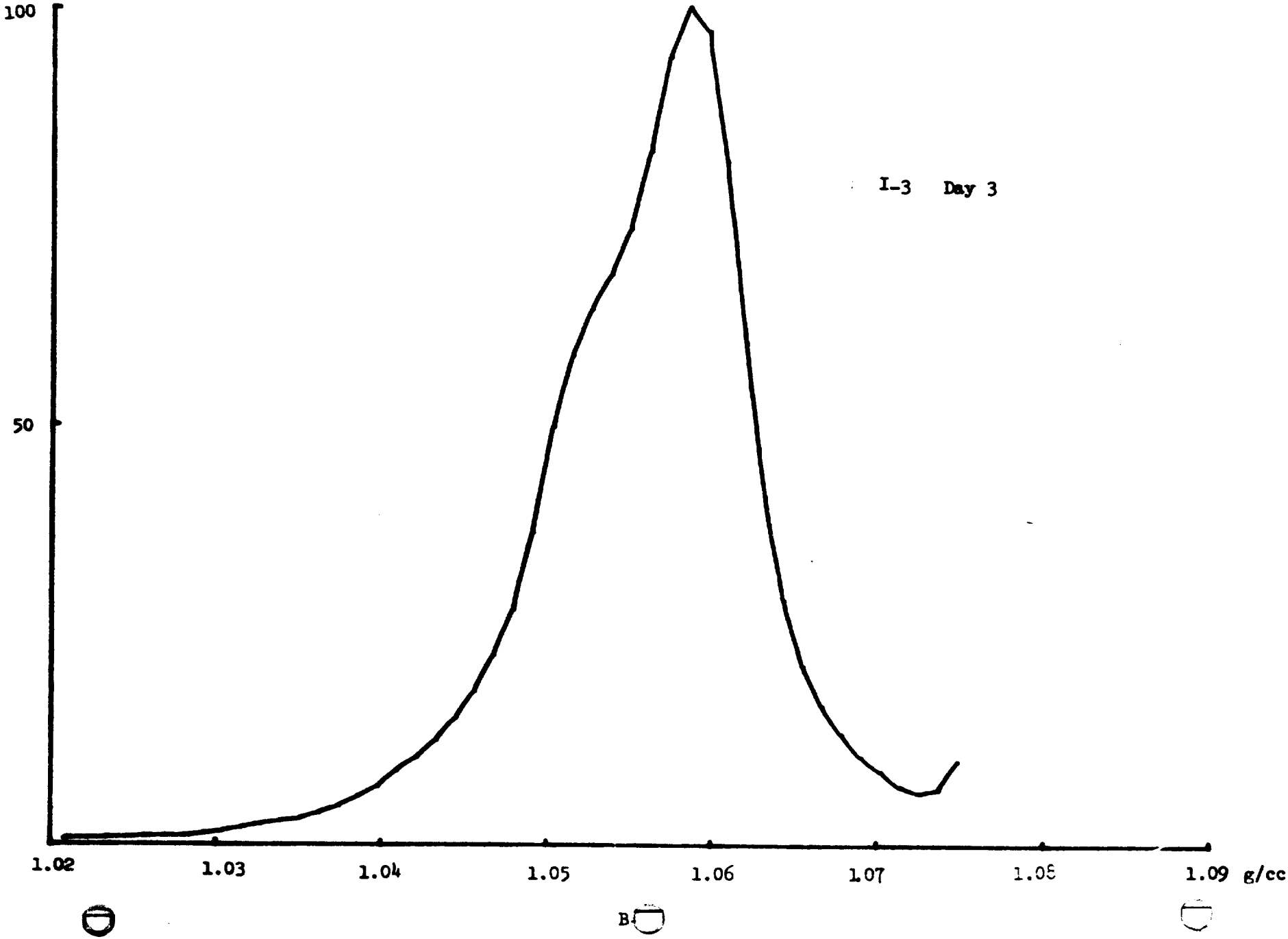
100
50
I-3 Day 3
1.02
1.03
1.04
1.05
1.06
1.07
1.08
1.09 g/cc

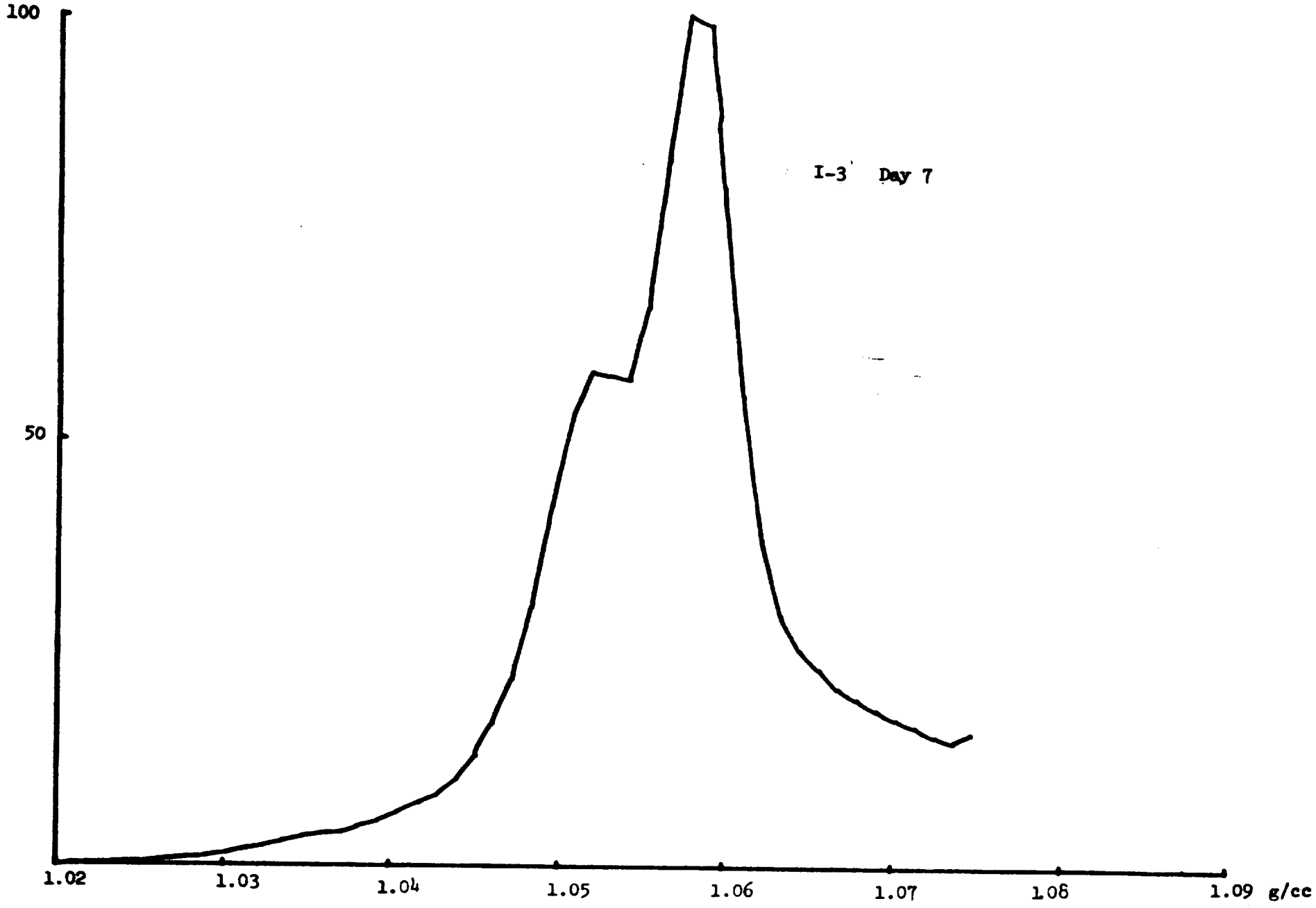
100
50
I-3 Day 7
1.02
1.03
1.04
1.05
1.06
1.07
1.08
1.09 g/cc

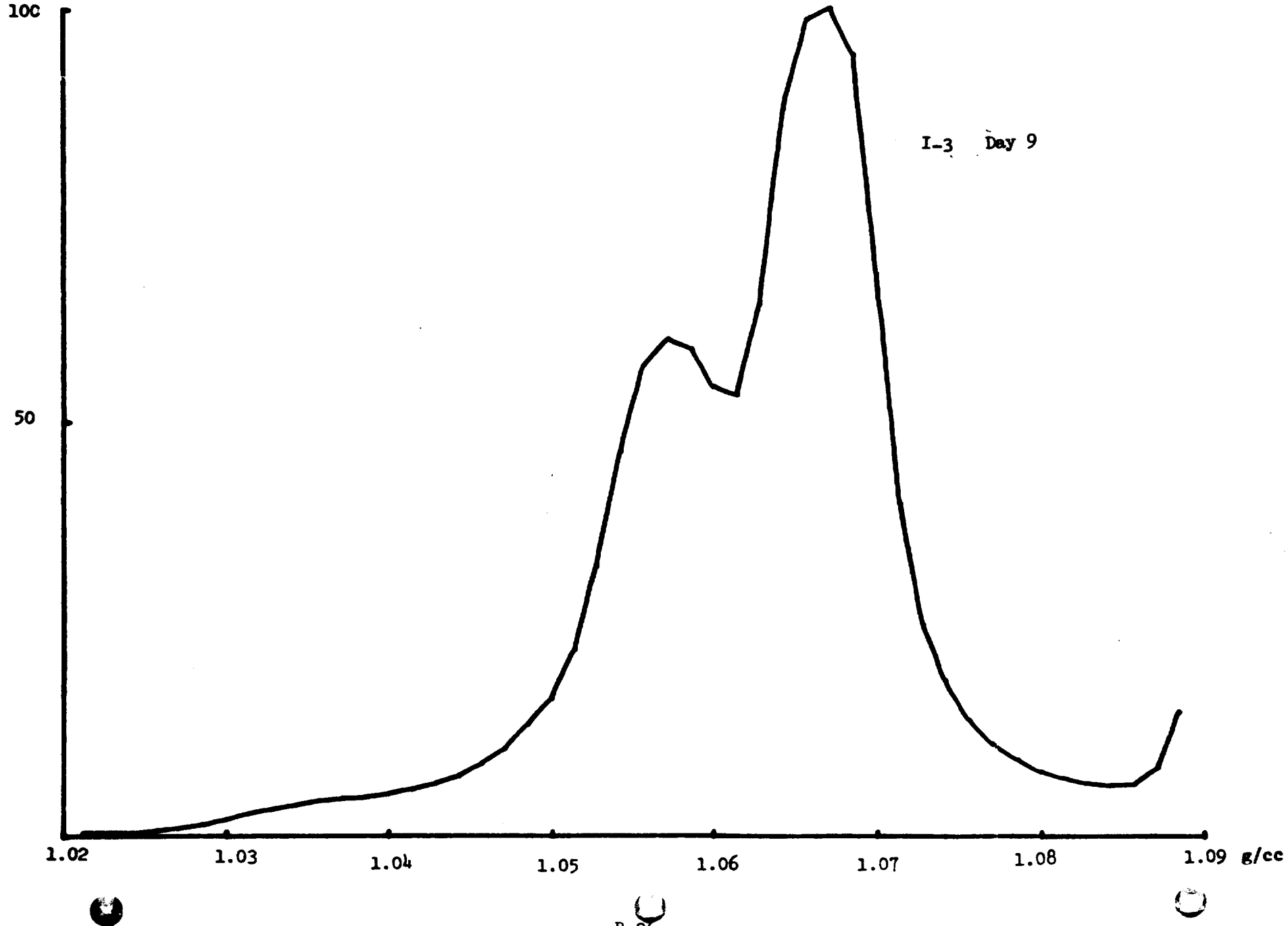
100
50
I-3 Day 9
1.02
1.03
1.04
1.05
1.06
1.07
1.08
1.09 g/cc

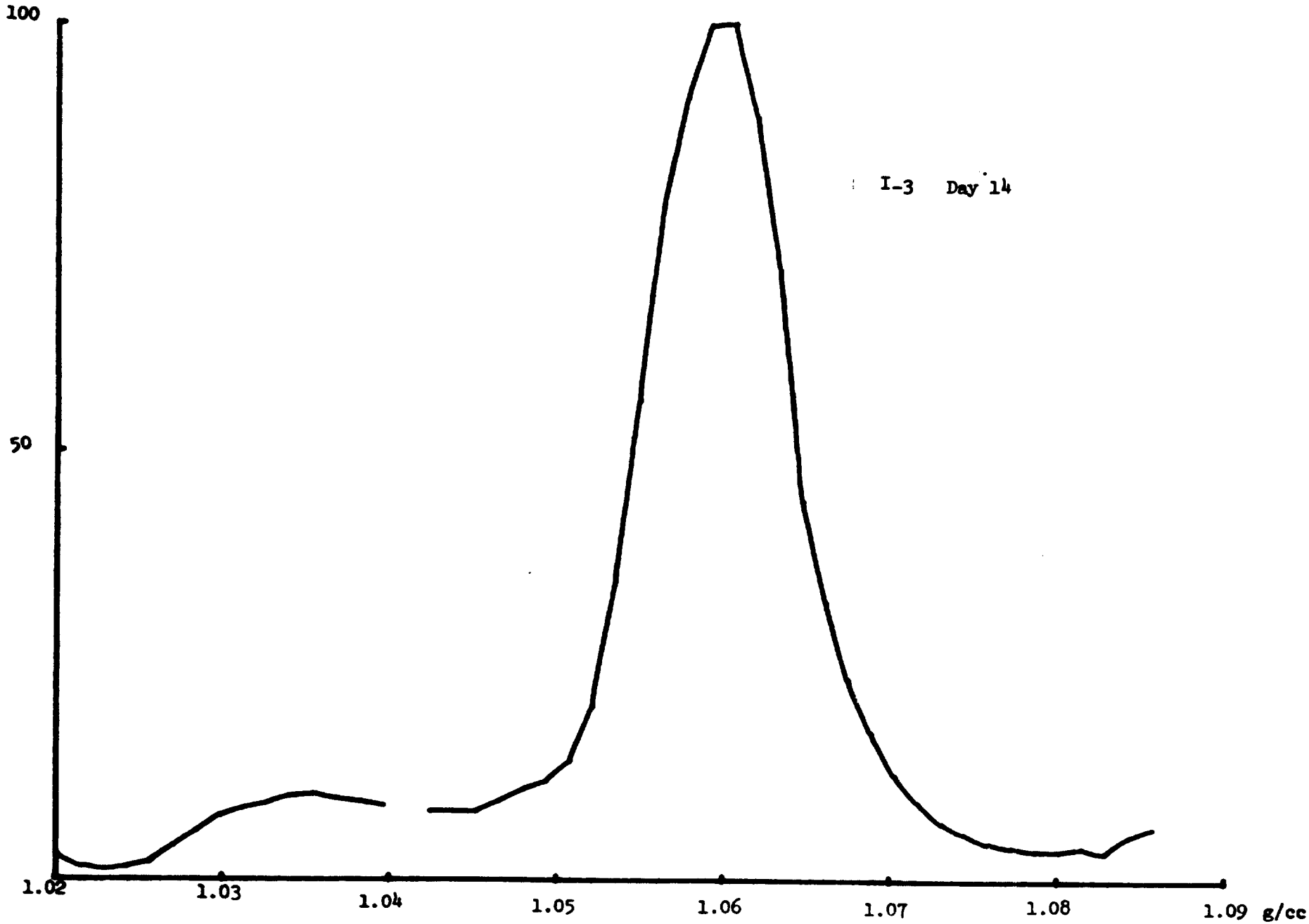
100
50
I-3 Day 14
1.02
1.03
1.04
1.05
1.06
1.07
1.08
1.09 g/cc

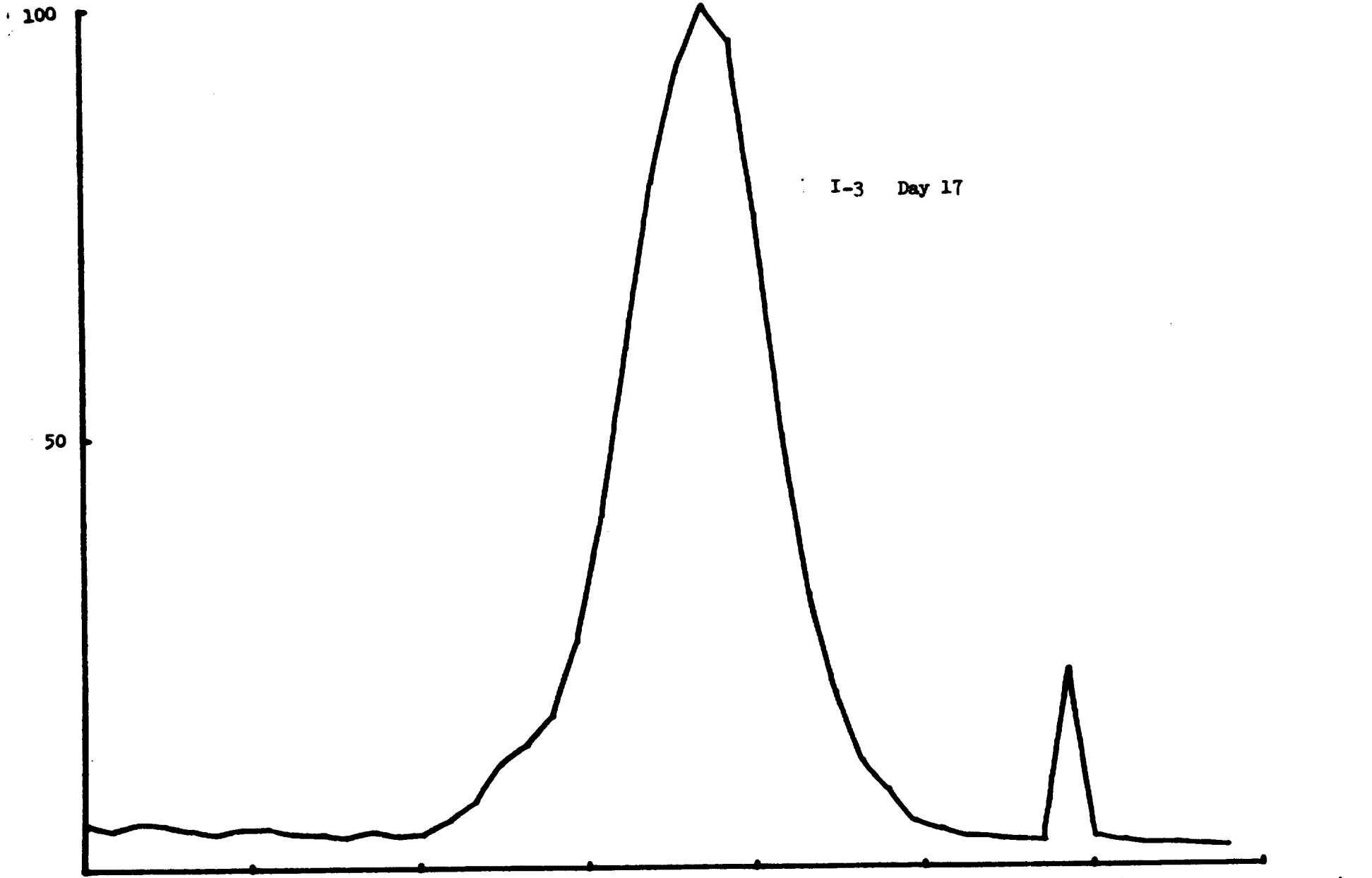
100
50
I-3 Day 17
1.02
1.03
1.04
1.05
1.06
1.07
1.08
1.09 g/cc

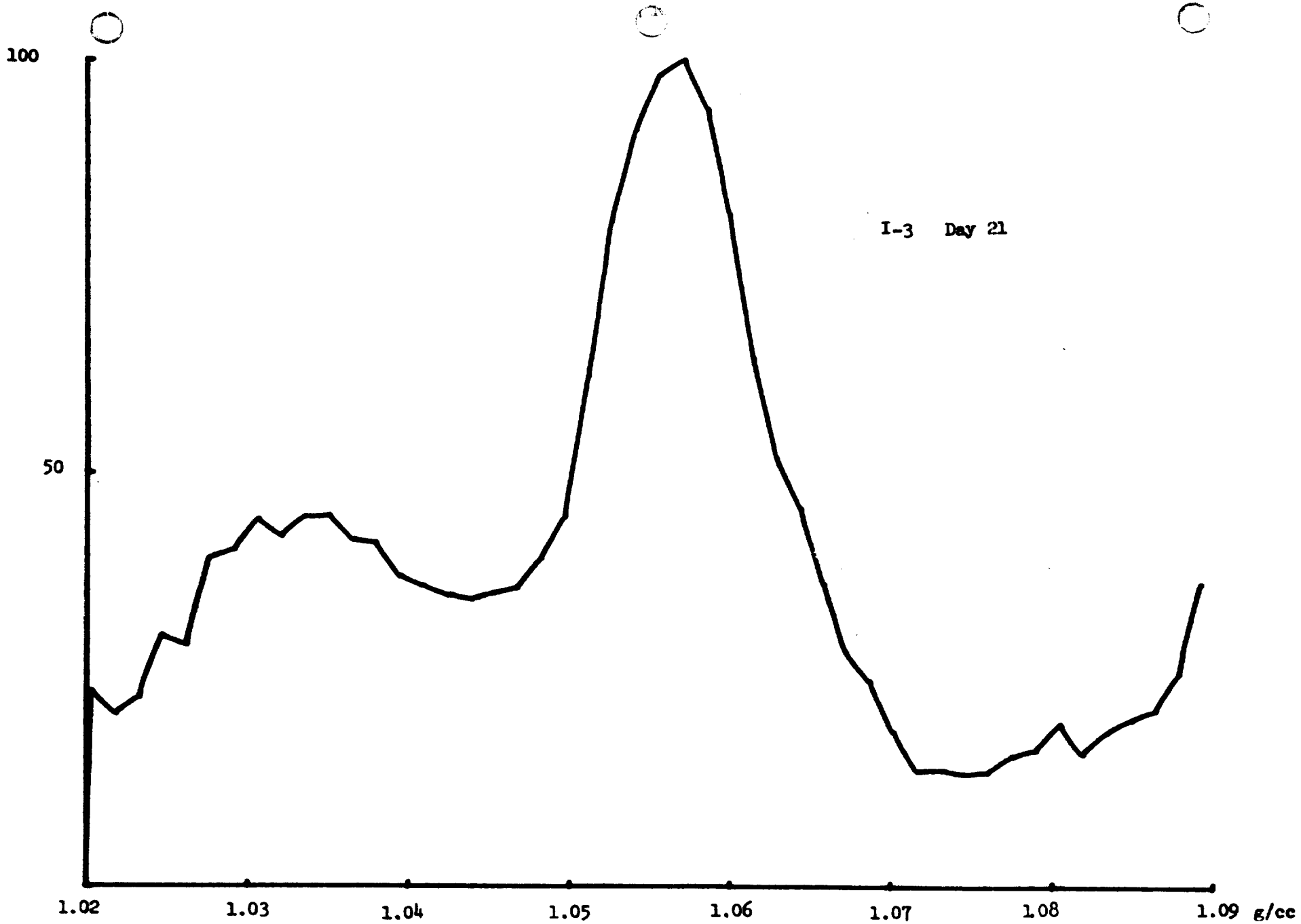
100
50
I-3 Day 21
1.02
1.03
1.04
1.05
1.06
1.07
1.08
1.09 g/cc

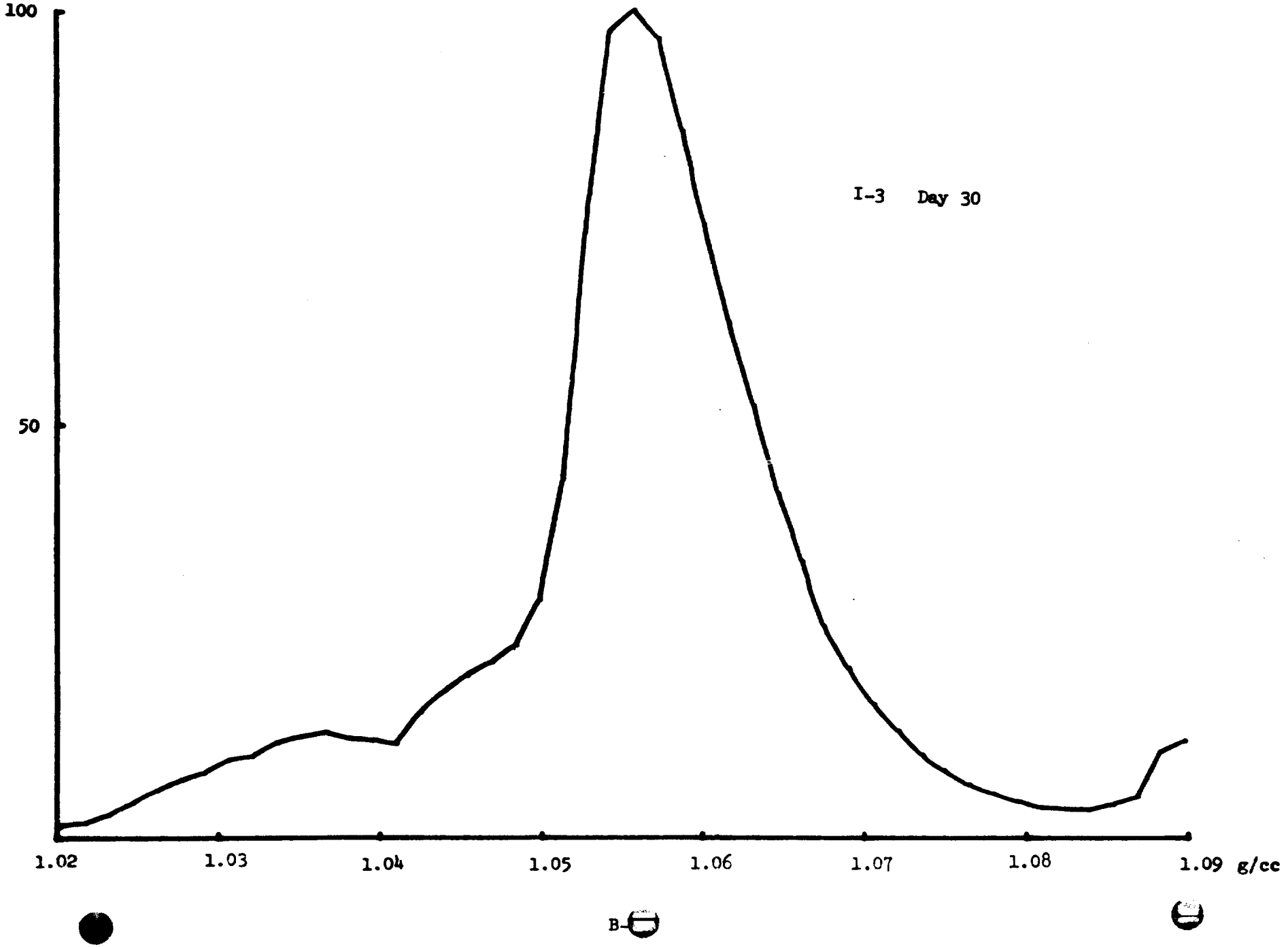
100
50
I-3 Day 30
1.02
1.03
1.04
1.05
1.06
1.07
1.08
1.09 g/cc

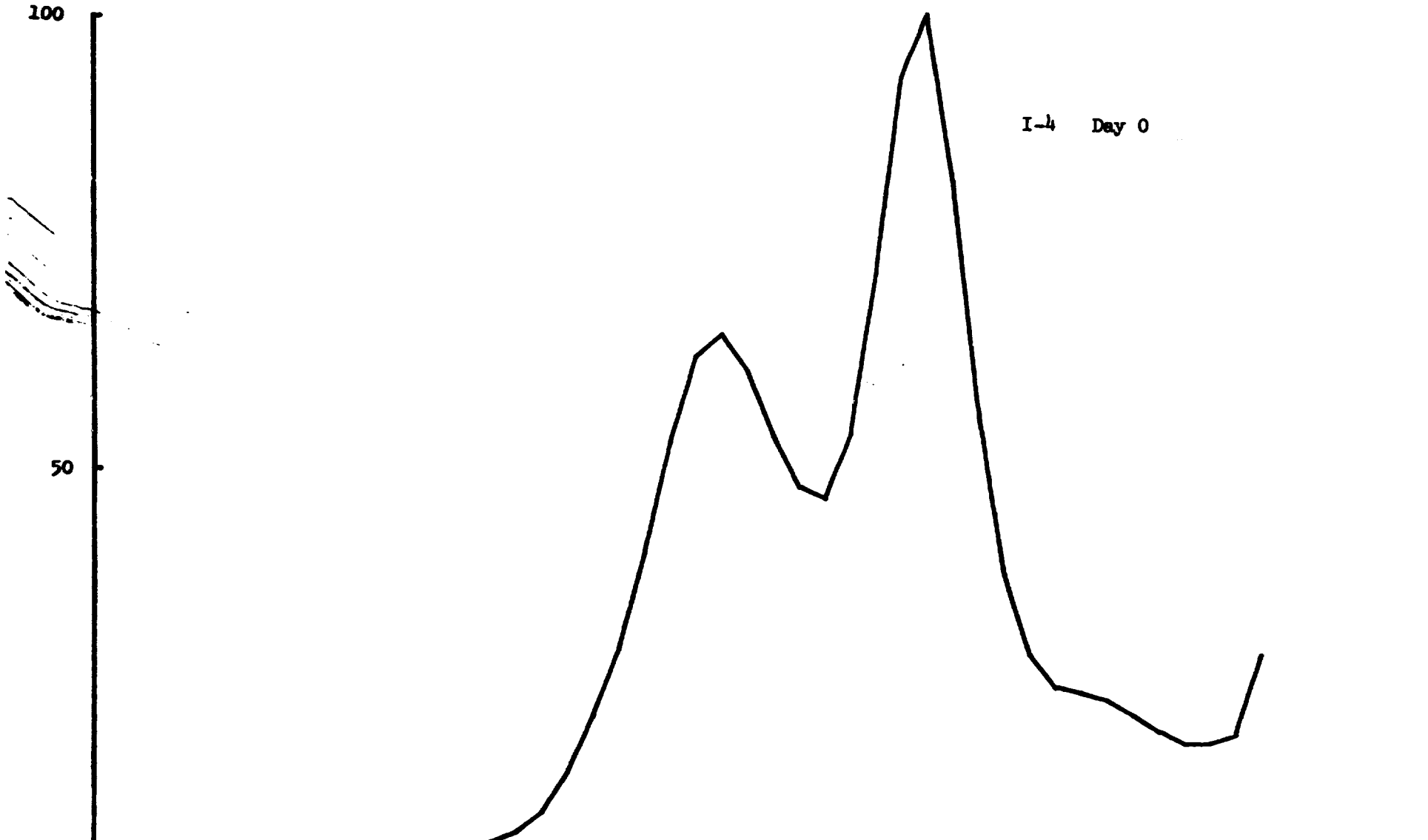
100
50
I-4 Day 0
1.02
1.03
1.04
1.05
1.06
1.07
1.08
1.09 g/cc

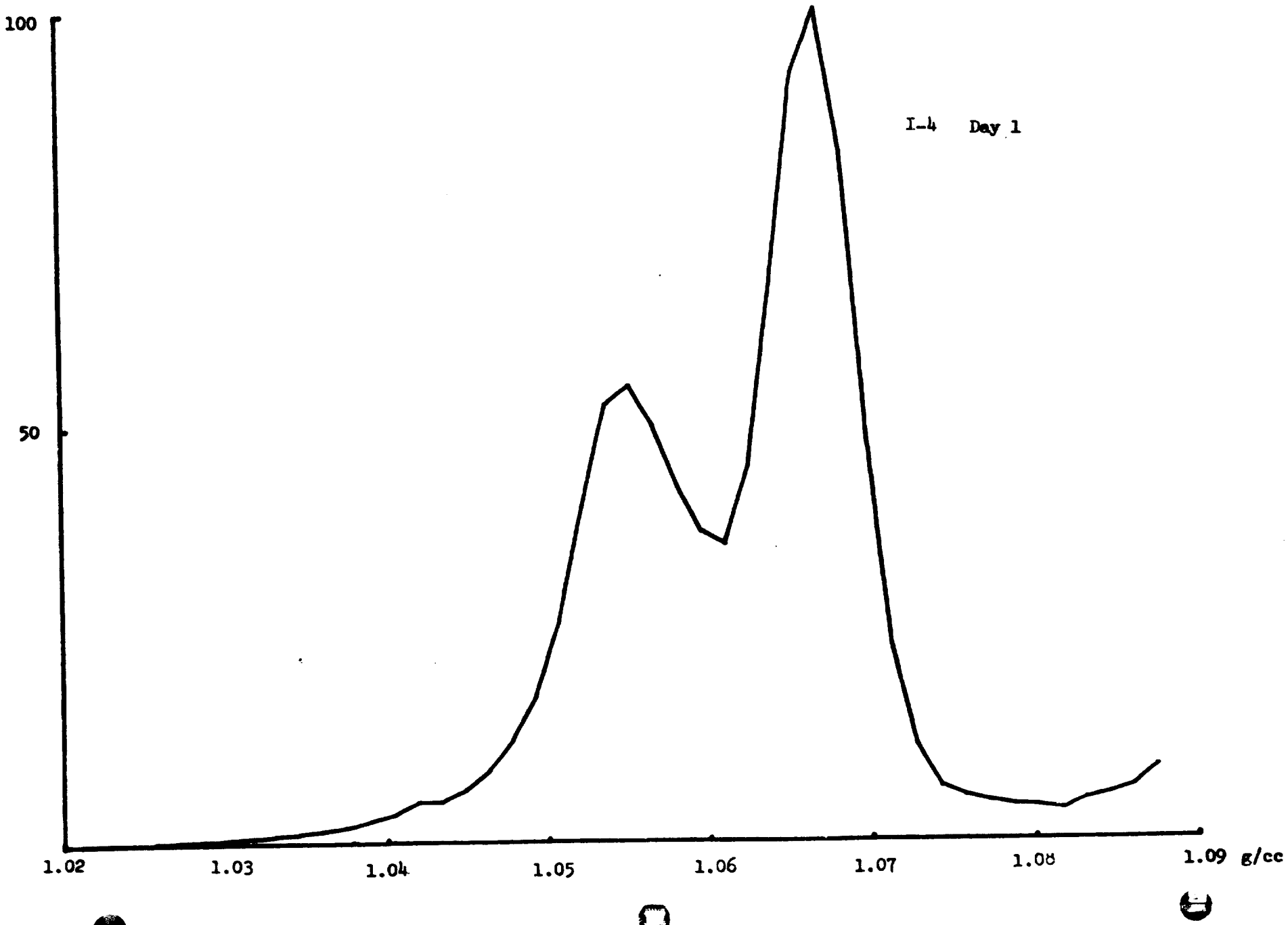
100
50
I-4 Day 1
1.02
1.03
1.04
1.05
1.06
1.07
1.08
1.09 g/cc

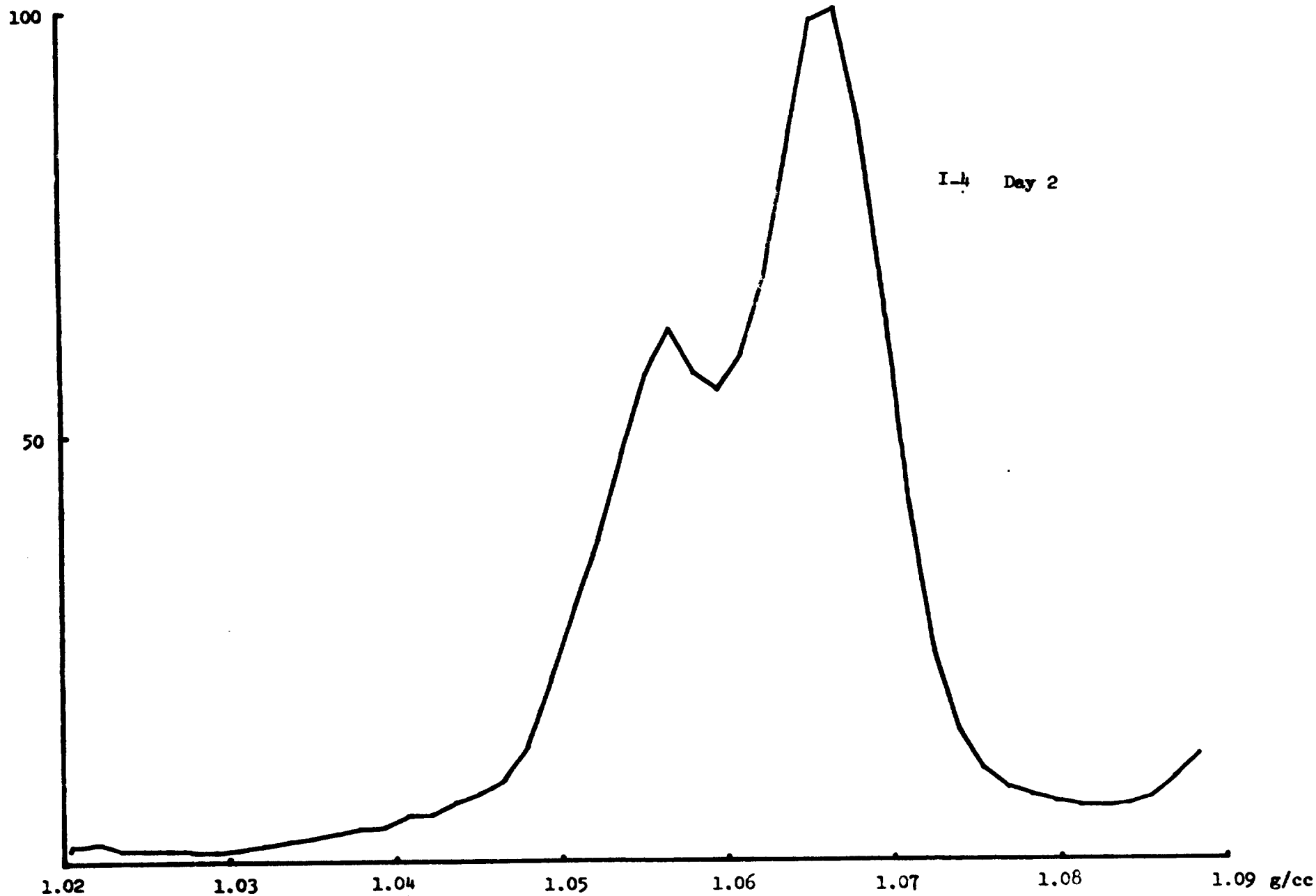
100
50
I-4 Day 2
1.02
1.03
1.04
1.05
1.06
1.07
1.08
1.09 g/cc

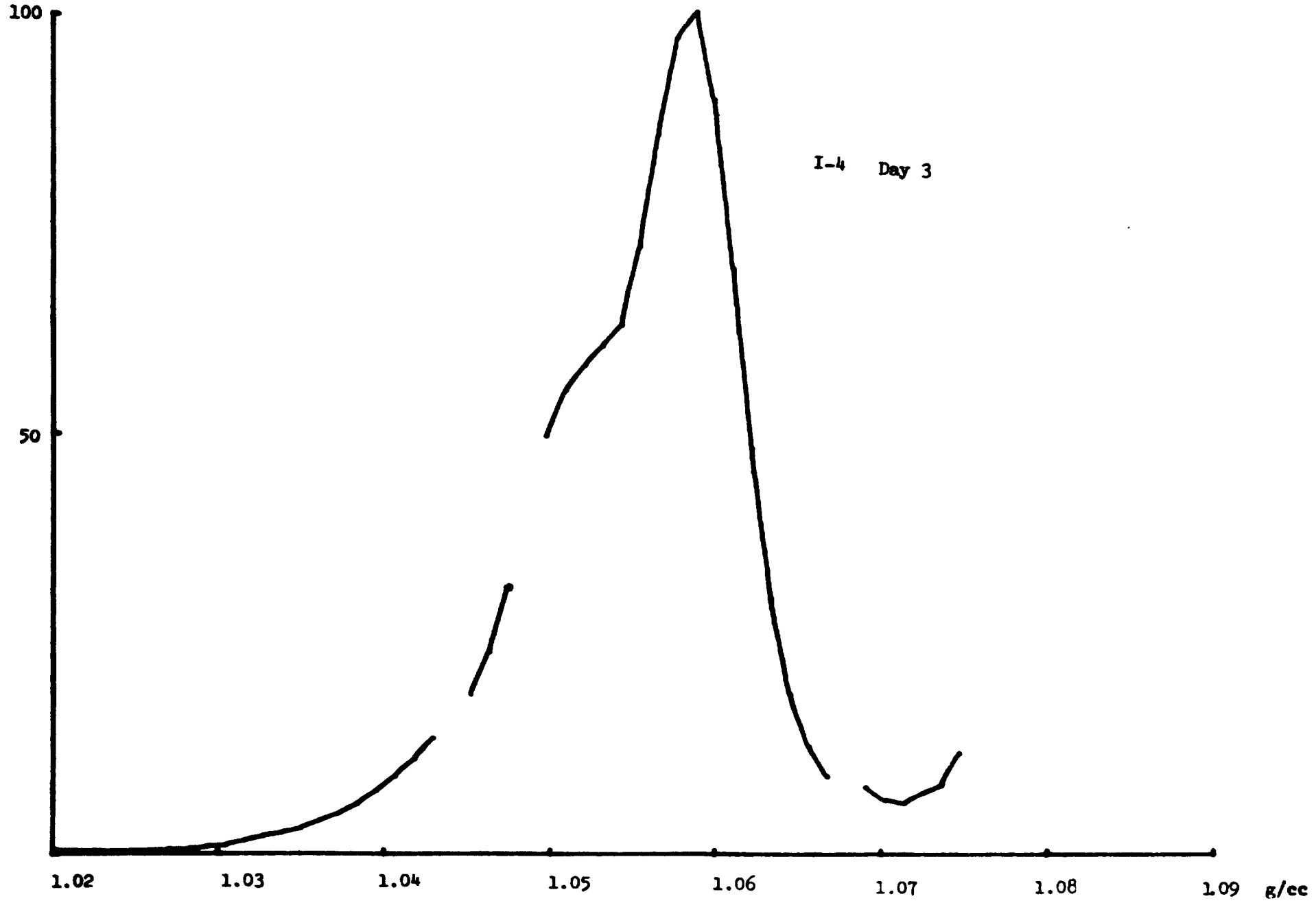
100
50
I-4 Day 3
1.02
1.03
1.04
1.05
1.06
1.07
1.08
1.09
g/cc

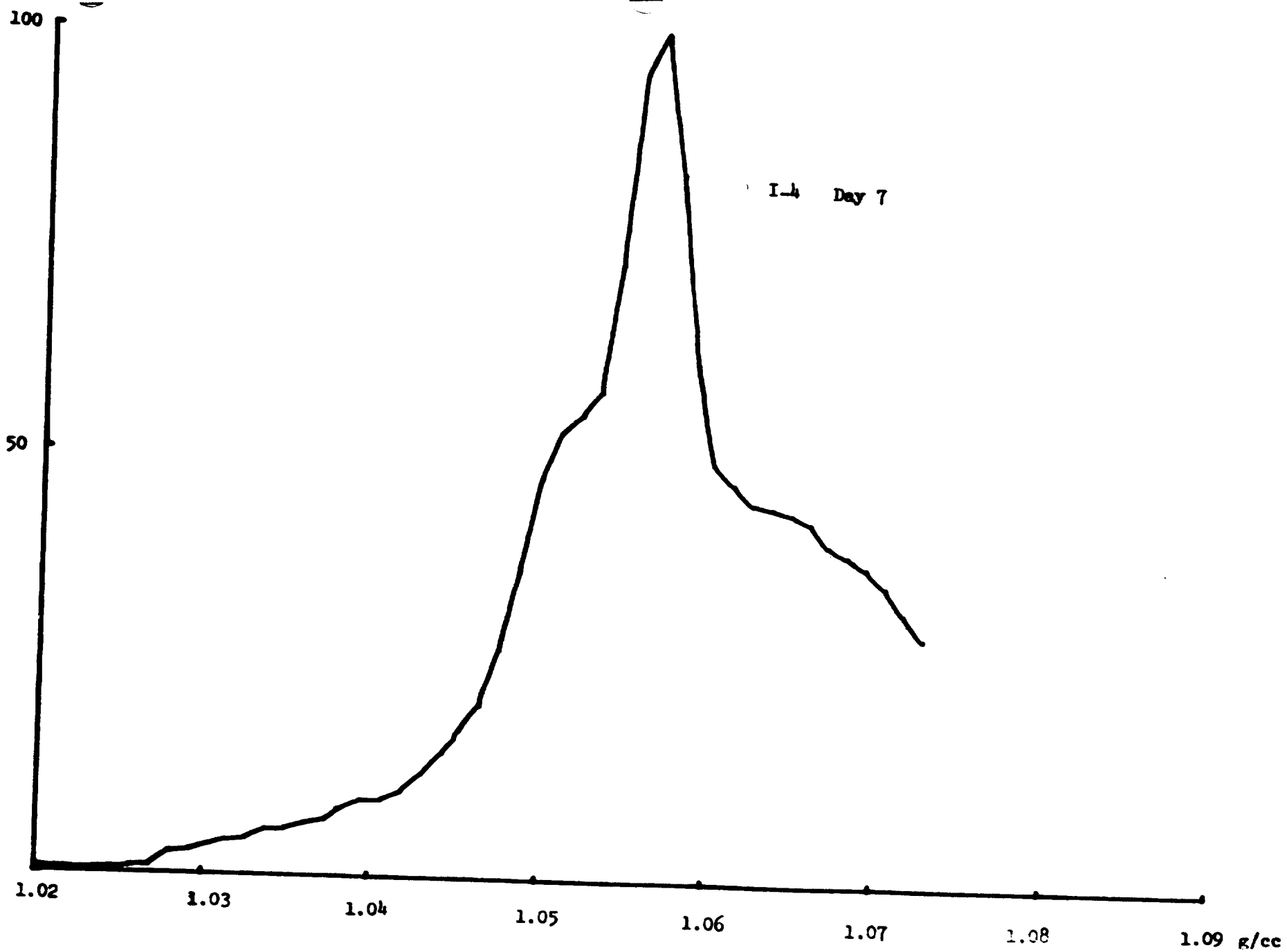
100
50
I-4 Day 7
1.02
1.03
1.04
1.05
1.06
1.07
1.08
1.09 g/cc

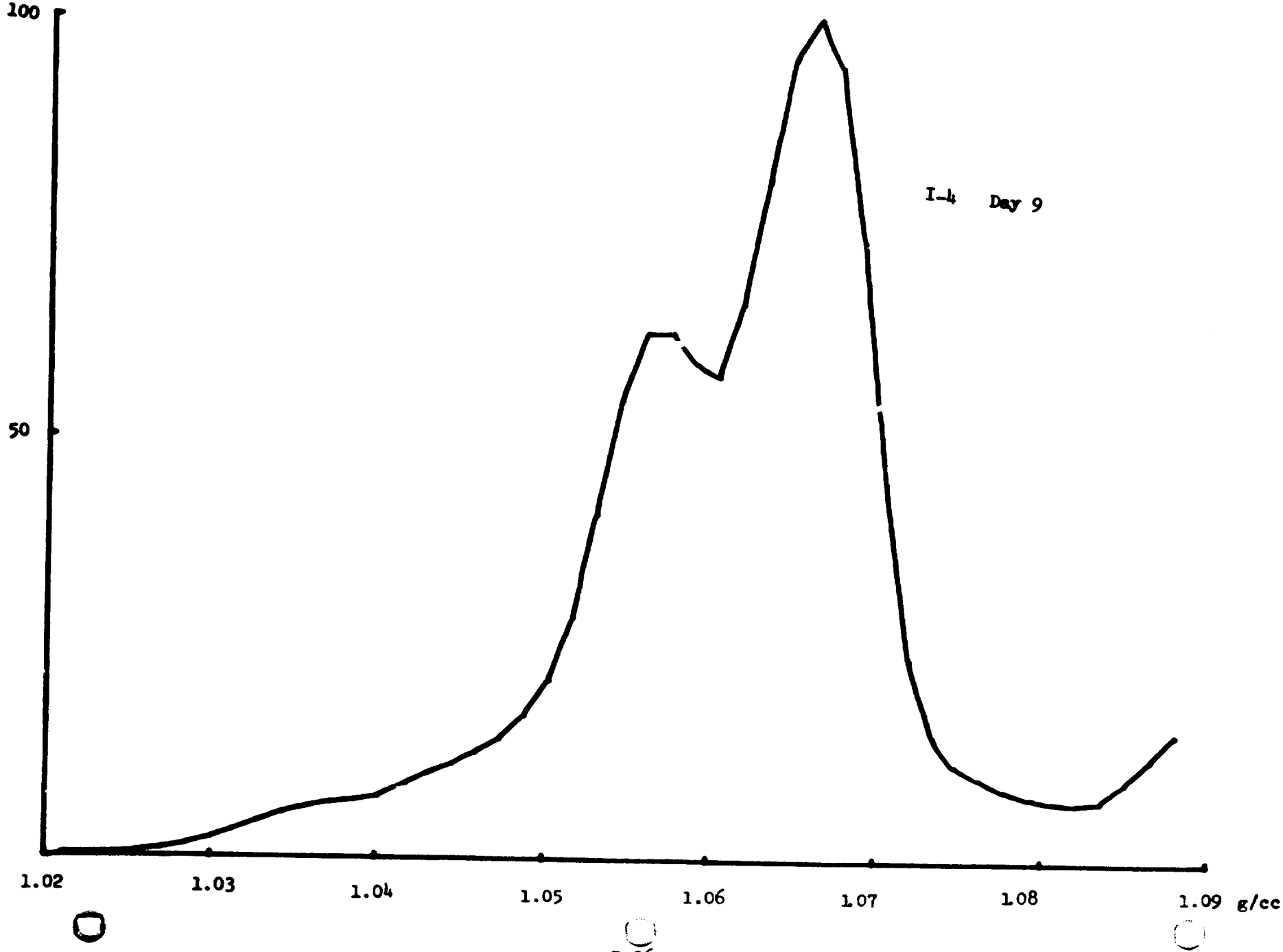
100
50
I-4 Day 9
1.02
1.03
1.04
1.05
1.06
1.07
1.08
1.09 g/cc

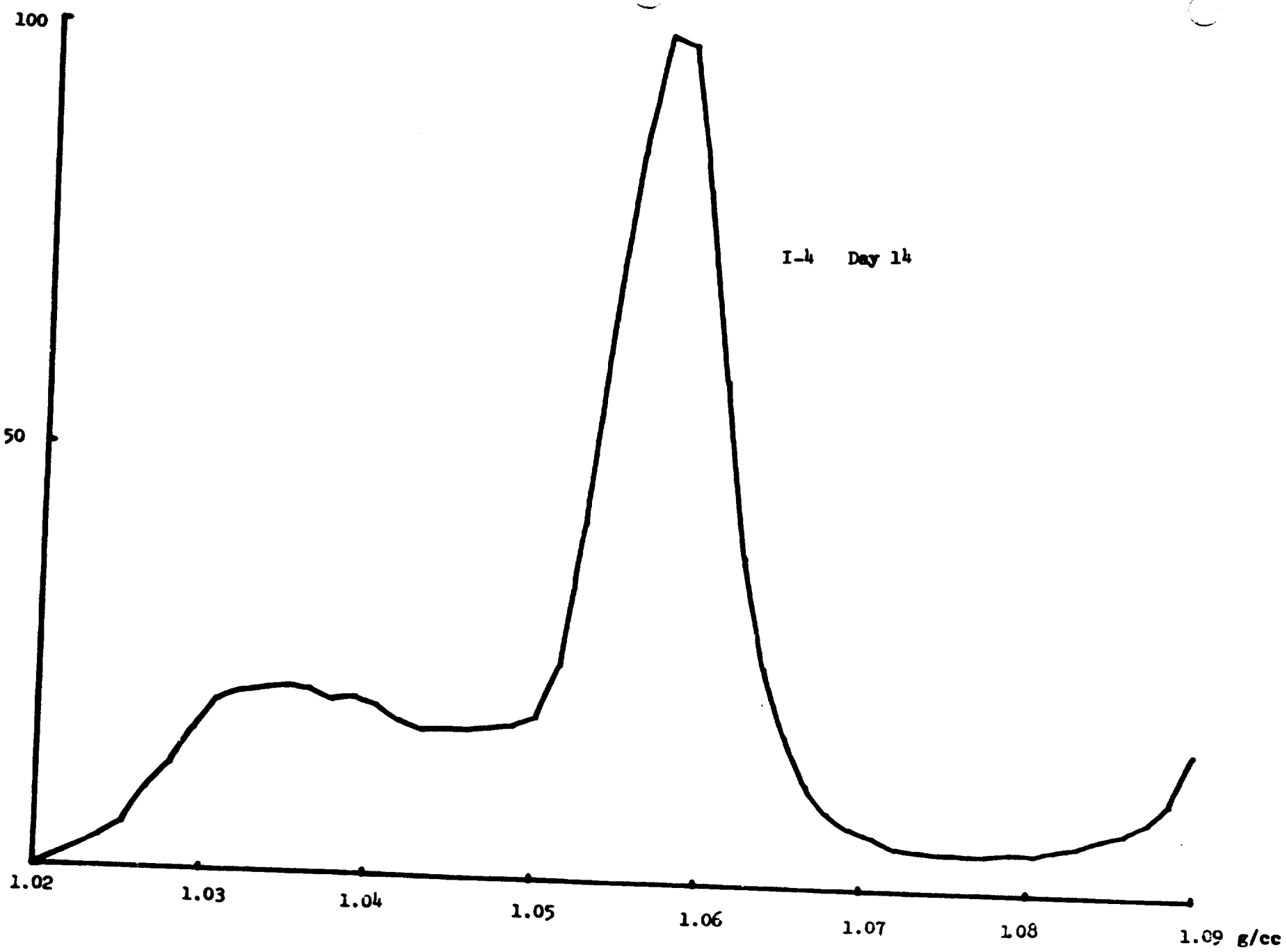
100
50
I-4 Day 14
1.02
1.03
1.04
1.05
1.06
1.07
1.08
1.09 g/cc

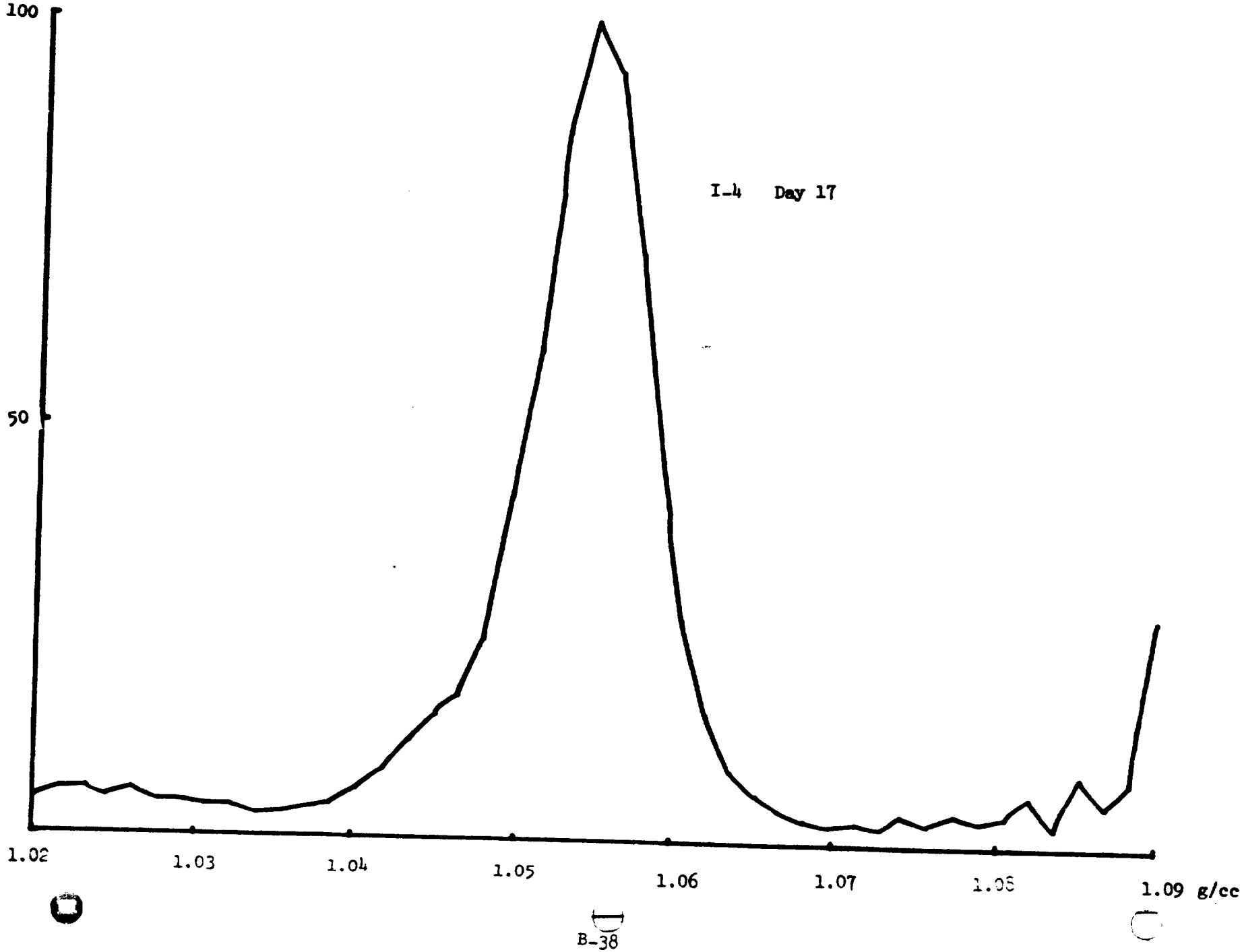
100
50
I-4 Day 17
1.02
1.03
1.04
1.05
1.06
1.07
1.08
1.09 g/cc

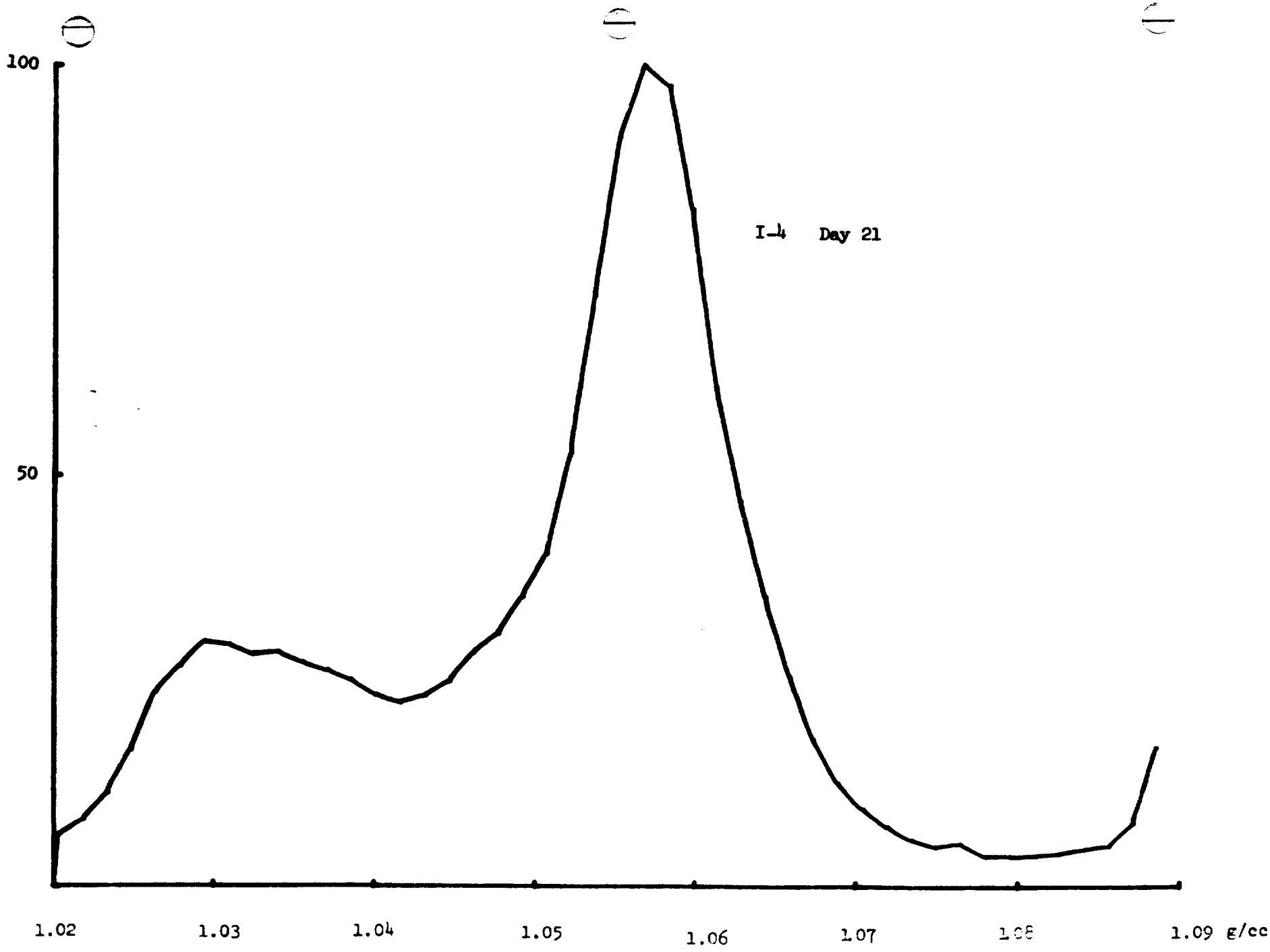
100
50
I-4 Day 21
1.02
1.03
1.04
1.05
1.06
1.07
1.08
1.09 g/cc

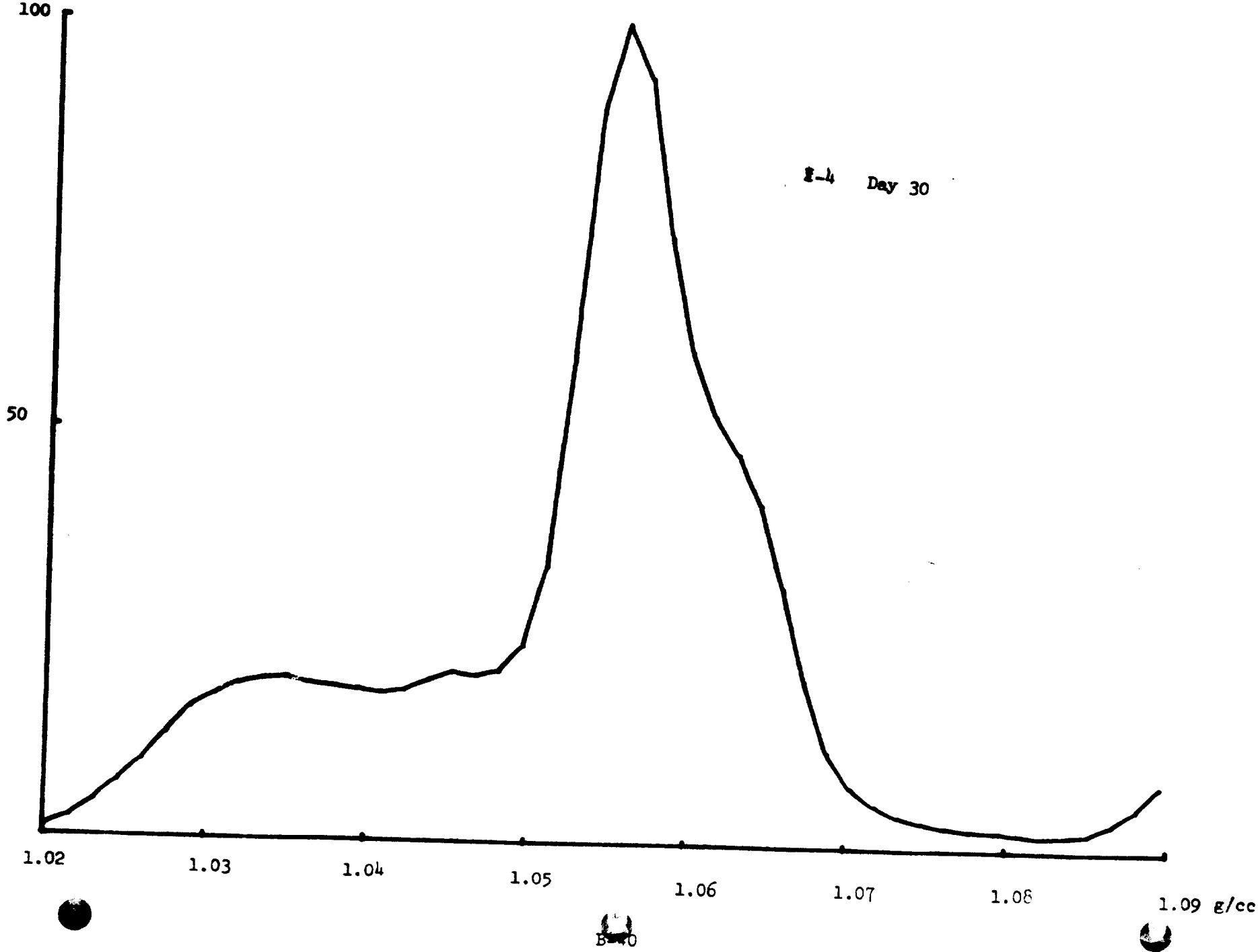
100
50
E-4 Day 30
1.02
1.03
1.04
1.05
1.06
1.07
1.08
1.09 g/cc

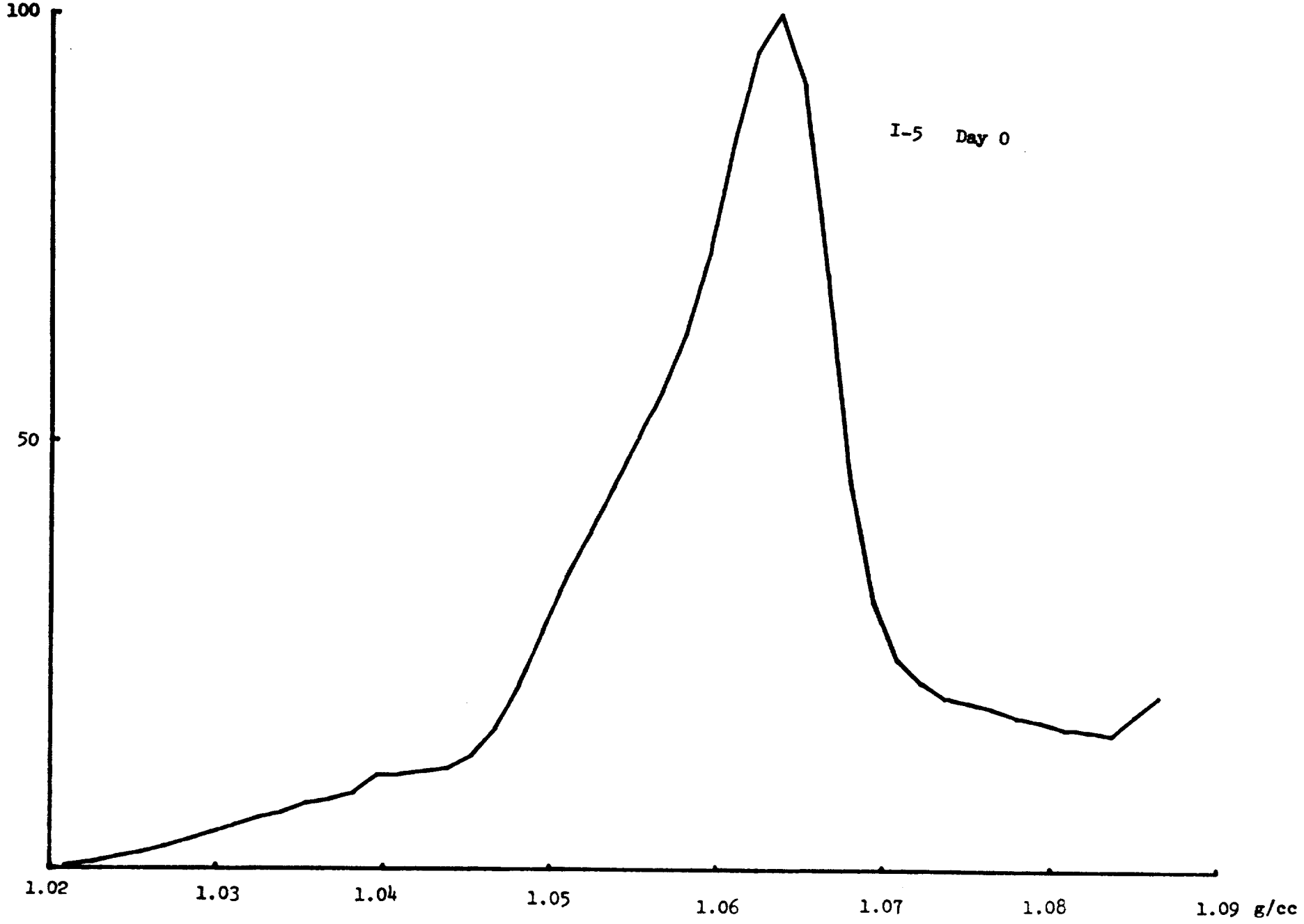
100
50
I-5 Day 0
1.02
1.03
1.04
1.05
1.06
1.07
1.08
1.09 g/cc

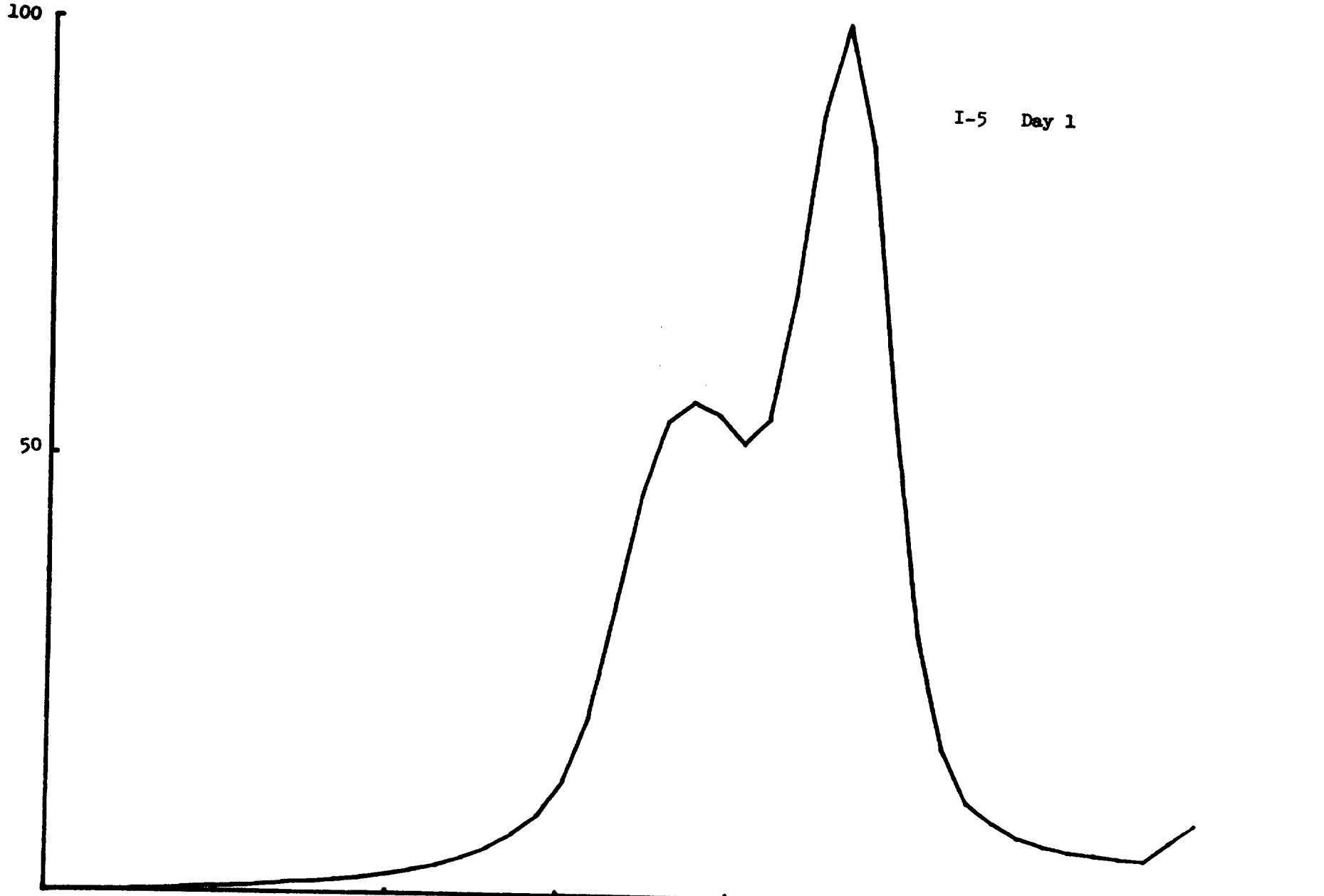
100
50
I-5 Day 1
1.02
1.03
1.04
1.05
1.06
1.07
1.08
1.09 g/cc

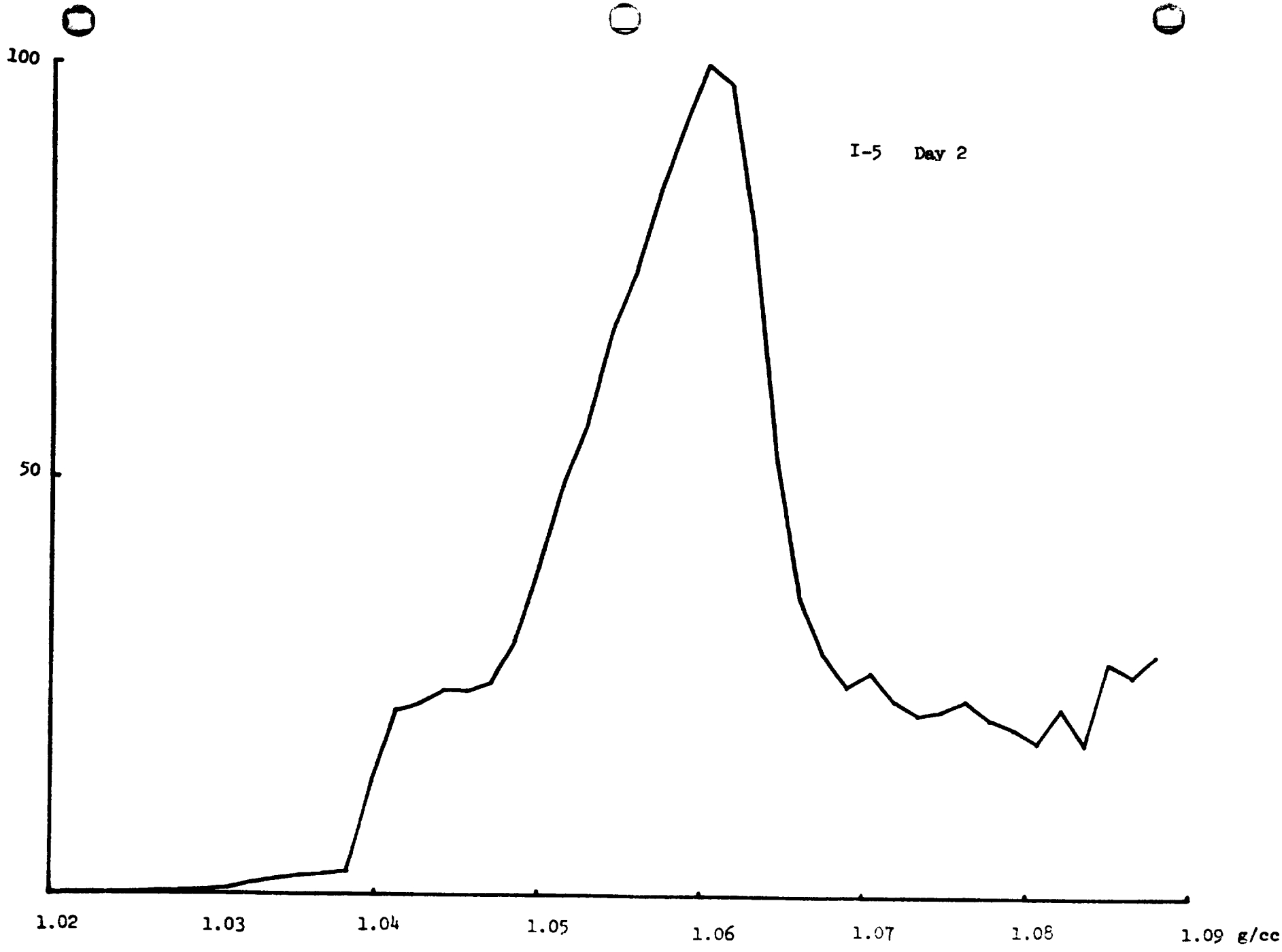
100
50
I-5 Day 2
1.02
1.03
1.04
1.05
1.06
1.07
1.08
1.09 g/cc

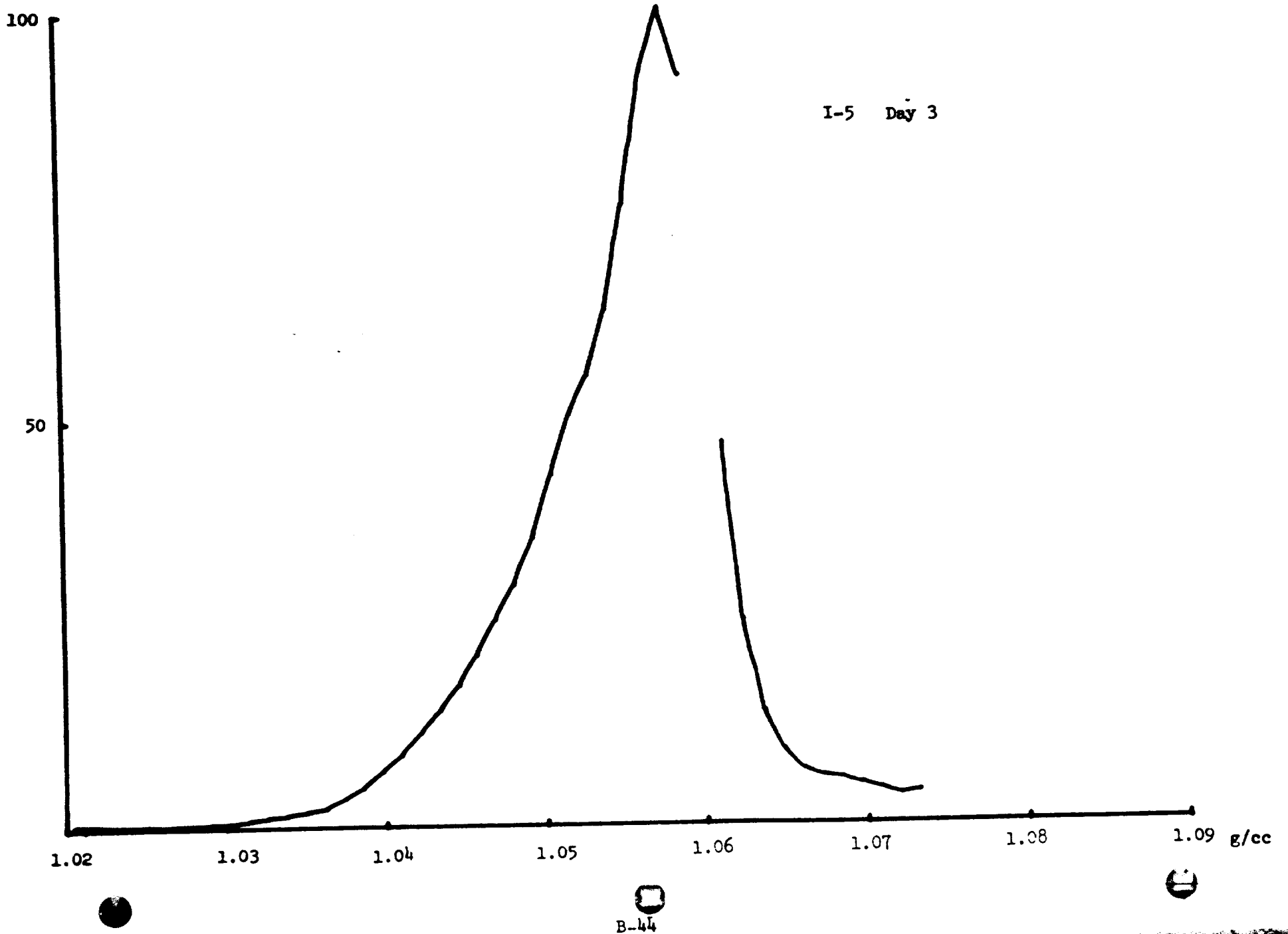
100
50
I-5 Day 3
1.02
1.03
1.04
1.05
1.06
1.07
1.08
1.09 g/cc

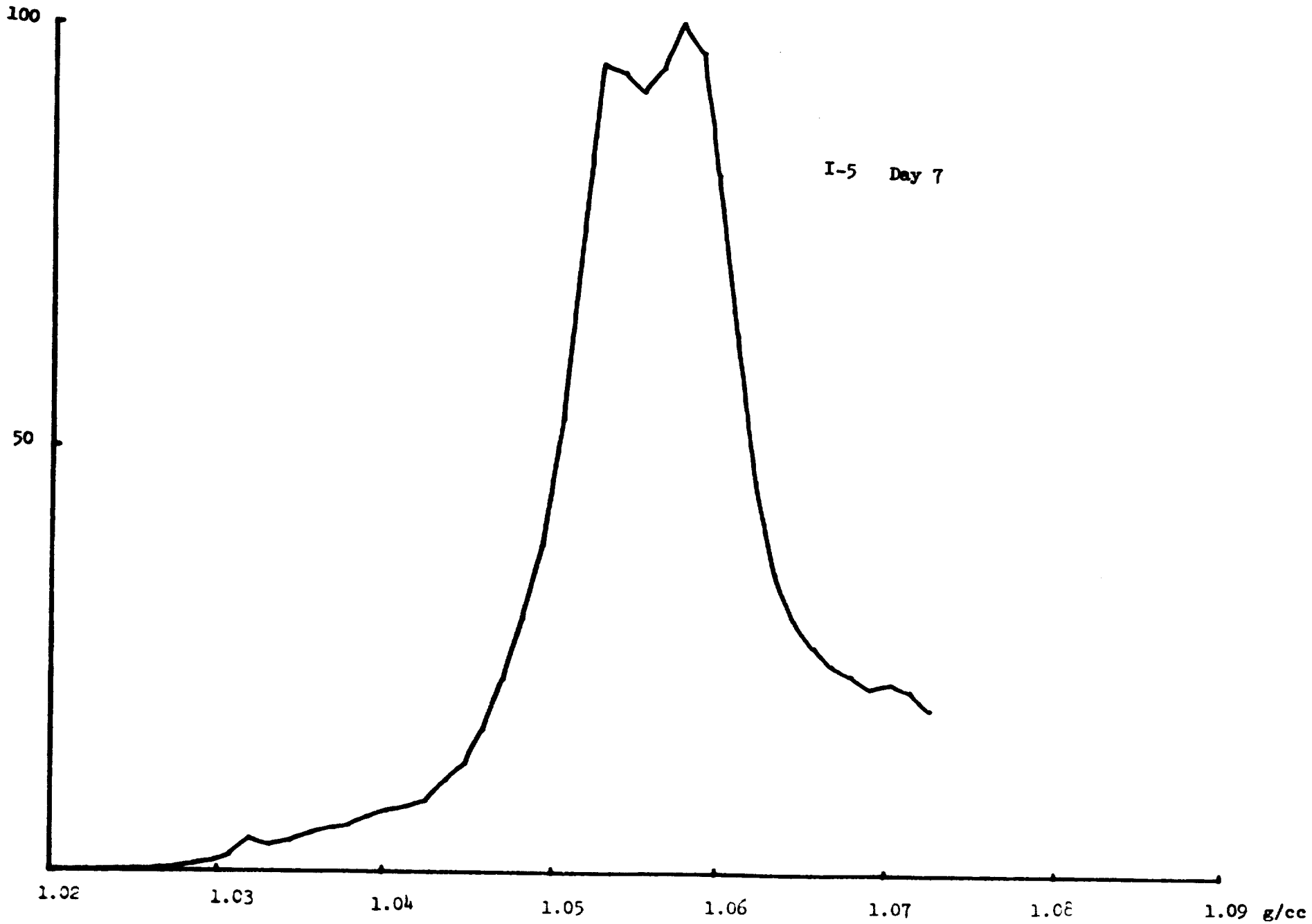
100
50
I-5 Day 7
1.02
1.03
1.04
1.05
1.06
1.07
1.08
1.09 g/cc

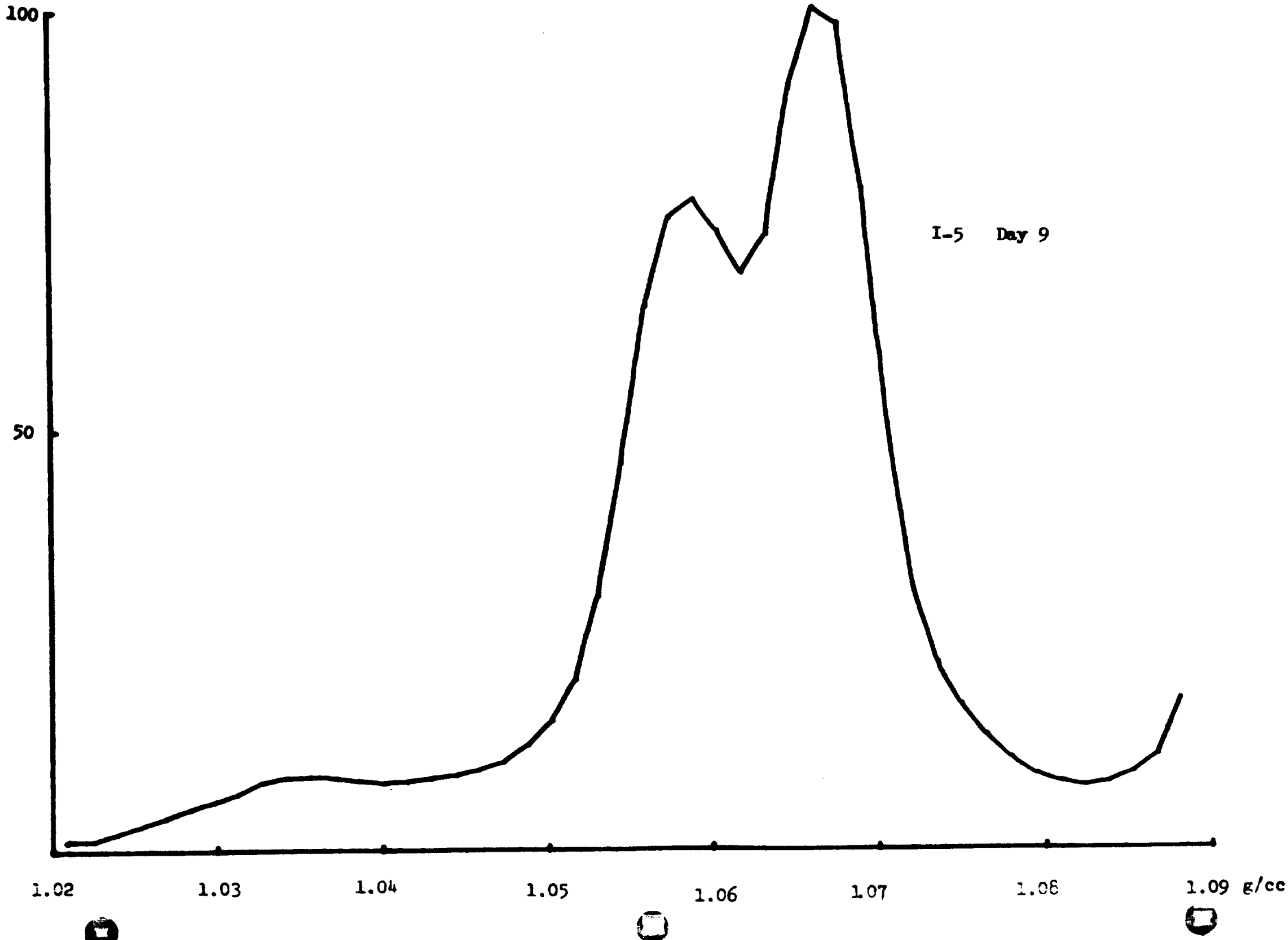
100
50
I-5 Day 9
1.02
1.03
1.04
1.05
1.06
1.07
1.08
1.09 g/cc

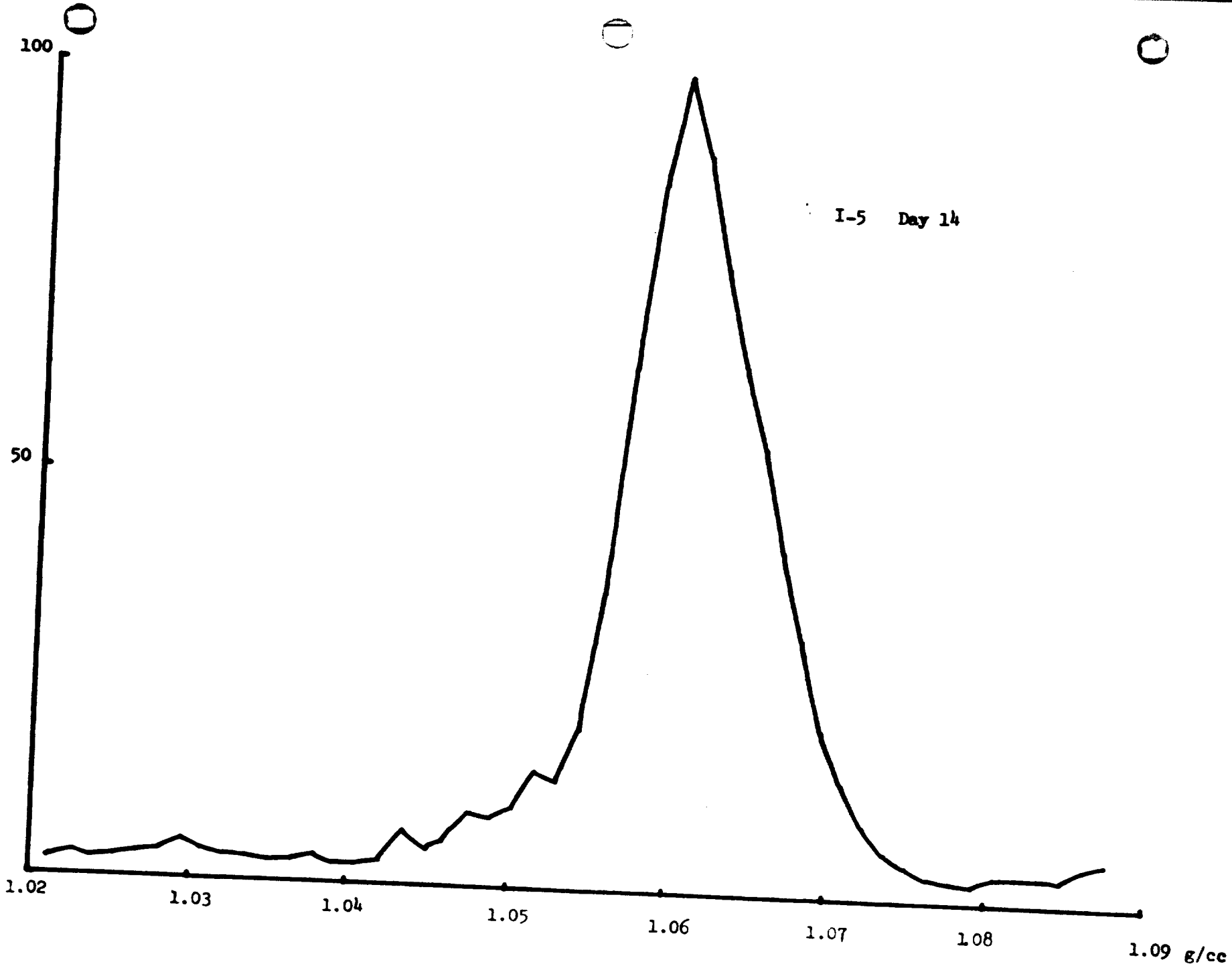
100
50
I-5 Day 14
1.02
1.03
1.04
1.05
1.06
1.07
1.08
1.09 g/cc

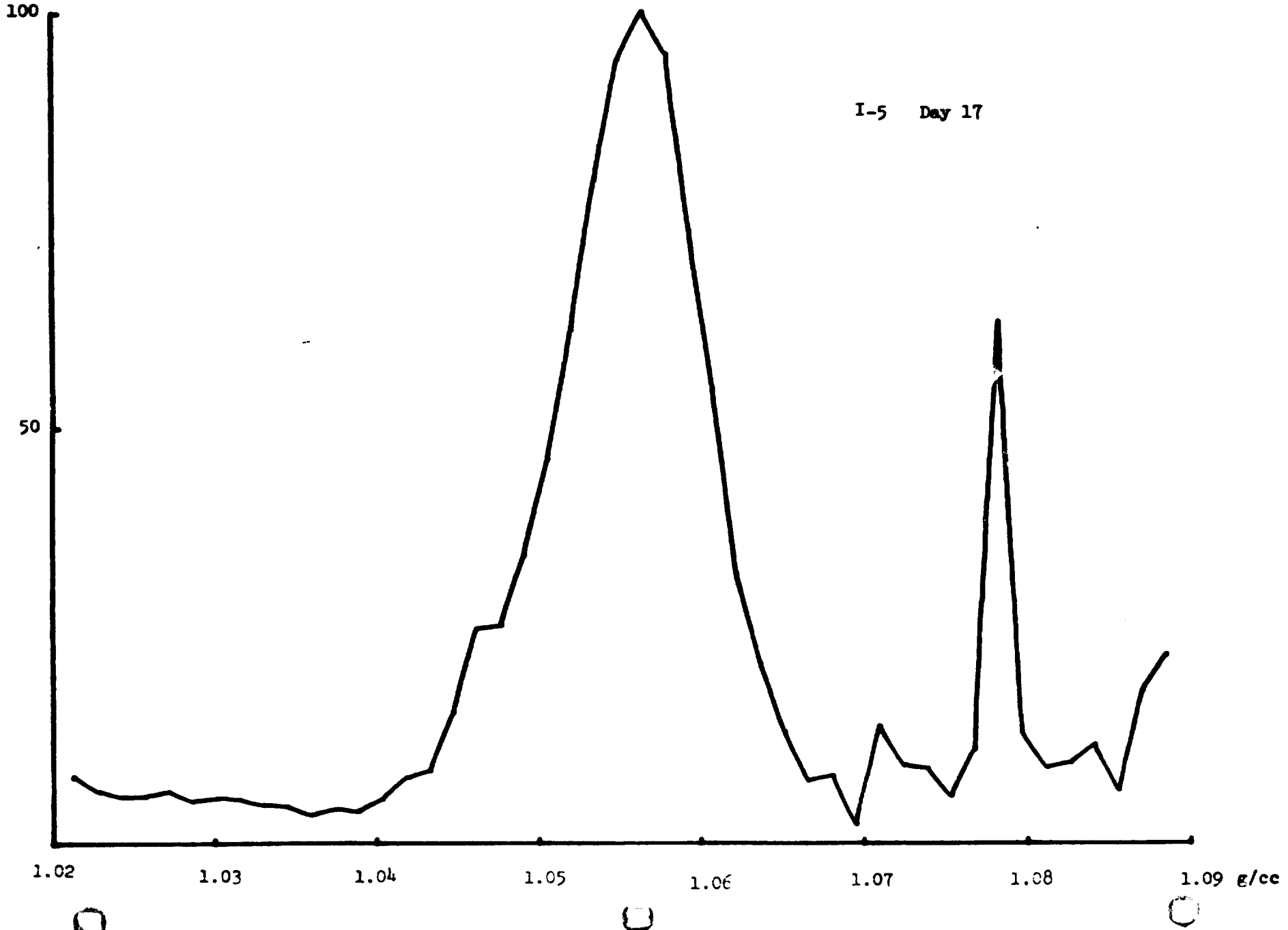
100
50
I-5 Day 17
1.02
1.03
1.04
1.05
1.06
1.07
1.08
1.09 g/cc

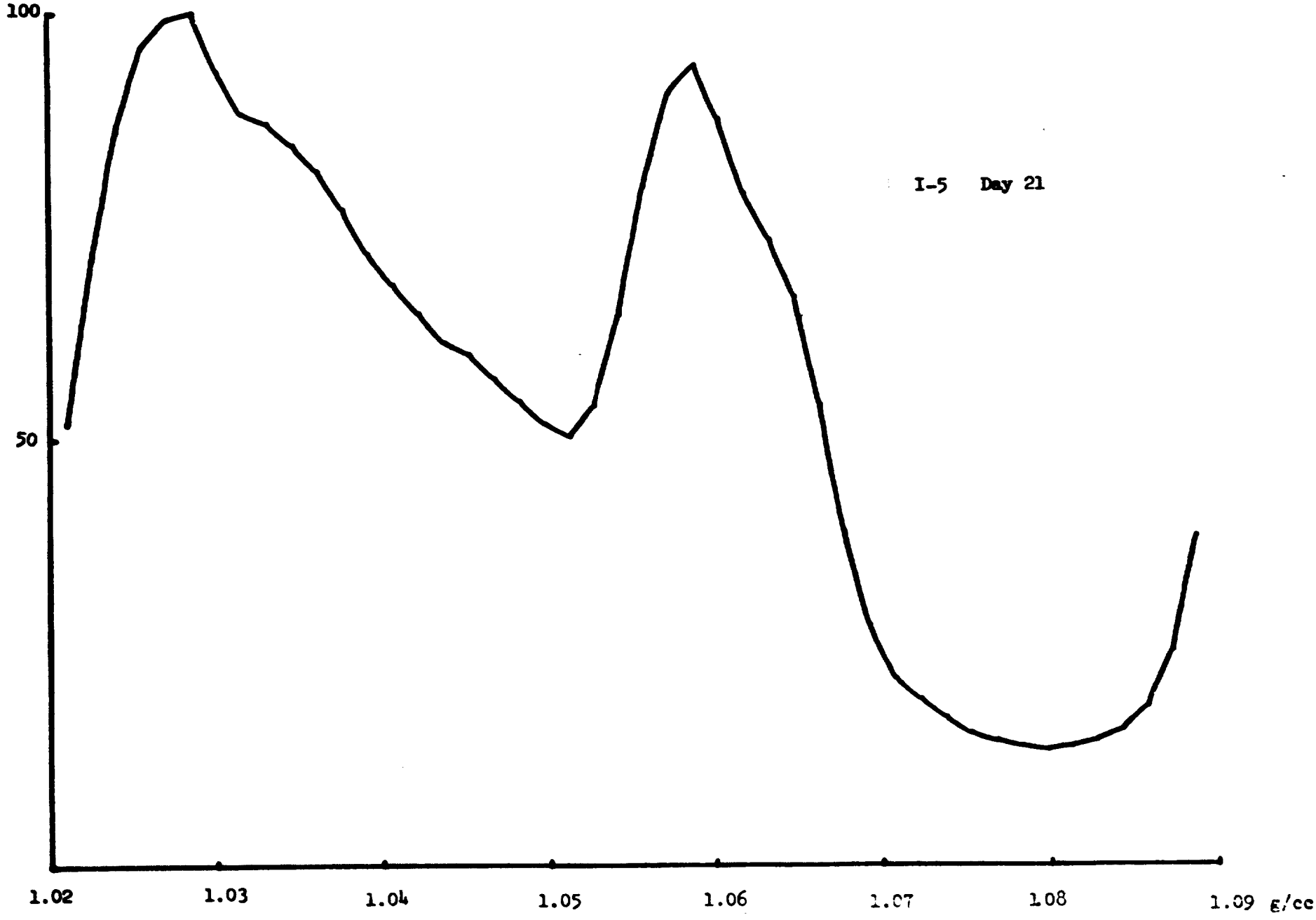
100
50
I-5 Day 21
1.02
1.03
1.04
1.05
1.06
1.07
1.08
1.09 g/cc

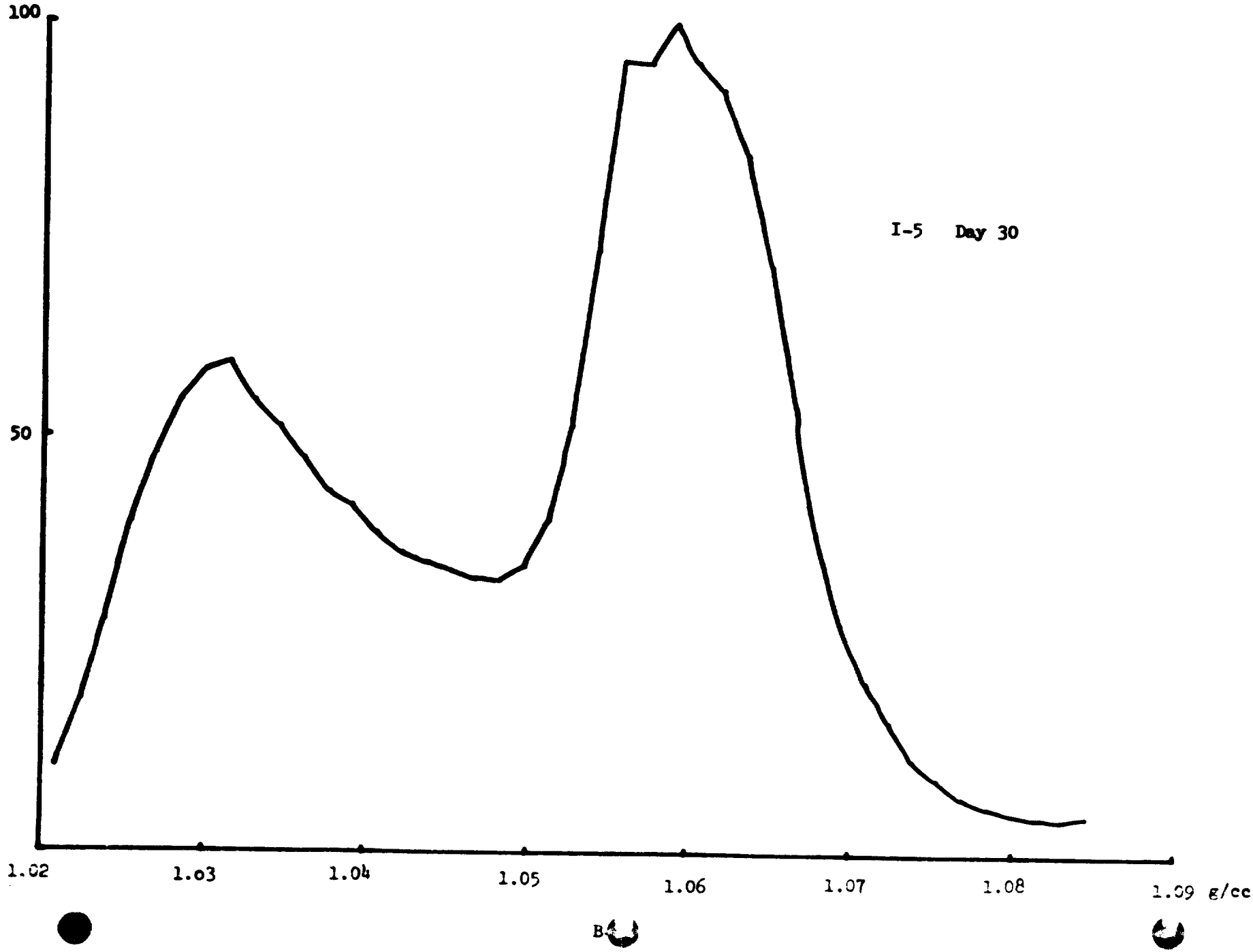
100
50
I-5 Day 30
1.02
1.03
1.04
1.05
1.06
1.07
1.08
1.09 g/cc

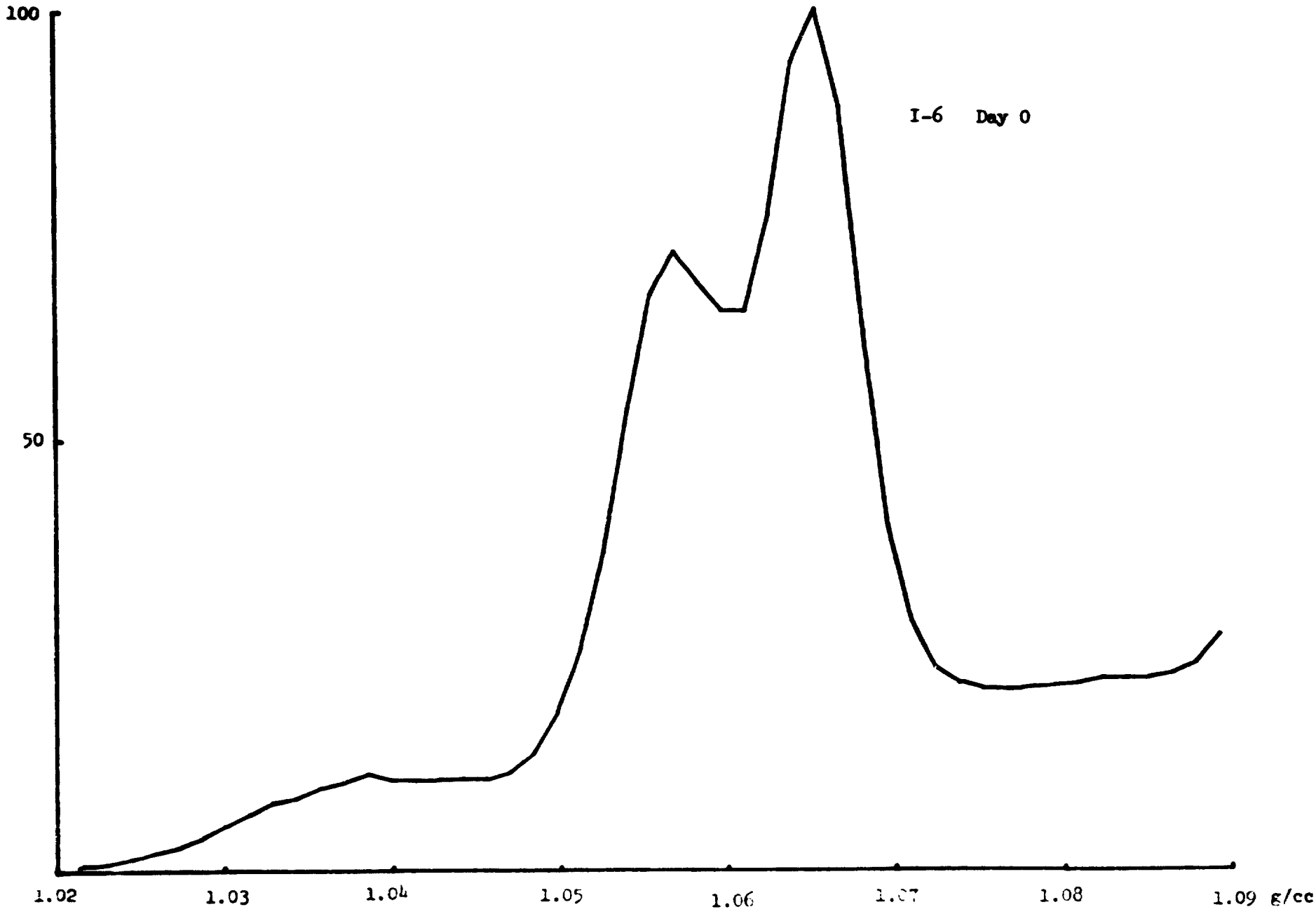
100
50
I-6 Day 0
1.02
1.03
1.04
1.05
1.06
1.07
1.08
1.09 g/cc

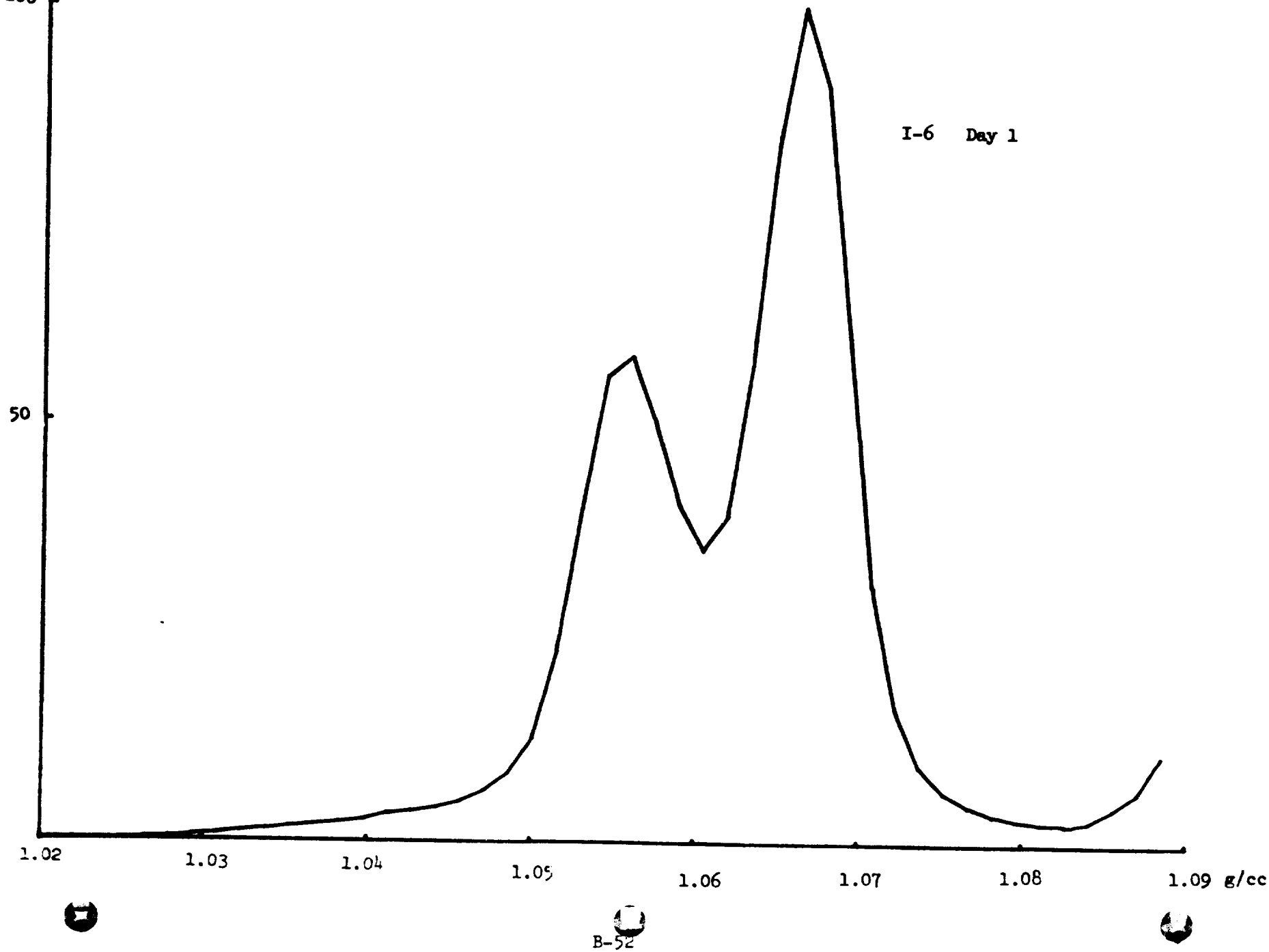
100
50
I-6 Day 1
1.02
1.03
1.04
1.05
1.06
1.07
1.08
1.09 g/cc

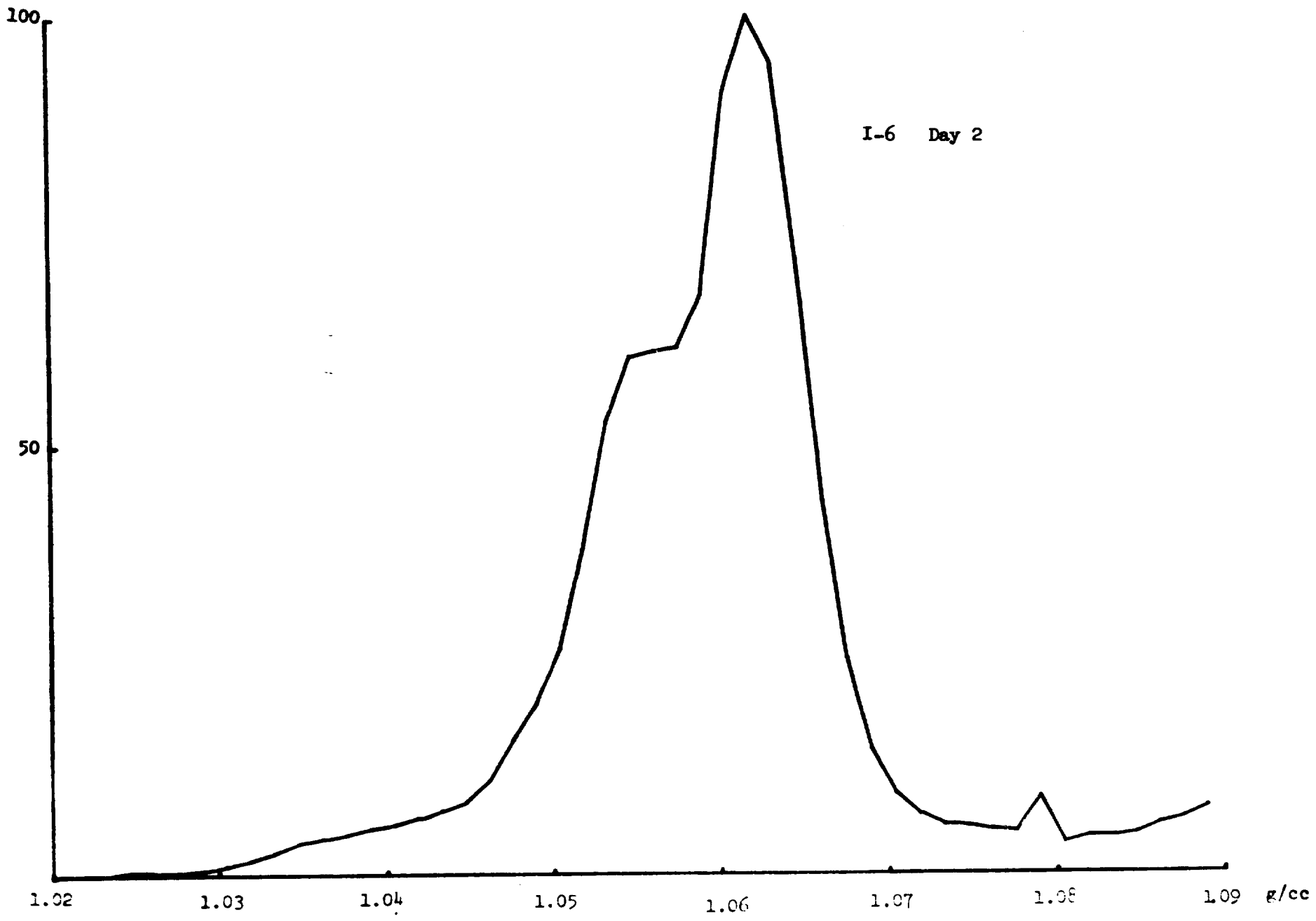
100
50
I-6 Day 2
1.02
1.03
1.04
1.05
1.06
1.07
1.08
1.09
g/cc

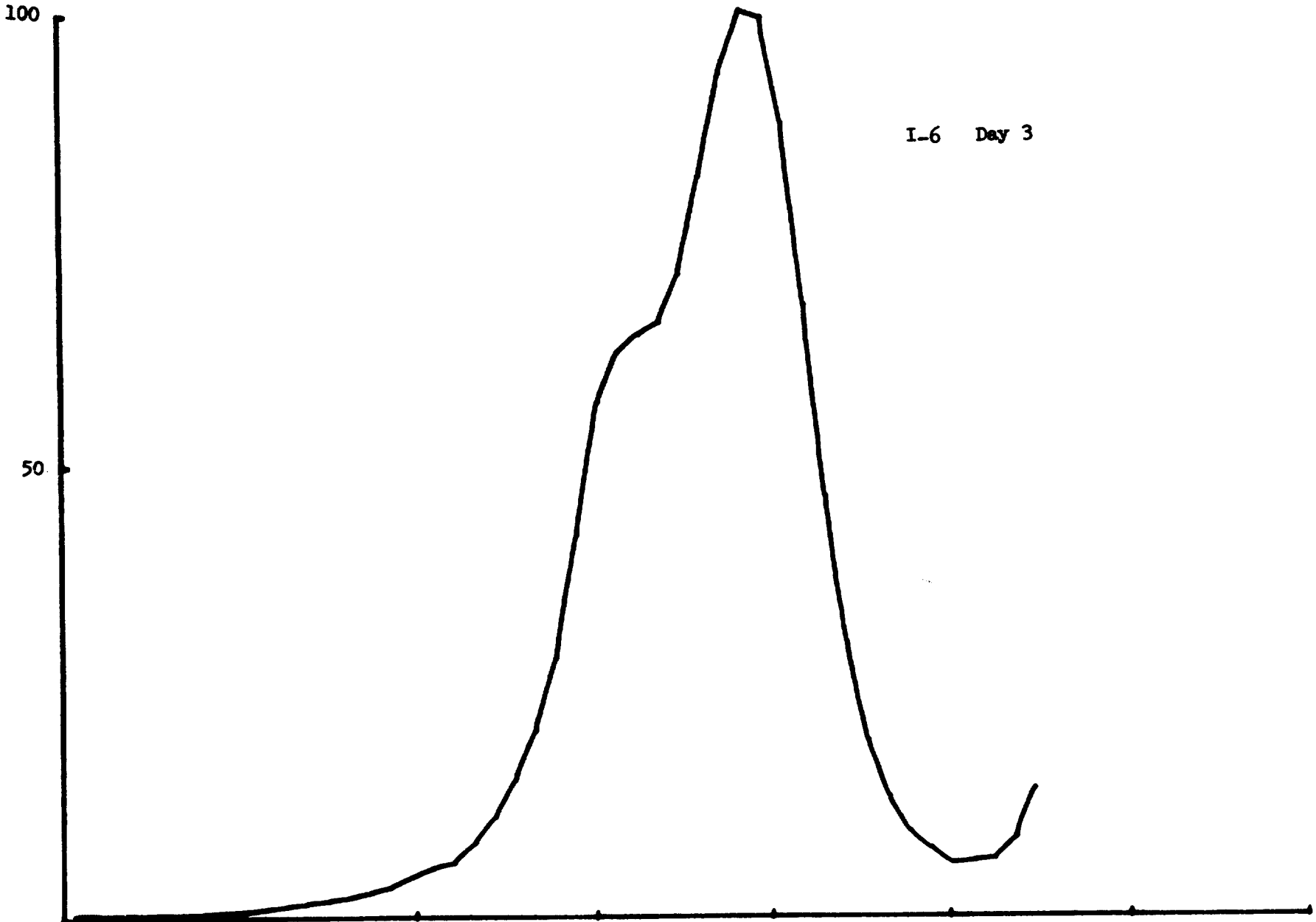
100
50
I-6 Day 3

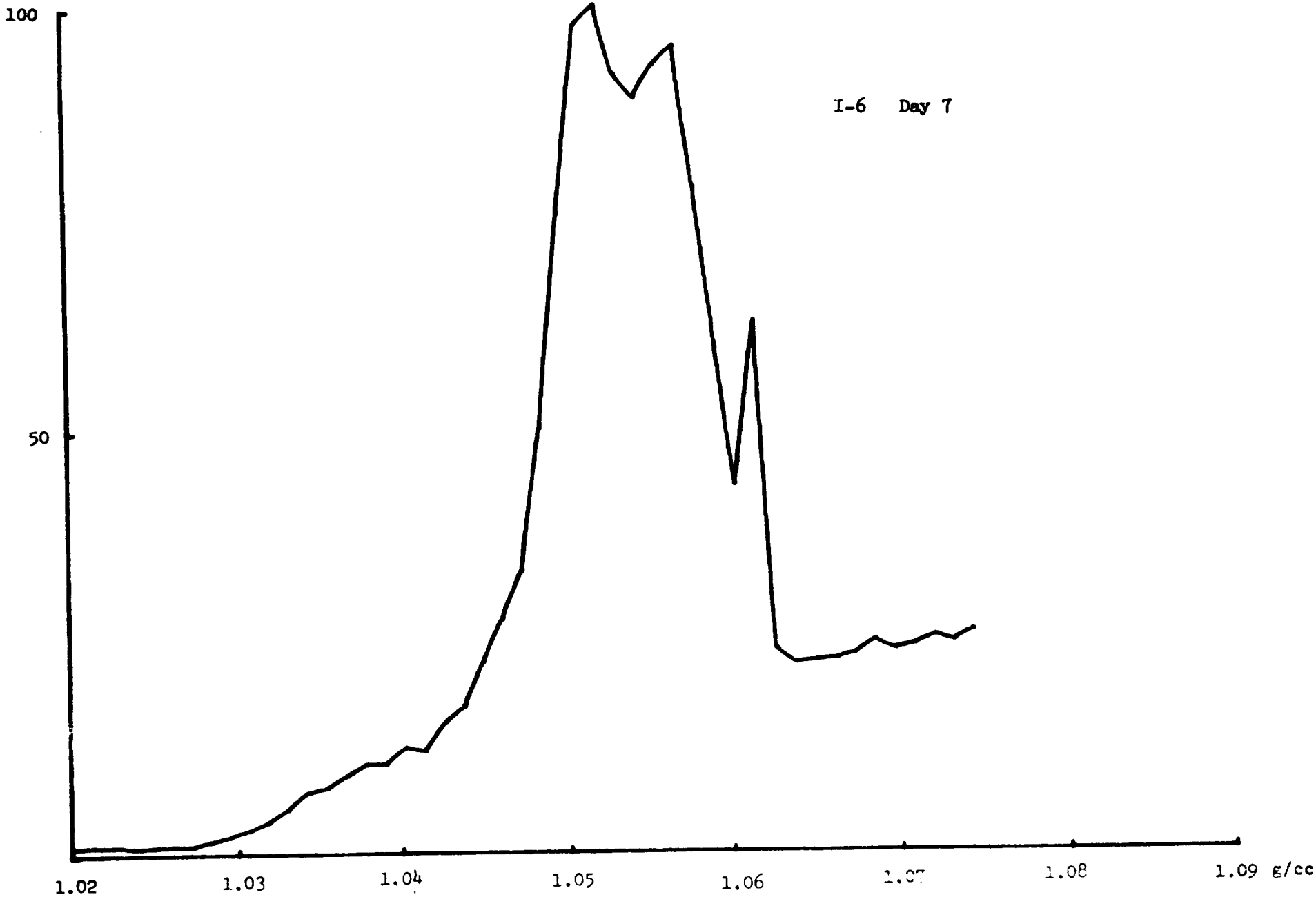
100
50
I-6 Day 7
1.02
1.03
1.04
1.05
1.06
1.07
1.08
1.09 g/cc

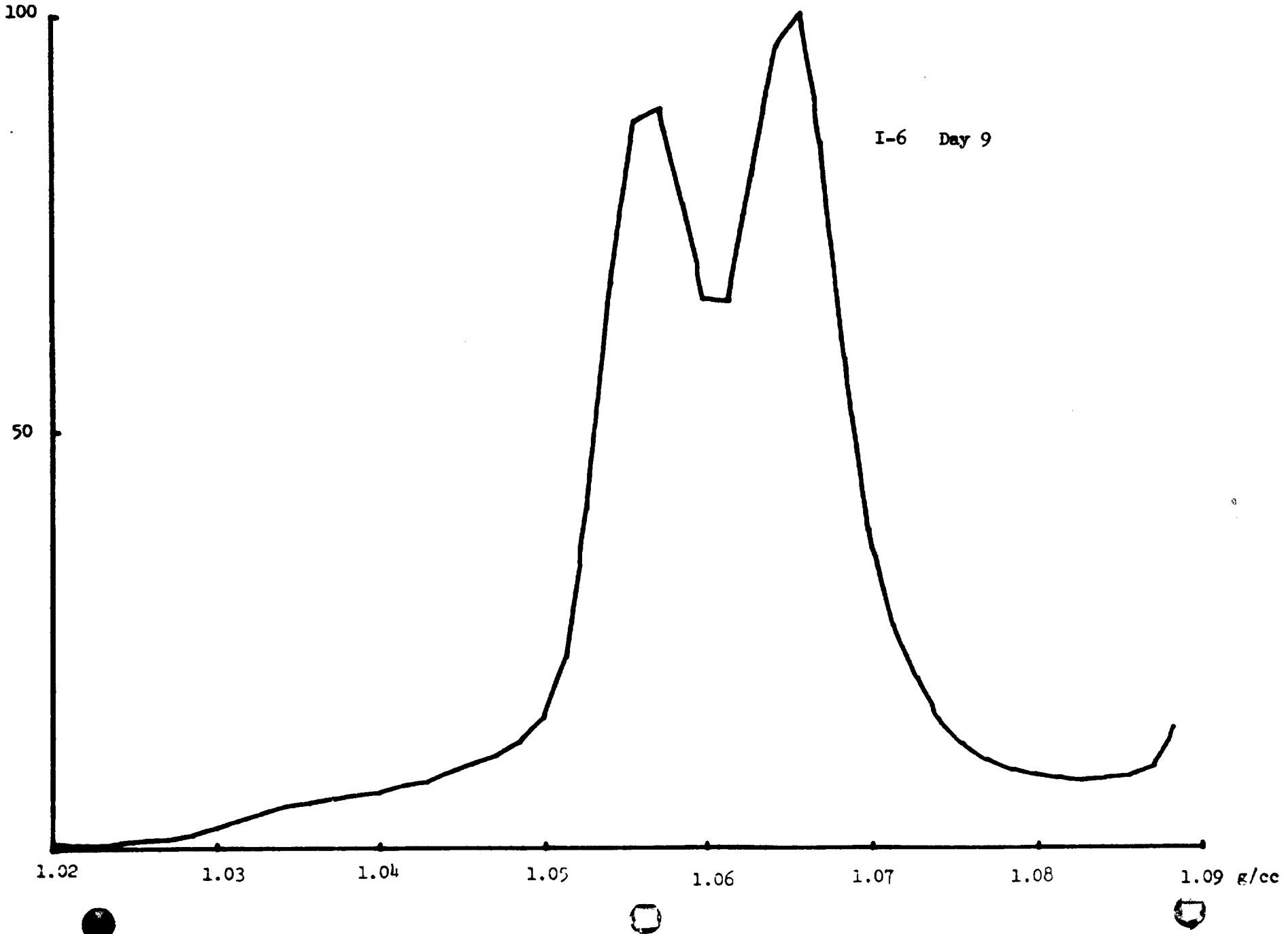
100
50
I-6 Day 9
1.02
1.03
1.04
1.05
1.06
1.07
1.08
1.09 g/cc

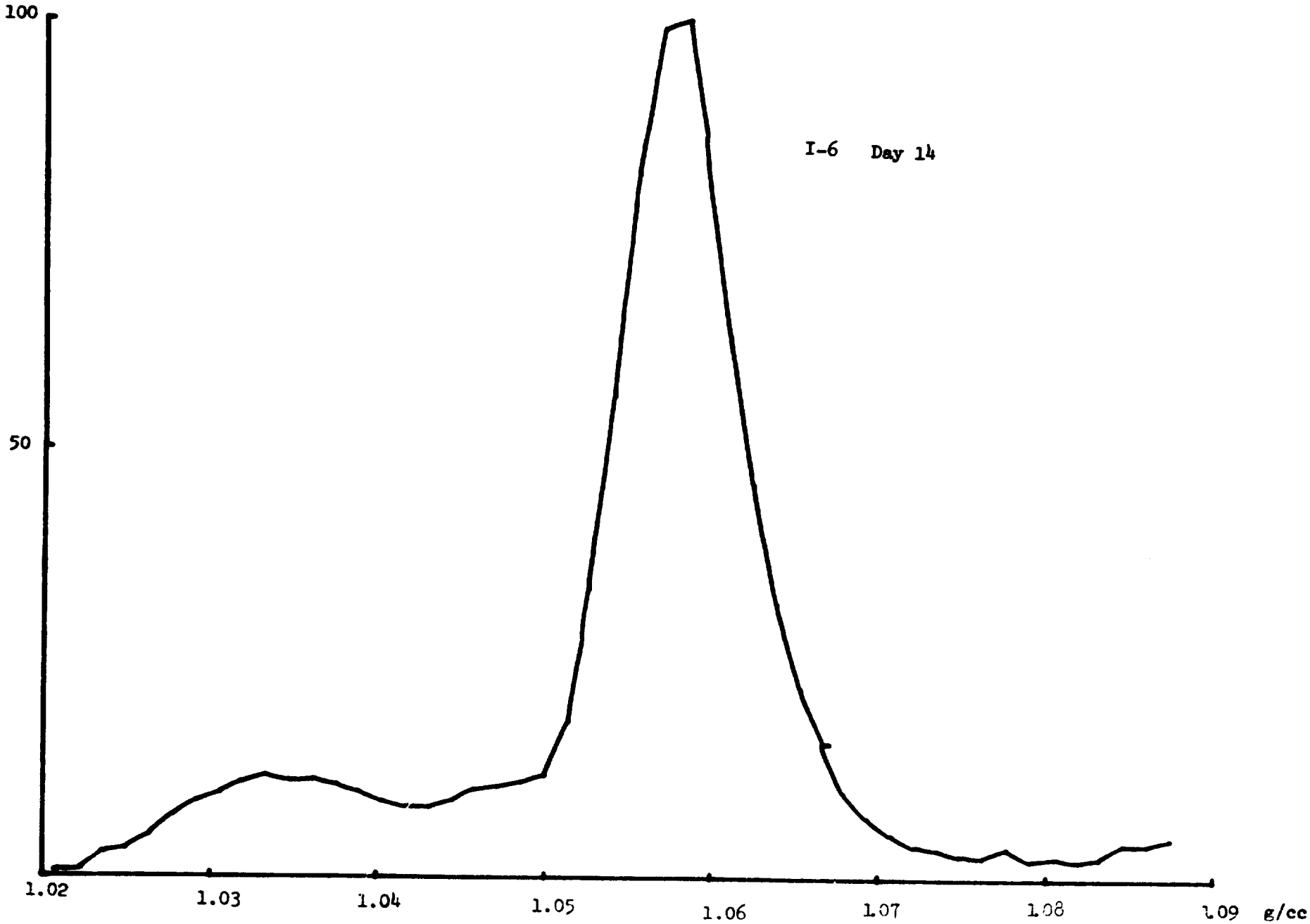
100
50
I-6 Day 14
1.02
1.03
1.04
1.05
1.06
1.07
1.08
1.09
g/cc

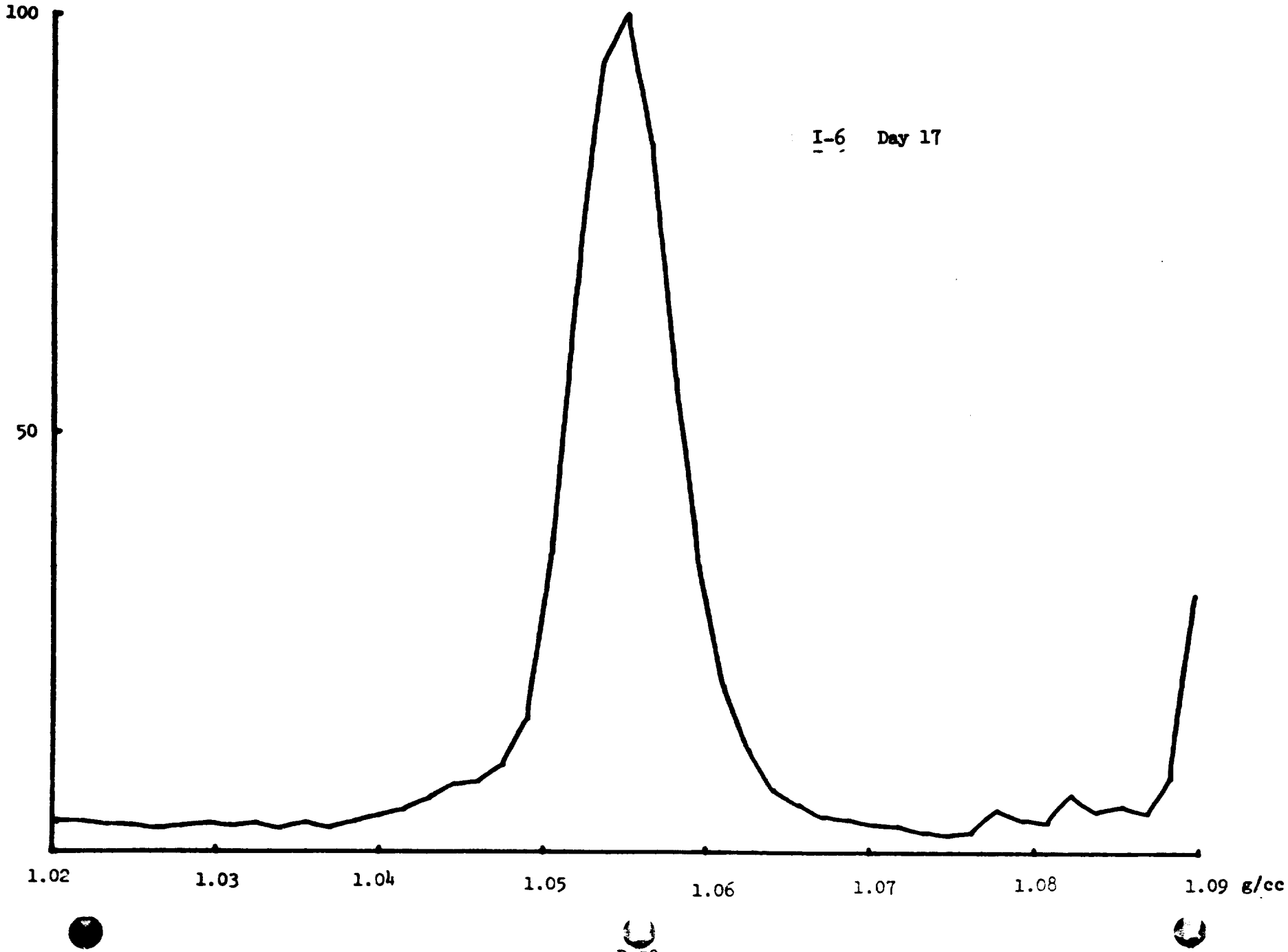
100
50
I-6 Day 17
1.02
1.03
1.04
1.05
1.06
1.07
1.08
1.09 g/cc

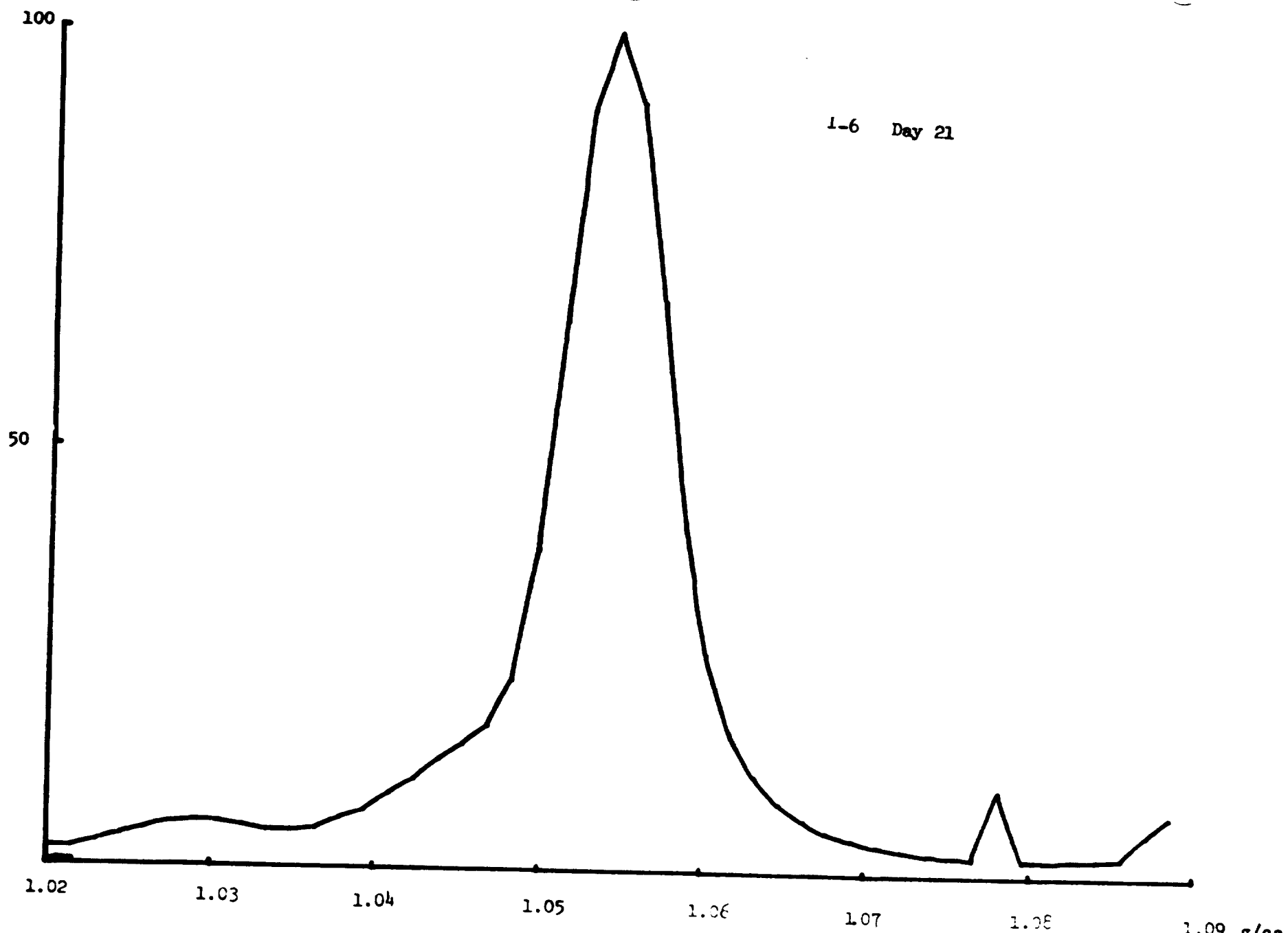
100
50
1-6 Day 21
1.02
1.03
1.04
1.05
1.06
1.07
1.08
1.09 g/cc

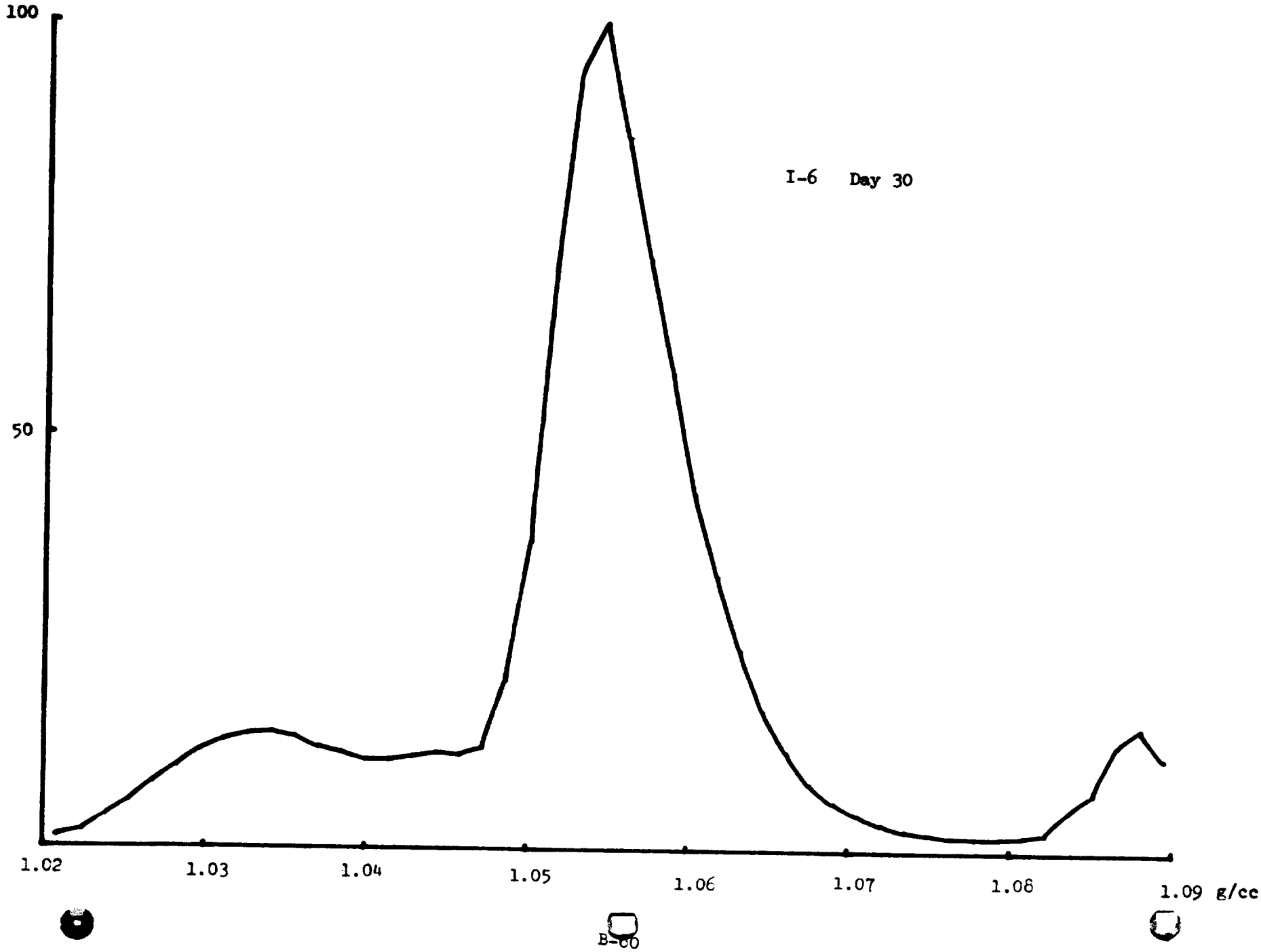
100
50
I-6 Day 30
1.02
1.03
1.04
1.05
1.06
1.07
1.08
1.09 g/cc
B-60

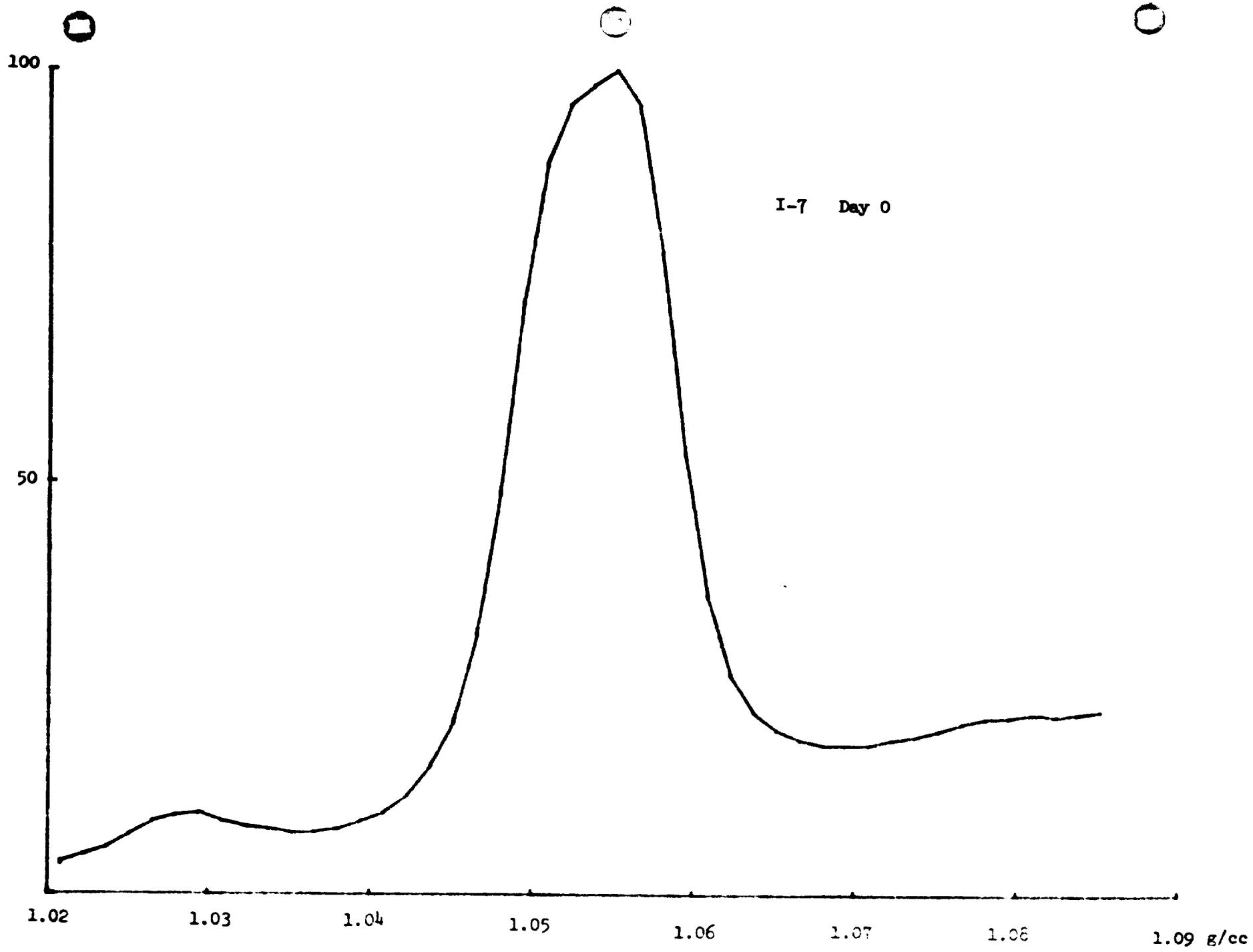
100
50
I-7 Day 0
1.02
1.03
1.04
1.05
1.06
1.07
1.08
1.09 g/cc

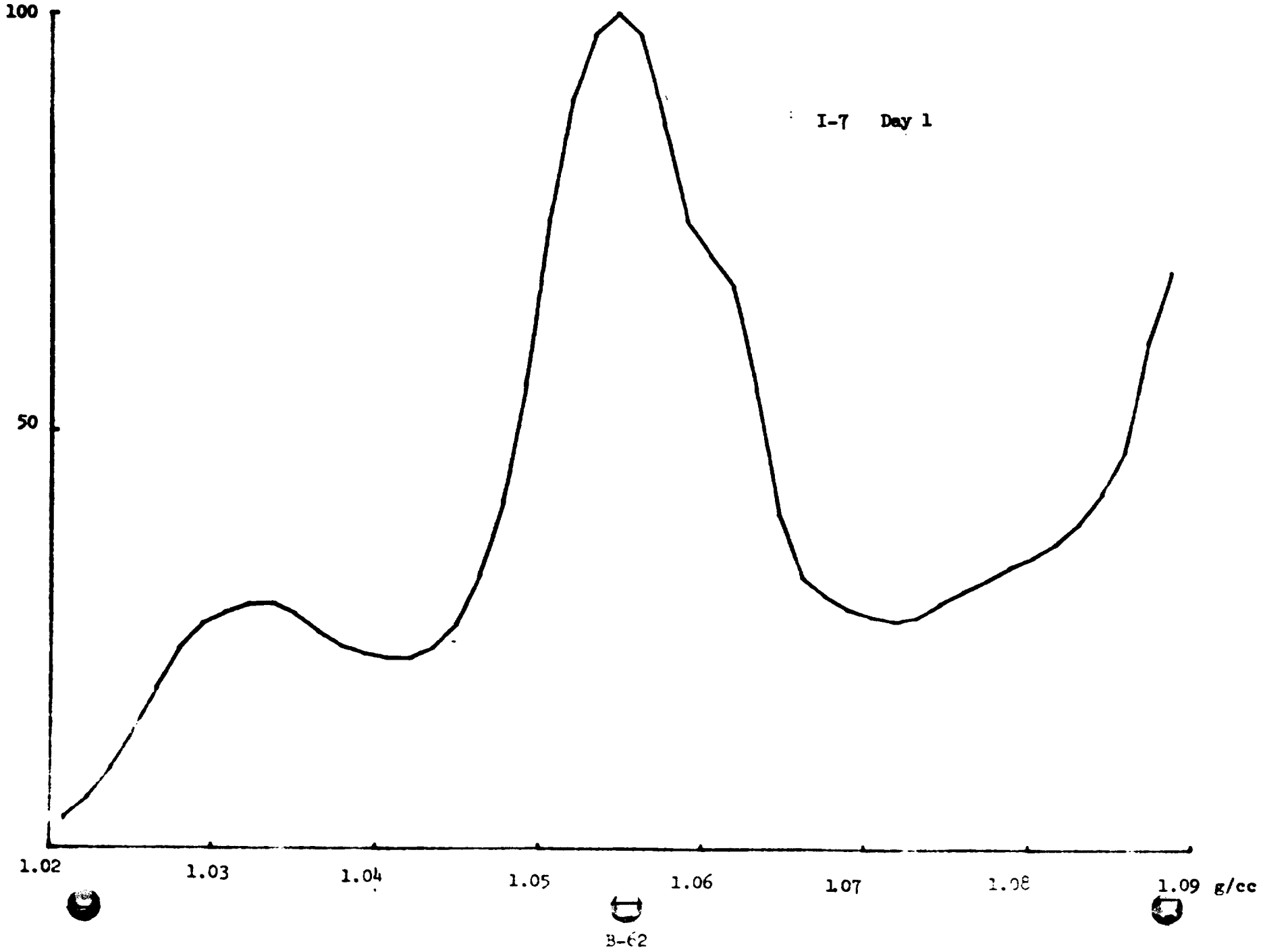
100
50
I-7 Day 1
1.02
1.03
1.04
1.05
1.06
1.07
1.08
1.09 g/cc

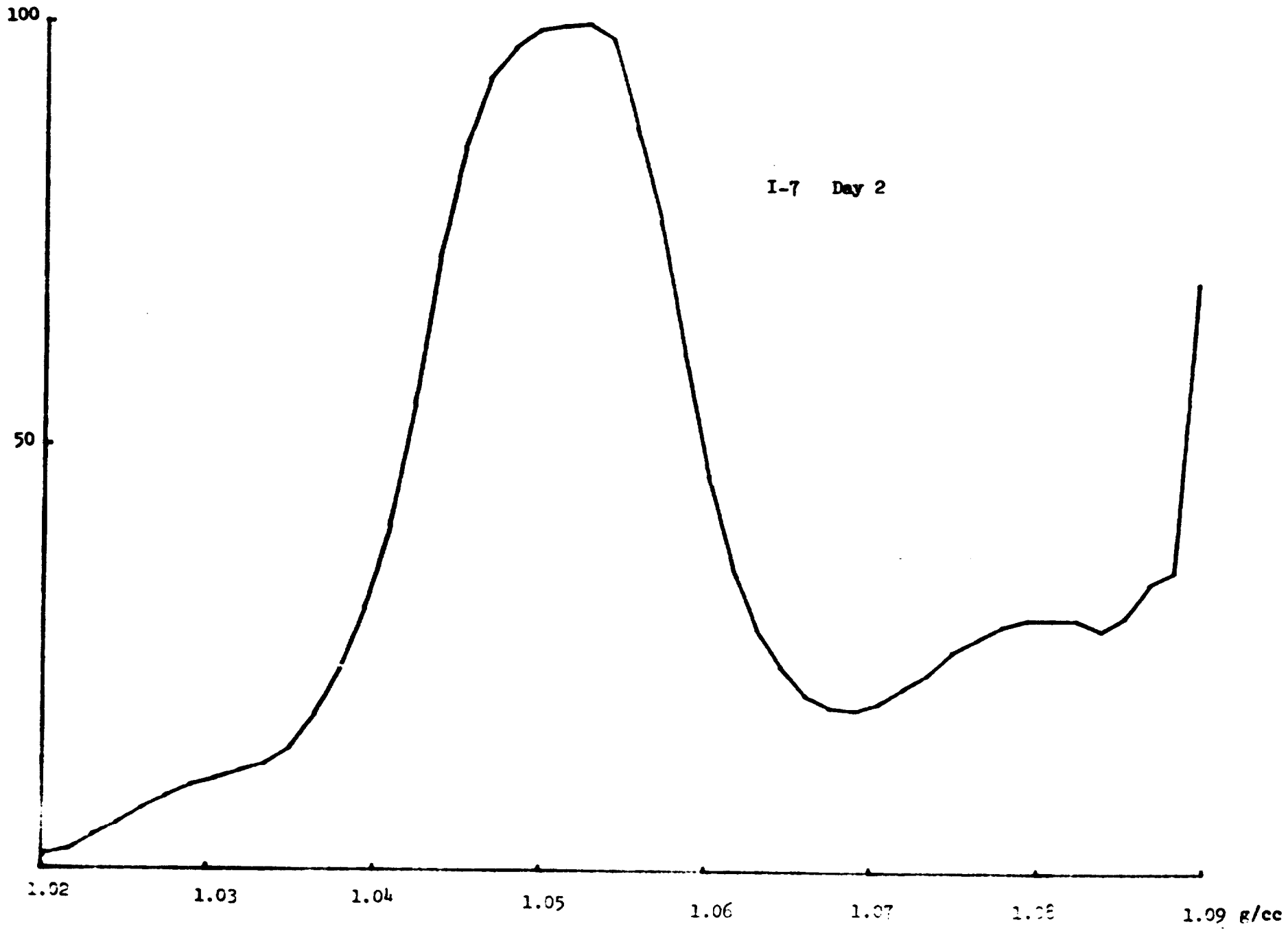
100
50
I-7 Day 2
1.02
1.03
1.04
1.05
1.06
1.07
1.08
1.09 g/cc

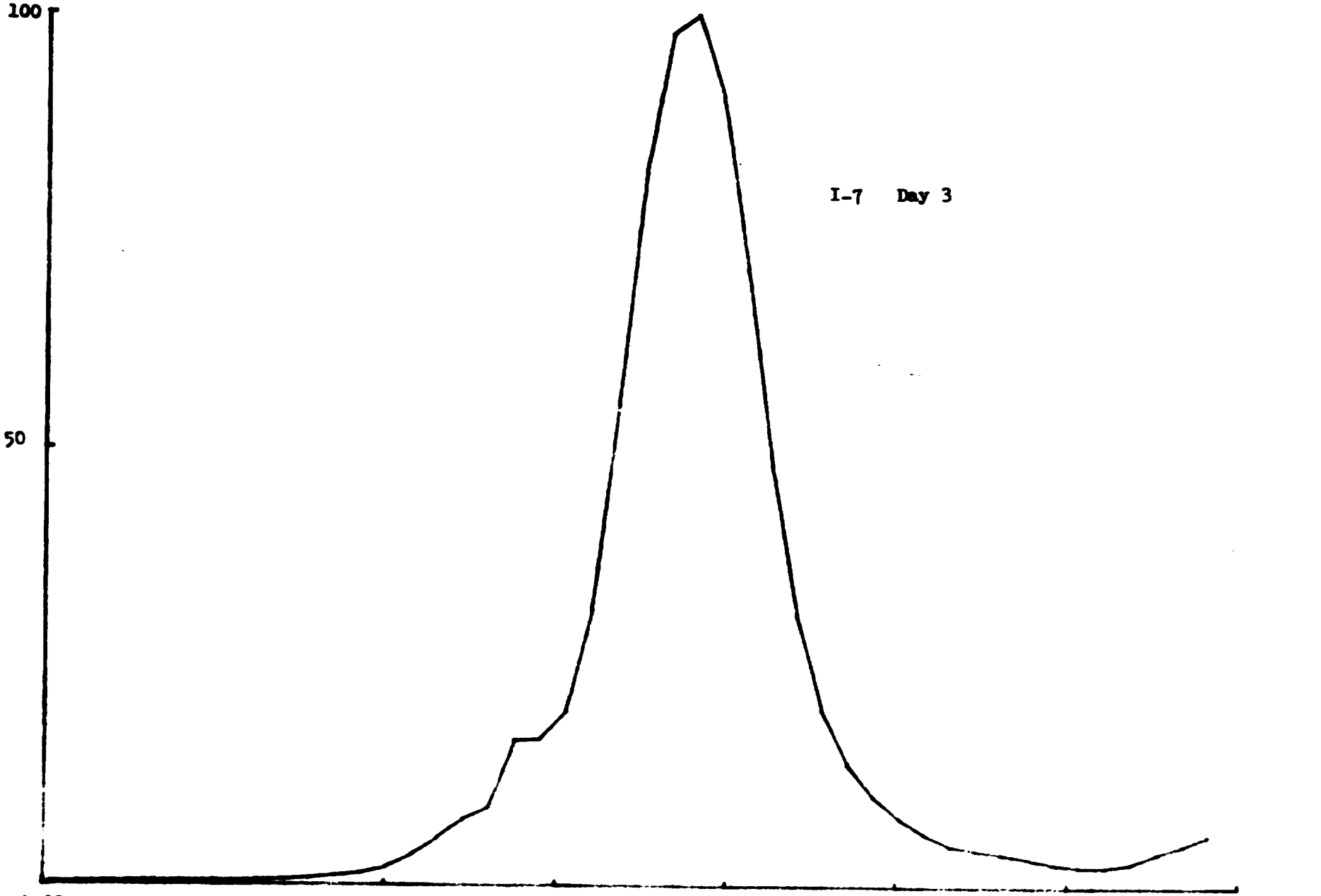
100
50
I-7 Day 3
1.02
1.03
1.04
1.05
1.06
1.07
1.08
1.09 g/cc

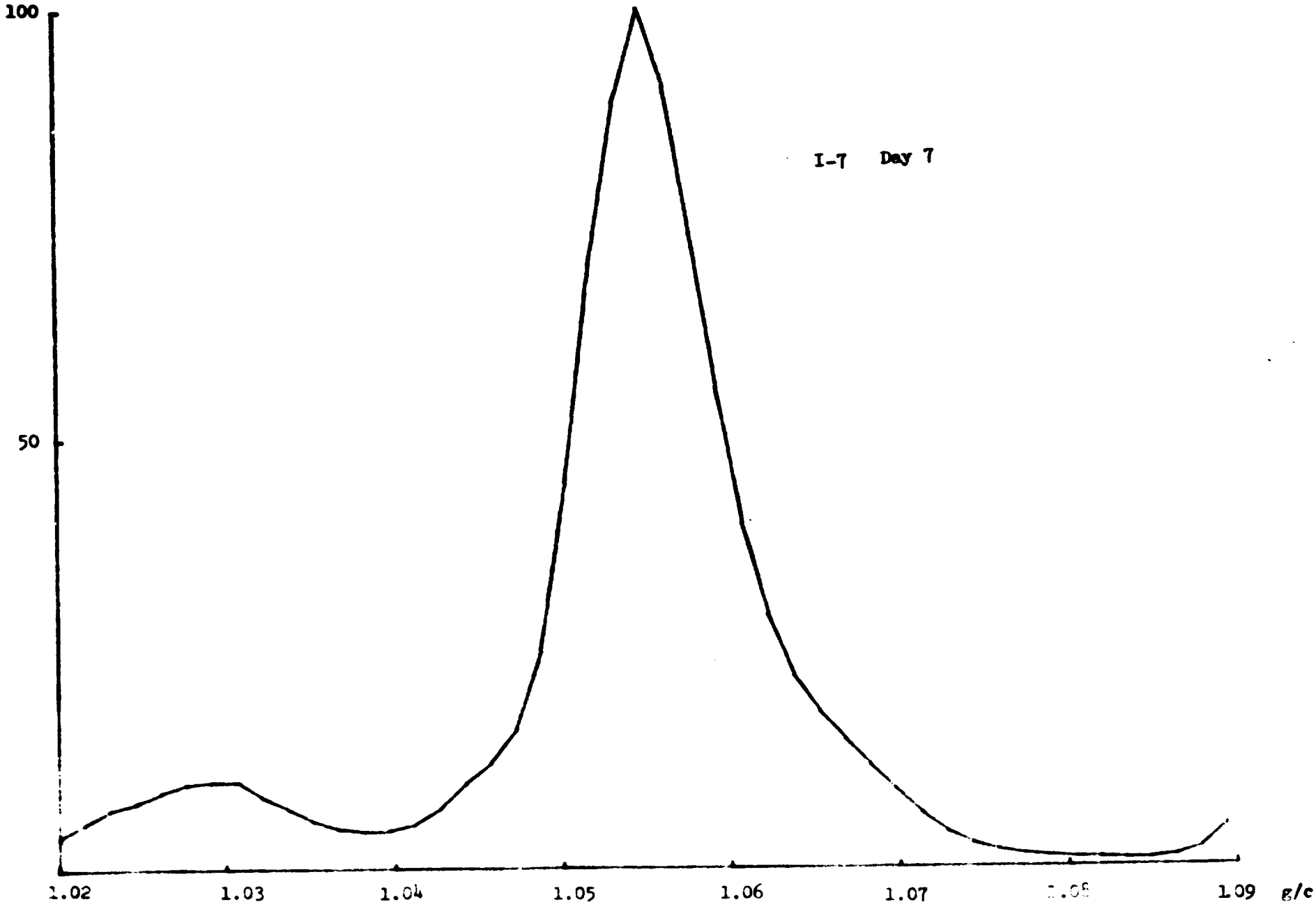
100
50
I-7 Day 7
1.02
1.03
1.04
1.05
1.06
1.07
1.09
g/c

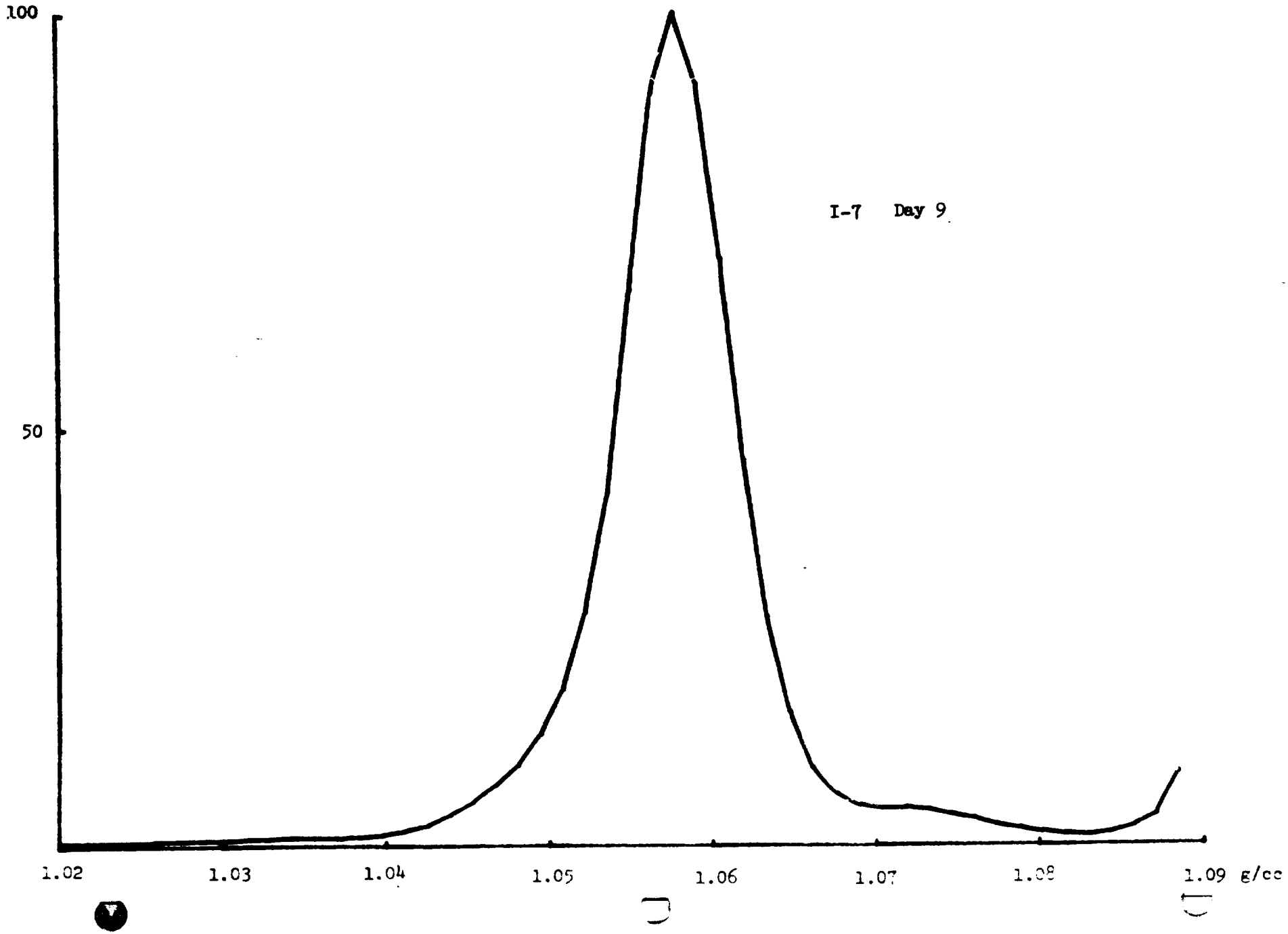
100
50
I-7 Day 9
1.02
1.03
1.04
1.05
1.06
1.07
1.08
1.09 g/cc

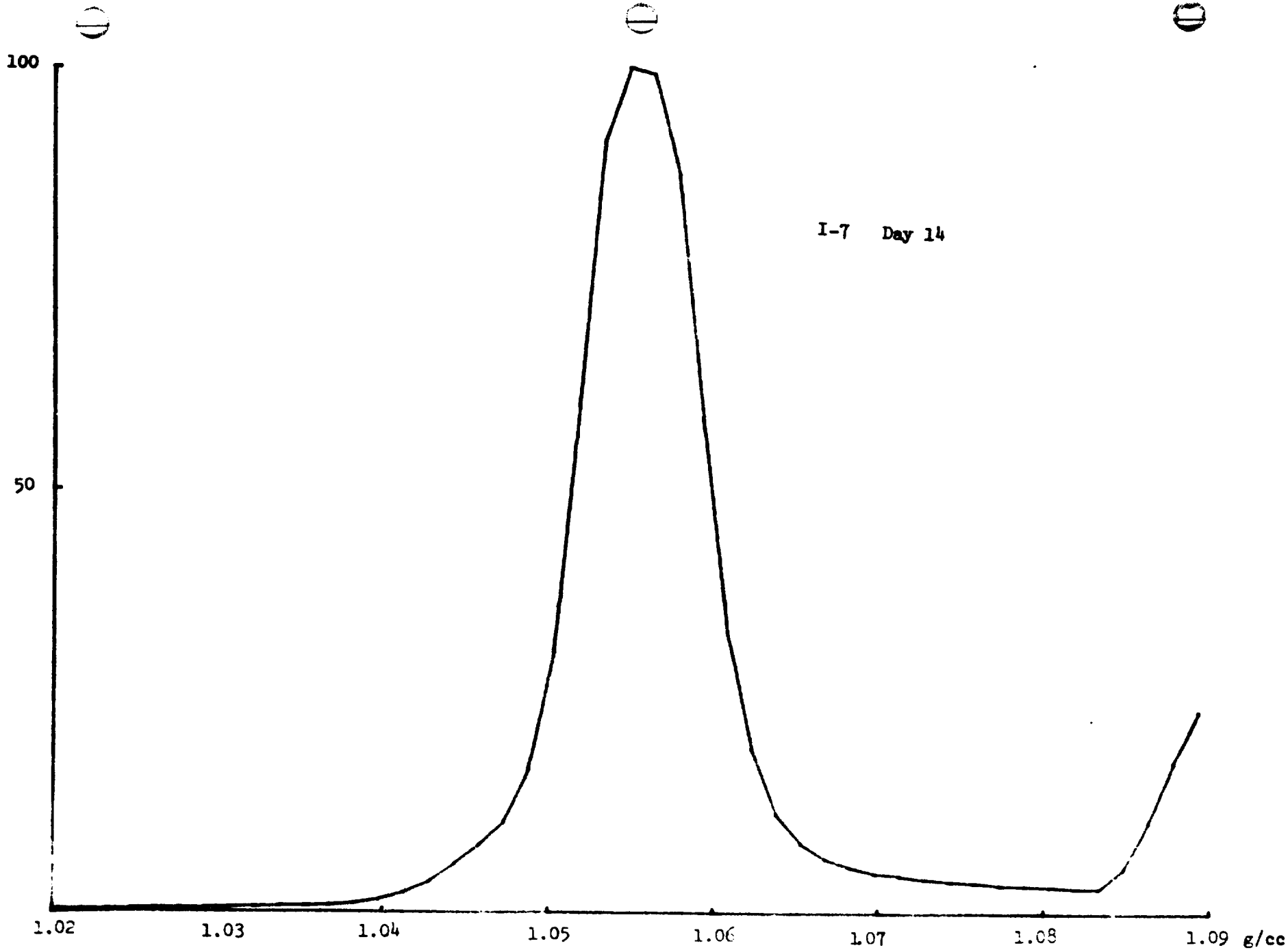
100
50
I-7 Day 14
1.02
1.03
1.04
1.05
1.06
1.07
1.08
1.09 g/cc

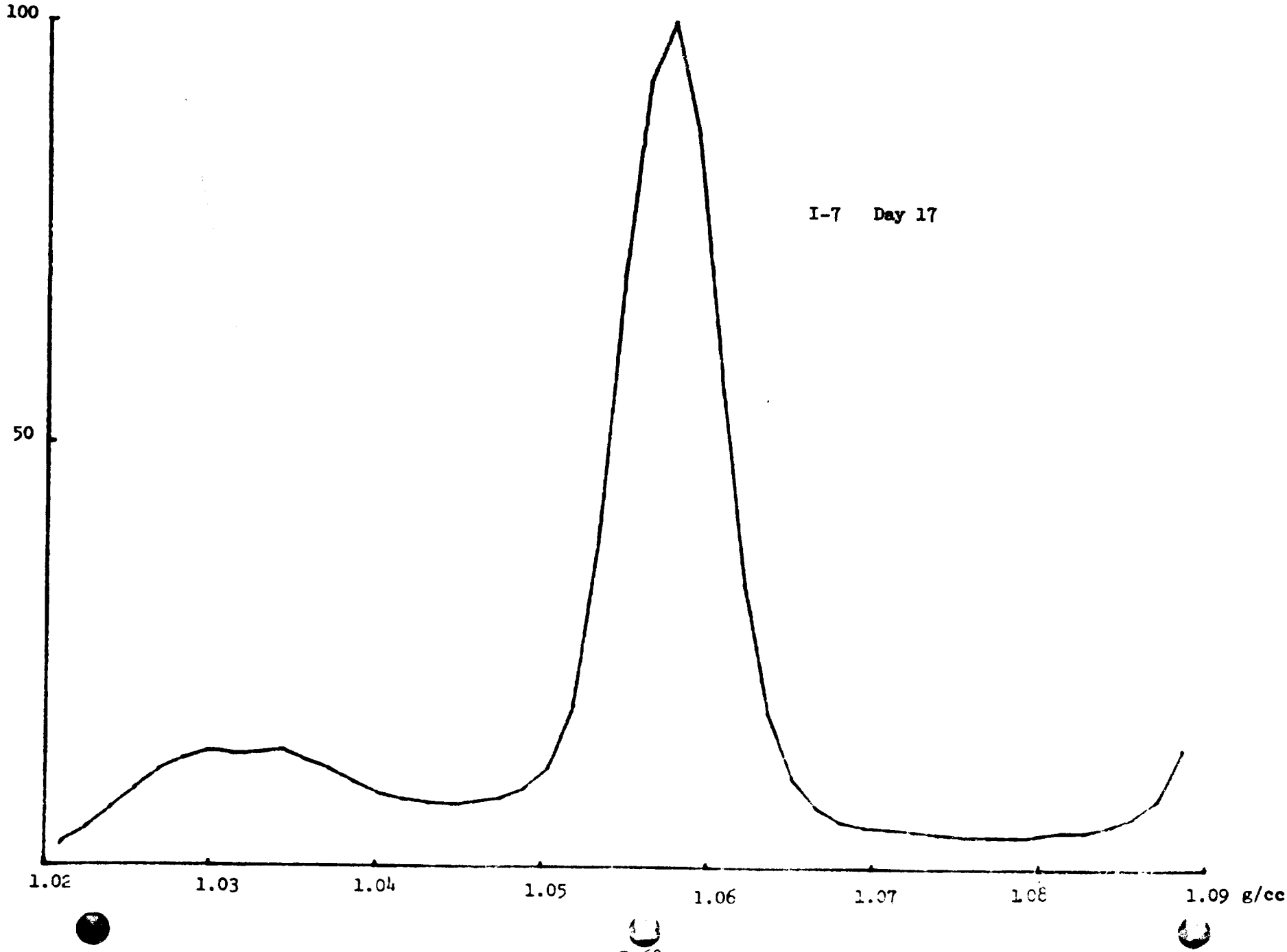
100
50
I-7 Day 17
1.02
1.03
1.04
1.05
1.06
1.07
1.08
1.09 g/cc

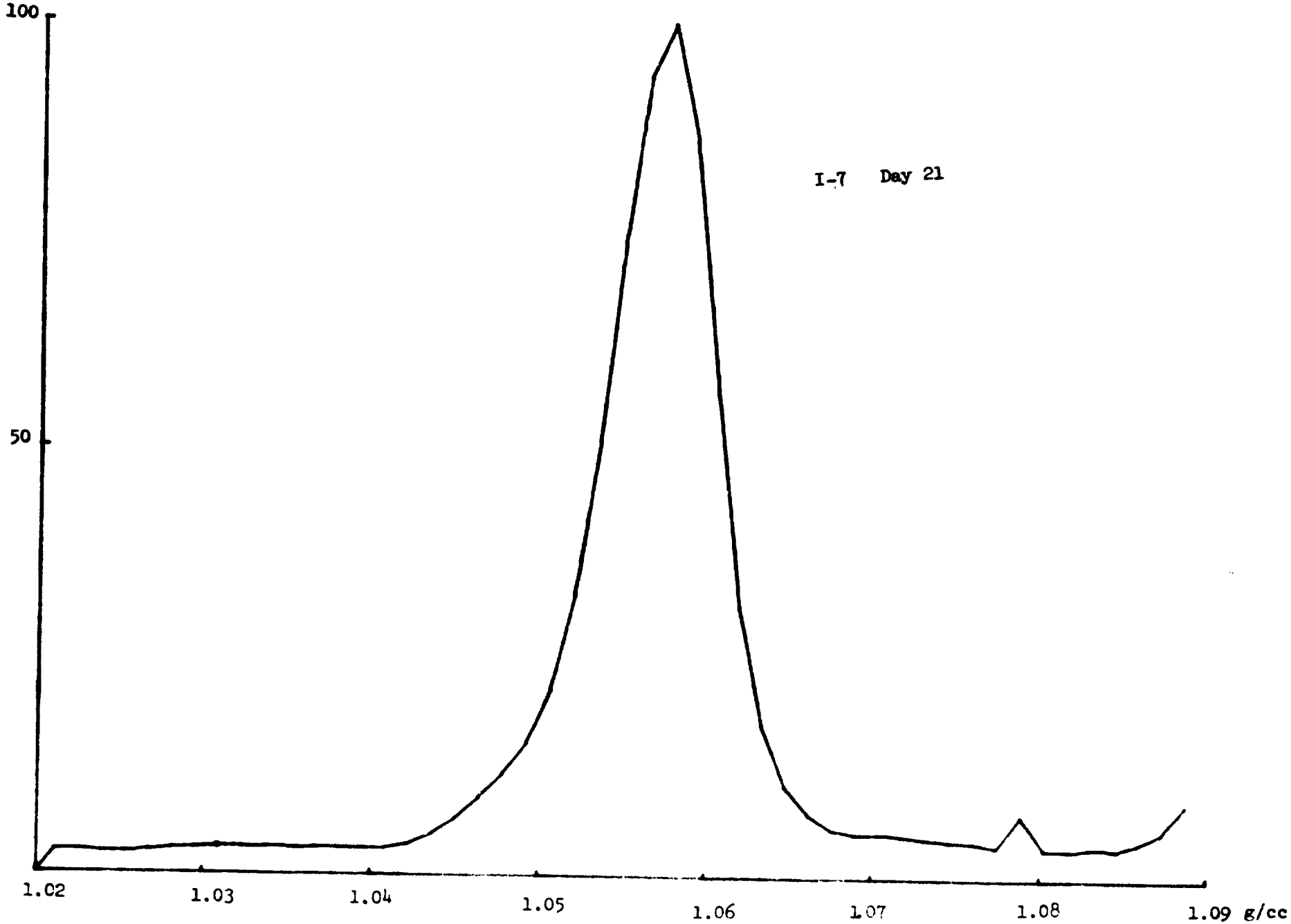
100
50
I-7 Day 21
1.02
1.03
1.04
1.05
1.06
1.07
1.08
1.09 g/cc

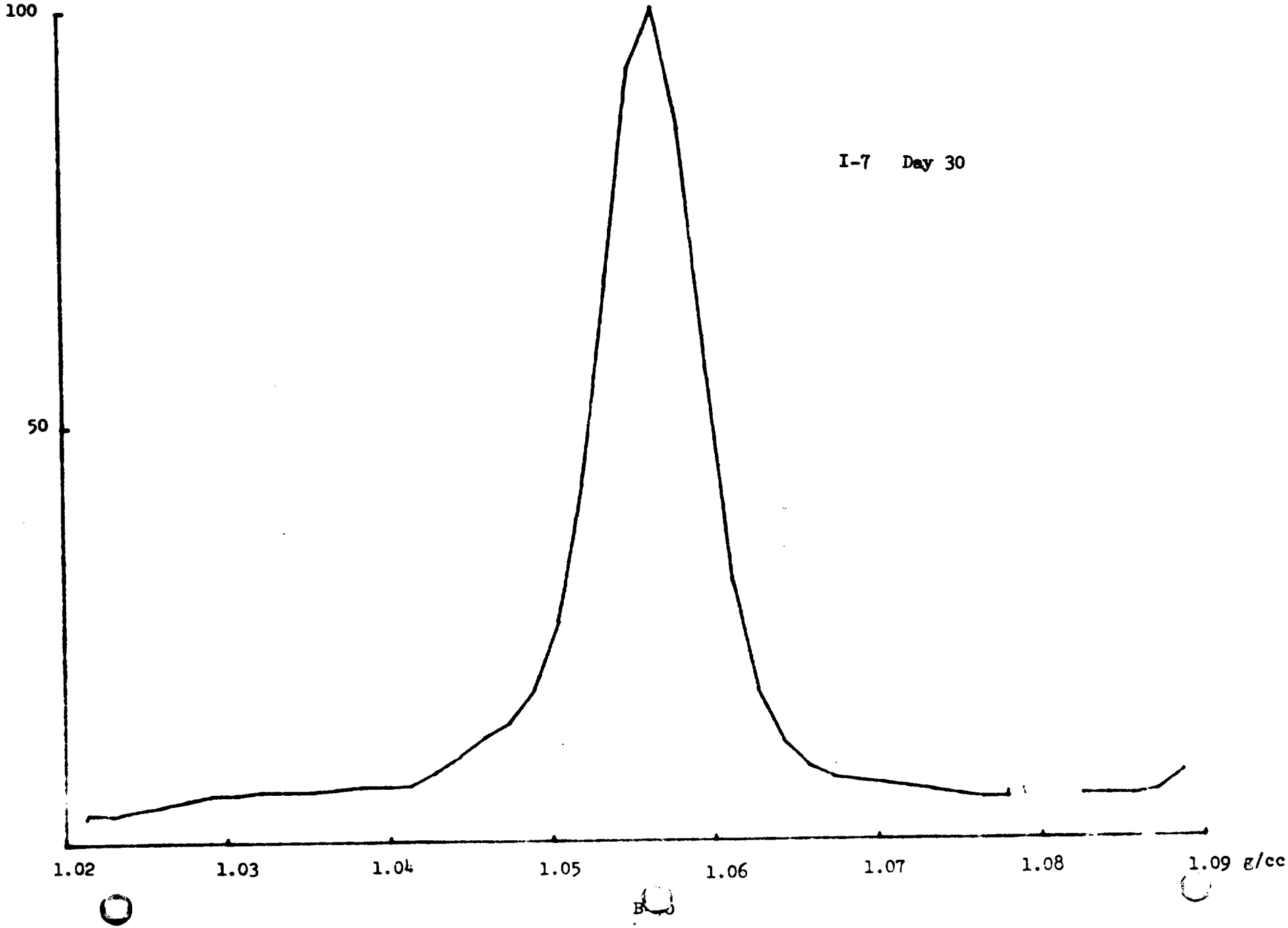
100
50
I-7 Day 30
1.02
1.03
1.04
1.05
1.06
1.07
1.08
1.09 g/cc

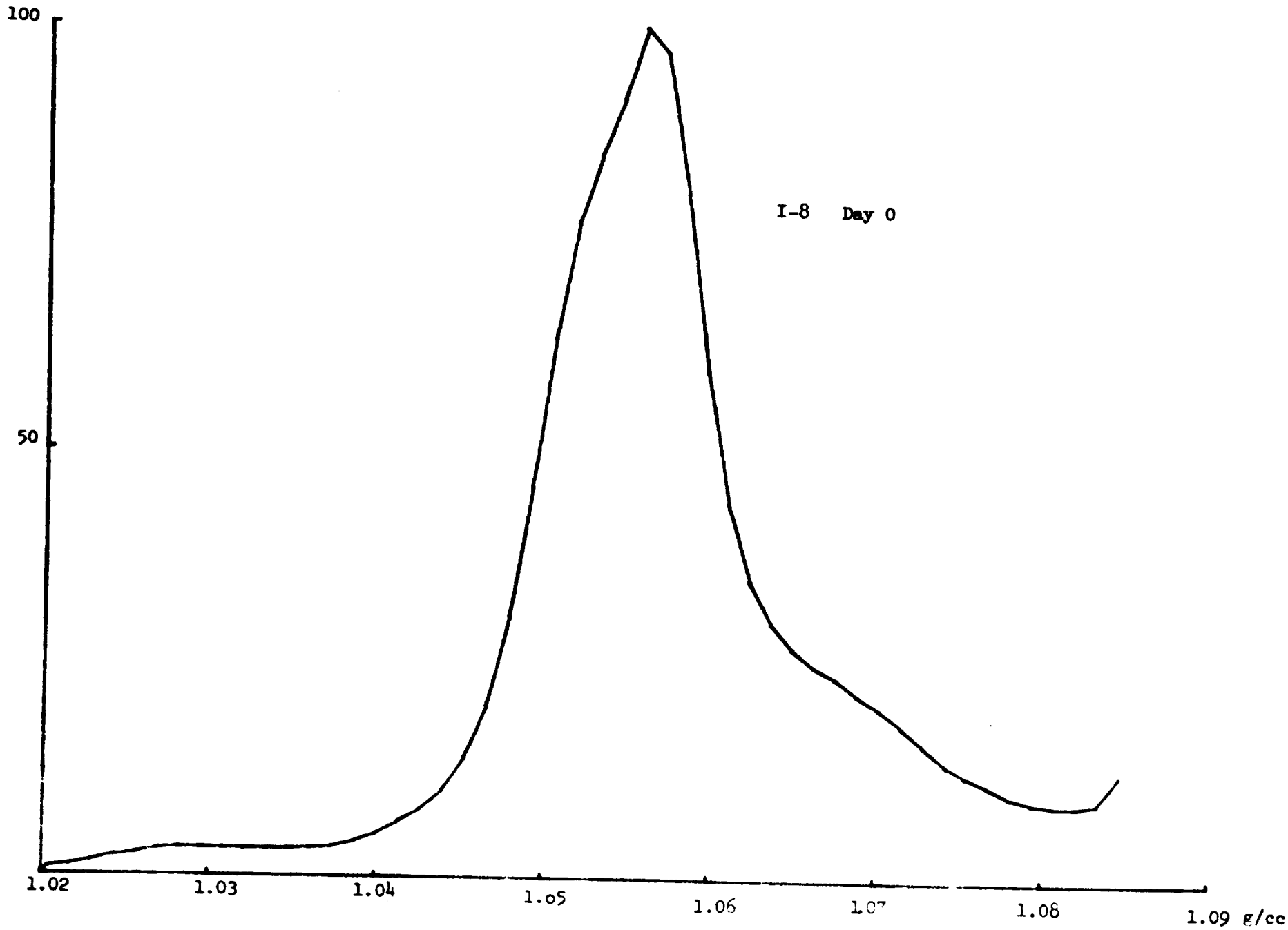
100
50
I-8 Day 0
1.02
1.03
1.04
1.05
1.06
1.07
1.08
1.09 g/cc

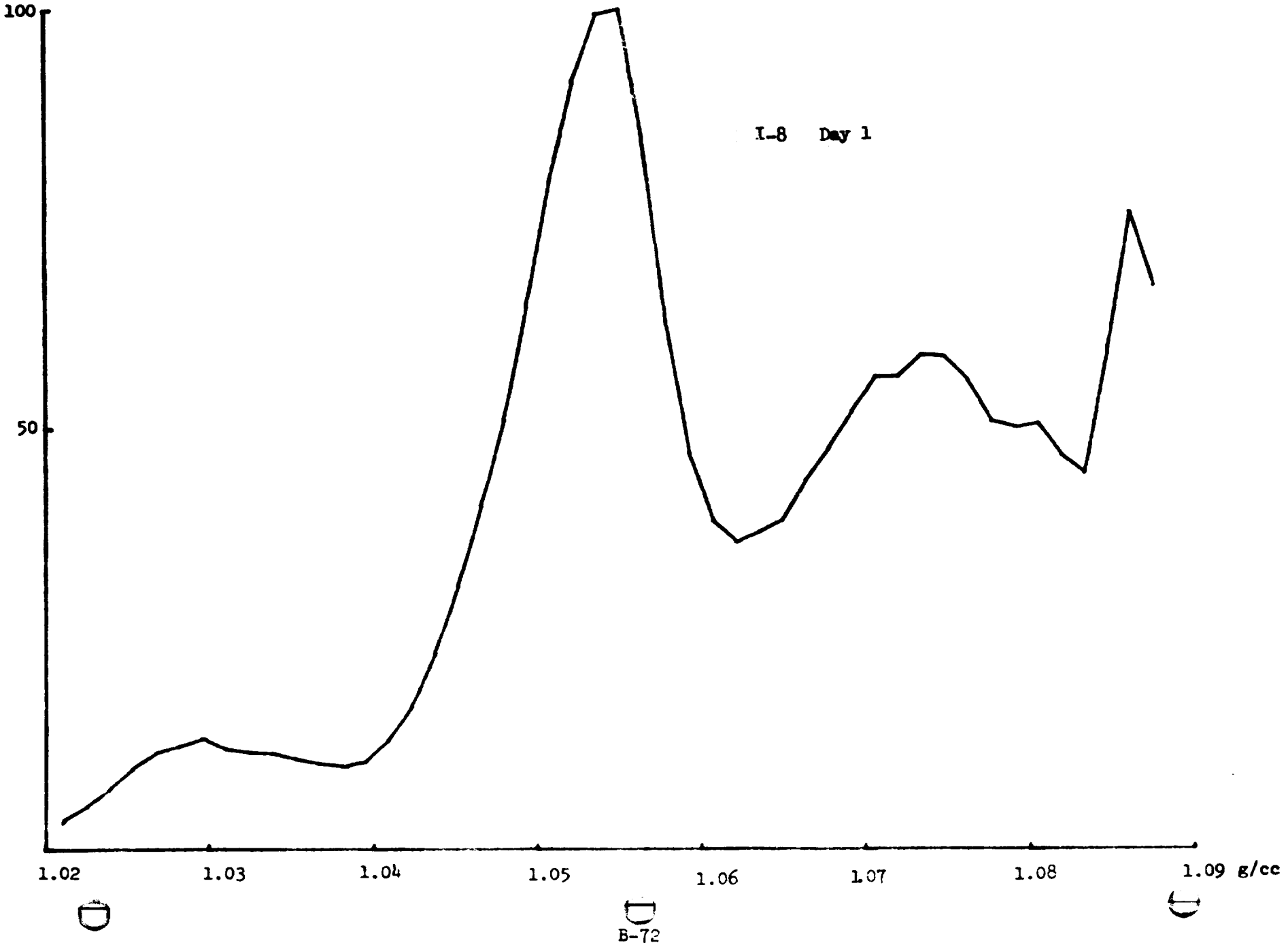
100
50
I-8 Day 1
1.02
1.03
1.04
1.05
1.06
1.07
1.08
1.09 g/cc

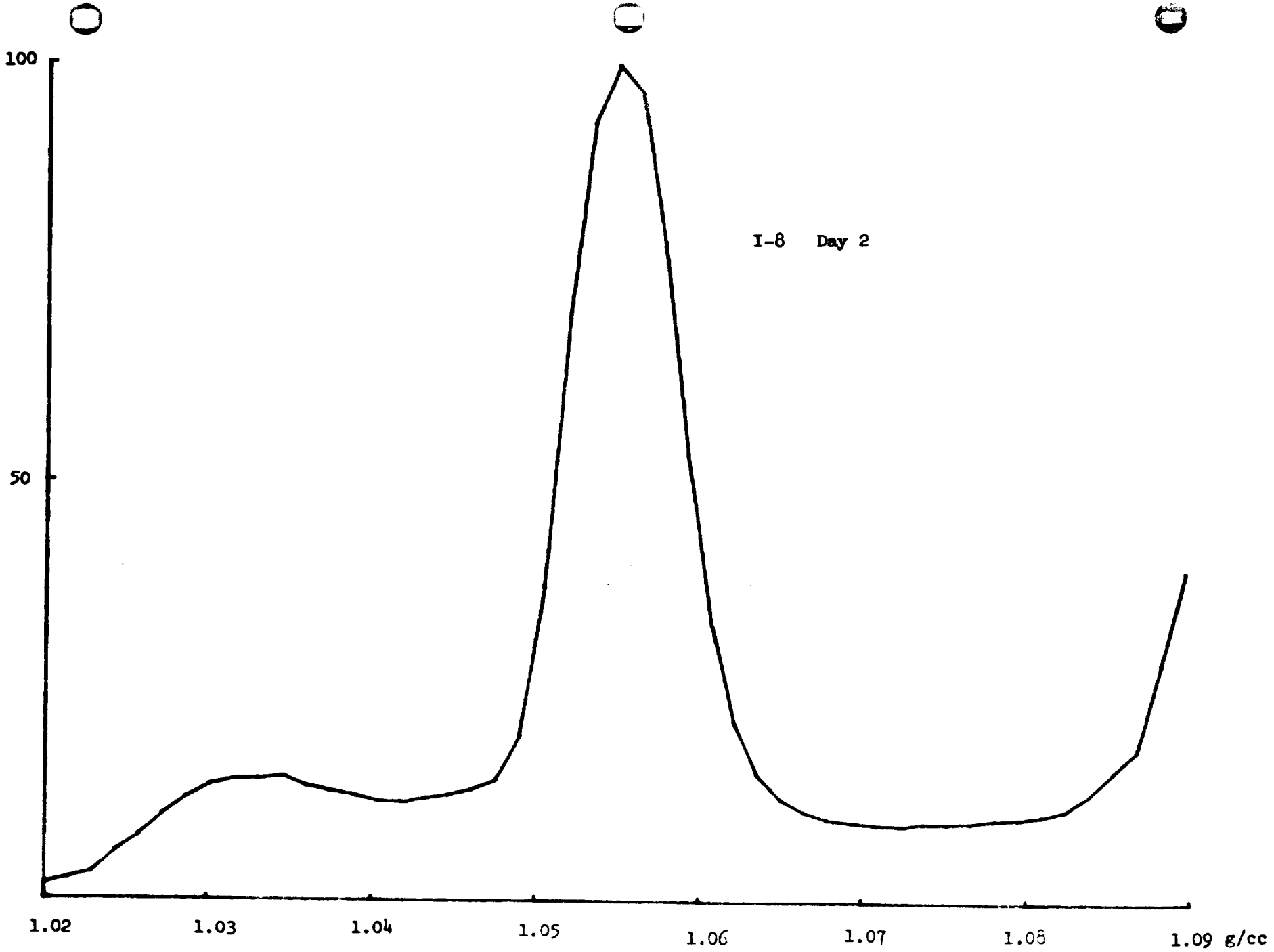
100
50
I-8 Day 2
1.02
1.03
1.04
1.05
1.06
1.07
1.08
1.09 g/cc

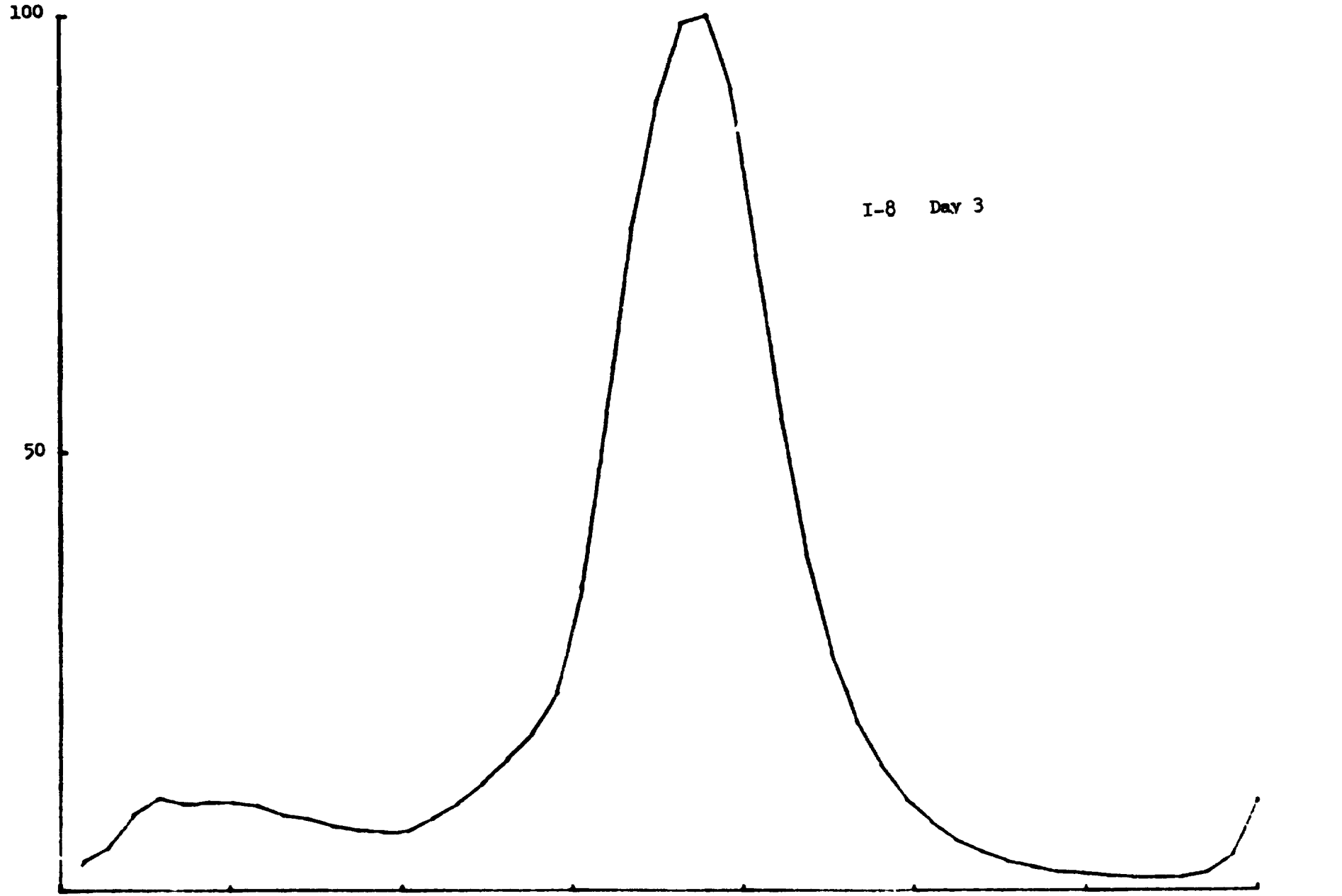
100
50
I-8 Day 3
1.02
1.03
1.04
1.05
1.06
1.07
1.08
1.09 g/cc

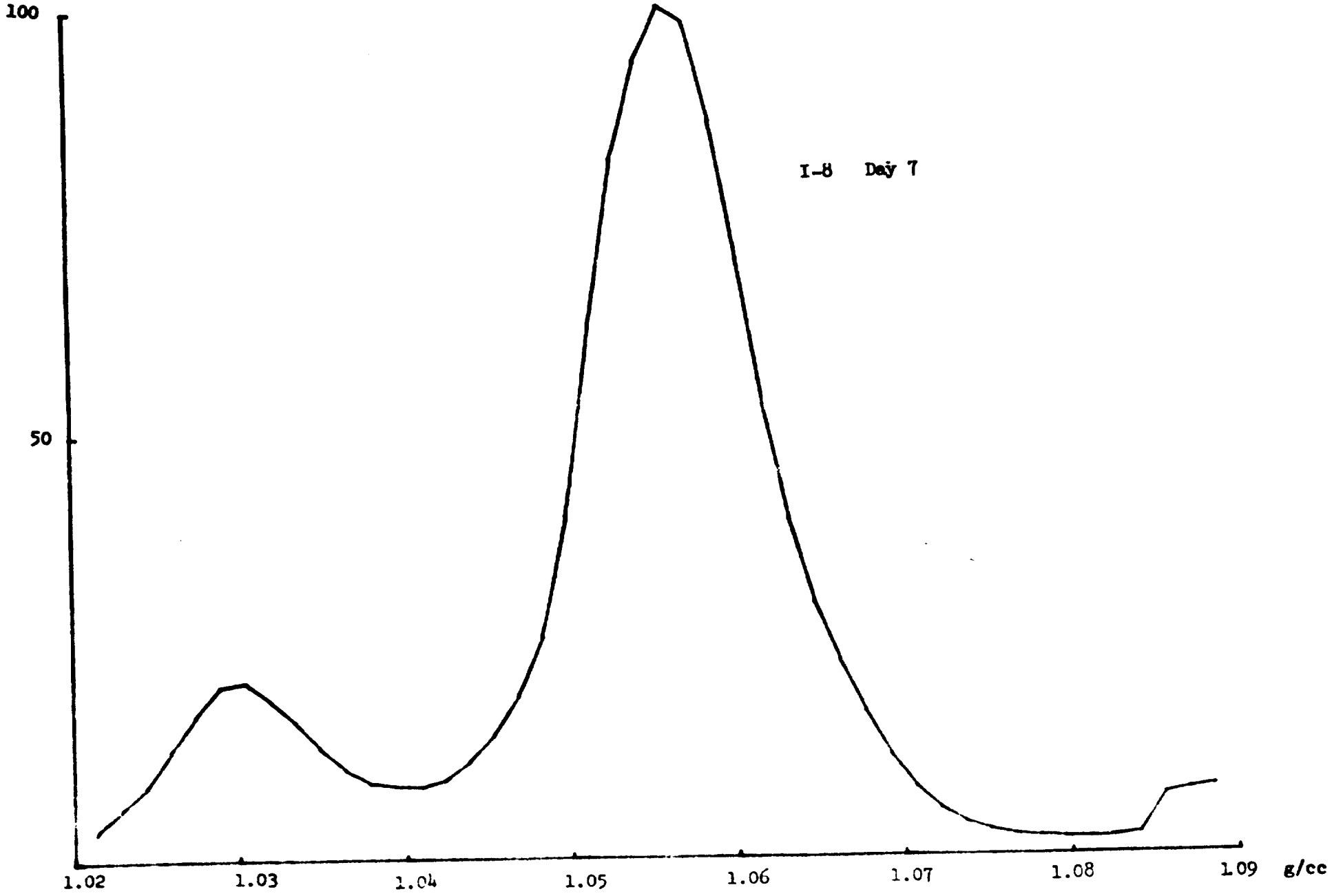
100
50
I-8 Day 7
1.02
1.03
1.04
1.05
1.06
1.07
1.08
1.09
g/cc

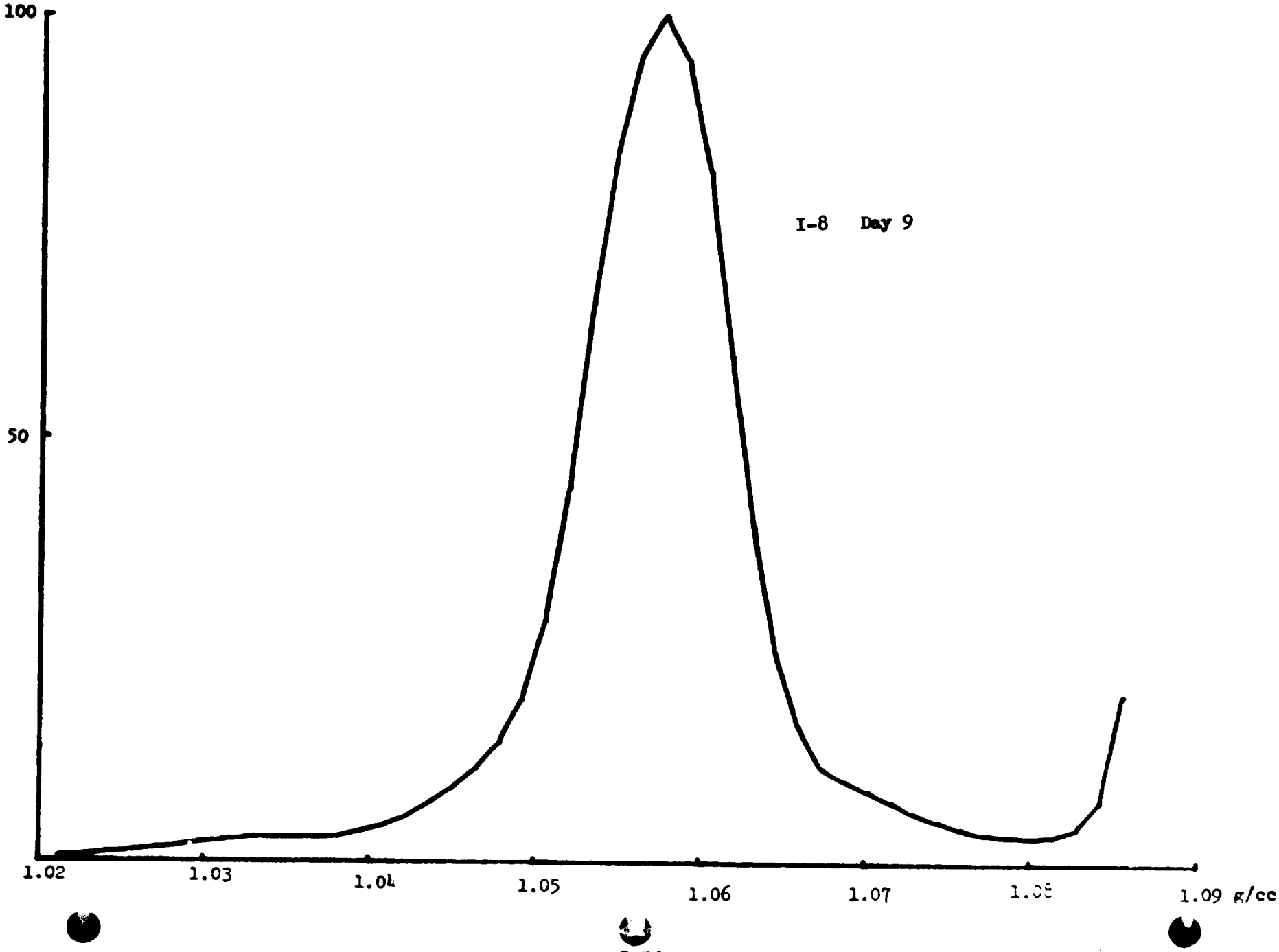
100
50
I-8 Day 9
1.02
1.03
1.04
1.05
1.06
1.07
1.08
1.09 g/cc

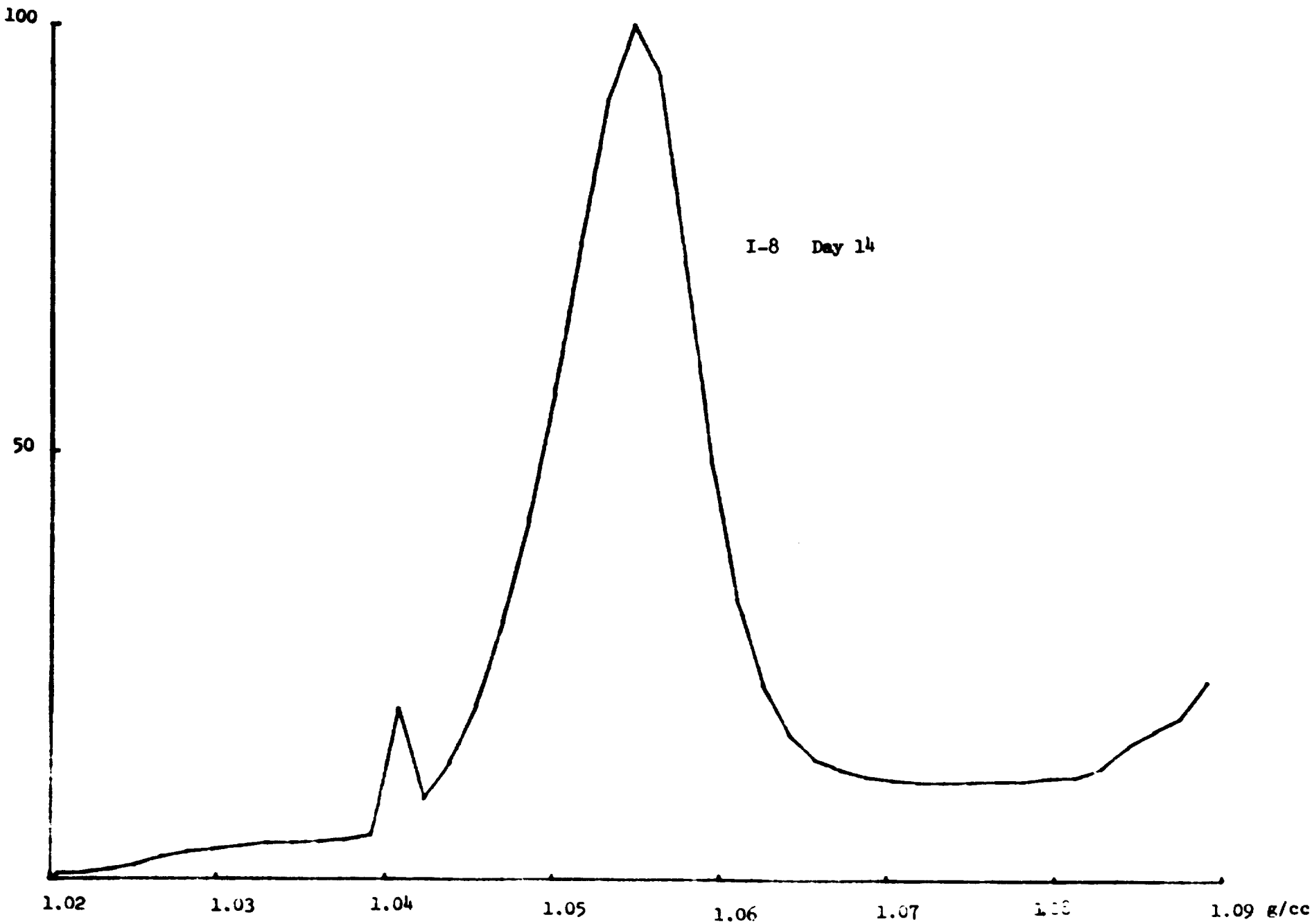
100
50
I-8 Day 14
1.02
1.03
1.04
1.05
1.06
1.07
1.09 g/cc

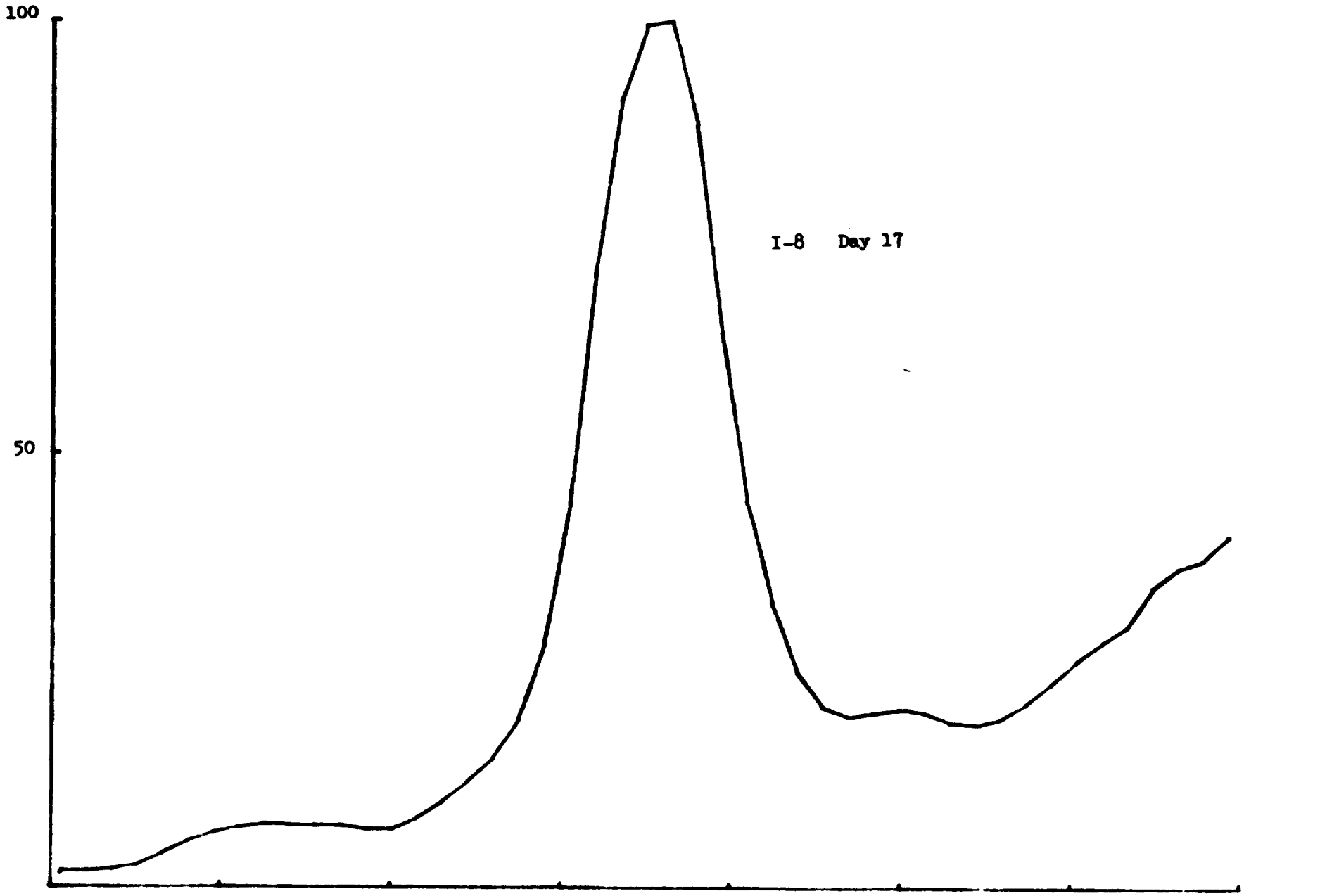
100
50
I-8 Day 17
1.02
1.03
1.04
1.05
1.06
1.07
1.08
1.09 g/cc

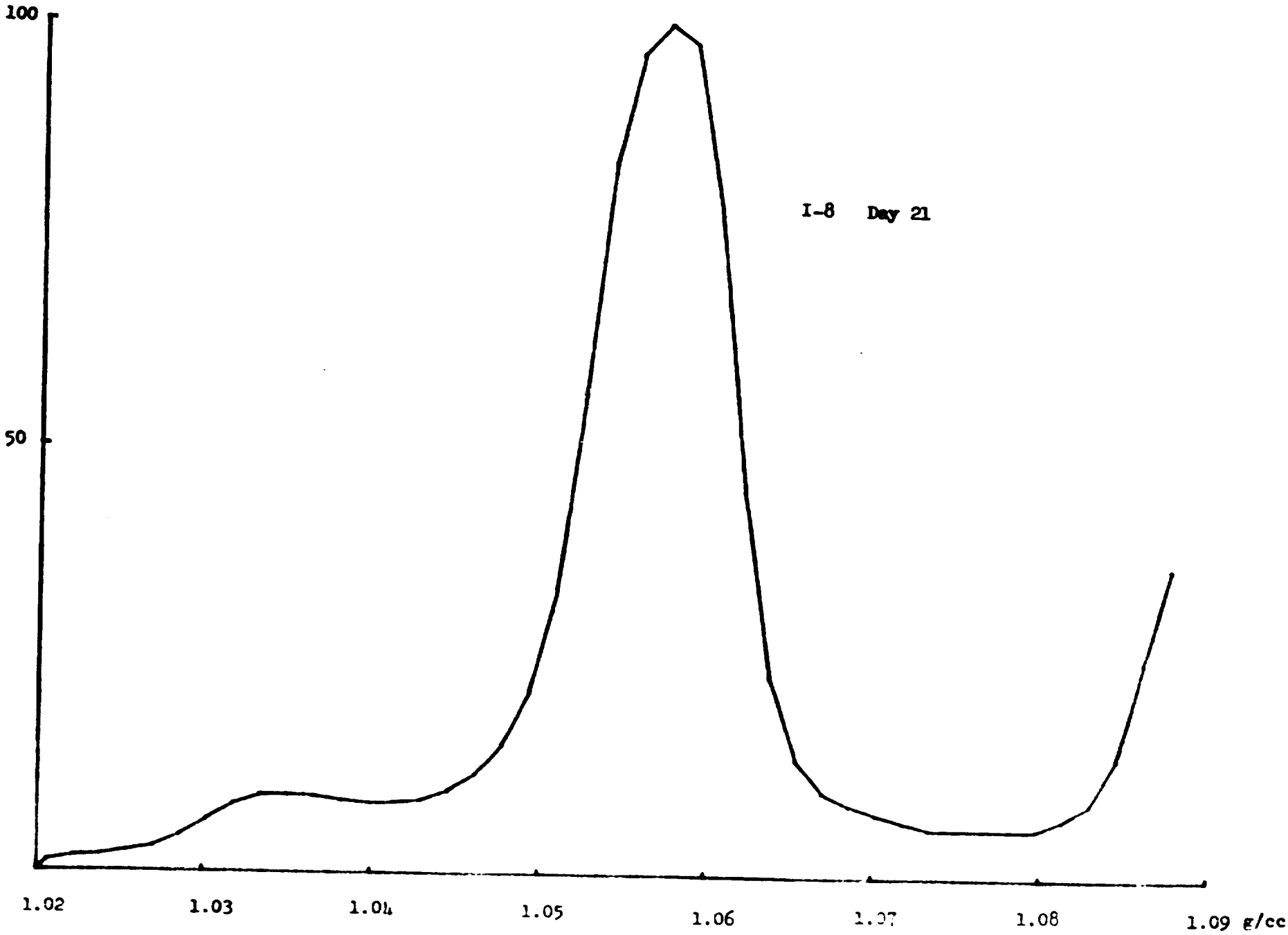
100
50
I-8 Day 21
1.02
1.03
1.04
1.05
1.06
1.07
1.08
1.09 g/cc

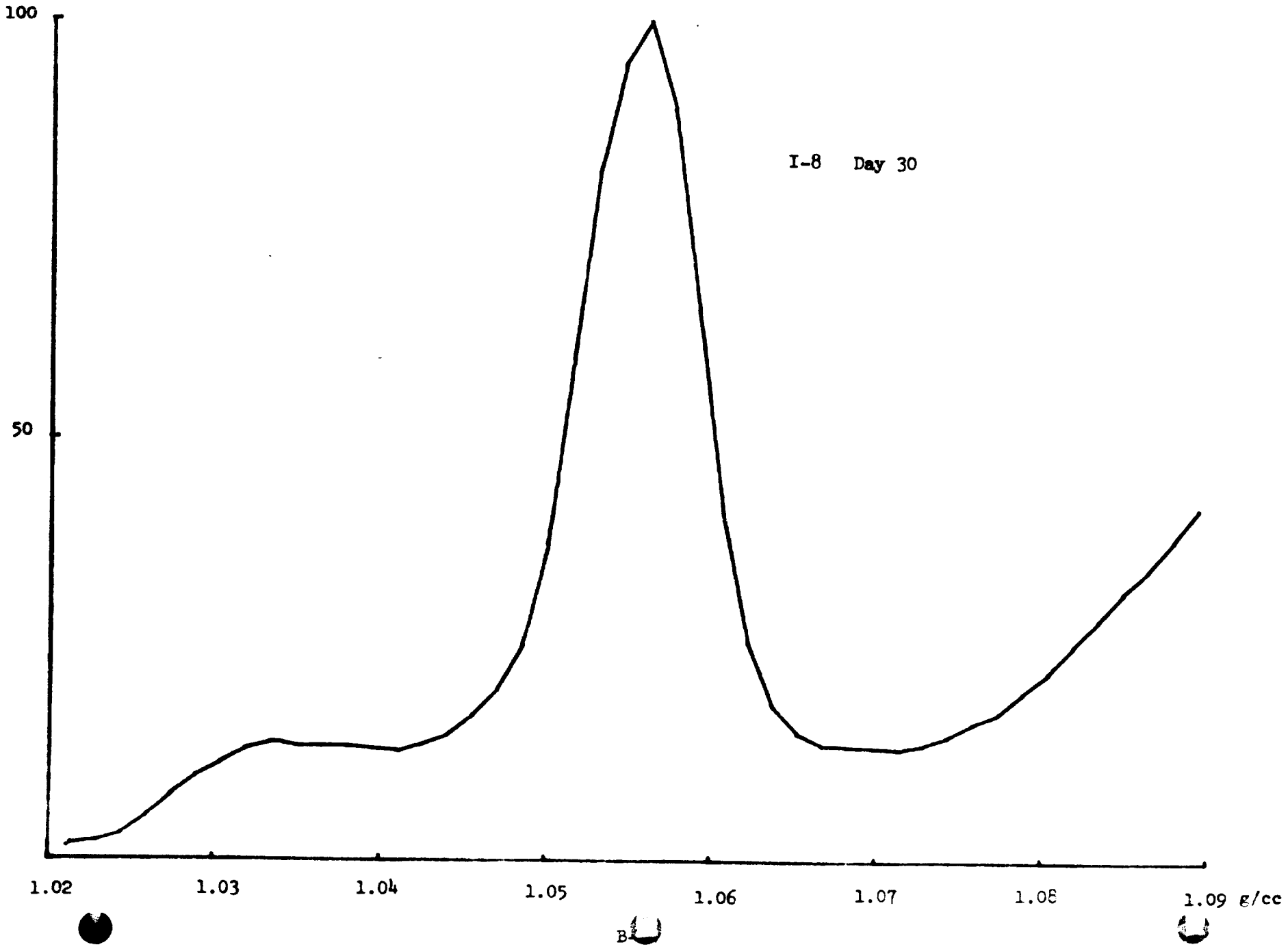
100
50
I-8 Day 30
1.02
1.03
1.04
1.05
1.06
1.07
1.08
1.09 g/cc

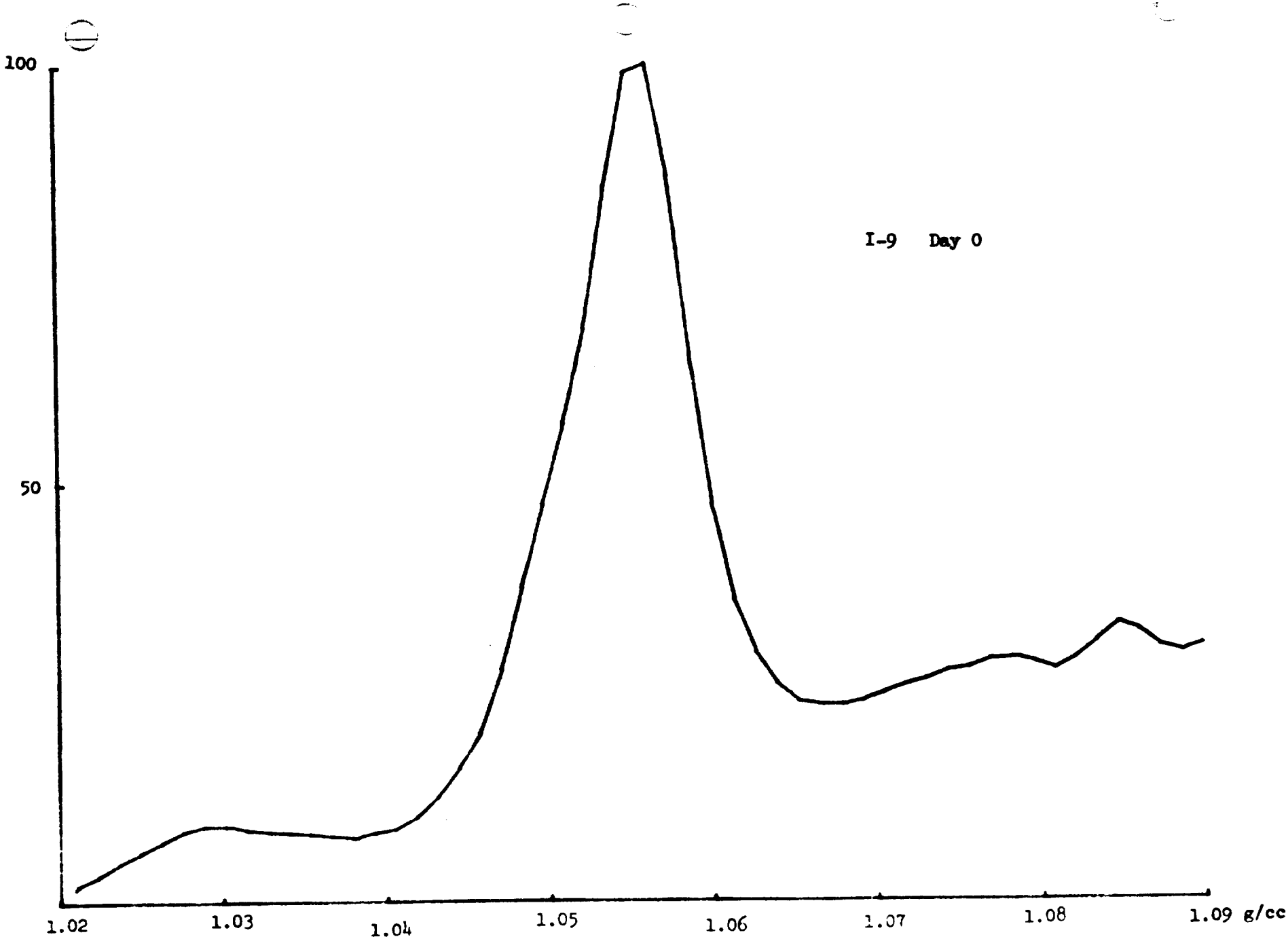
100
50
I-9 Day 0
1.02
1.03
1.04
1.05
1.06
1.07
1.08
1.09 g/cc

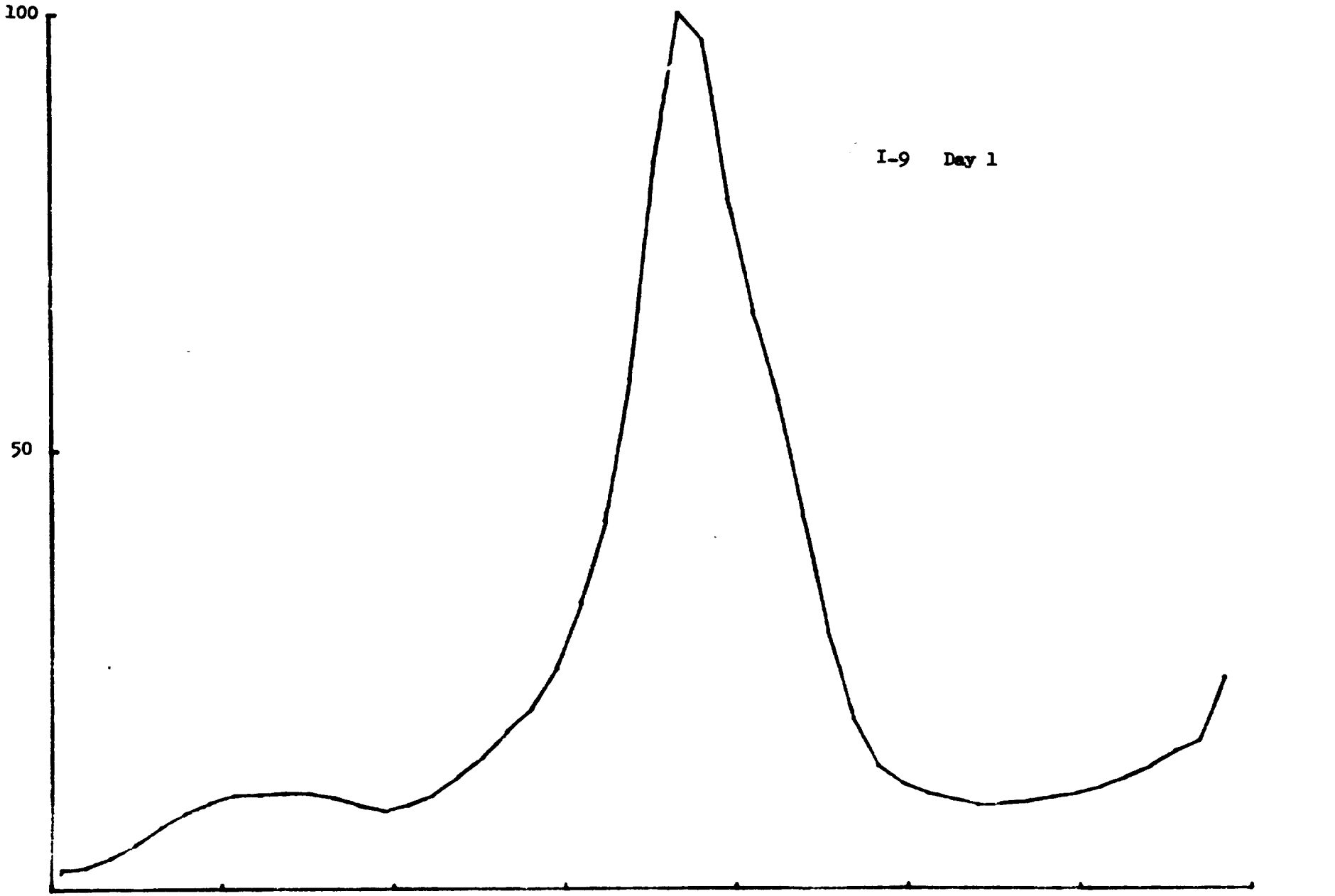
100
50
I-9 Day 1
1.02
1.03
1.04
1.05
1.06
1.07
1.08
1.09 ε/cc

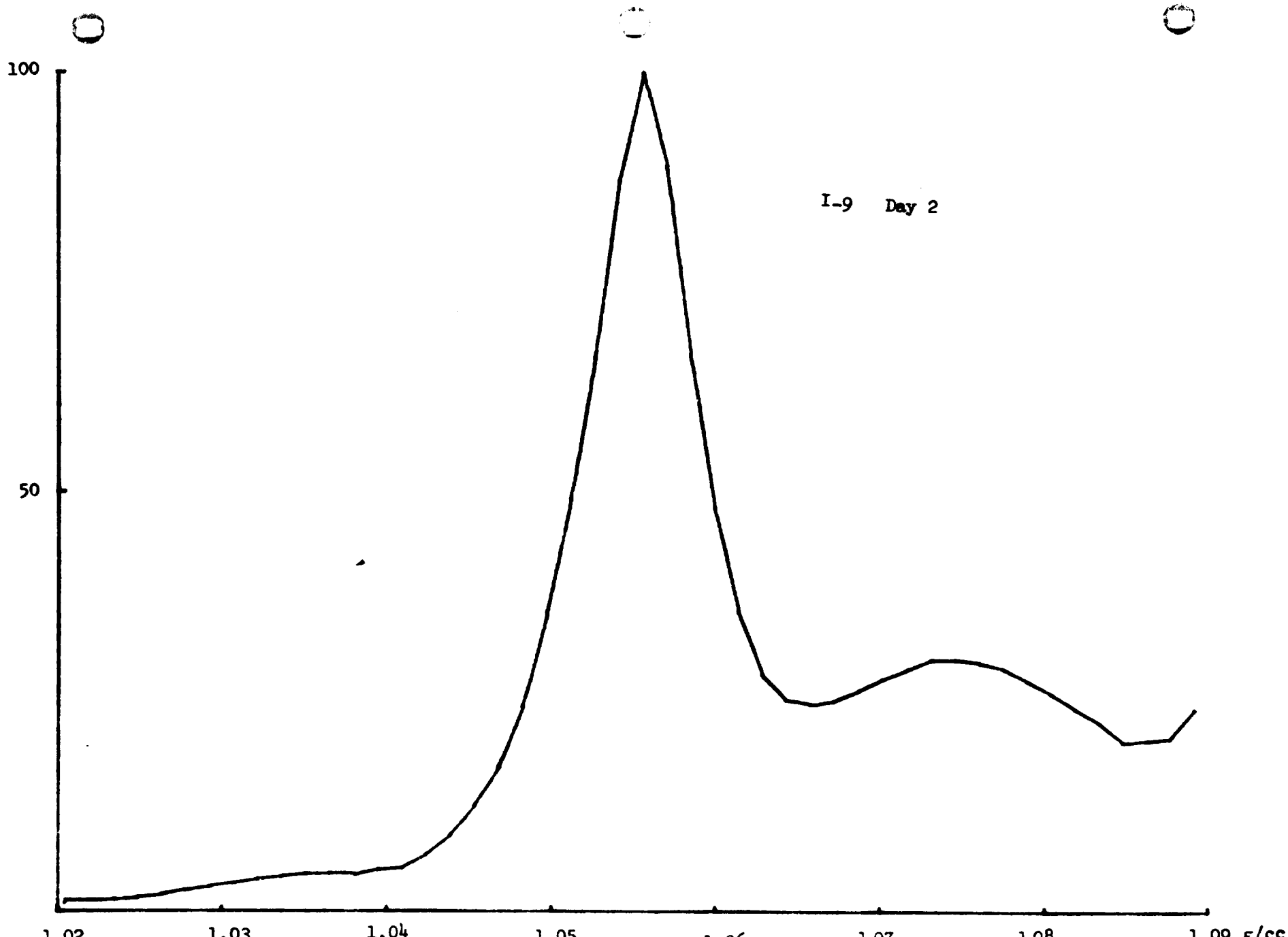
100
50
I-9 Day 2
1.02
1.03
1.04
1.05
1.06
1.07
1.08
1.09 g/cc

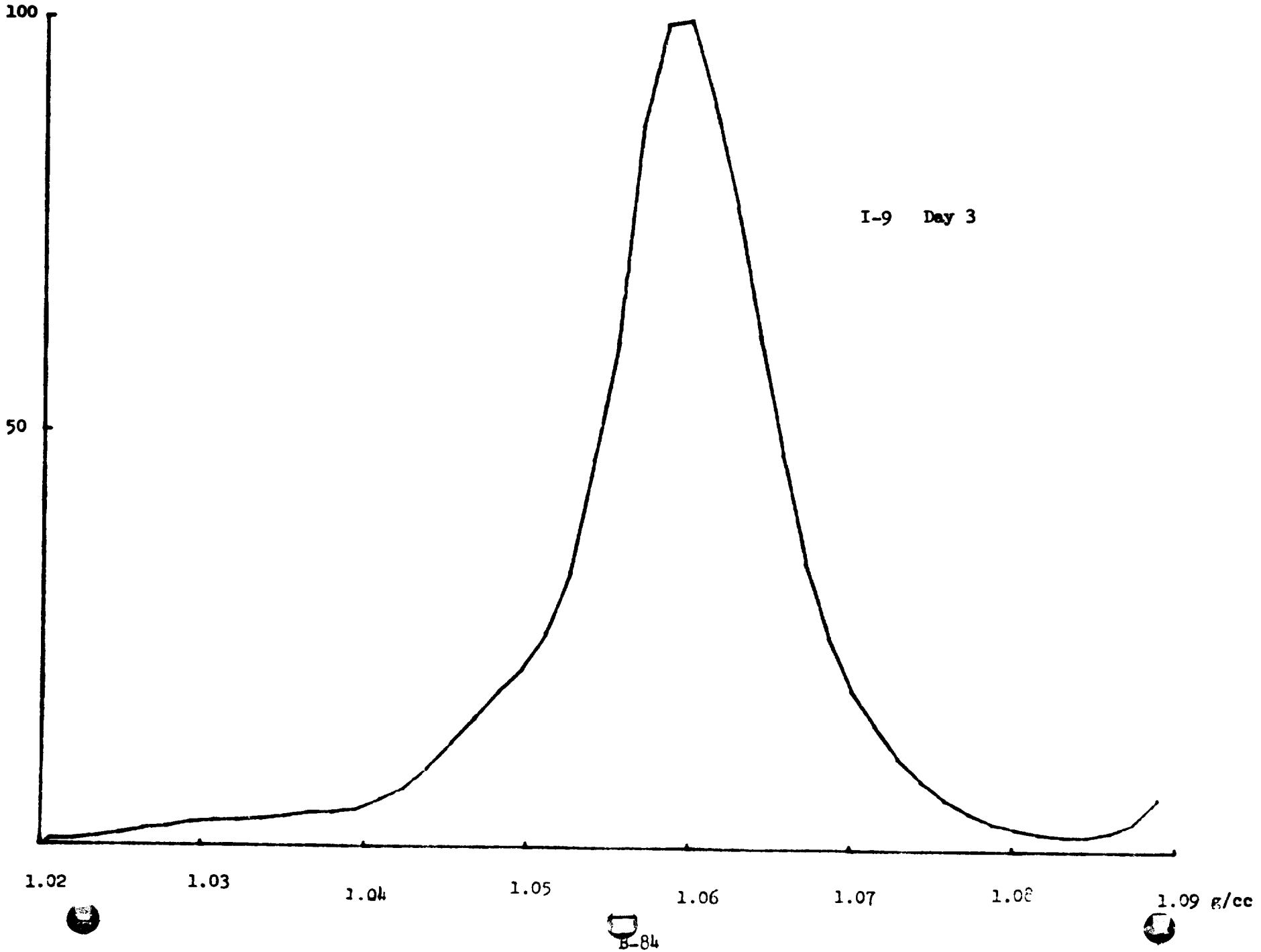
100
50
I-9 Day 3
1.02
1.03
1.04
1.05
1.06
1.07
1.08
1.09 g/cc

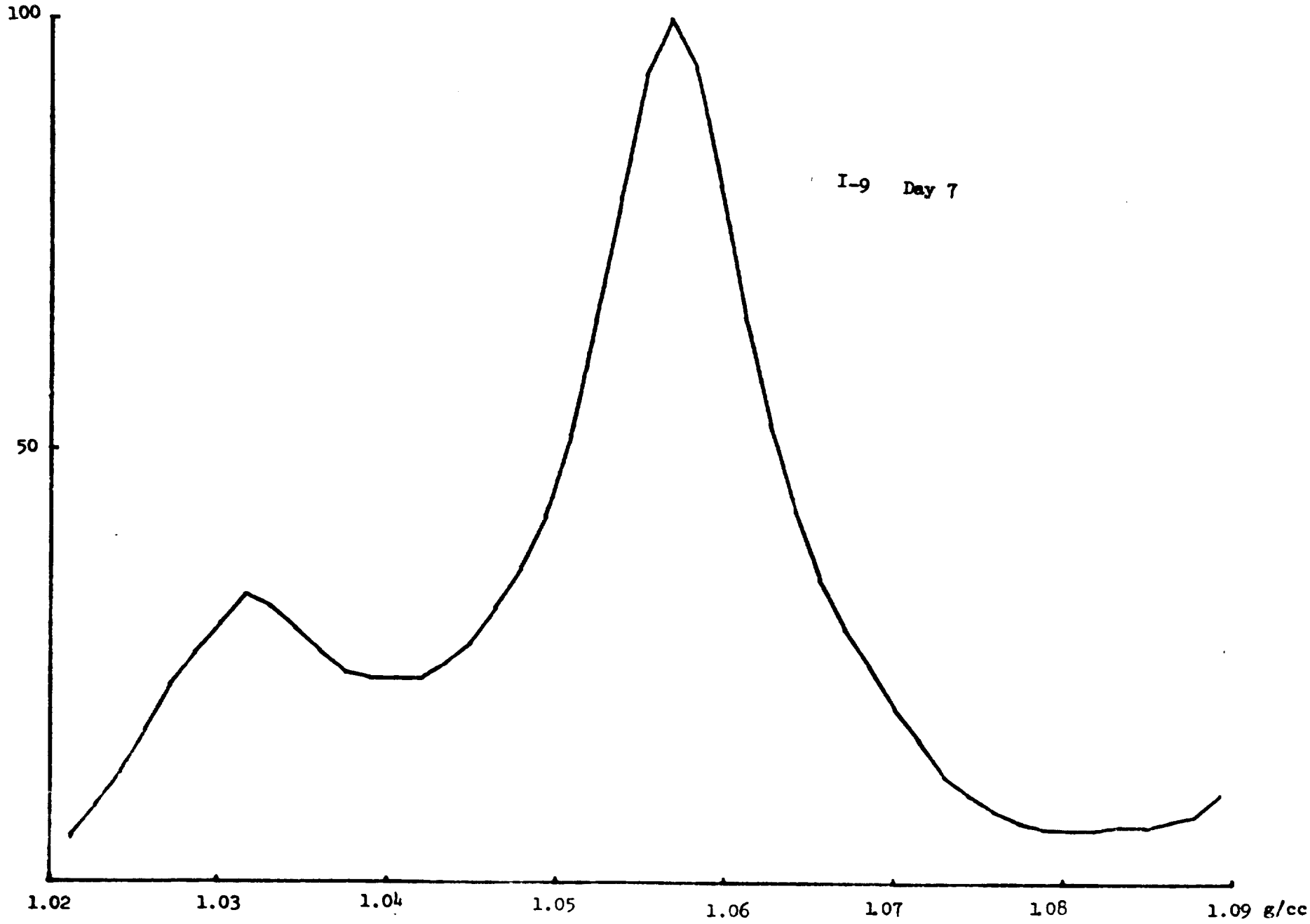
100
50
I-9 Day 7
1.02
1.03
1.04
1.05
1.06
1.07
1.08
1.09 g/cc

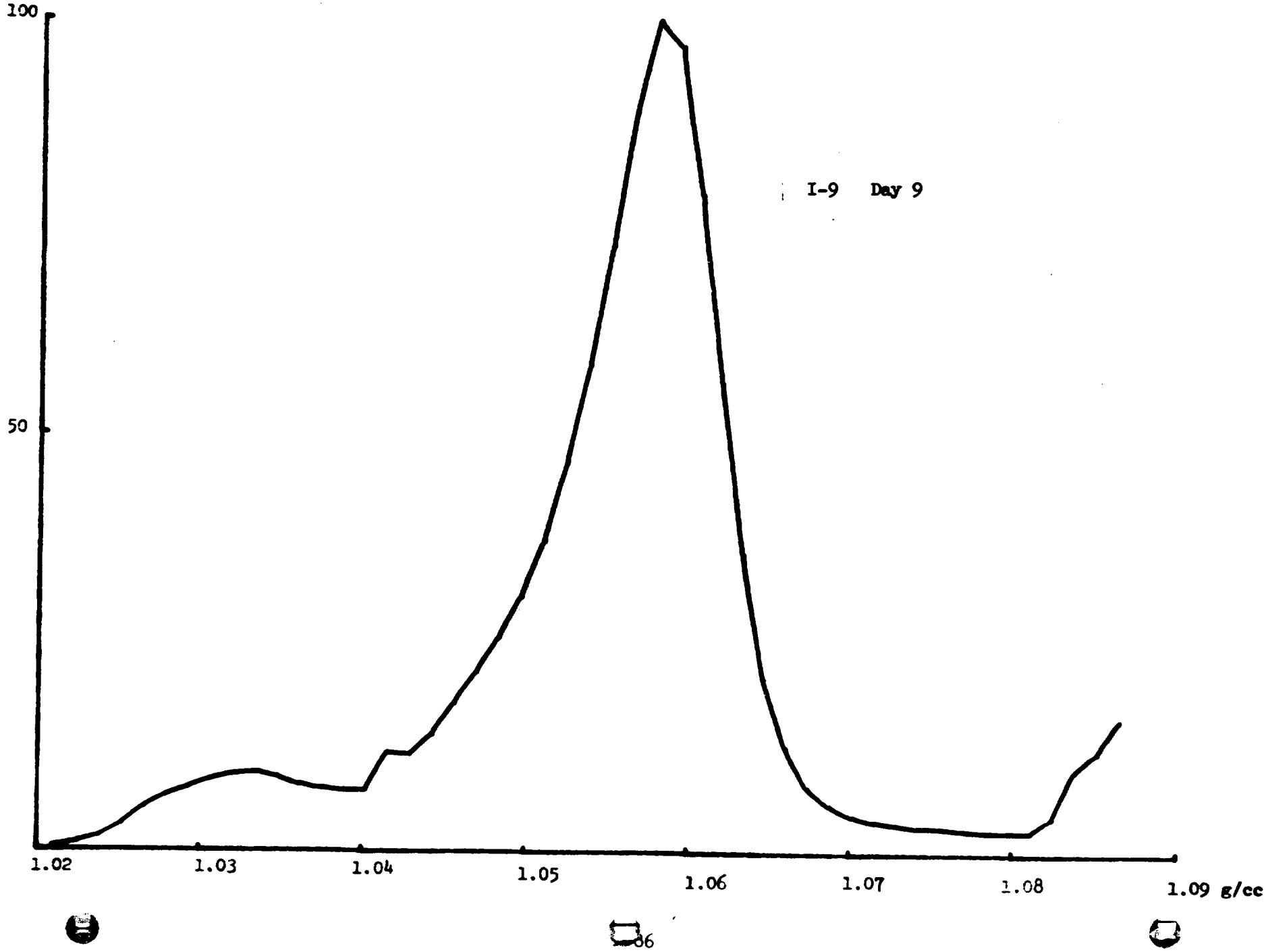
100
50
I-9 Day 9
1.02
1.03
1.04
1.05
1.06
1.07
1.08
1.09 g/cc

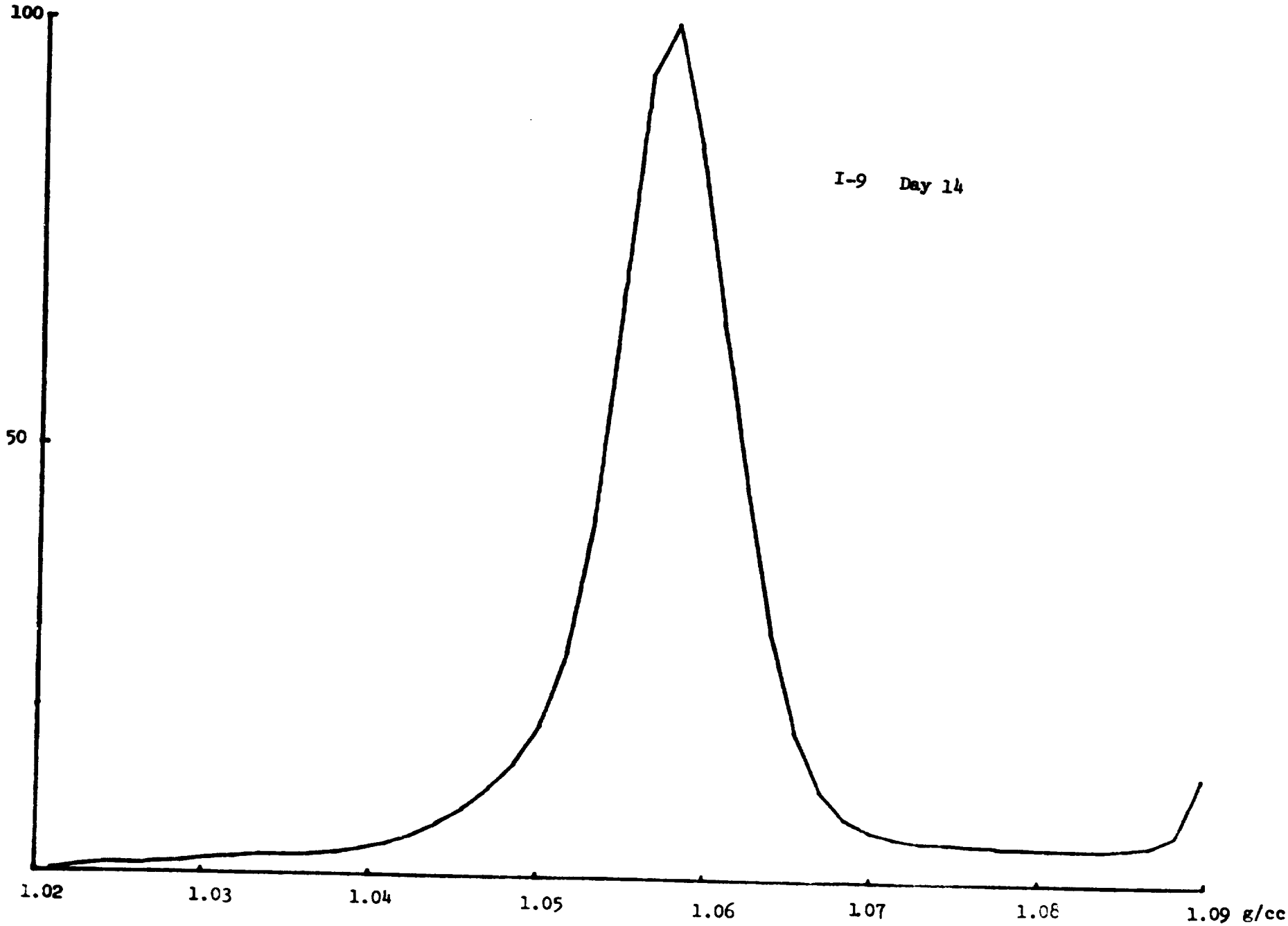
100
50
I-9 Day 14
1.02
1.03
1.04
1.05
1.06
1.07
1.08
1.09 g/cc

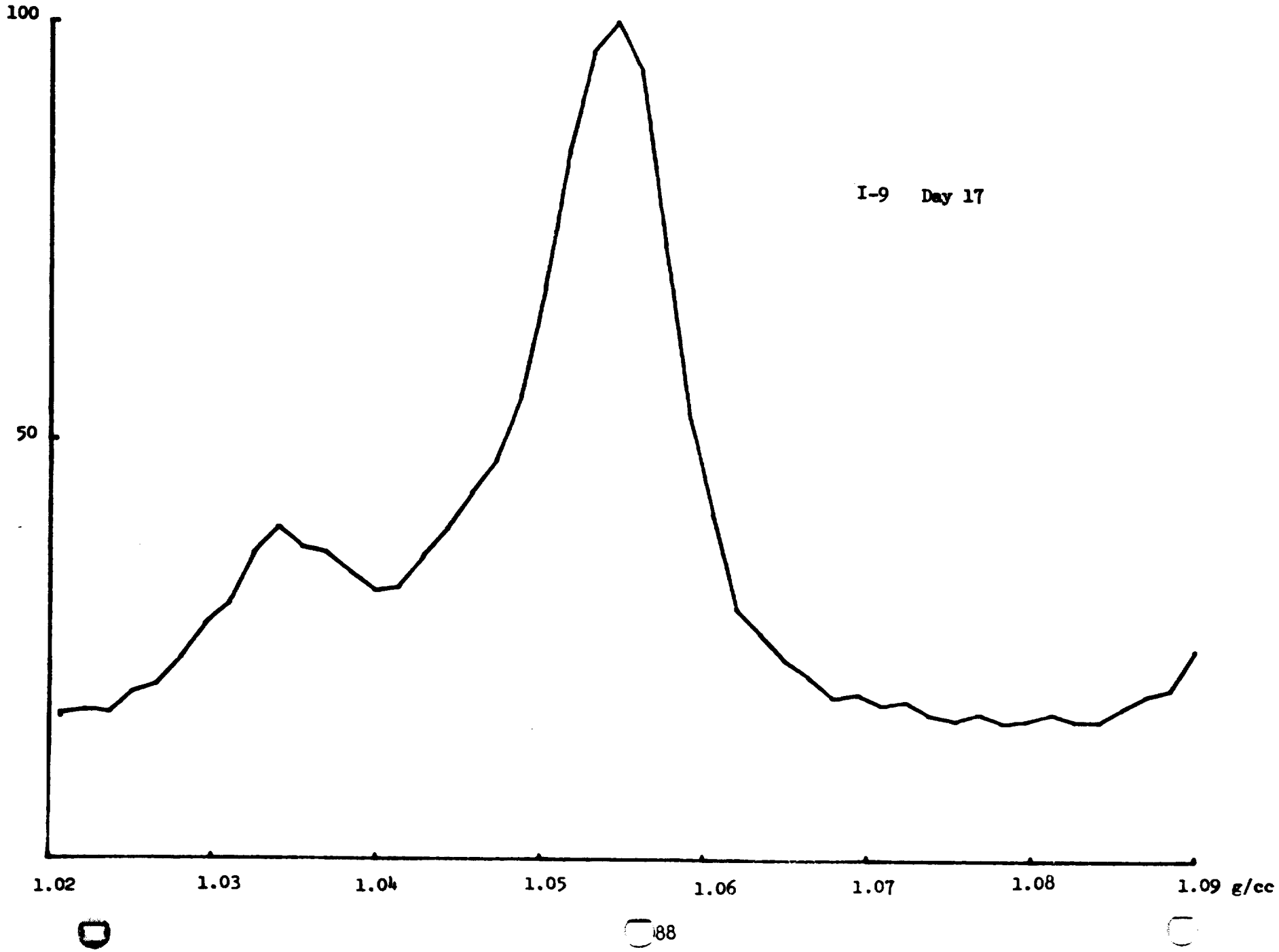
100
50
I-9 Day 17
1.02
1.03
1.04
1.05
1.06
1.07
1.08
1.09 g/cc

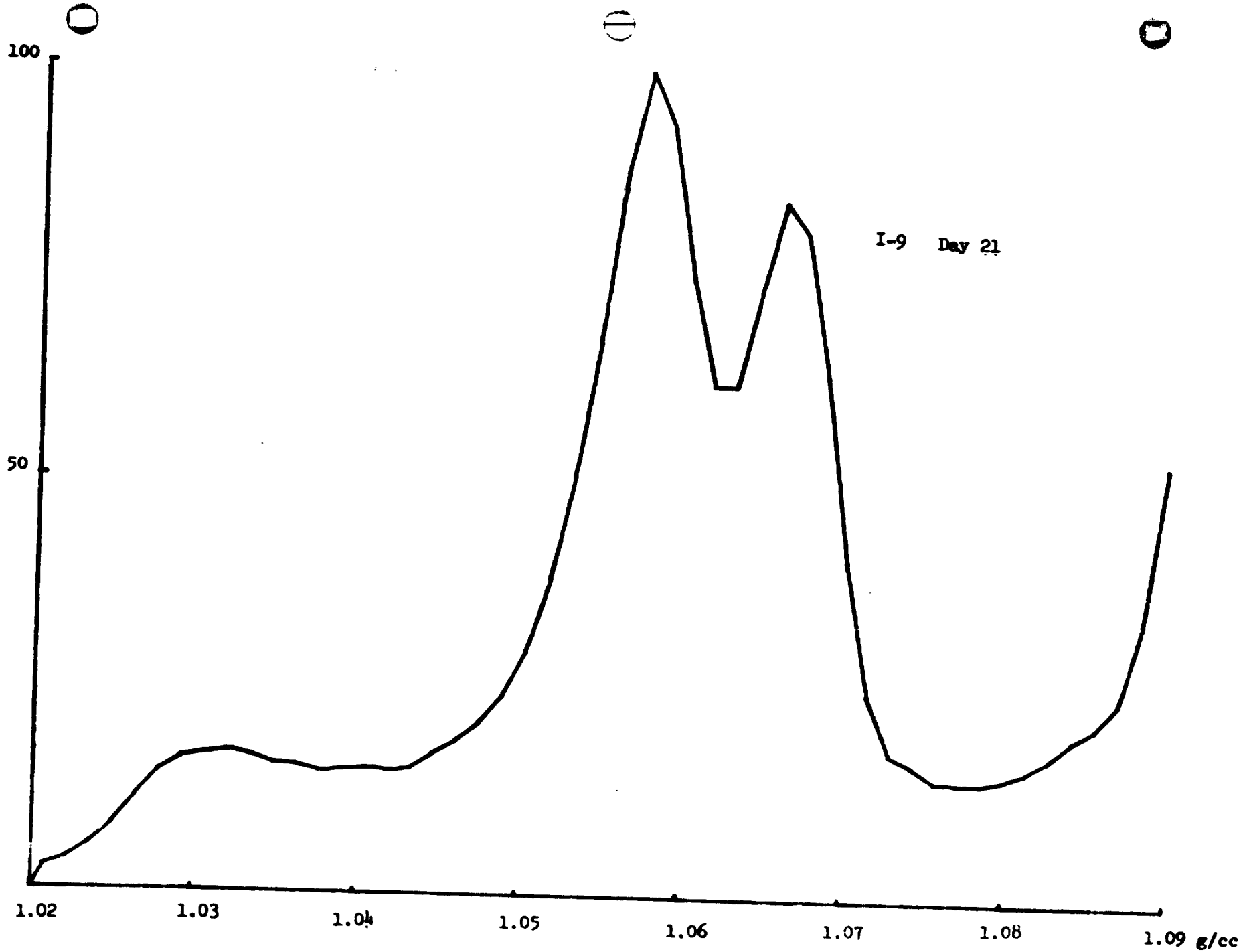
100
50
I-9 Day 21
1.02
1.03
1.04
1.05
1.06
1.07
1.08
1.09 g/cc

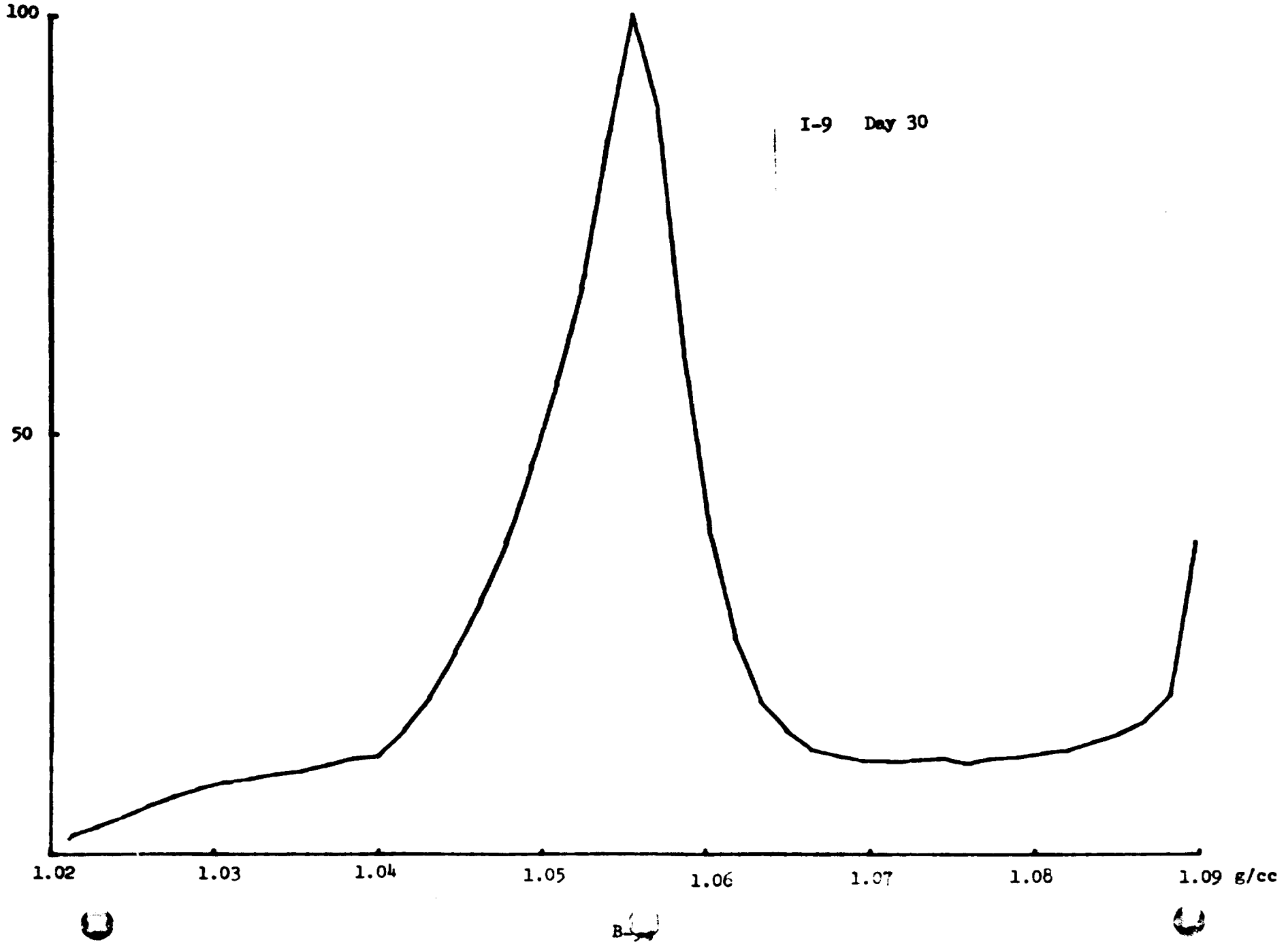
100
50
I-9 Day 30
1.02
1.03
1.04
1.05
1.06
1.07
1.08
1.09 g/cc

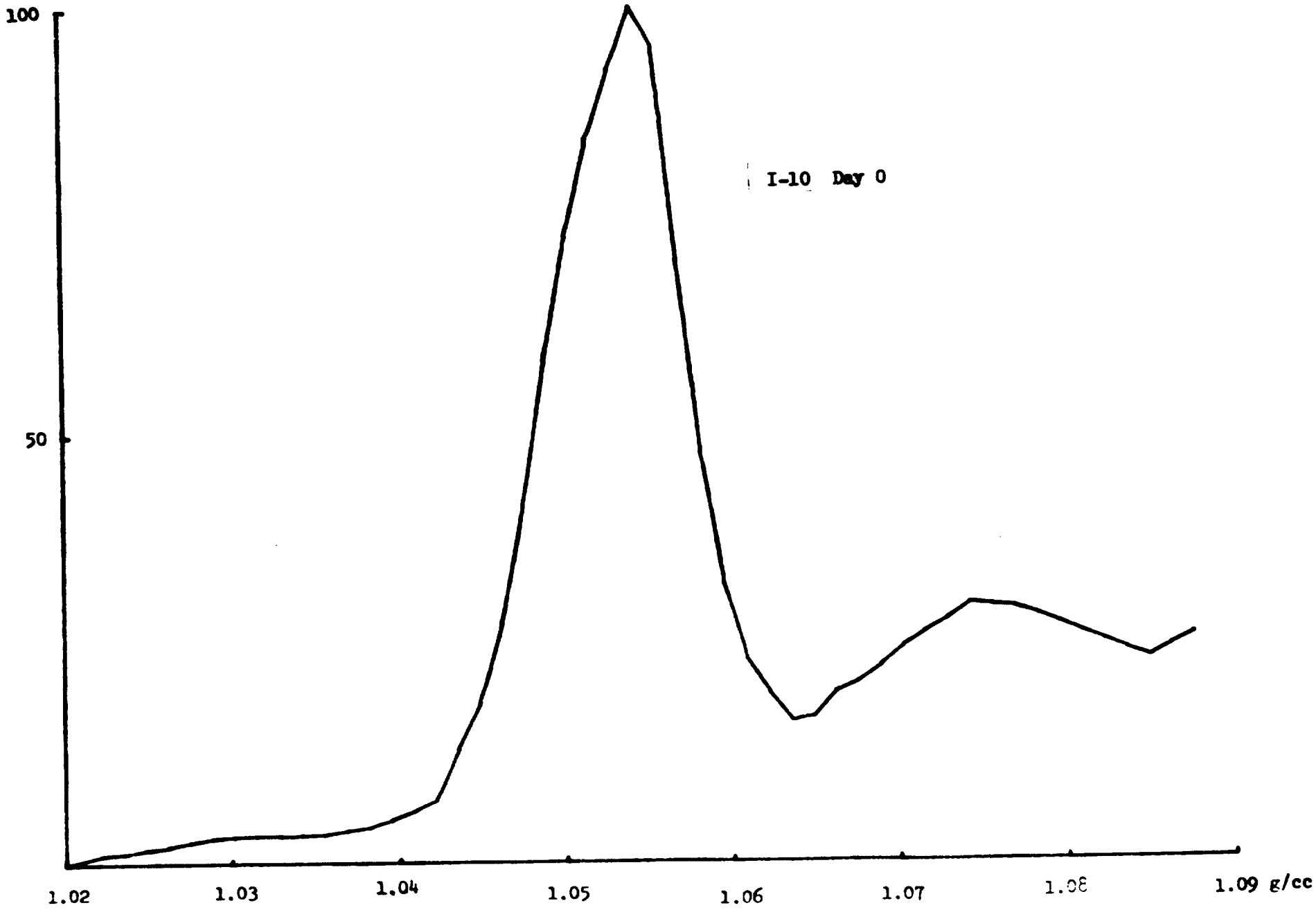
100
50
I-10 Day 0
1.02
1.03
1.04
1.05
1.06
1.07
1.08
1.09 g/cc

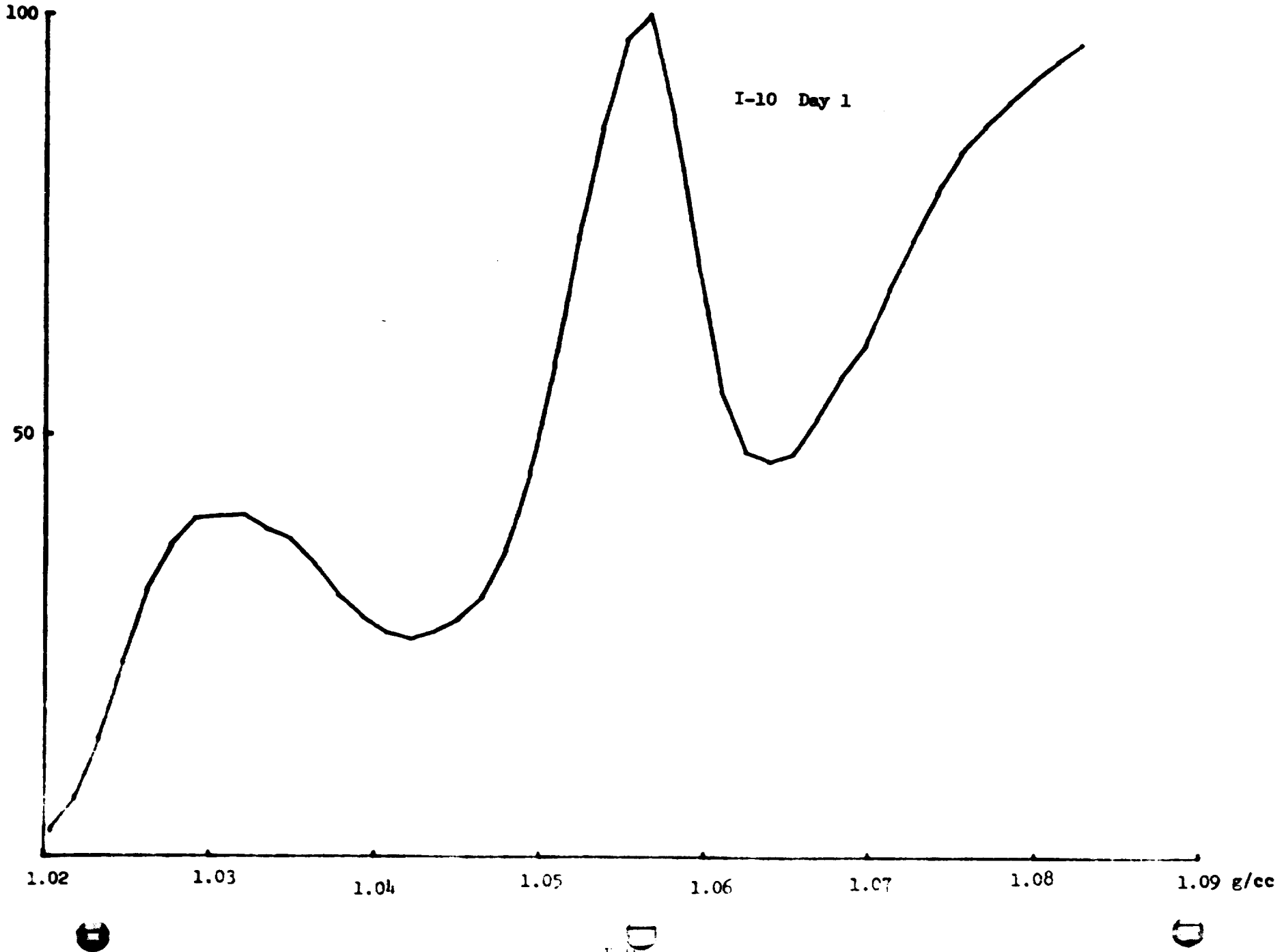
100
50
I-10 Day 1
1.02
1.03
1.04
1.05
1.06
1.07
1.08
1.09 g/cc

100
50
I-10 Day 2
1.02
1.03
1.04
1.05
1.06
1.07
1.08
1.09 g/cc

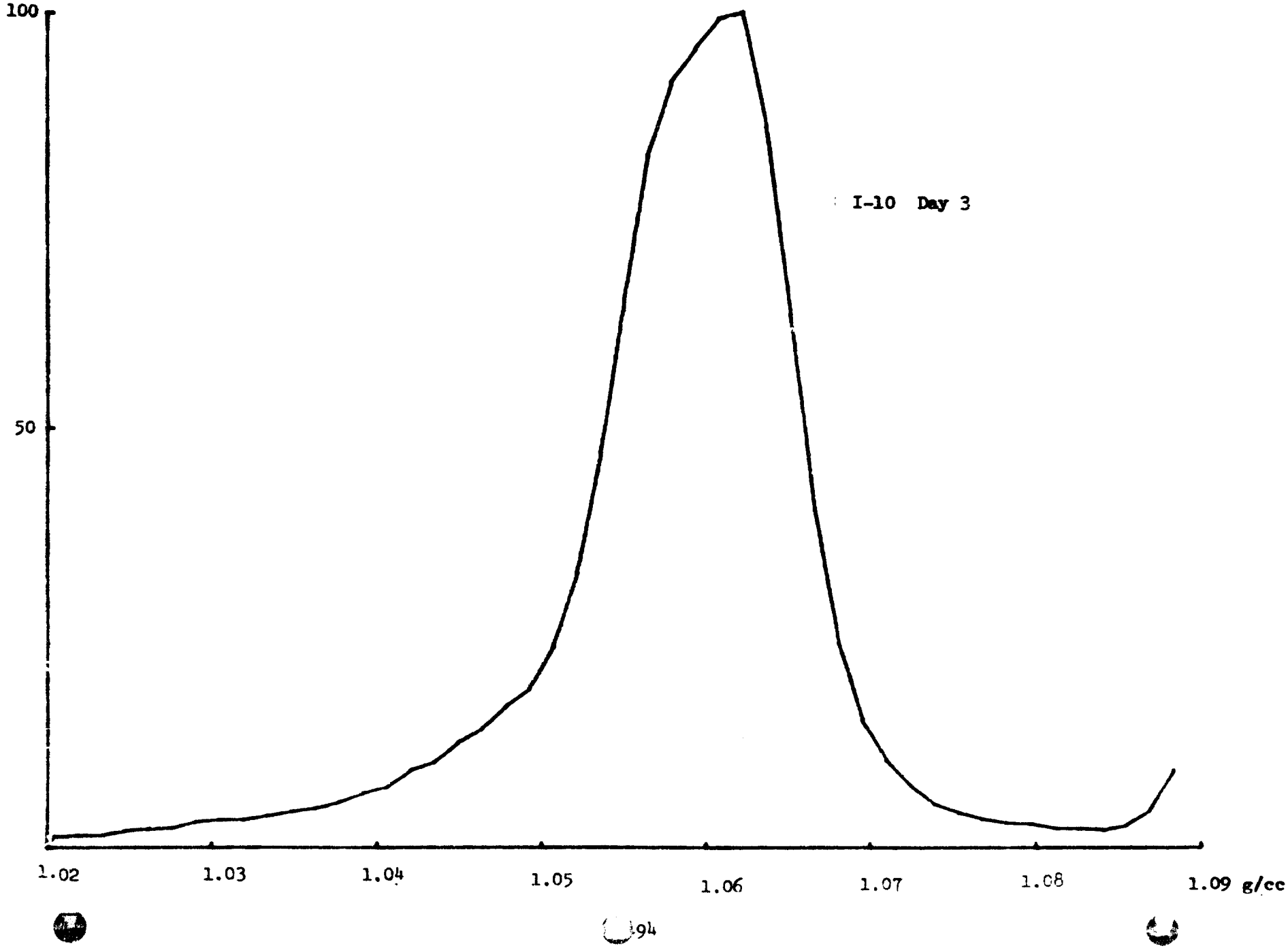
100
50
I-10 Day 3
1.02
1.03
1.04
1.05
1.06
1.07
1.08
1.09 g/cc

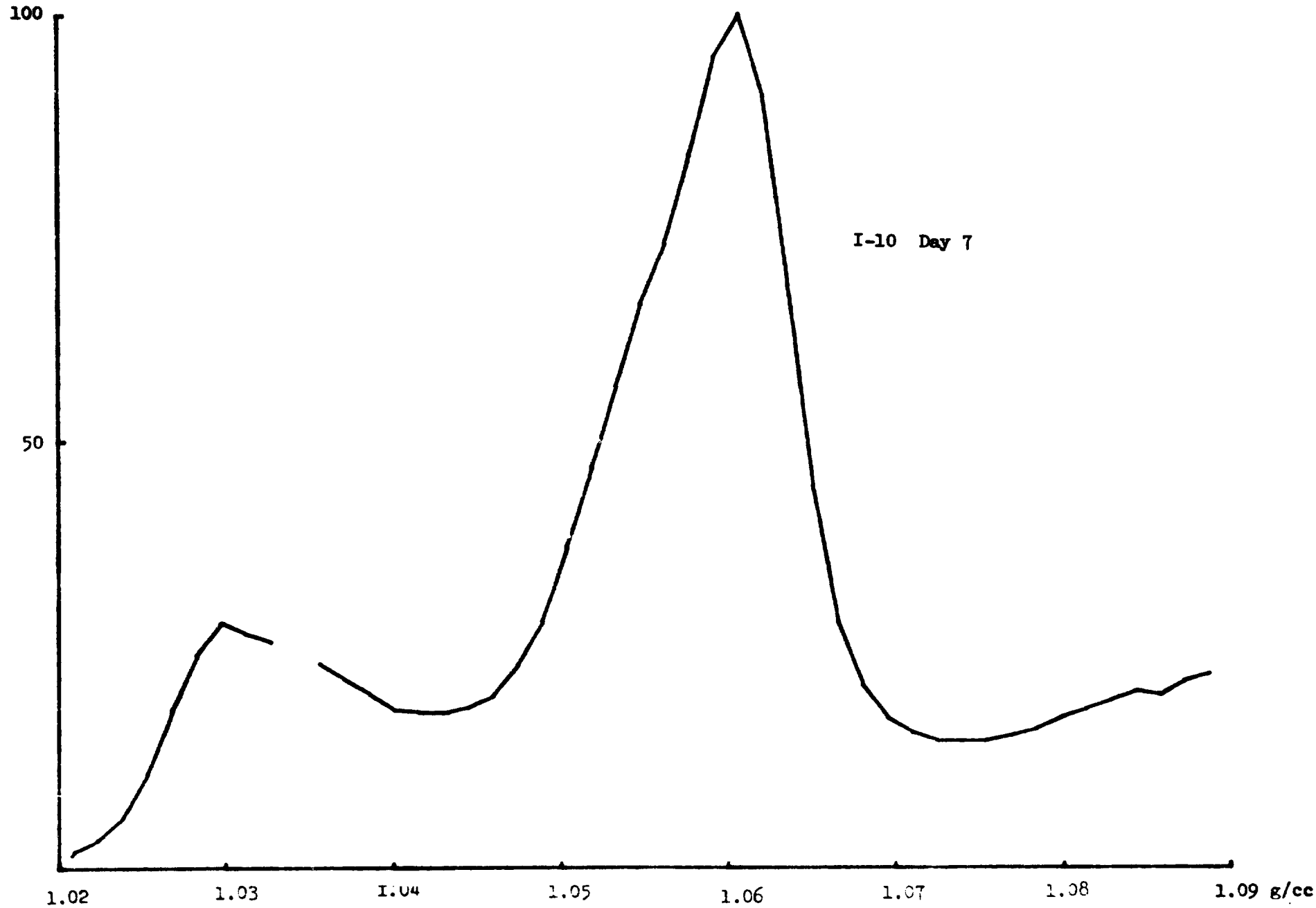
100
50
I-10 Day 7
1.02
1.03
1.04
1.05
1.06
1.07
1.08
1.09 g/cc

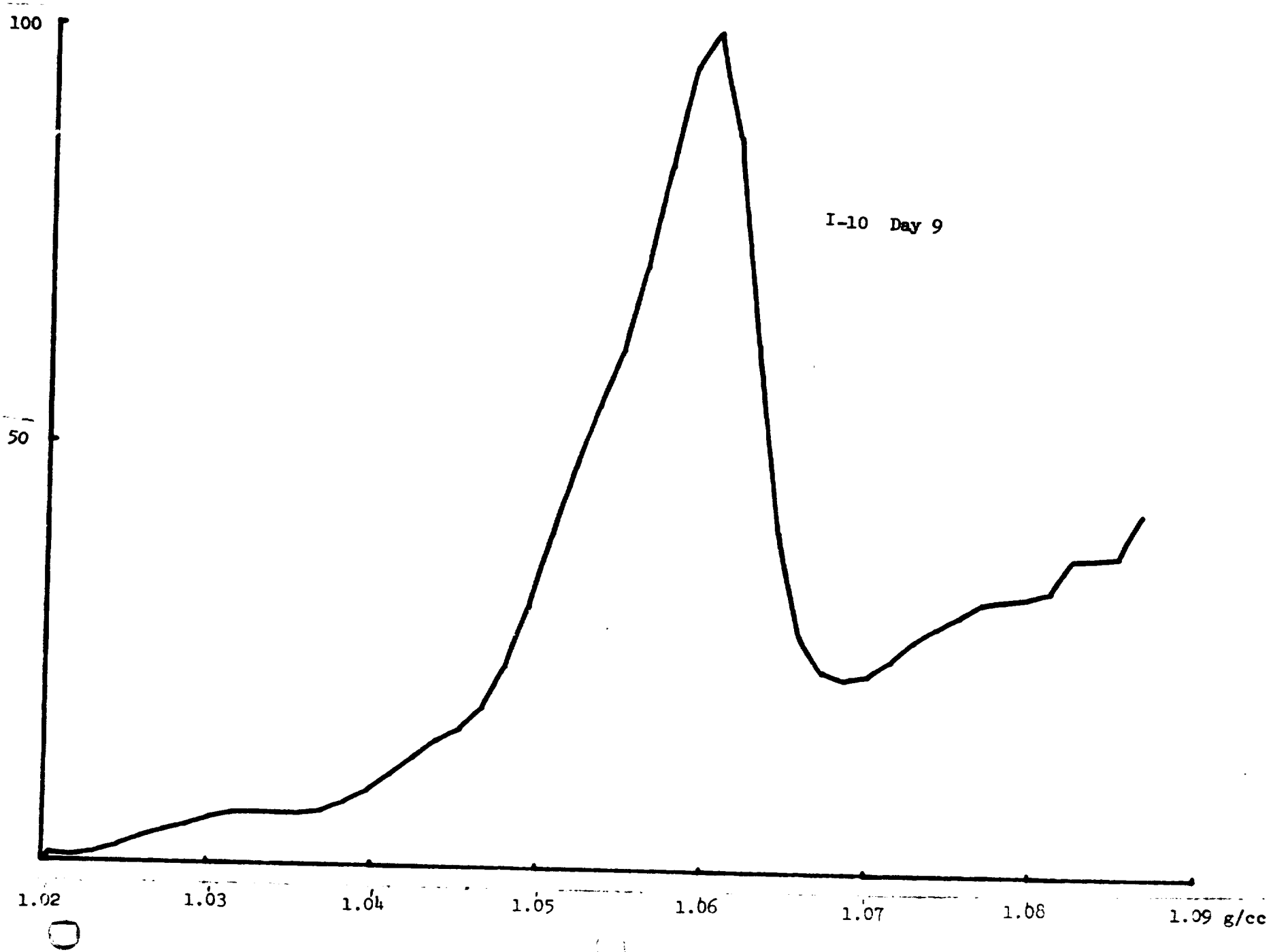
100
50
I-10 Day 9
1.02
1.03
1.04
1.05
1.06
1.07
1.08
1.09 g/cc

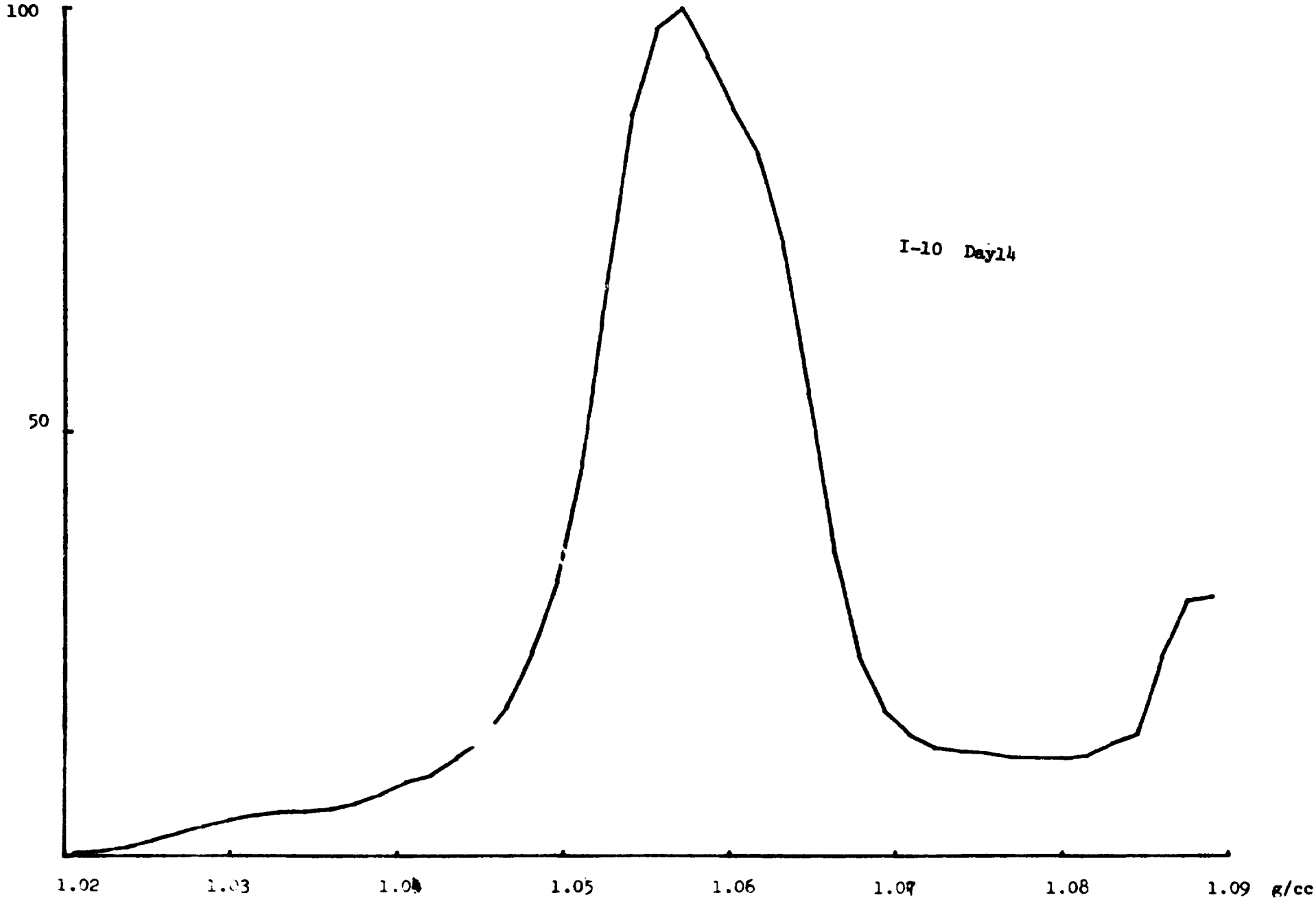
100
50
I-10 Day14
1.02
1.03
1.04
1.05
1.06
1.07
1.08
1.09
g/cc

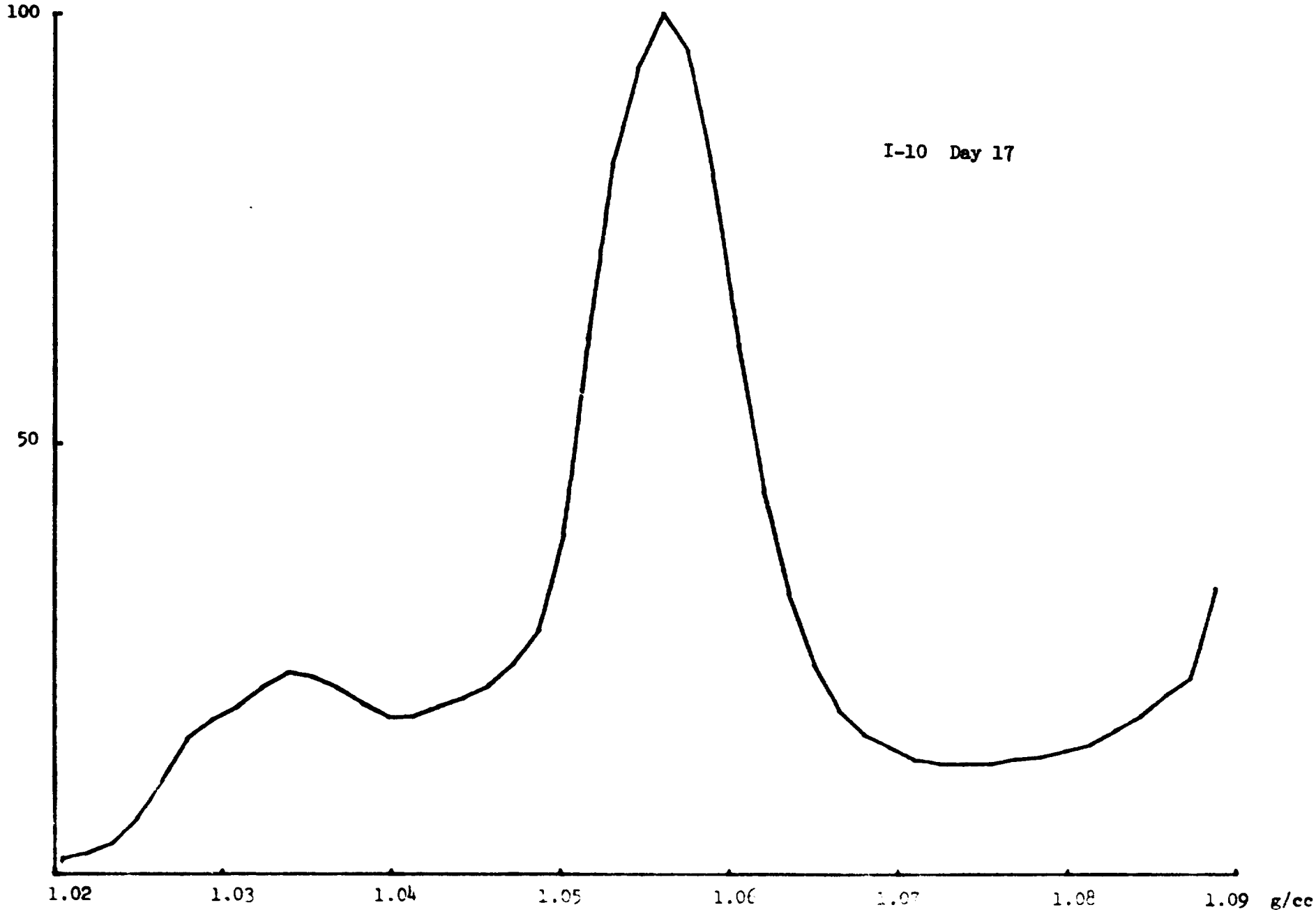
100
50
I-10 Day 17
1.02
1.03
1.04
1.05
1.06
1.07
1.08
1.09
g/cc

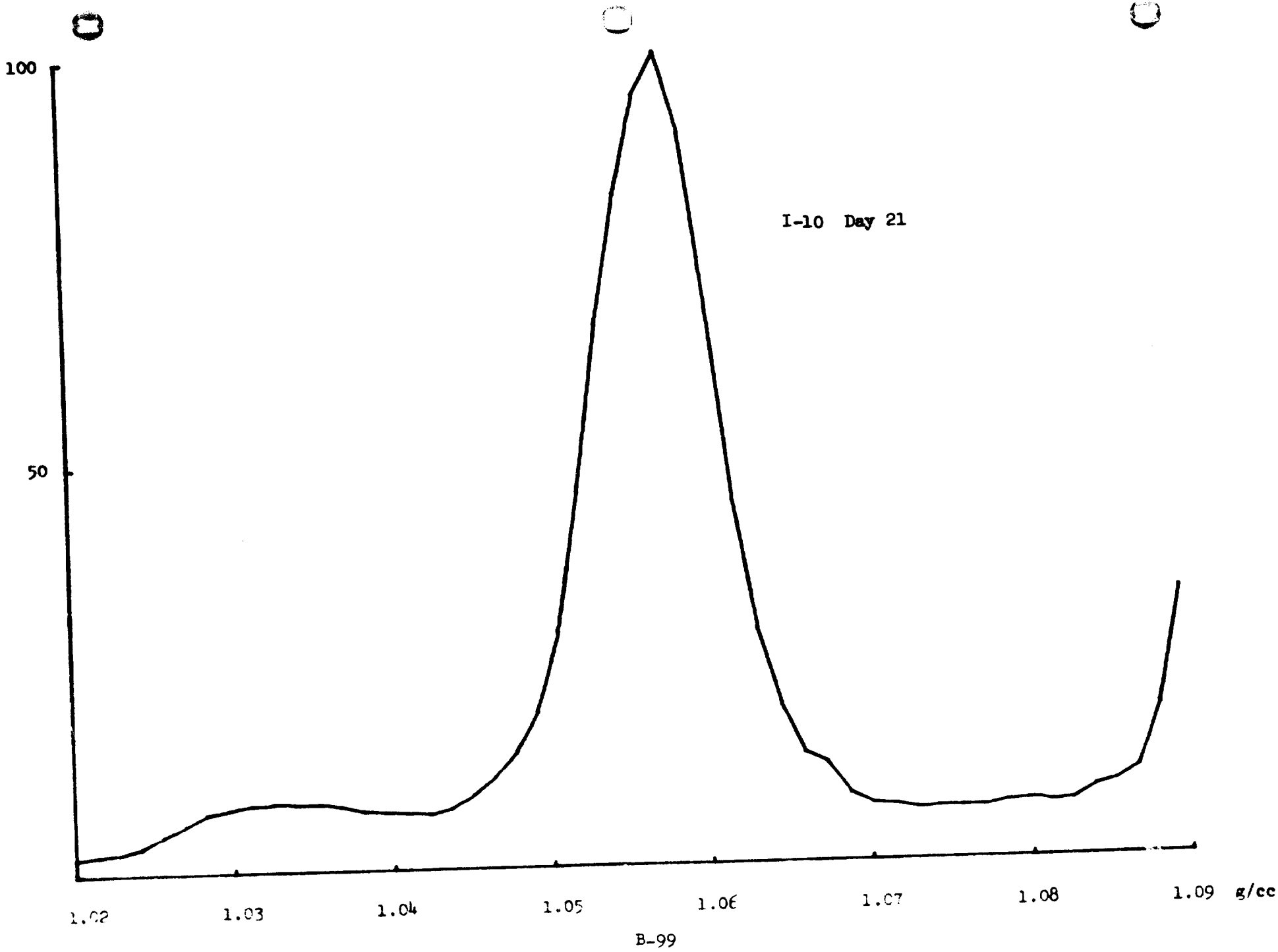
100
50
I-10 Day 21
1.02
1.03
1.04
1.05
1.06
1.07
1.08
1.09
g/cc

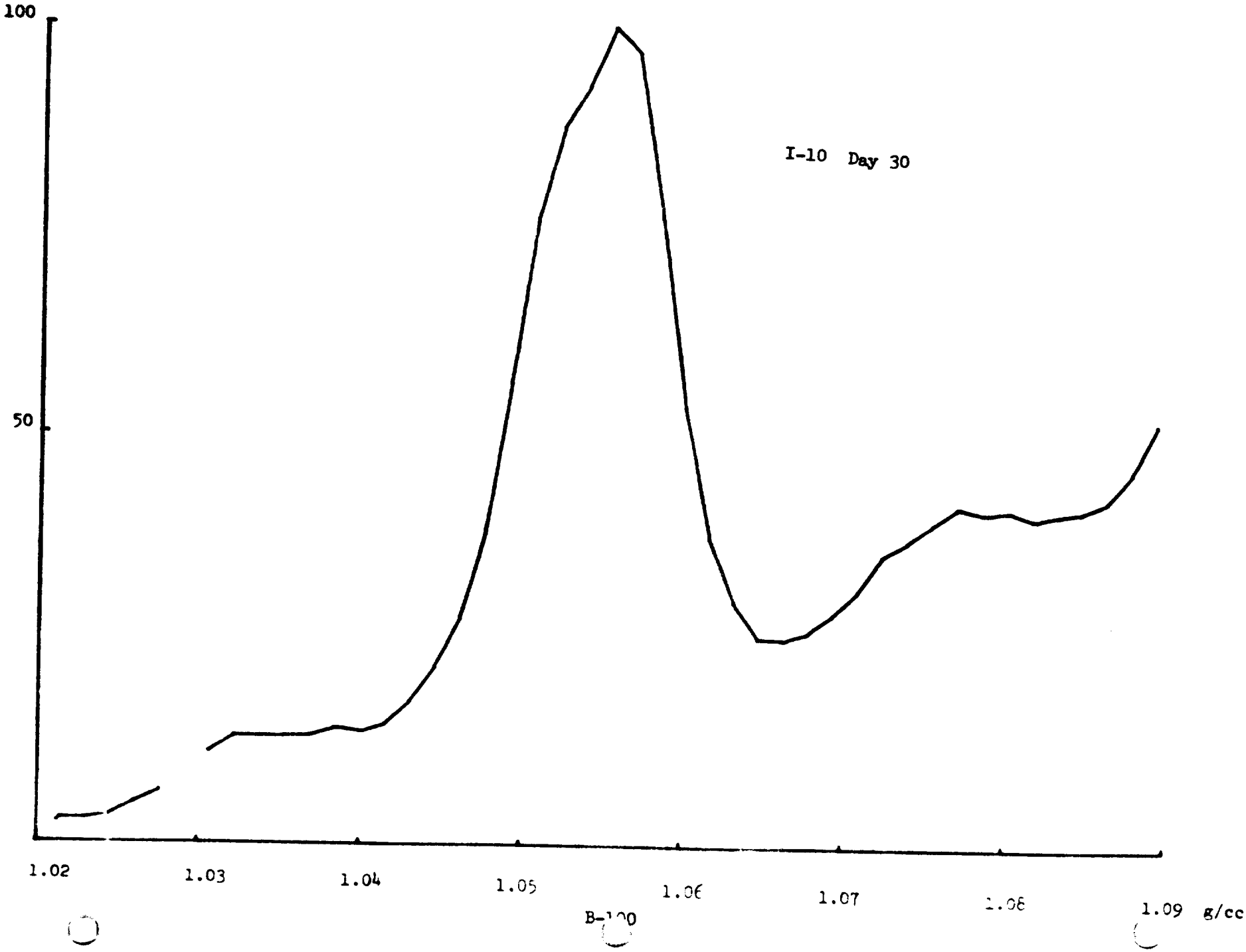
100
50
I-10 Day 30
1.02
1.03
1.04
1.05
1.06
1.07
1.08
1.09 g/cc

APPENDIX C

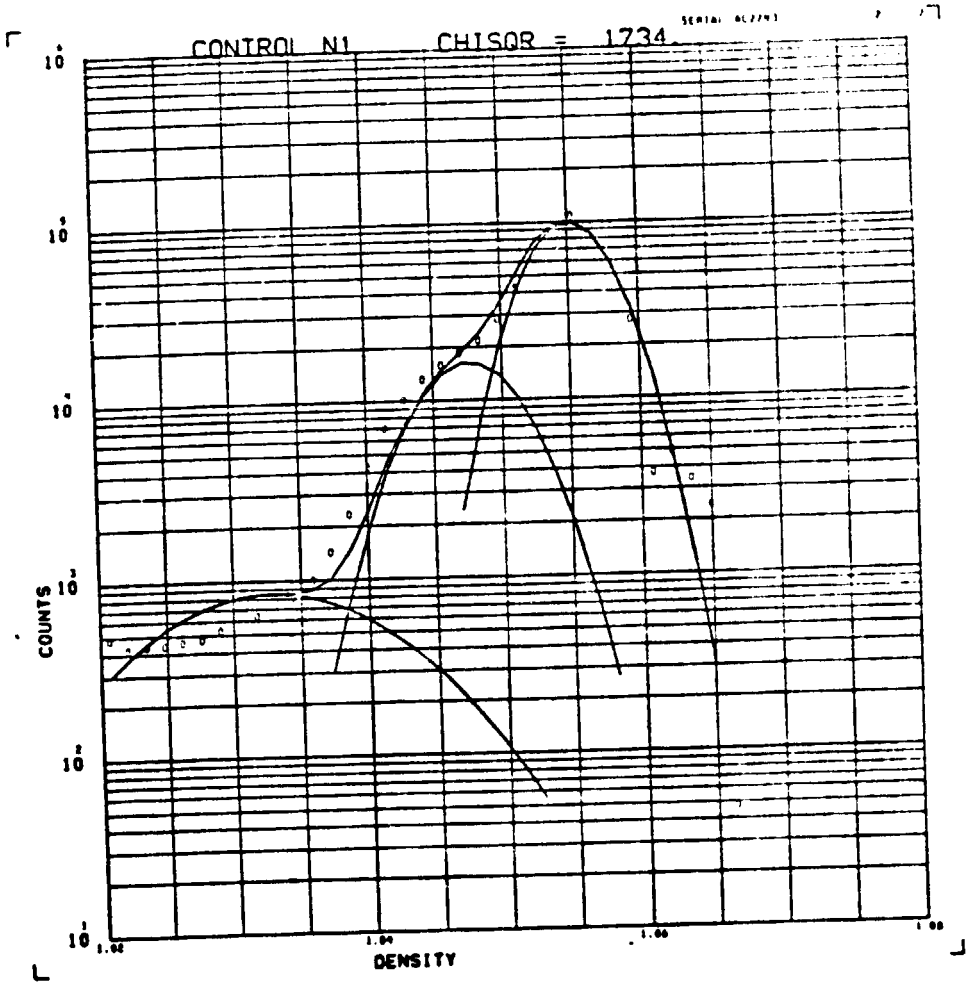

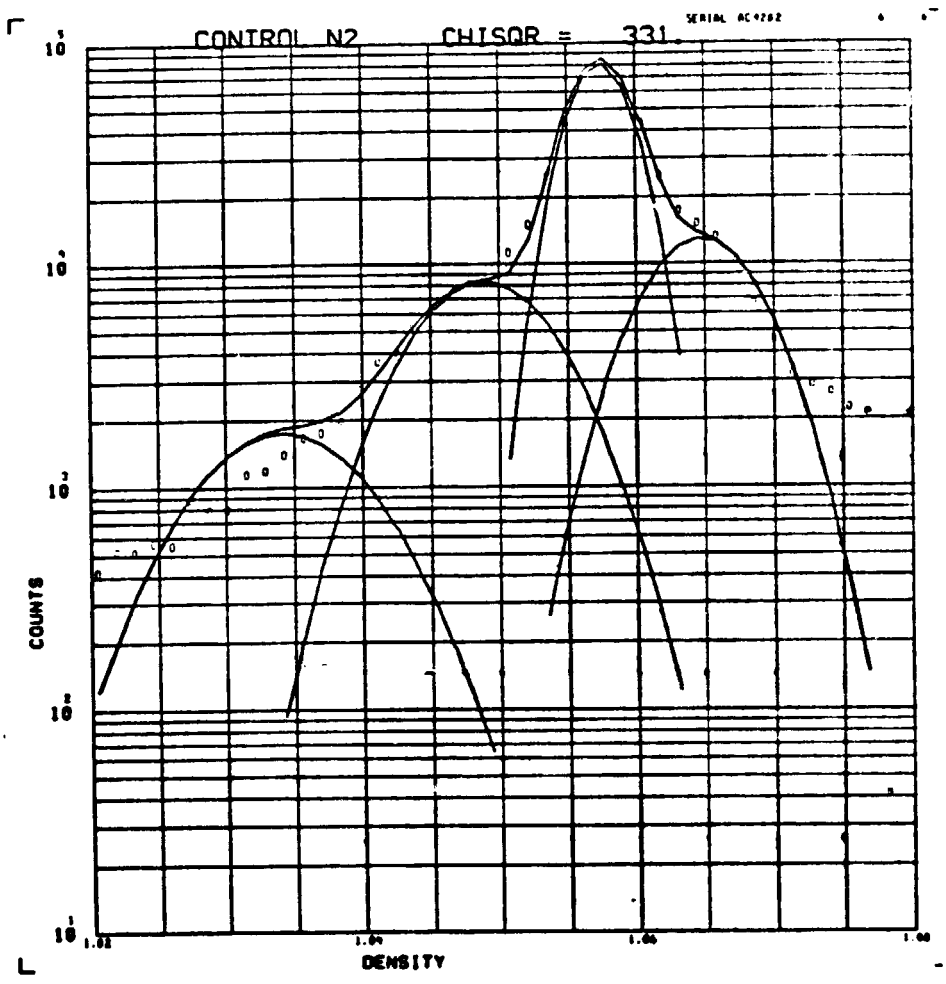
CONTROL N2
CHISQR = 331.
SERIAL AC4282
COUNTS
DENSITY

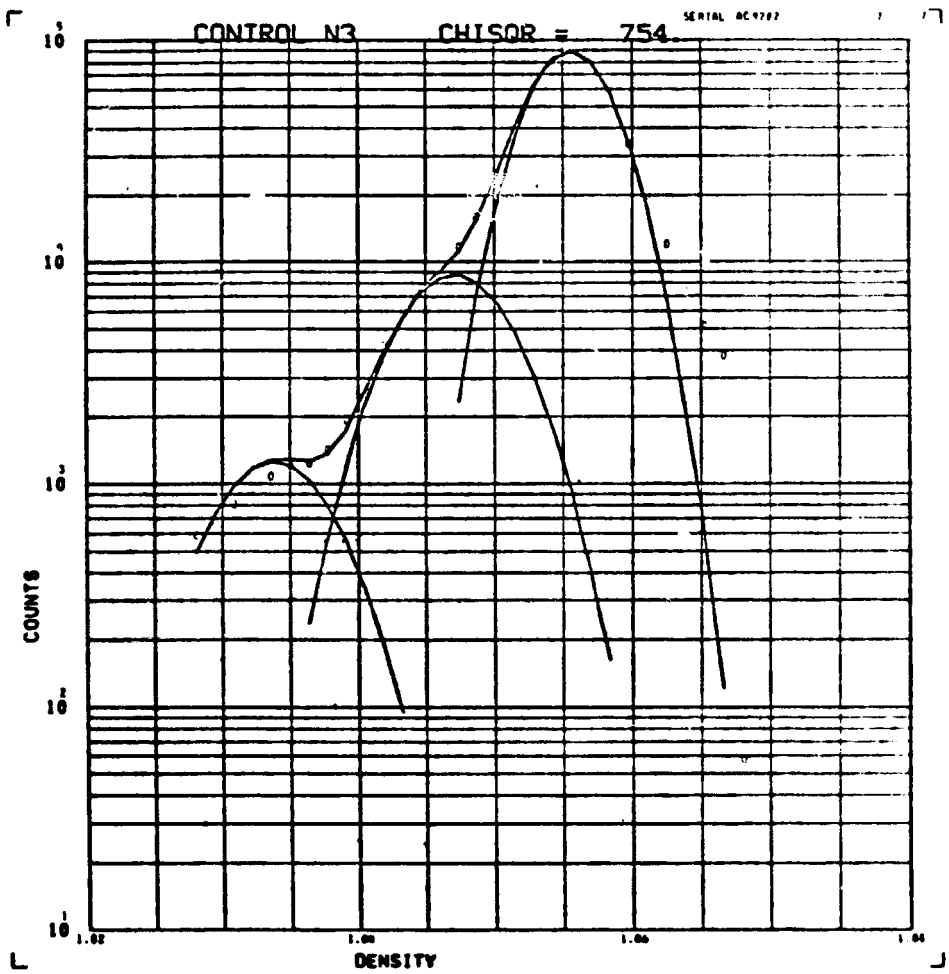
CONTROL N3
CHISQR = 754.
COUNTS
DENSITY

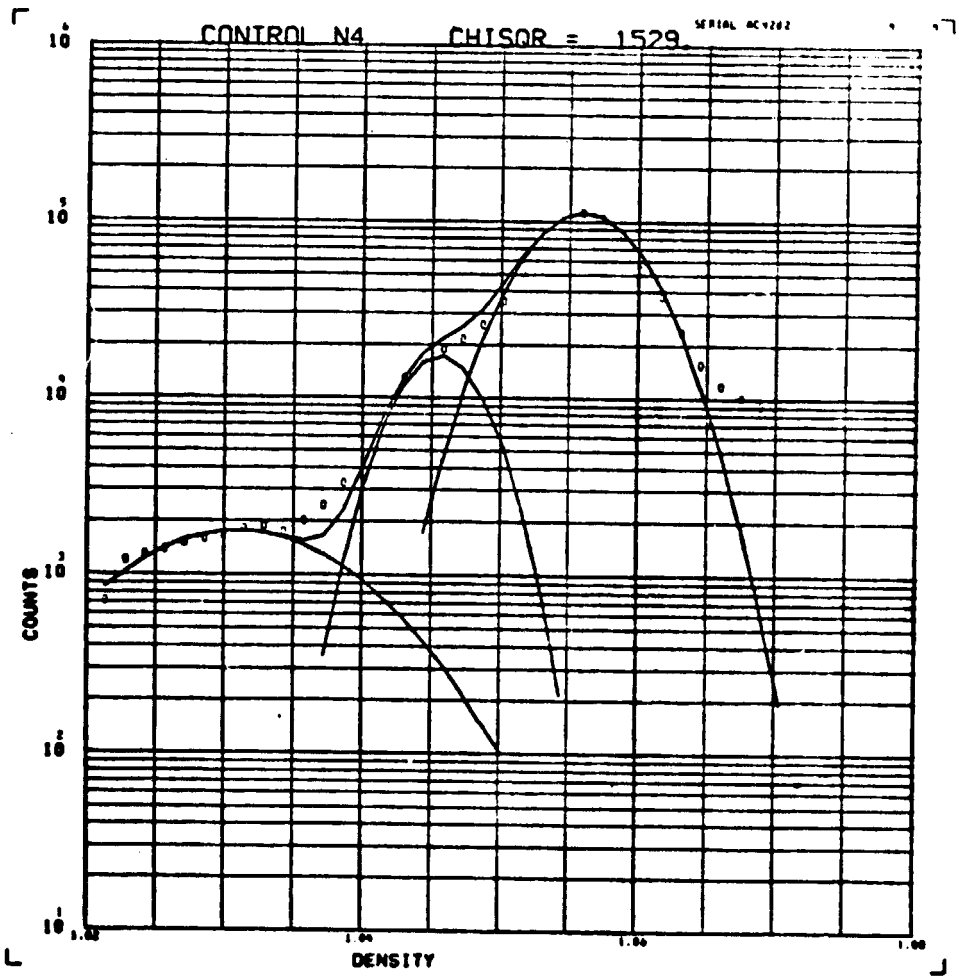
CONTROL N4
CHISQR = 1529.
COUNTS
DENSITY

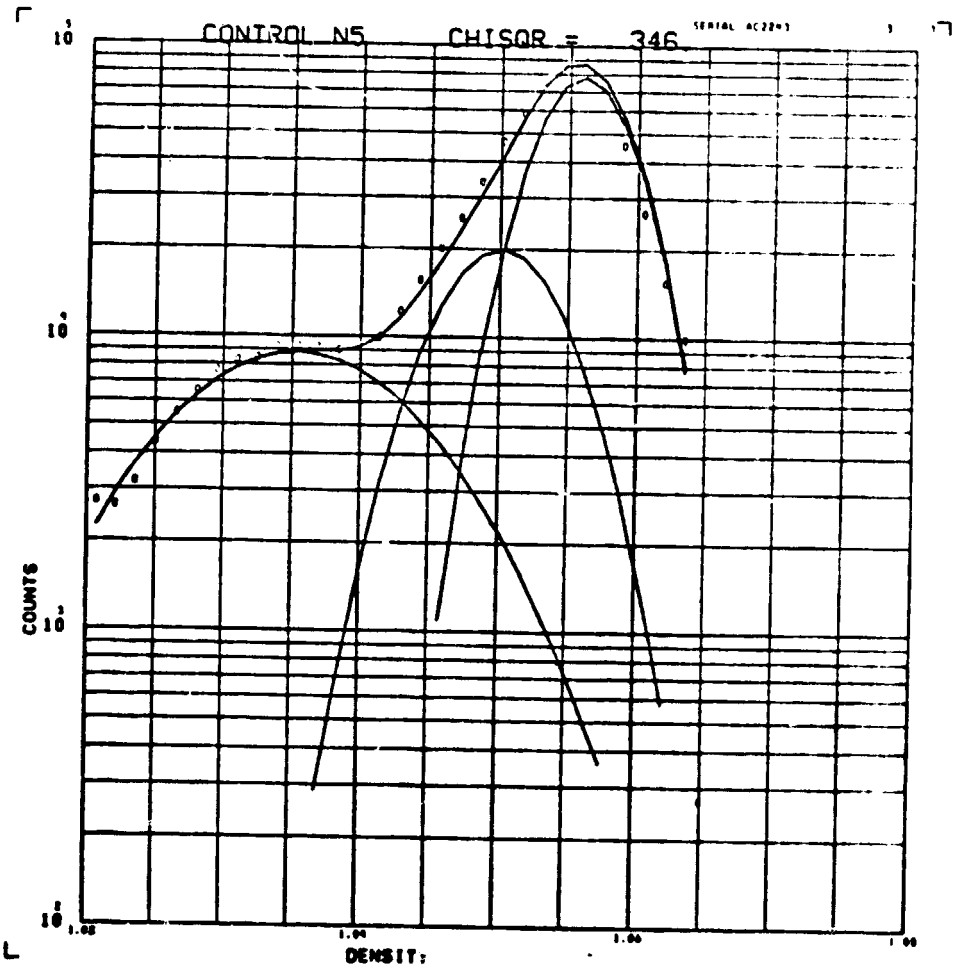
CONTROL N5
CHISQR = 346
COUNTS
DENSITY

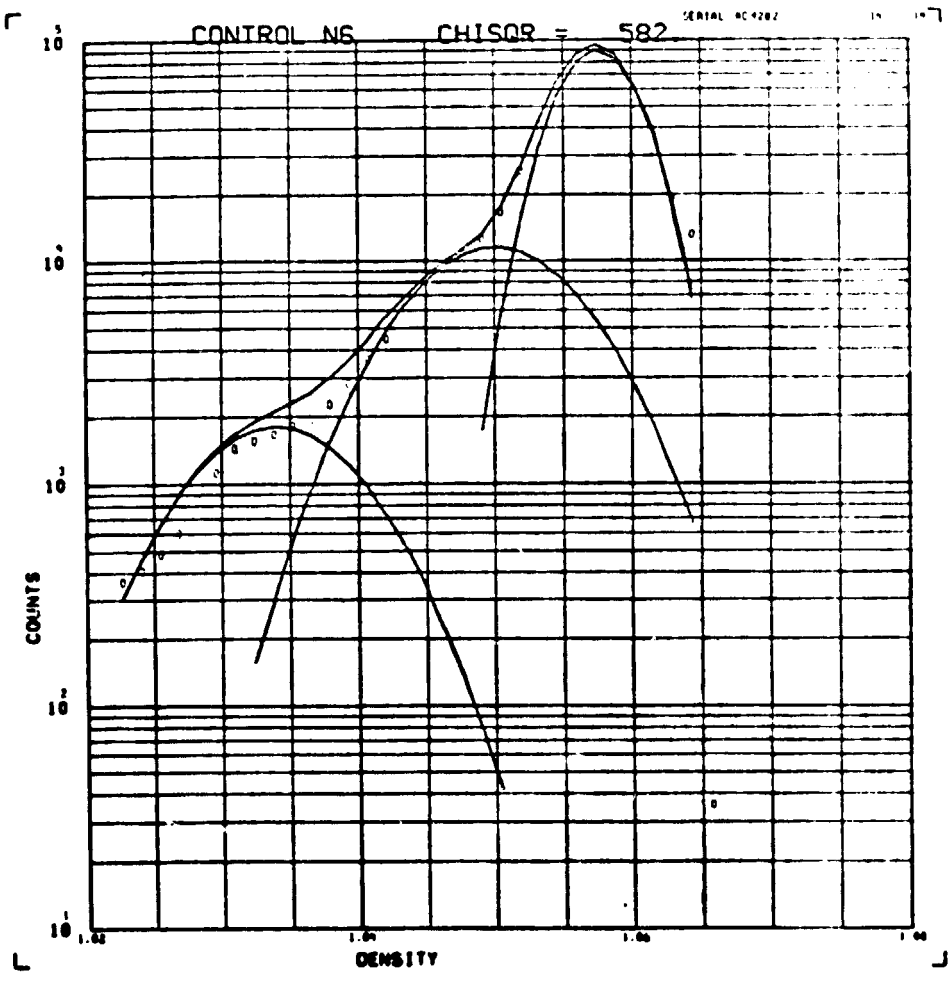
CONTROL NS
CHISQR = 582
COUNTS
DENSITY

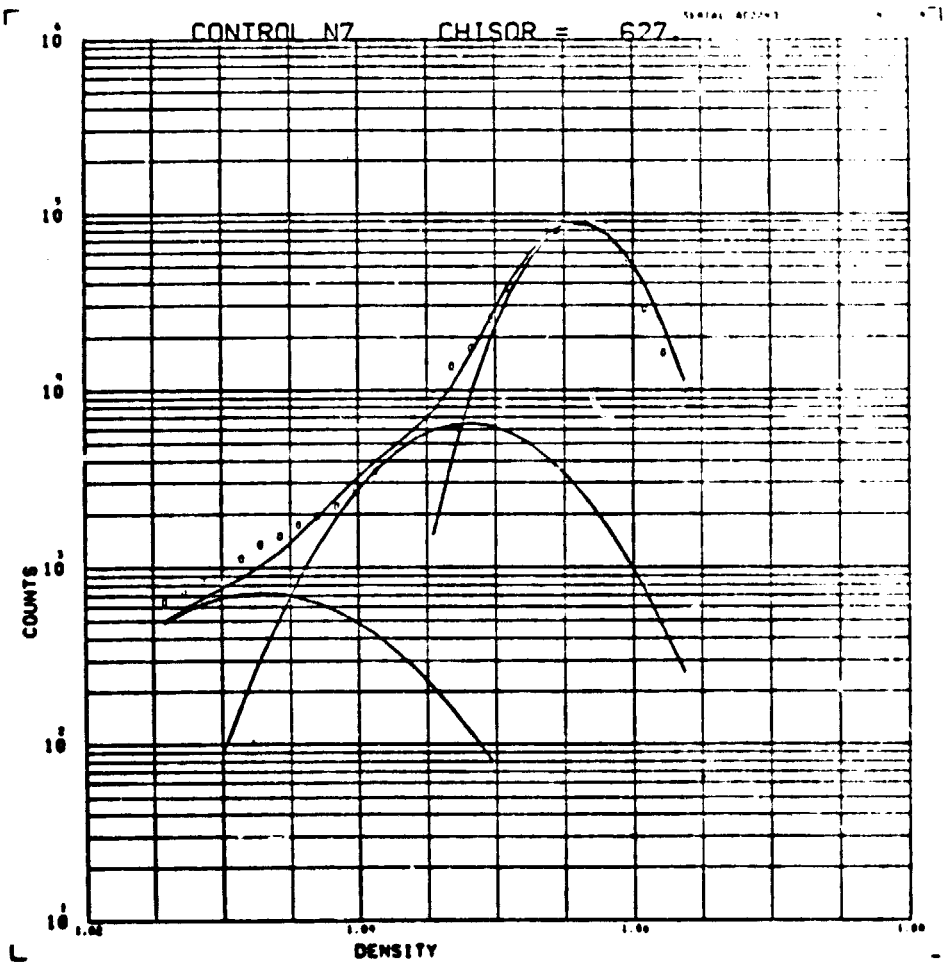
CONTROL N7 CHISQR = 627.
COUNTS
DENSITY

C-3

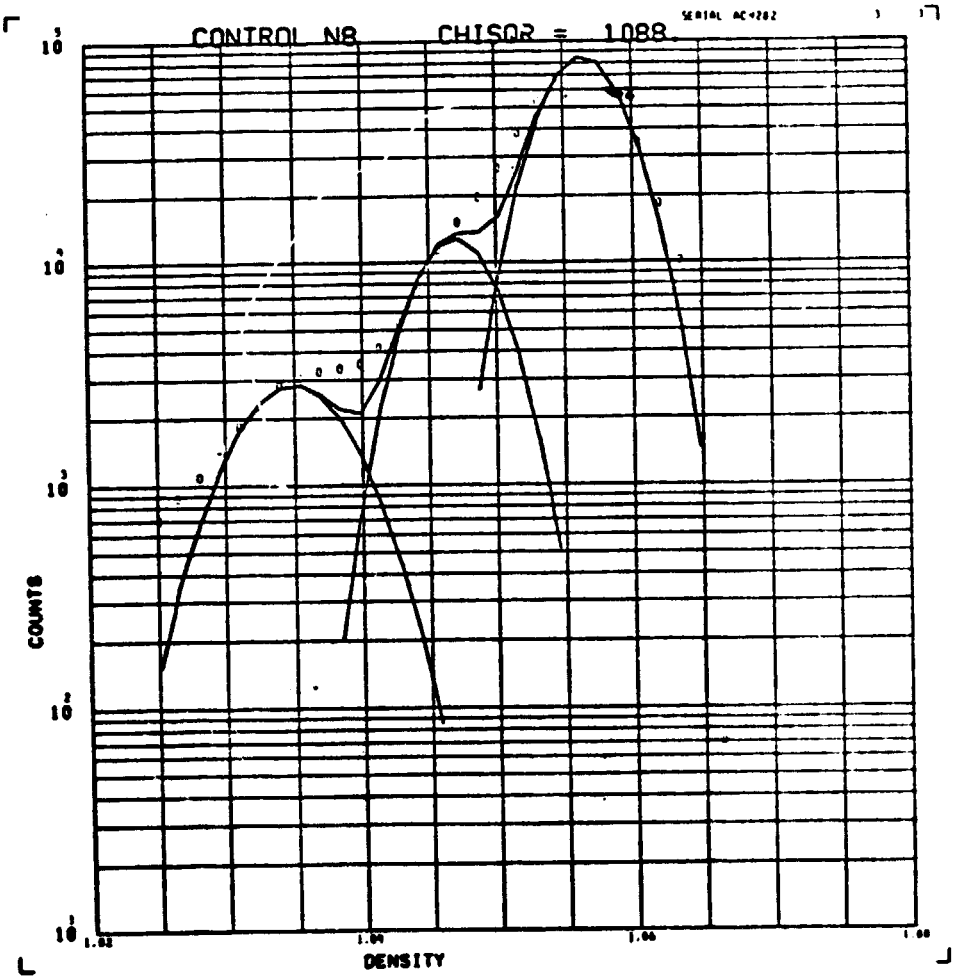

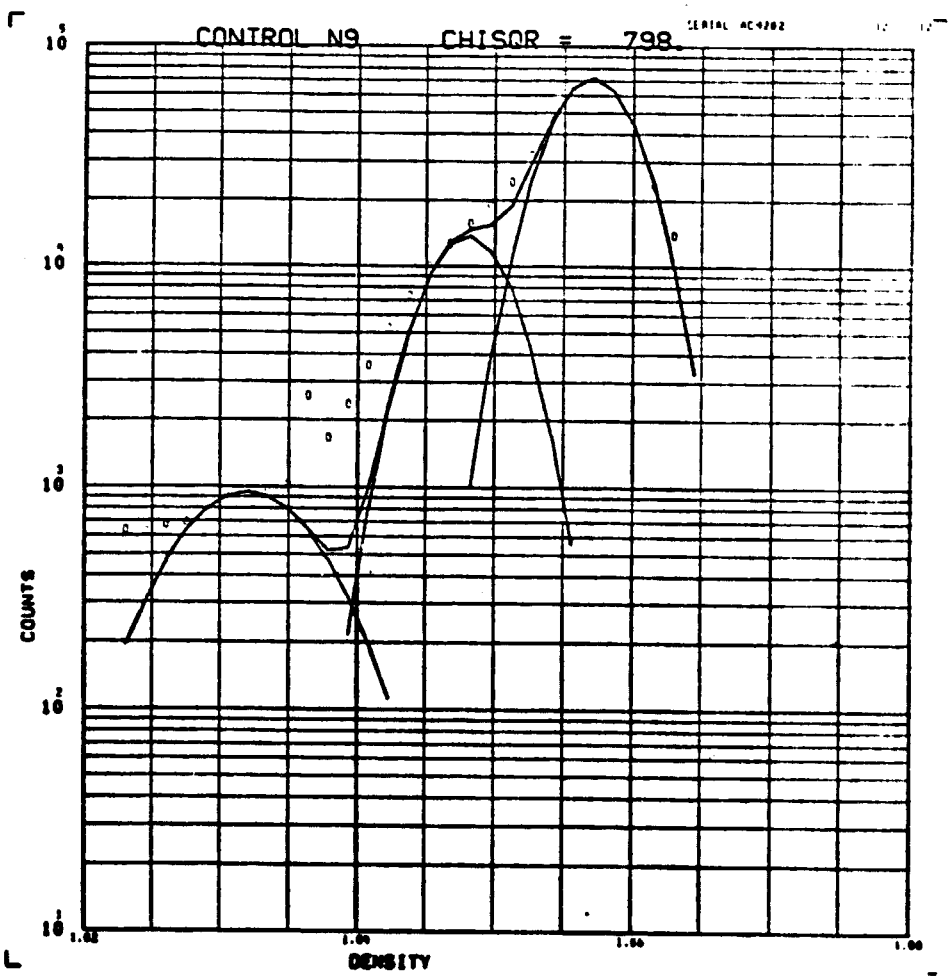
CONTROL N9
CHISQR = 798.
SERIAL AC4282
COUNTS
DENSITY

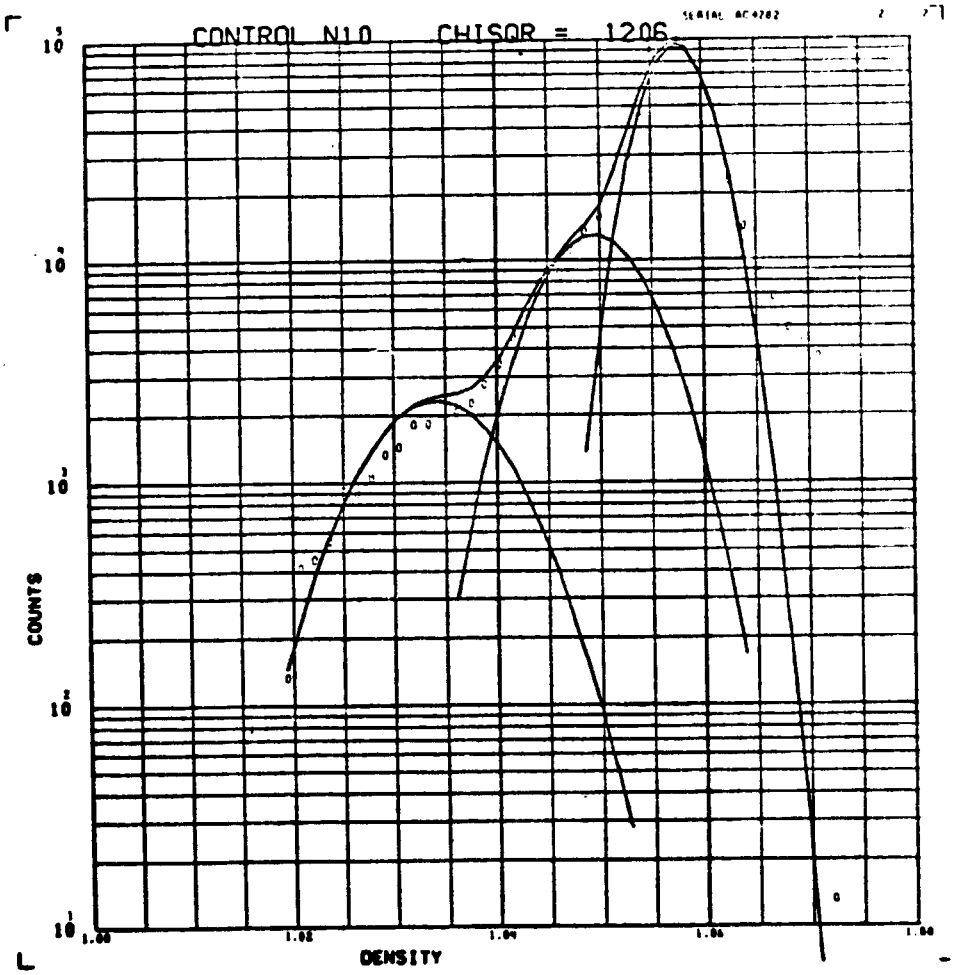
CONTROL N10 CHISQR = 1206
COUNTS
DENSITY

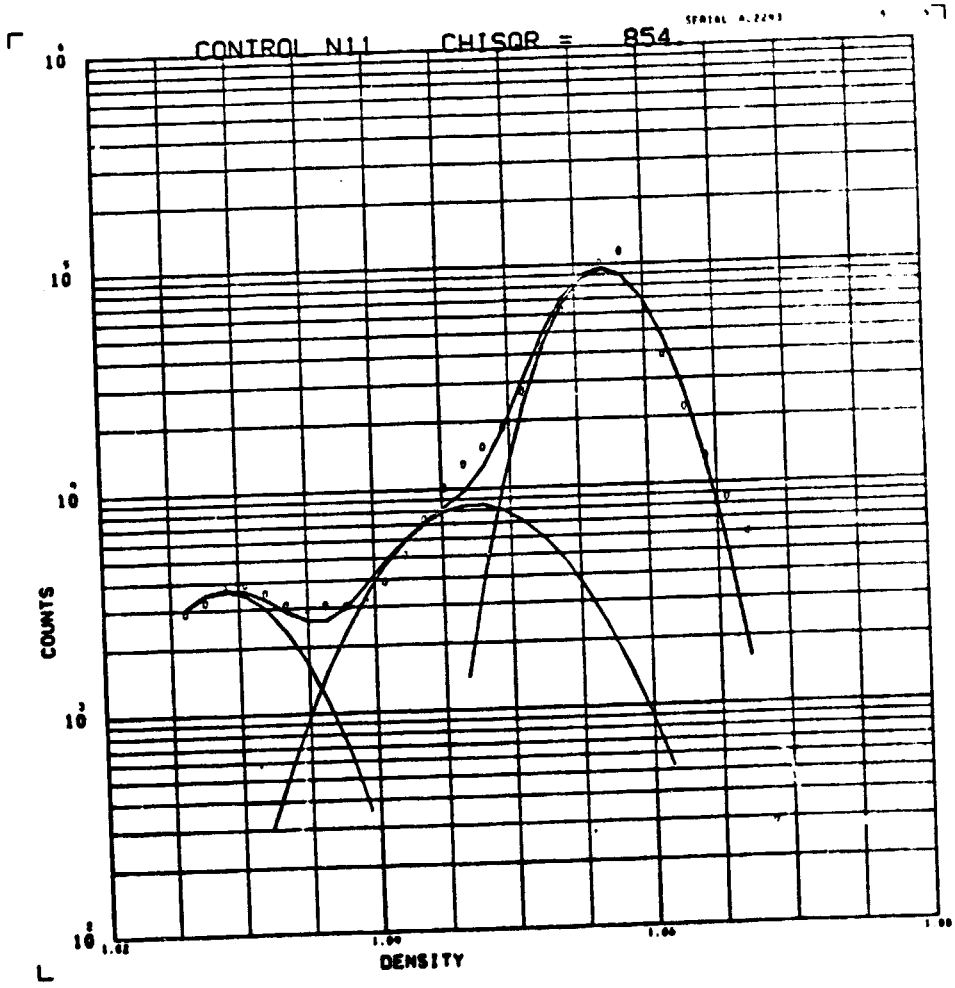
CONTROL N11 CHISQR = 854.
COUNTS
DENSITY

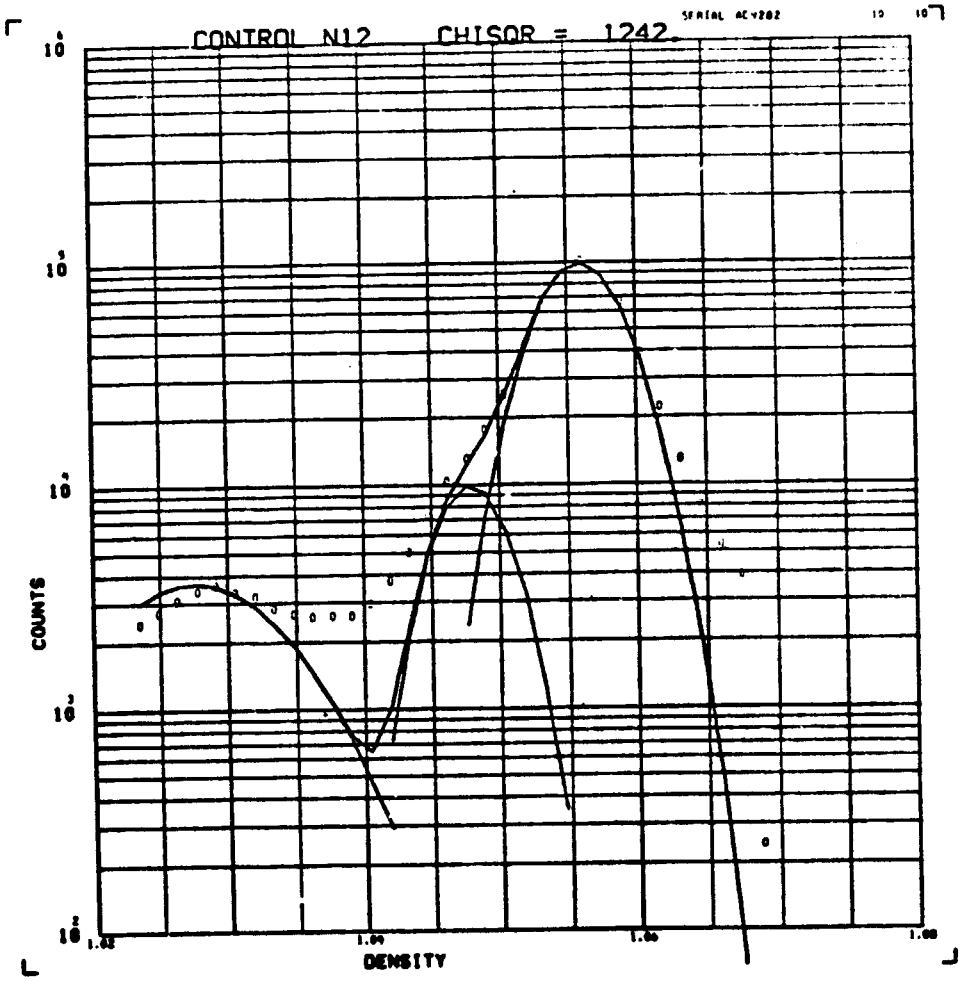
CONTROL N12 CHISQR = 1242
SERIAL AC-282
COUNTS
DENSITY

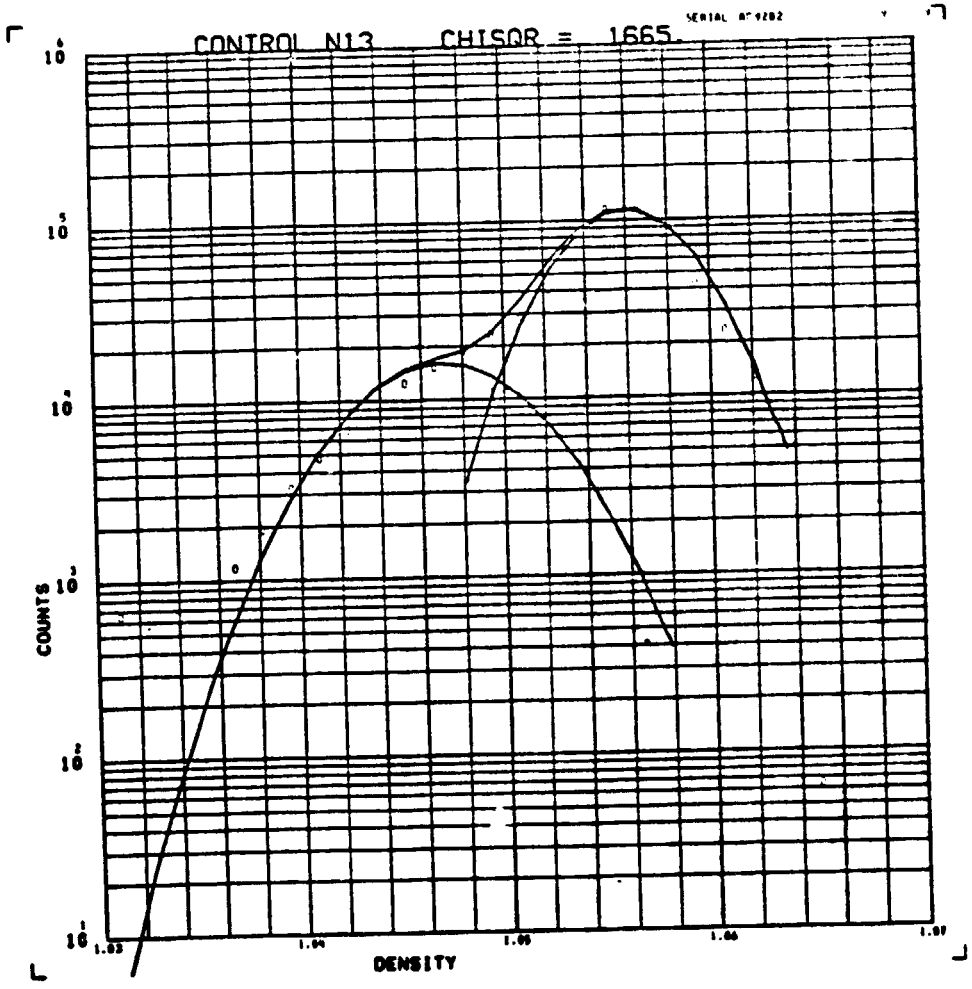
CONTROL N13 CHISQR = 1665.
COUNTS
DENSITY

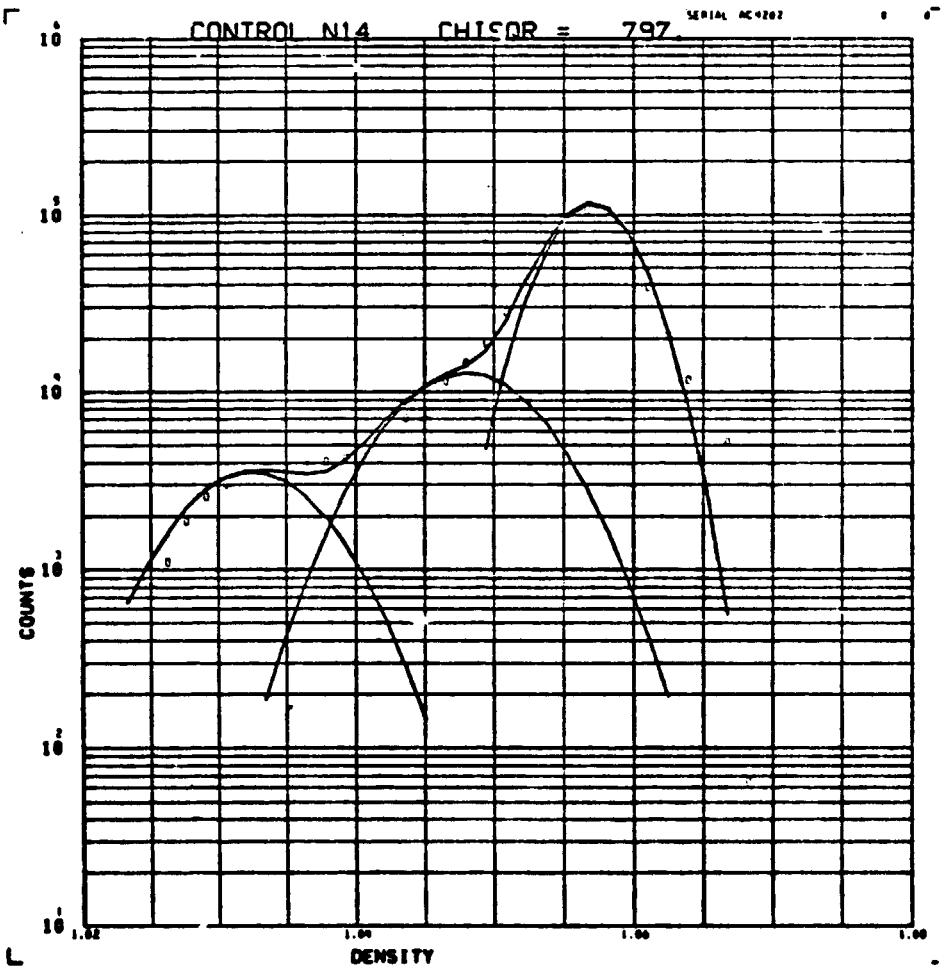
CONTROL N14 CHISQR = 797.
COUNTS
DENSITY

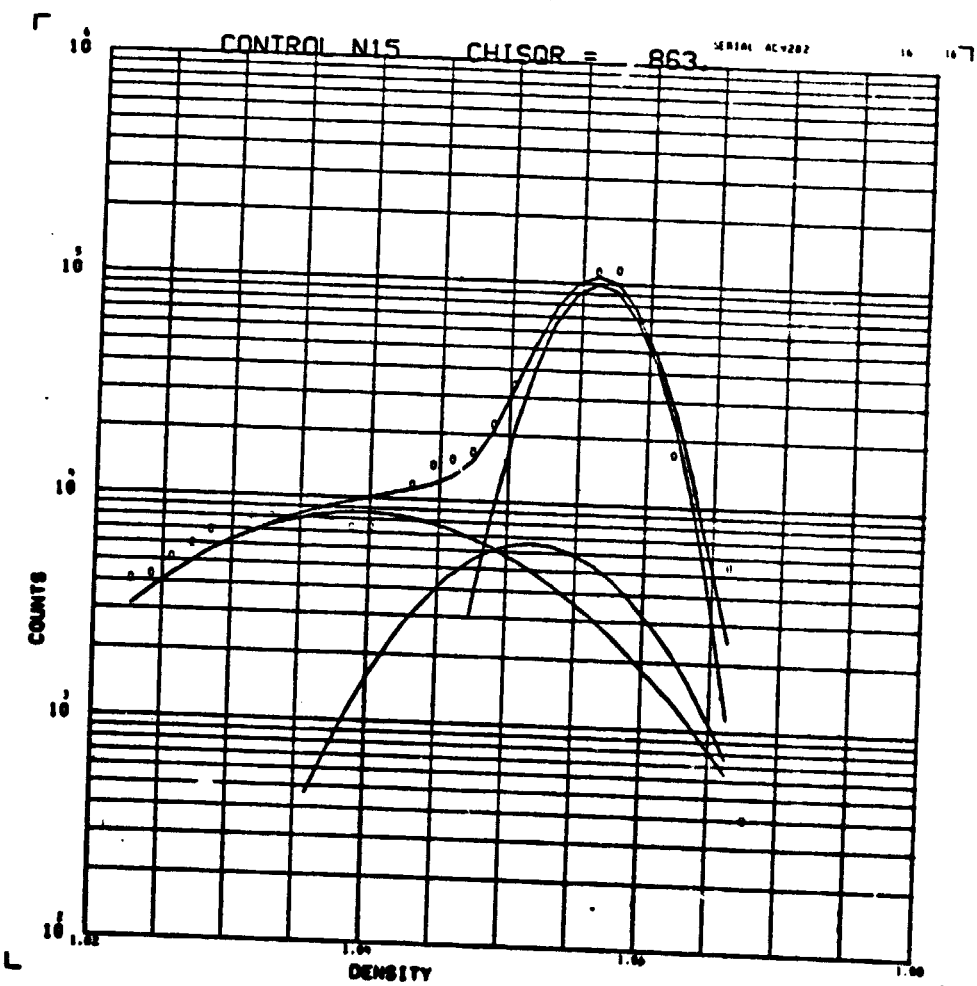
CONTROL N15 CHISQR = 863.
COUNTS
DENSITY

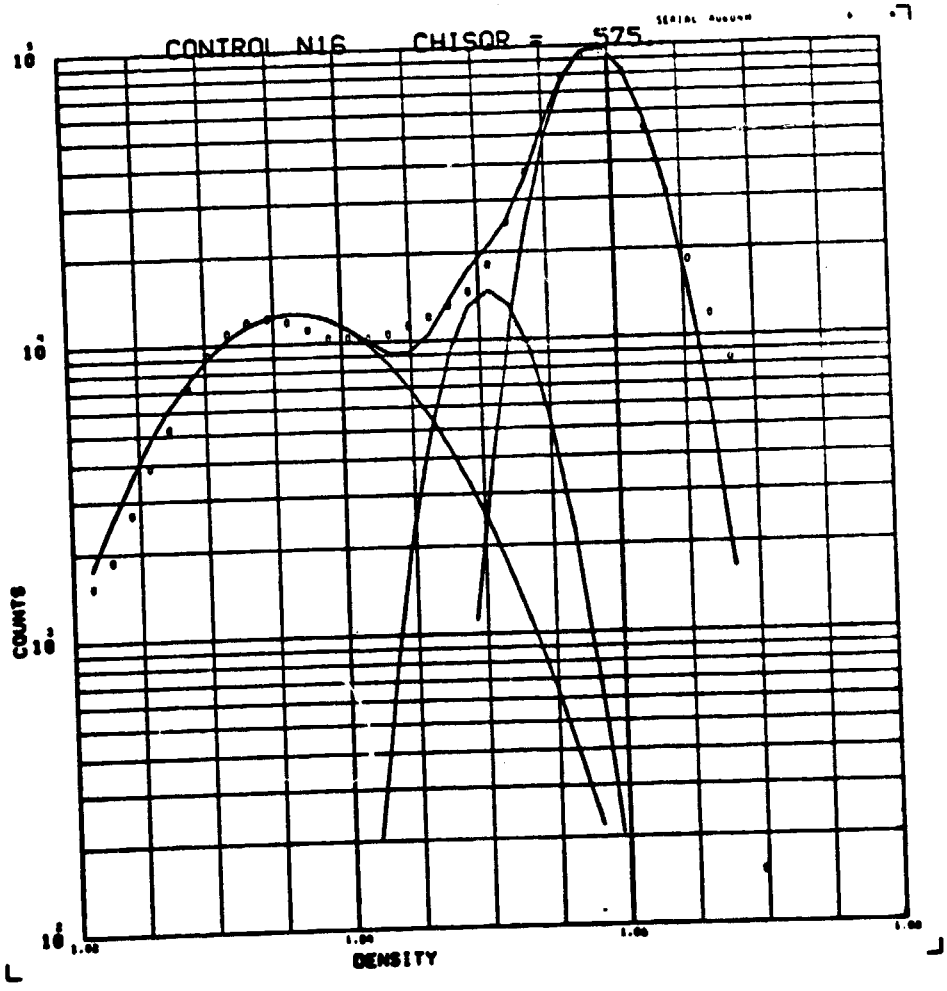
CONTROL N16 CHISQR = 575.
COUNTS
DENSITY

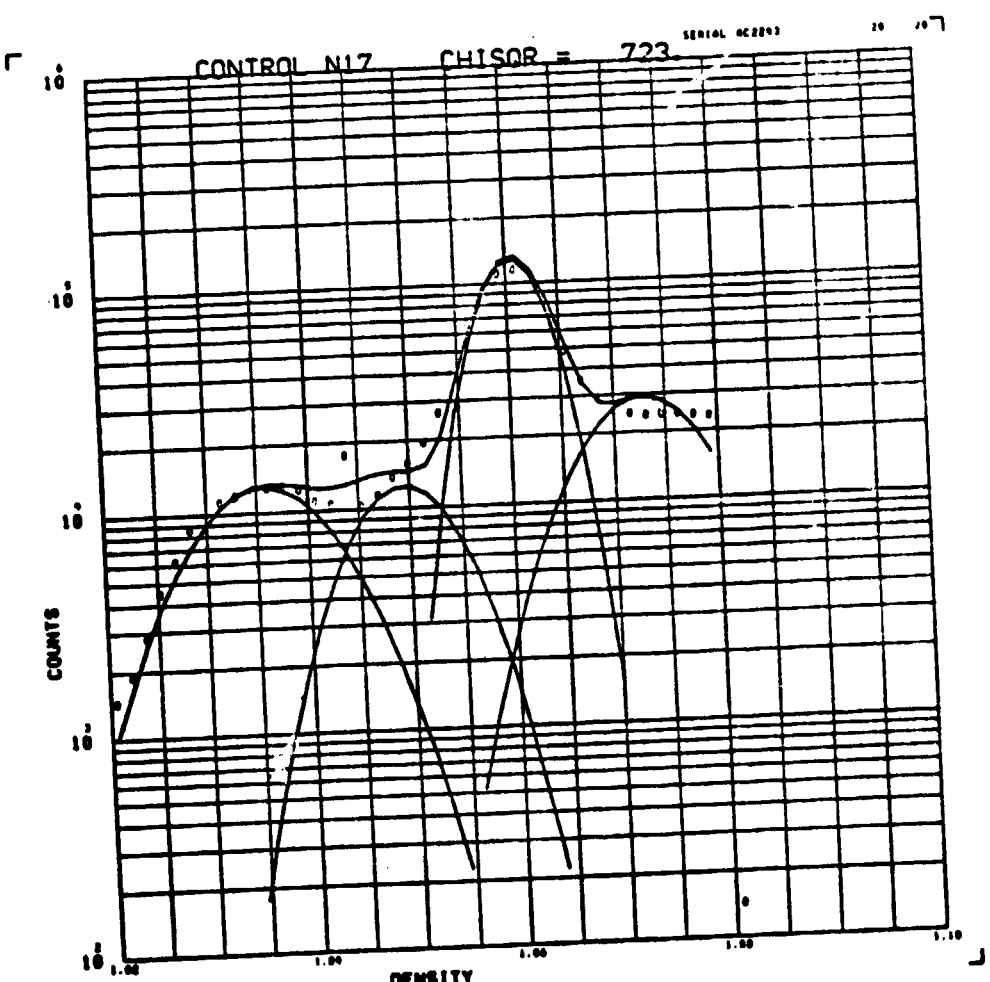
CONTROL N17 CHISQR = 723.
COUNTS
DENSITY

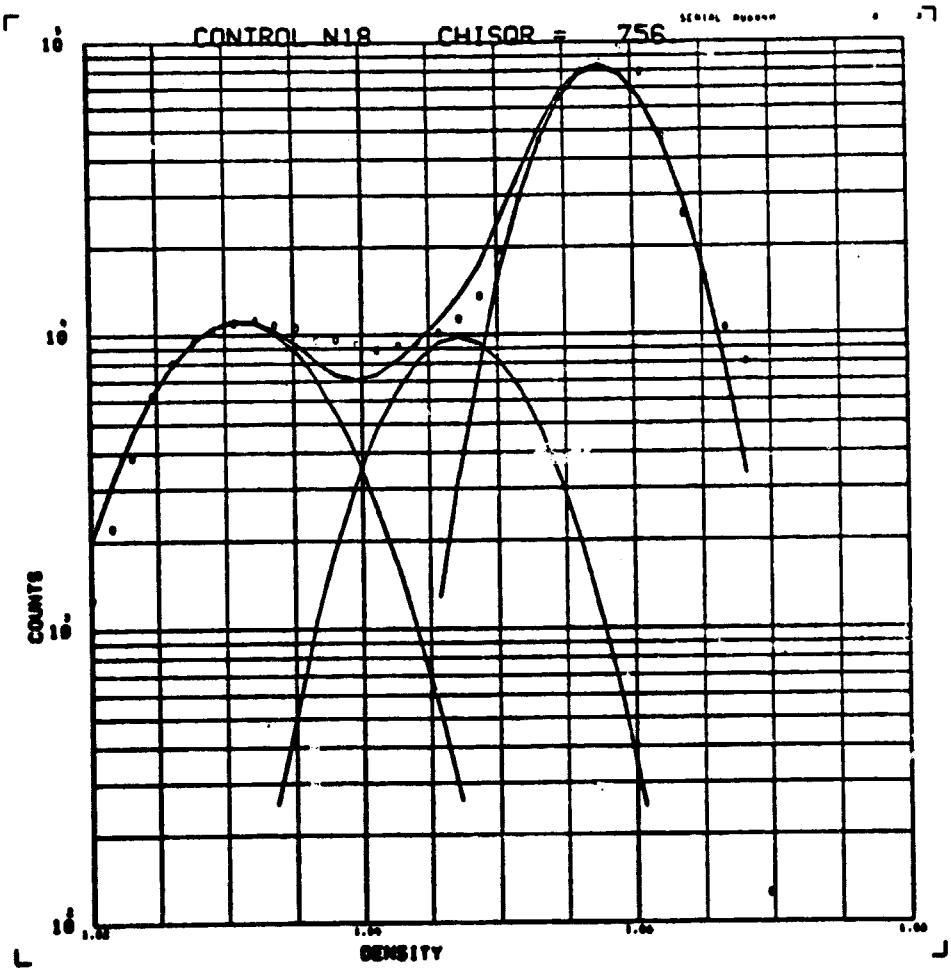
CONTROL N18 CHISQR = 756
COUNTS
DENSITY

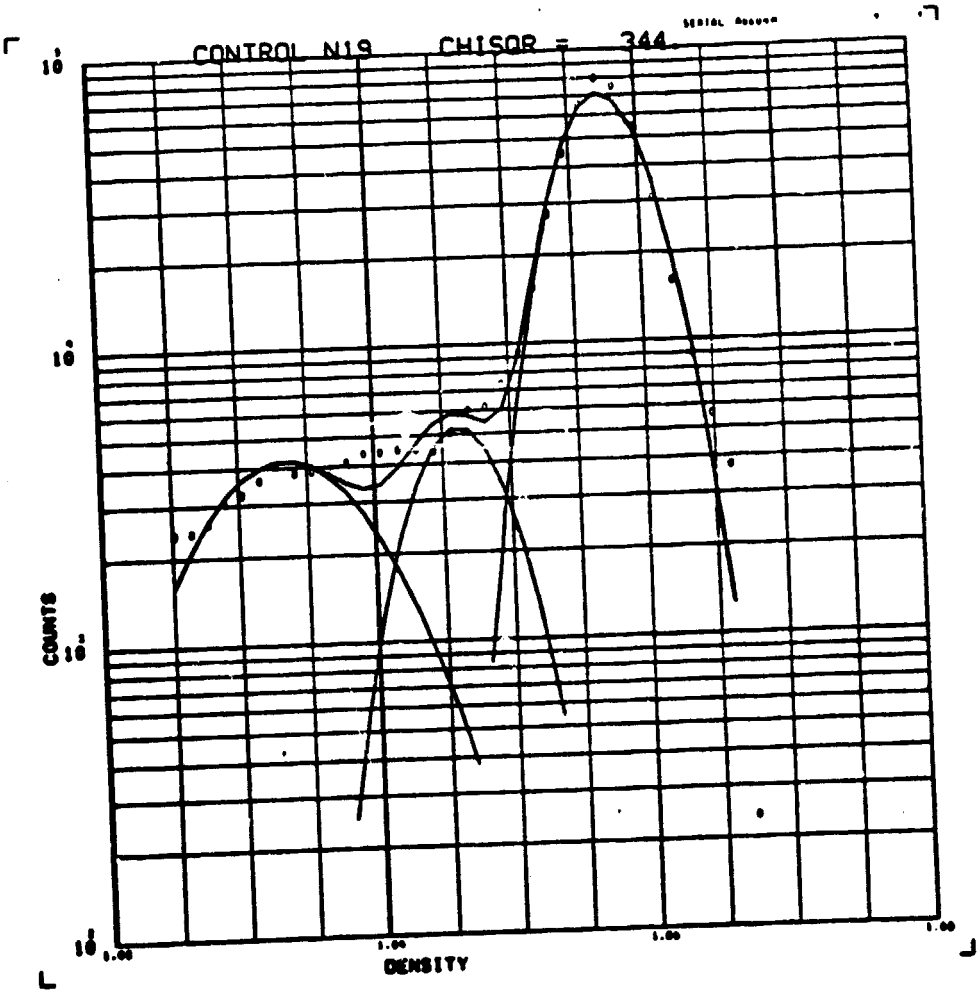
CONTROL N19 CHISQR = 344.
COUNTS
DENSITY
1.00
1.00
1.00
1.00

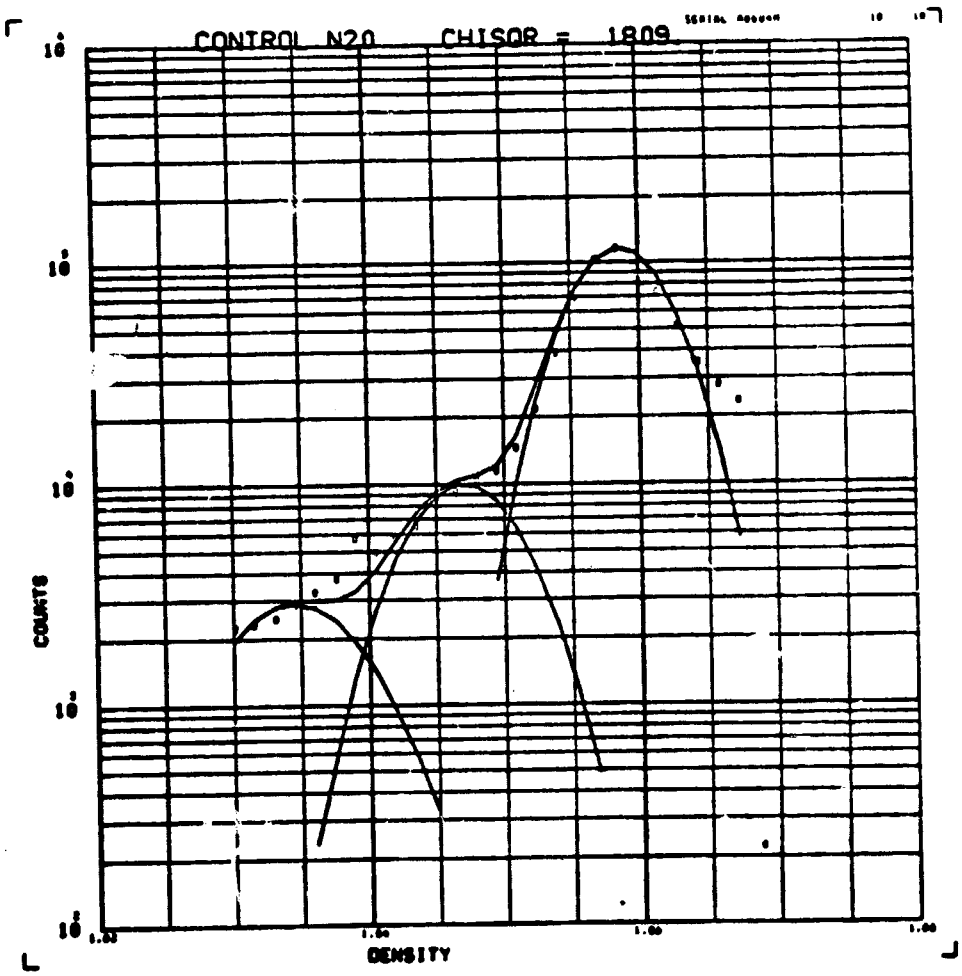
CONTROL N20 CHISQR = 1809.
COUNTS
DENSITY

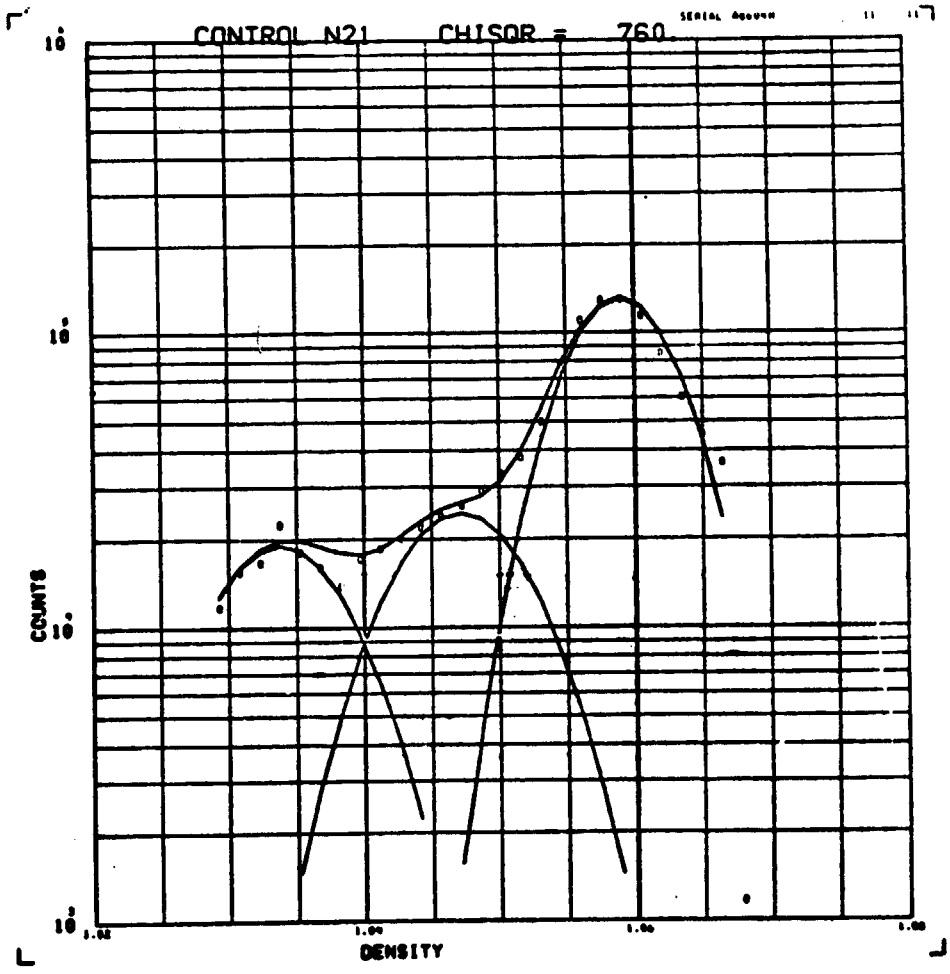
CONTROL N21 CHISQR = 760
COUNTS
DENSITY

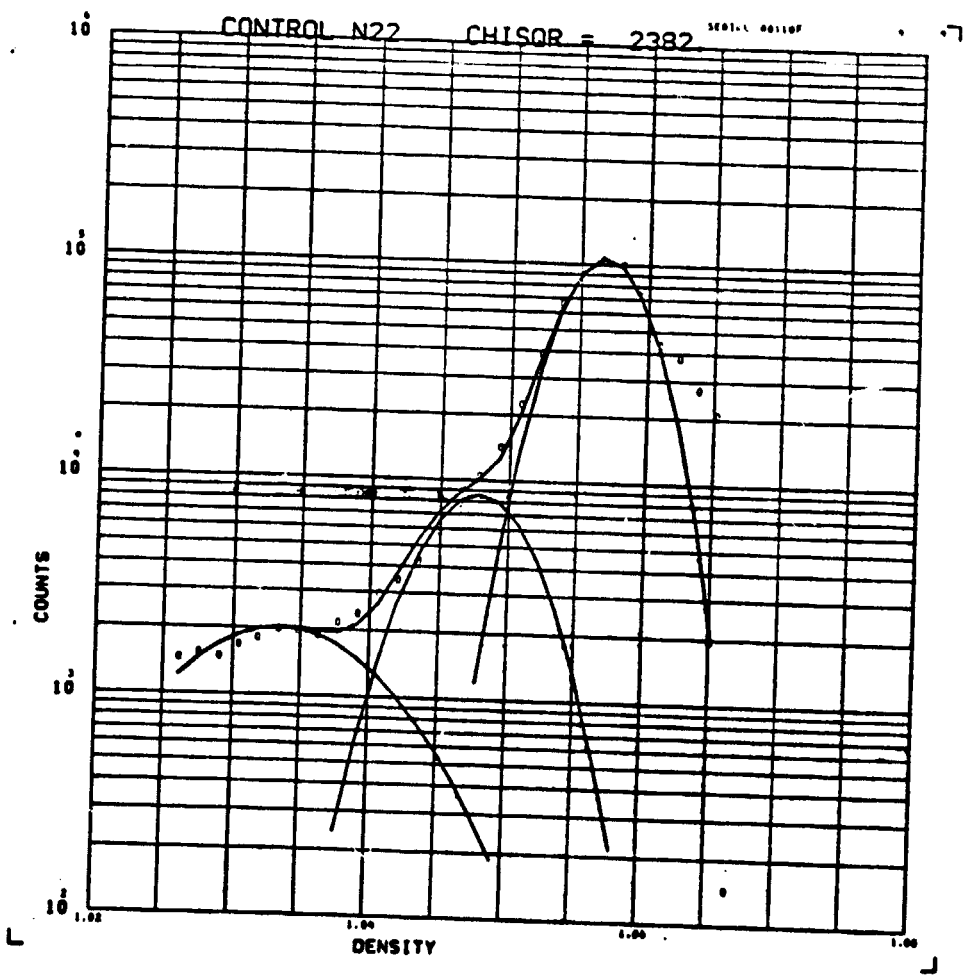
CONTROL N22 CHISQR = 2382
COUNTS
DENSITY

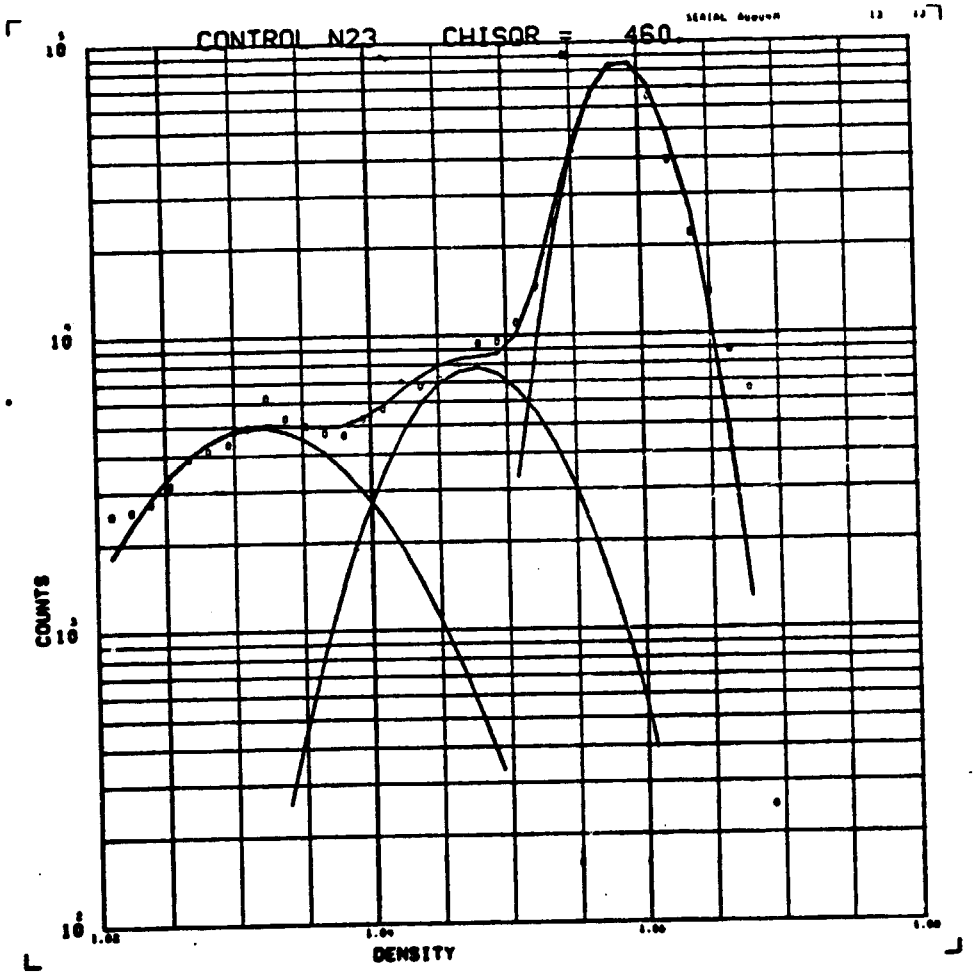
CONTROL N23 CHISQR = 460.
COUNTS
DENSITY

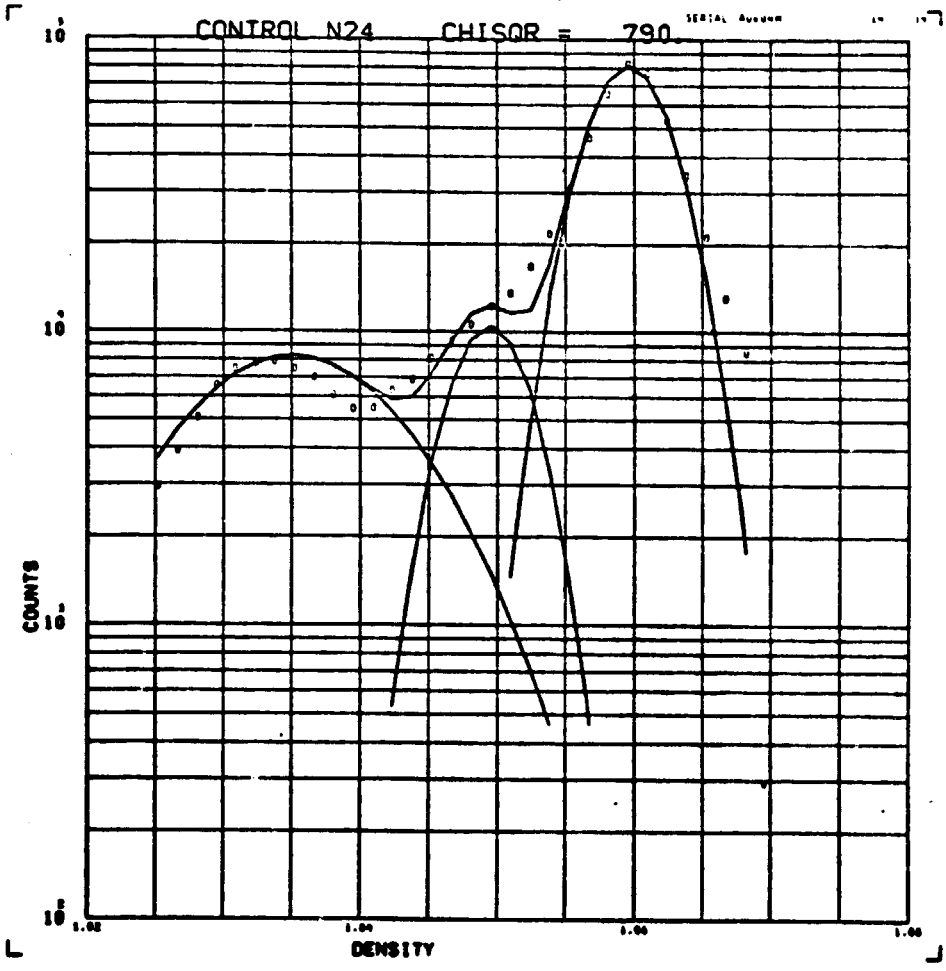
CONTROL N24 CHISQR = 790.
COUNTS
DENSITY

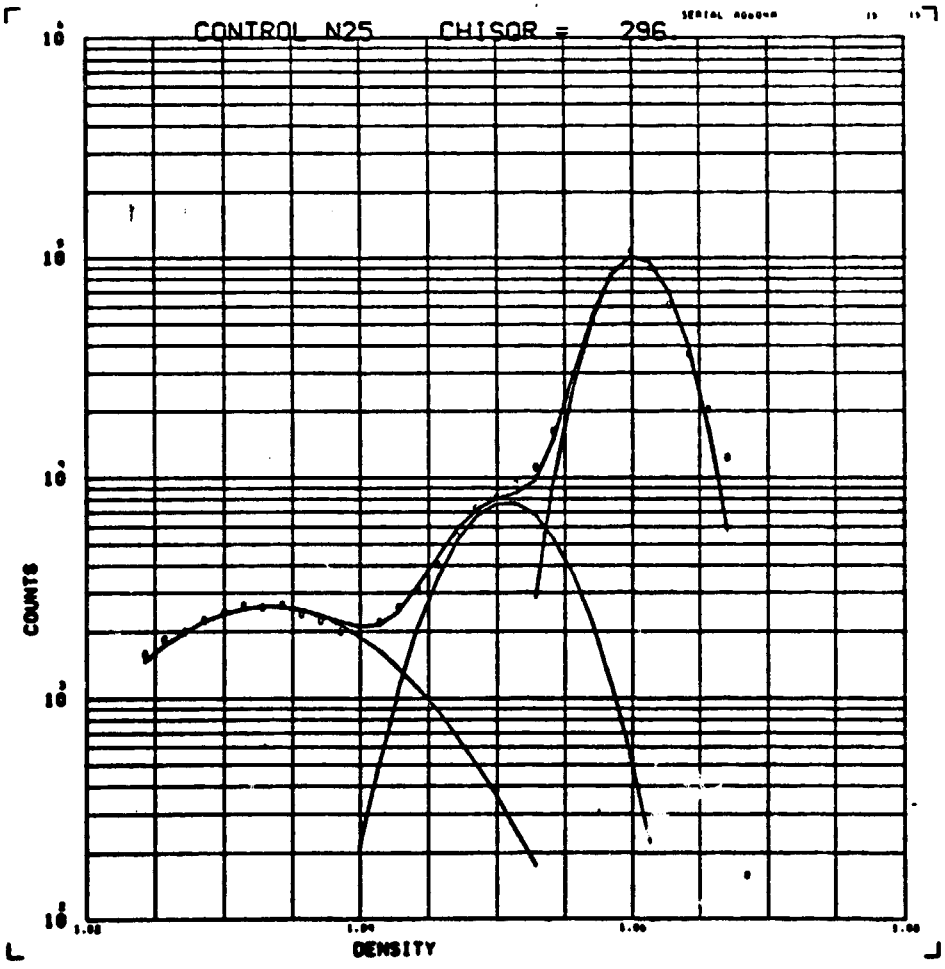
CONTROL N25 CHISQR = 296
COUNTS
DENSITY

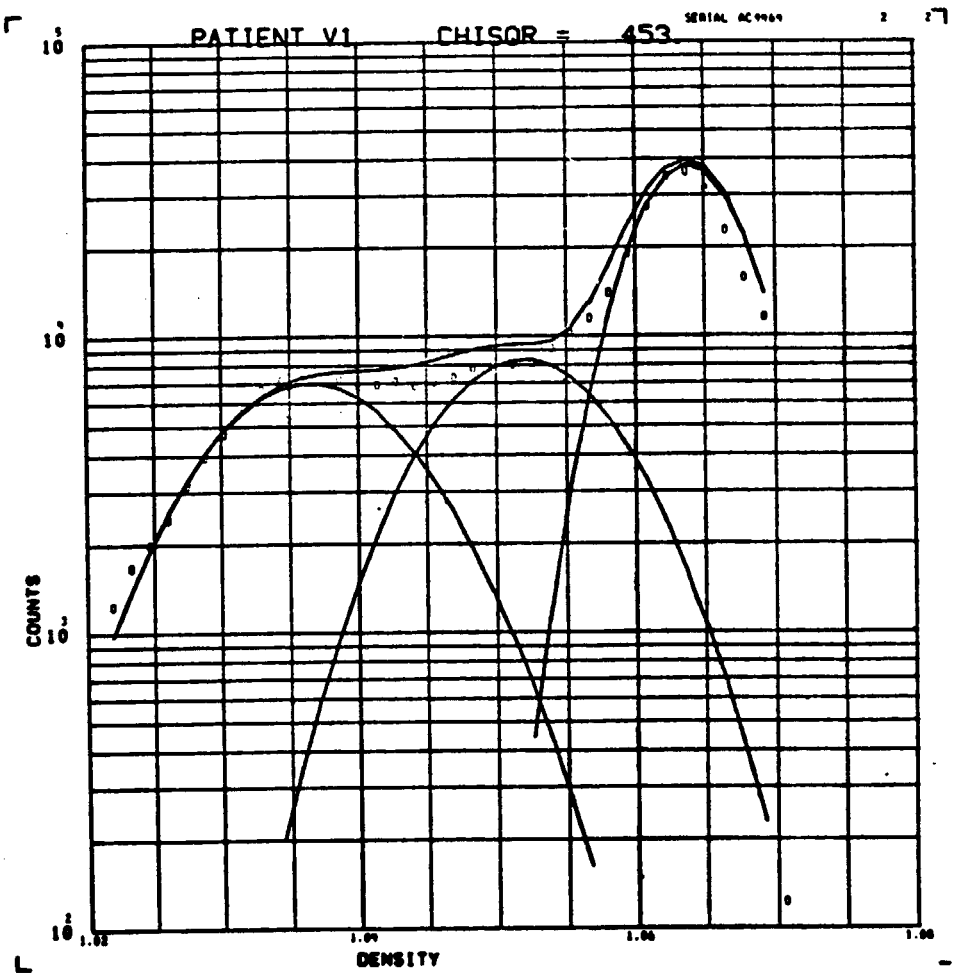
PATIENT V1 CHISQR = 453.
COUNTS
DENSITY

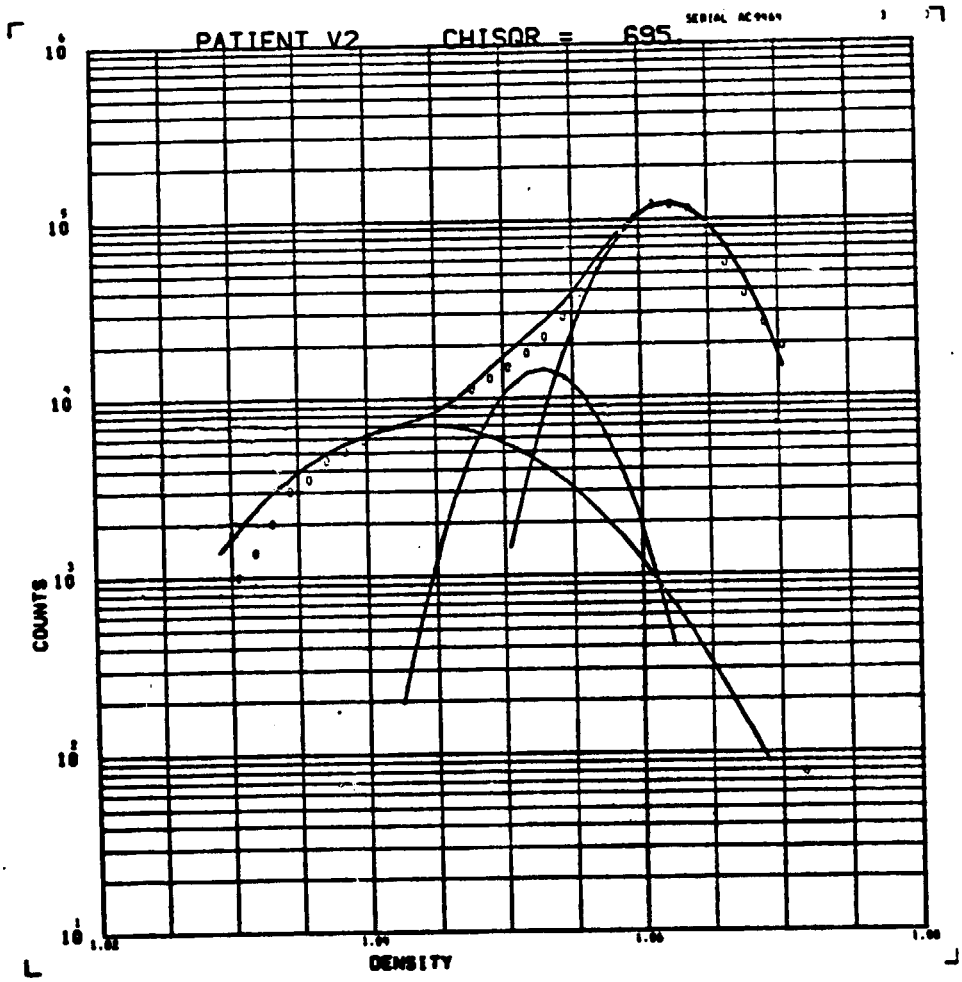
PATIENT V2
CHISQR = 695.
COUNTS
DENSITY

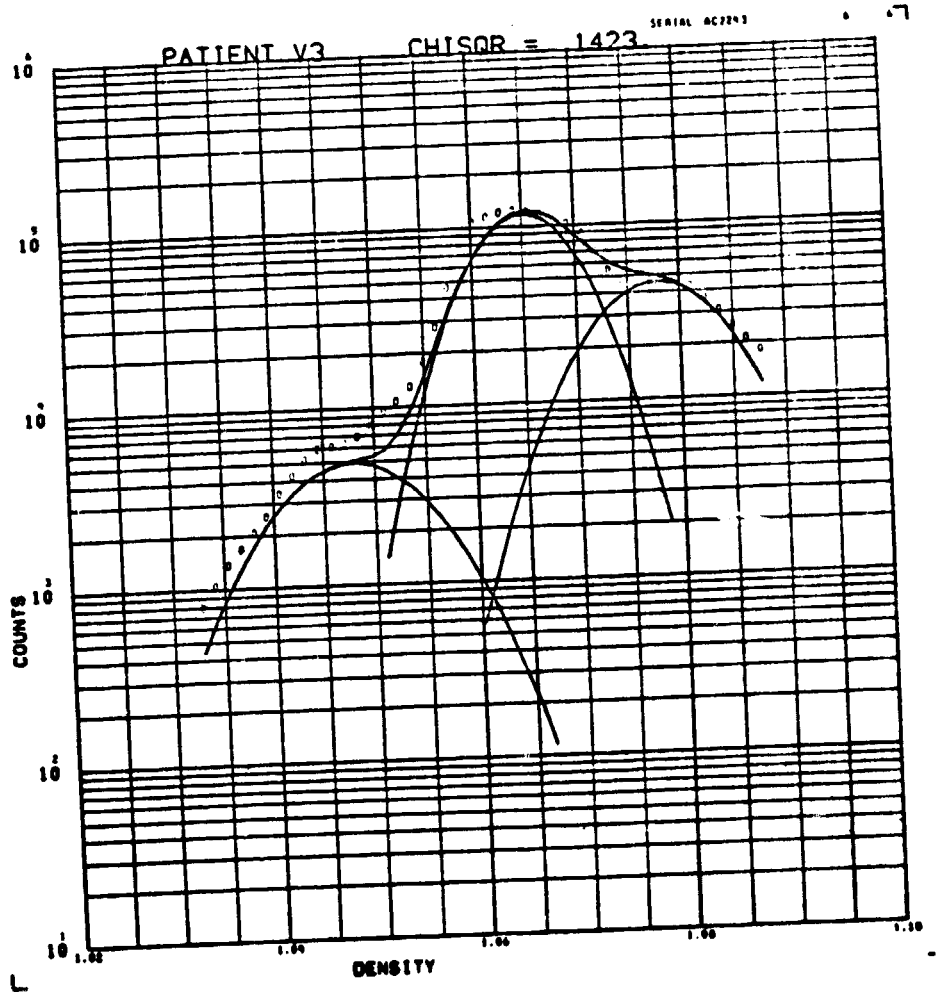
PATIENT V3 CHISQR = 1423.
COUNTS
DENSITY

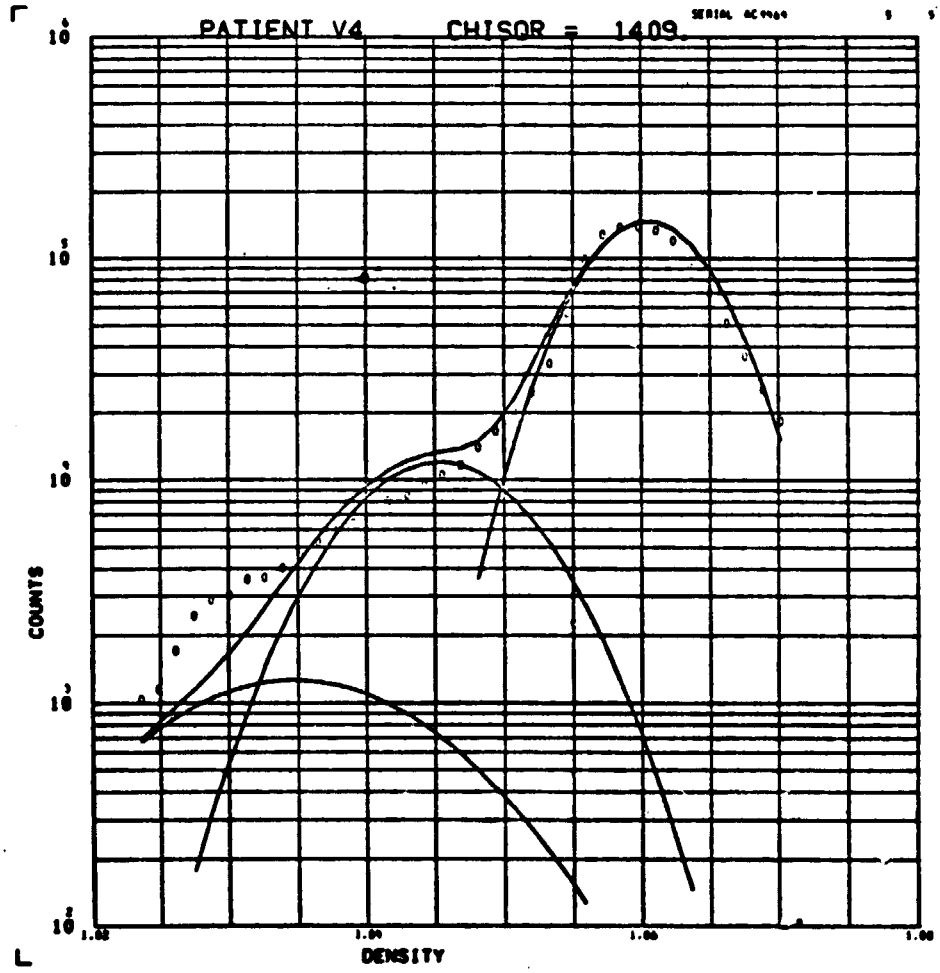
PATIENT V4 CHISQR = 1409
COUNTS
DENSITY

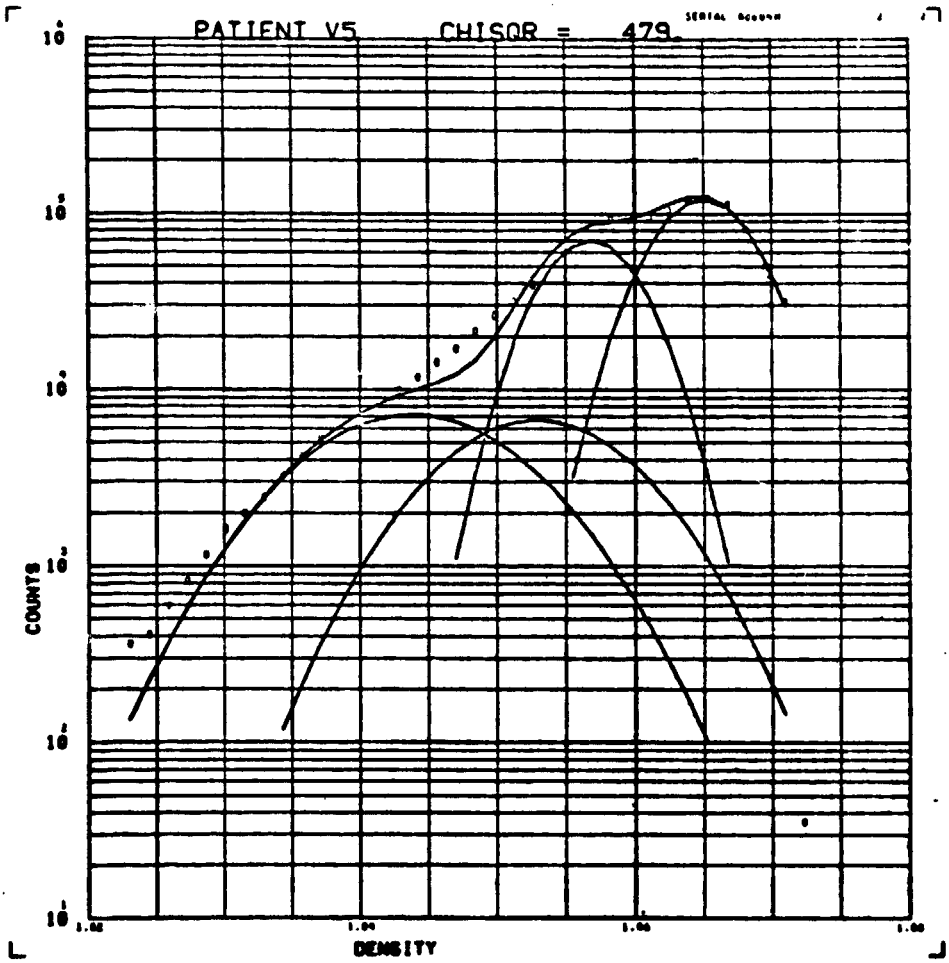
PATIENT V5 CHISQR = 479
COUNTS
DENSITY

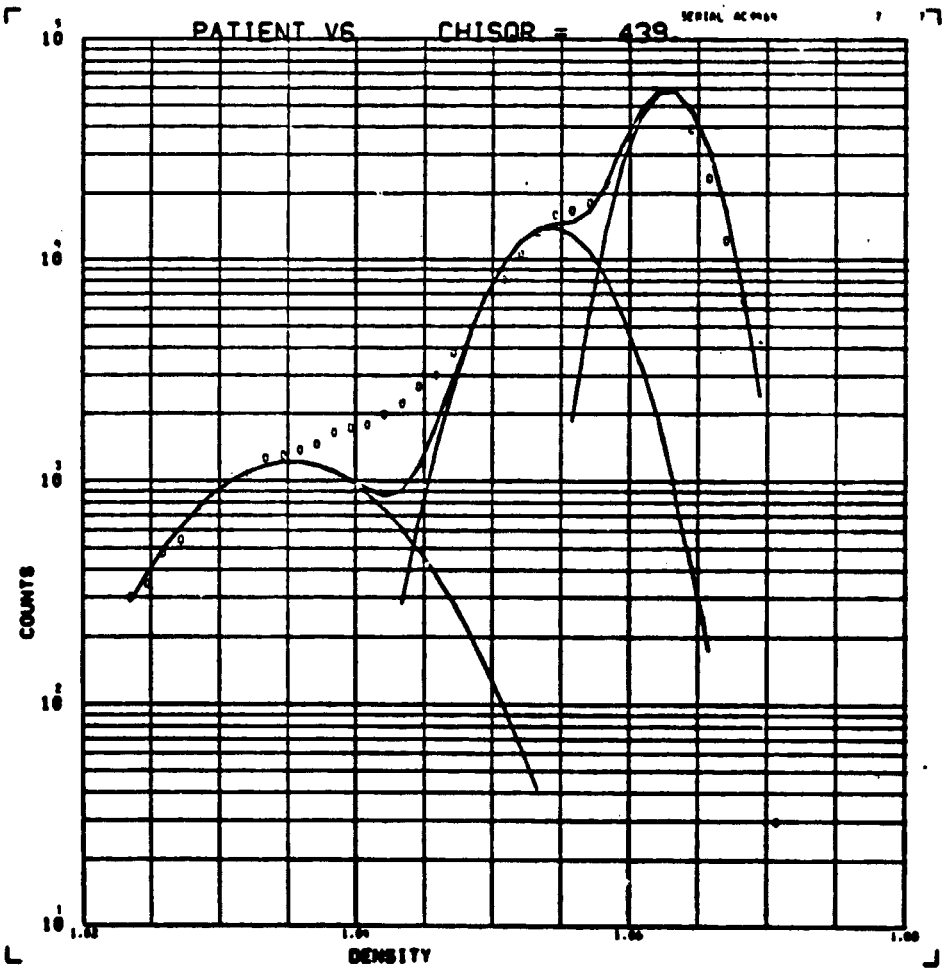
PATIENT V6 CHISQR = 439.
COUNTS
DENSITY

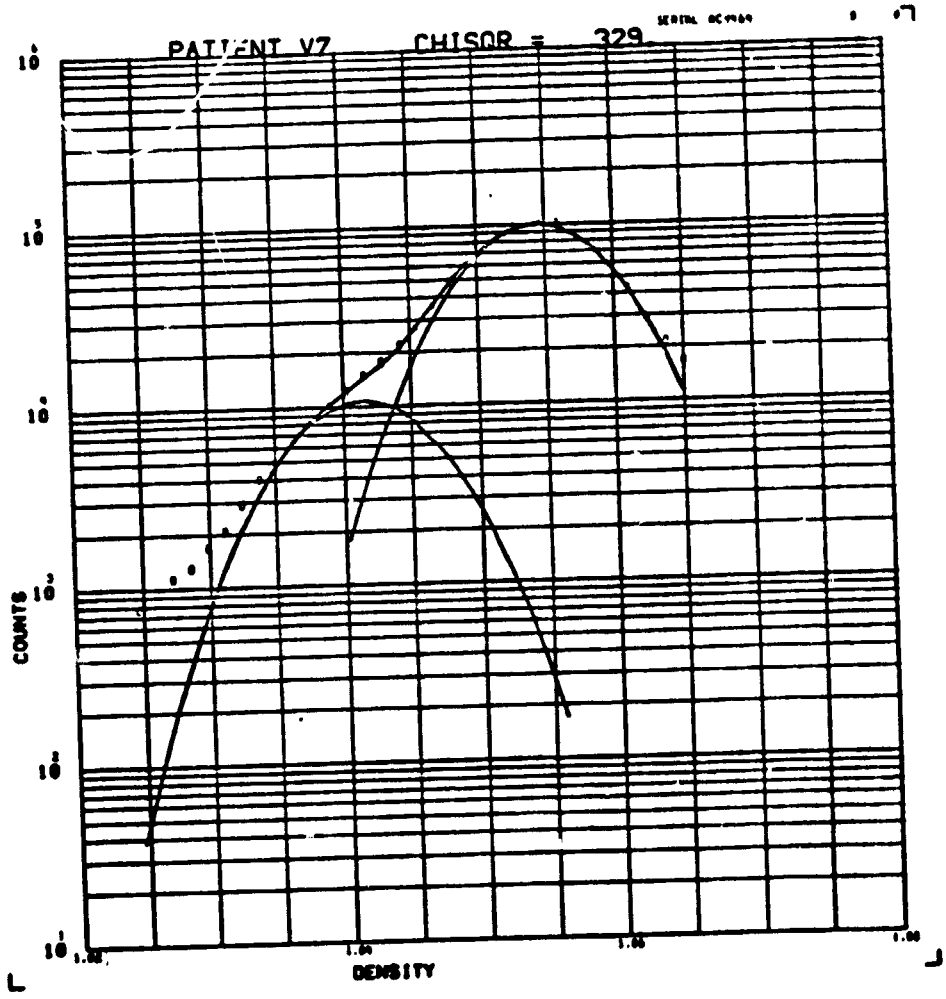
PATIENT V7
CHISQR = 329
COUNTS
DENSITY

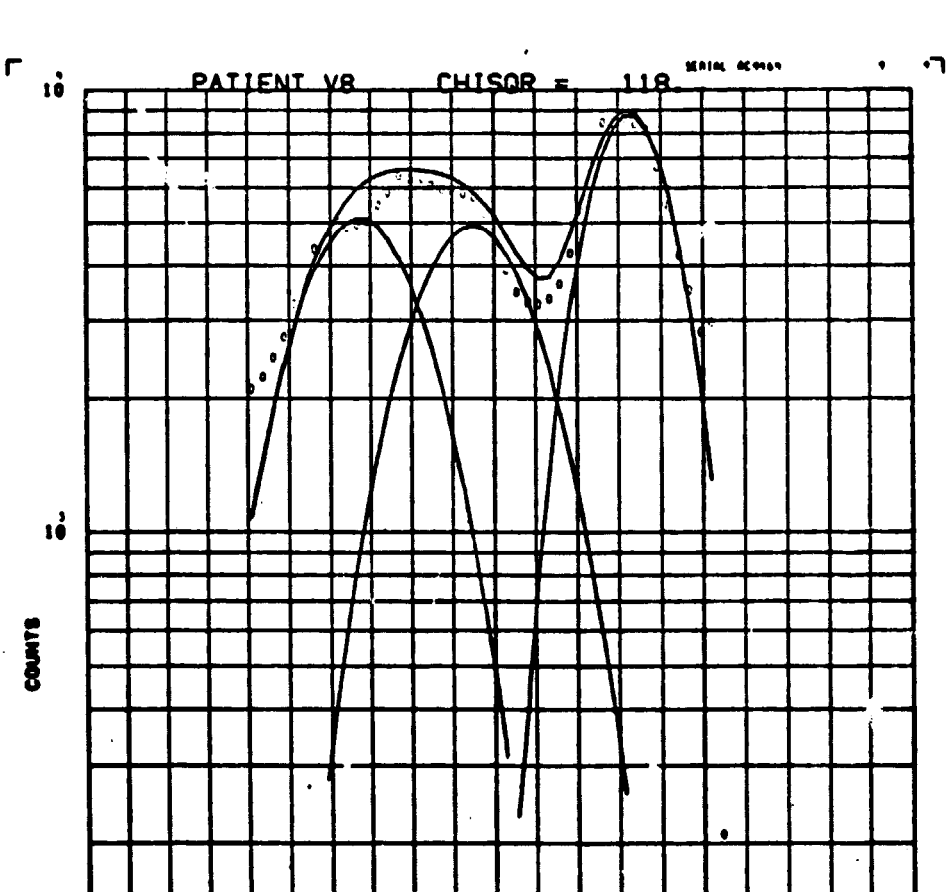
PATIENT V8 CHISQR = 118.
COUNTS
DENSITY

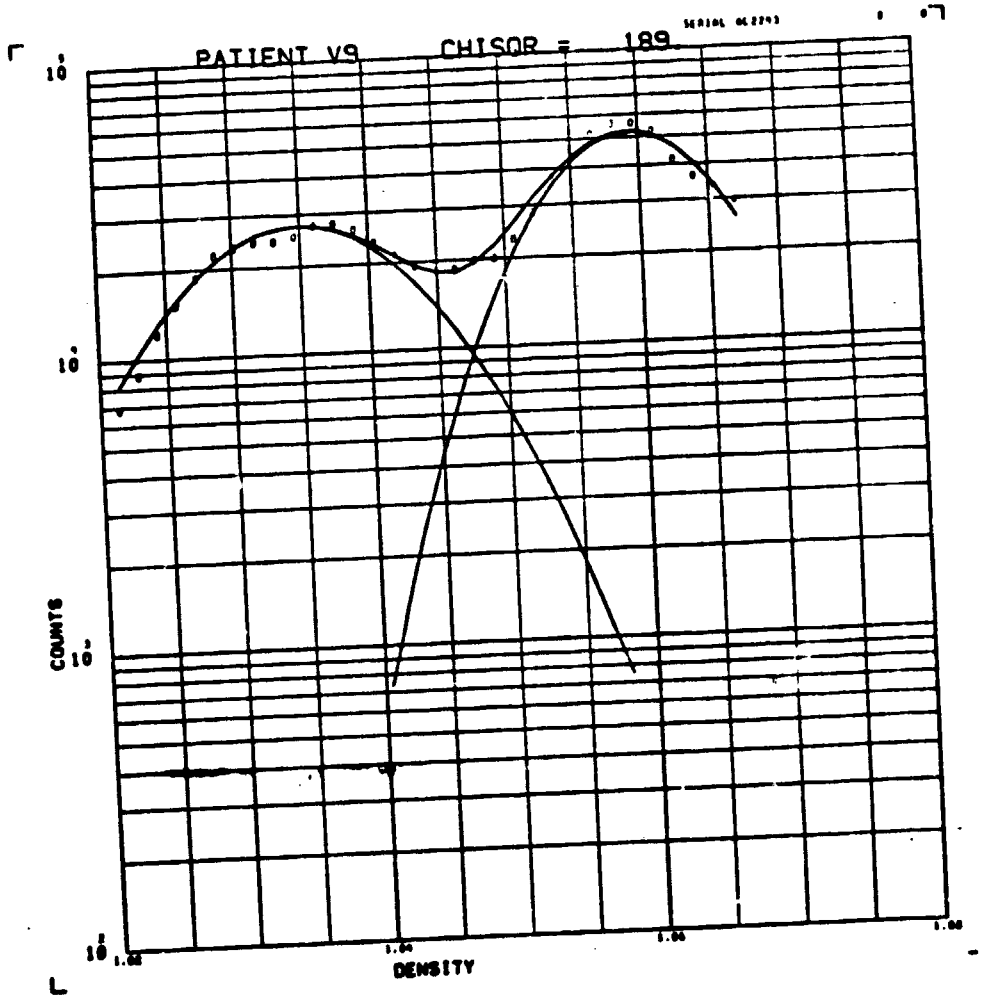
PATIENT V9 CHISQR = 189.
COUNTS
DENSITY

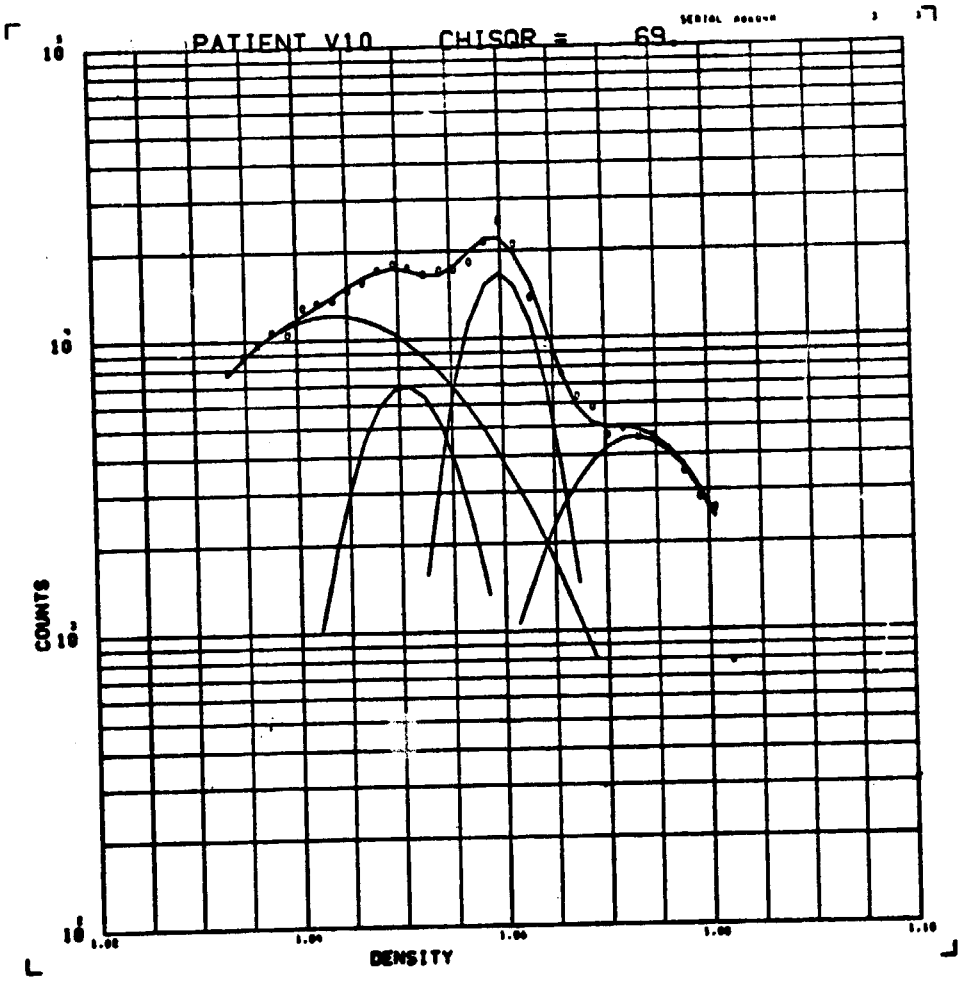
PATIENT V10 CHISQR = 69.
COUNTS
DENSITY

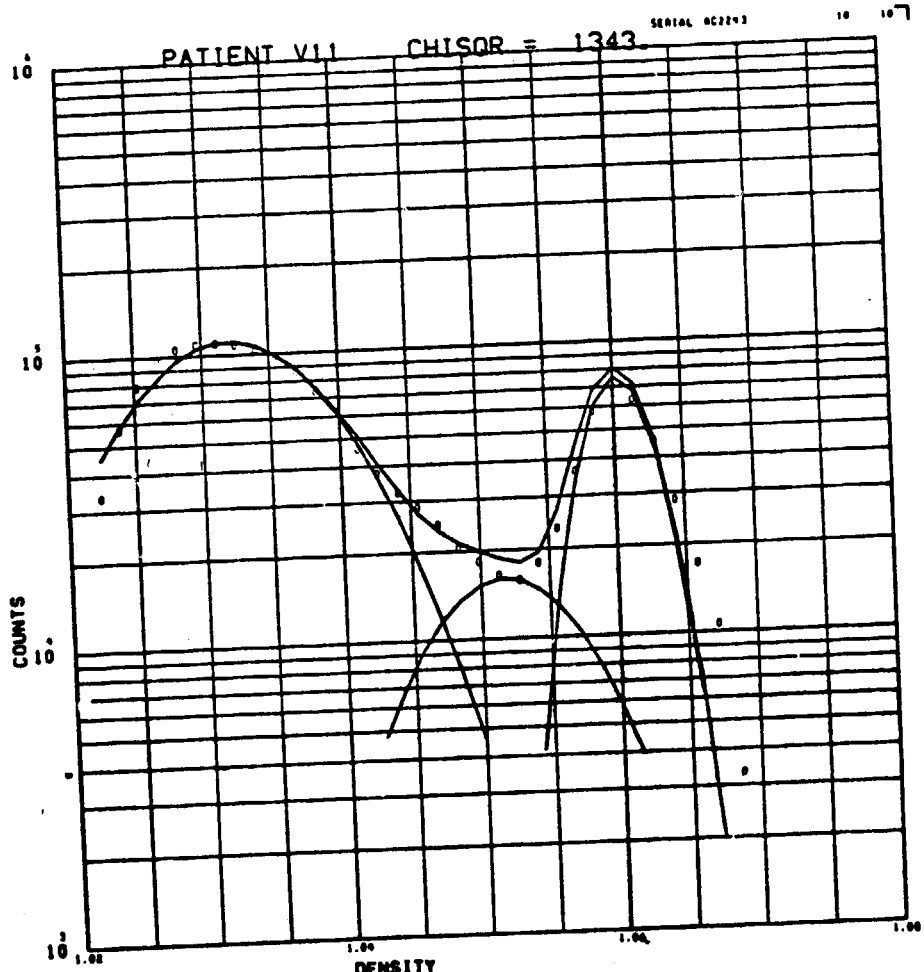
PATIENT V11 CHISQR = 1343.
COUNTS
DENSITY

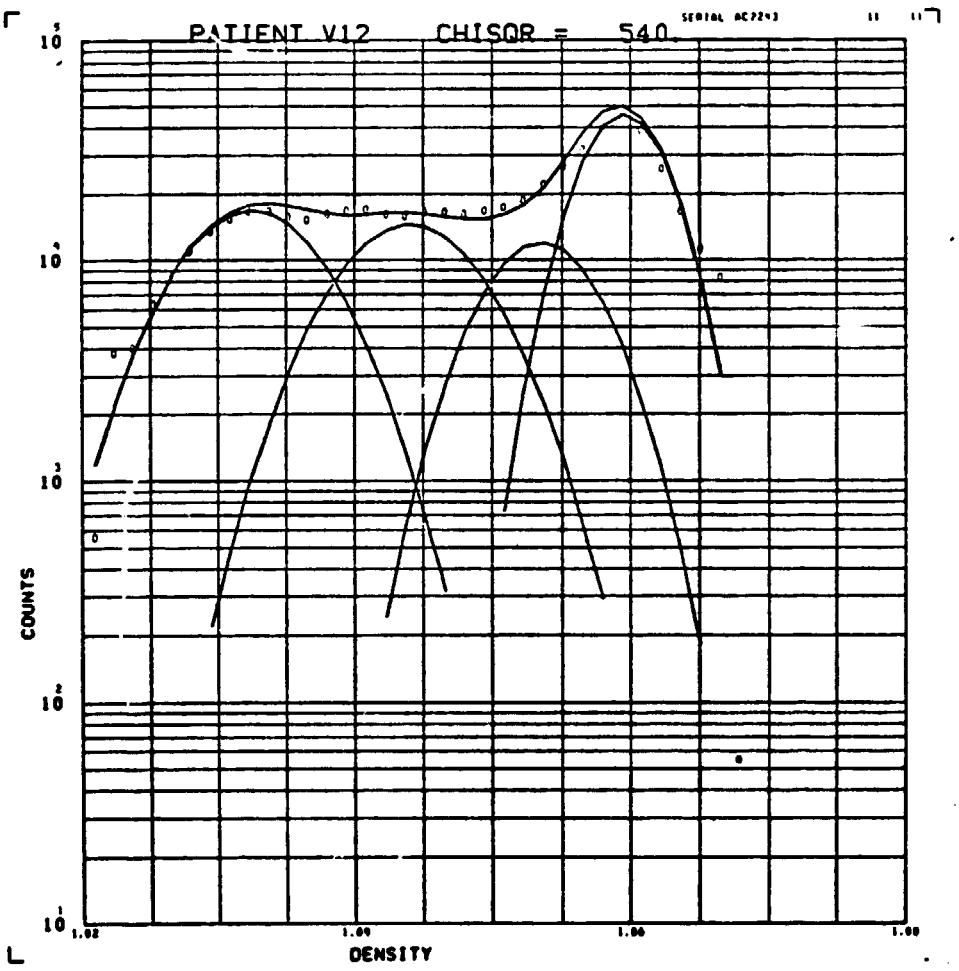
PATIENT V12 CHISQR = 540
COUNTS
DENSITY

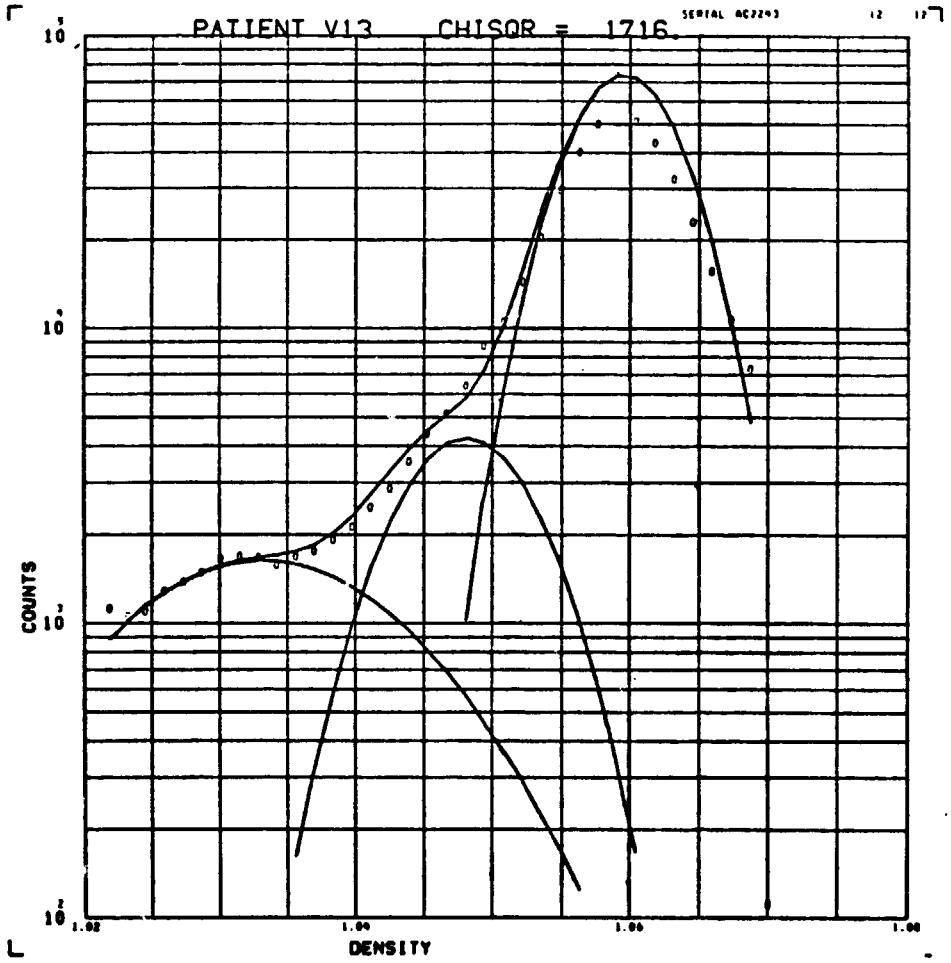
PATIENT V13 CHISQR = 1716.
COUNTS
DENSITY
1.02
1.04
1.06
1.08

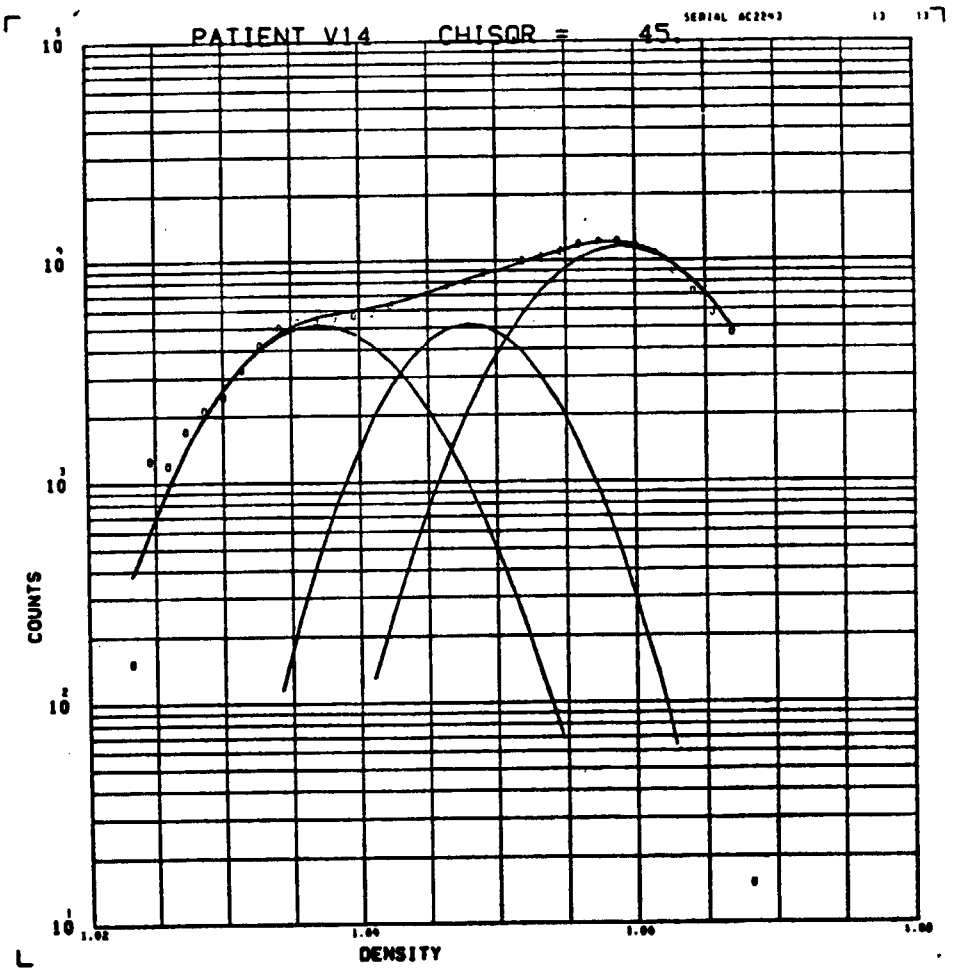
PATIENT V14 CHISQR = 45.
SERIAL AC2293
COUNTS
DENSITY
1.02
1.04
1.06
1.08

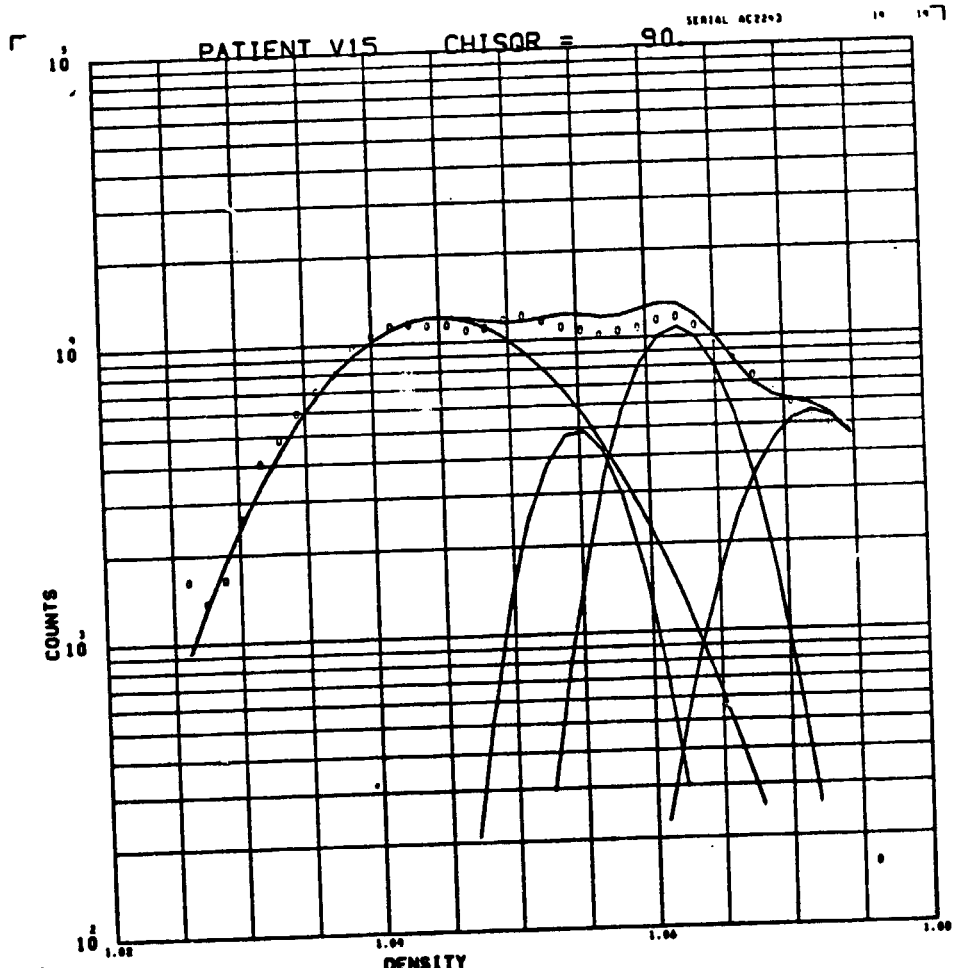
PATIENT V15 CHISQR = 90.
COUNTS
DENSITY

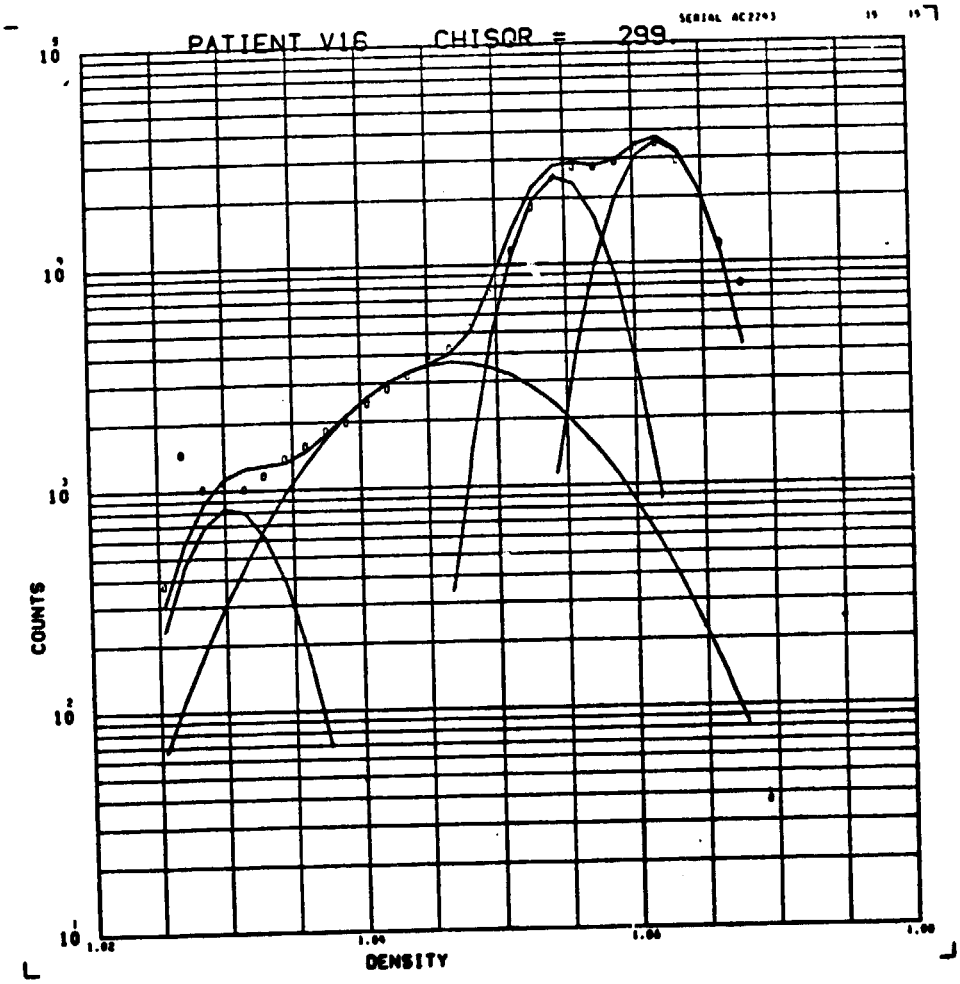
PATIENT V16 CHISQR = 299.
COUNTS
DENSITY

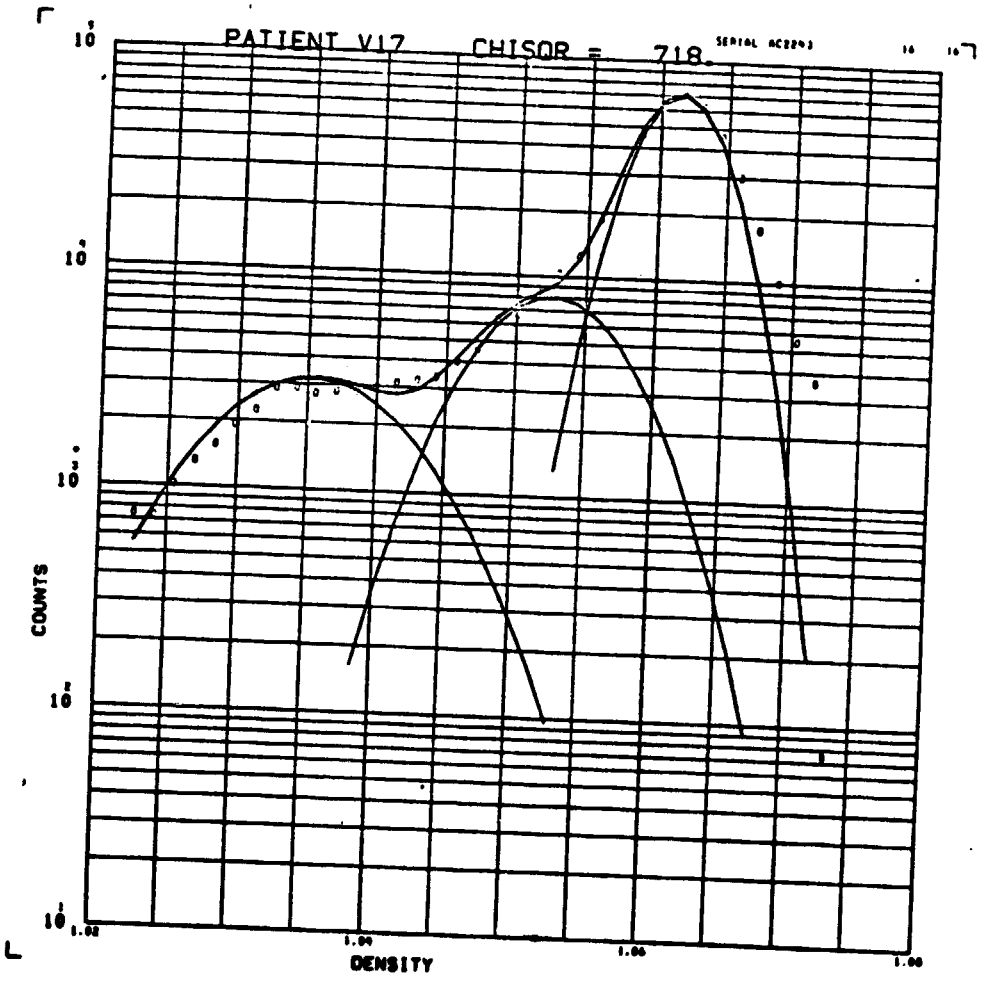
PATIENT V17 CHISQR = 718.
COUNTS
DENSITY
1.02
1.04
1.06
1.08

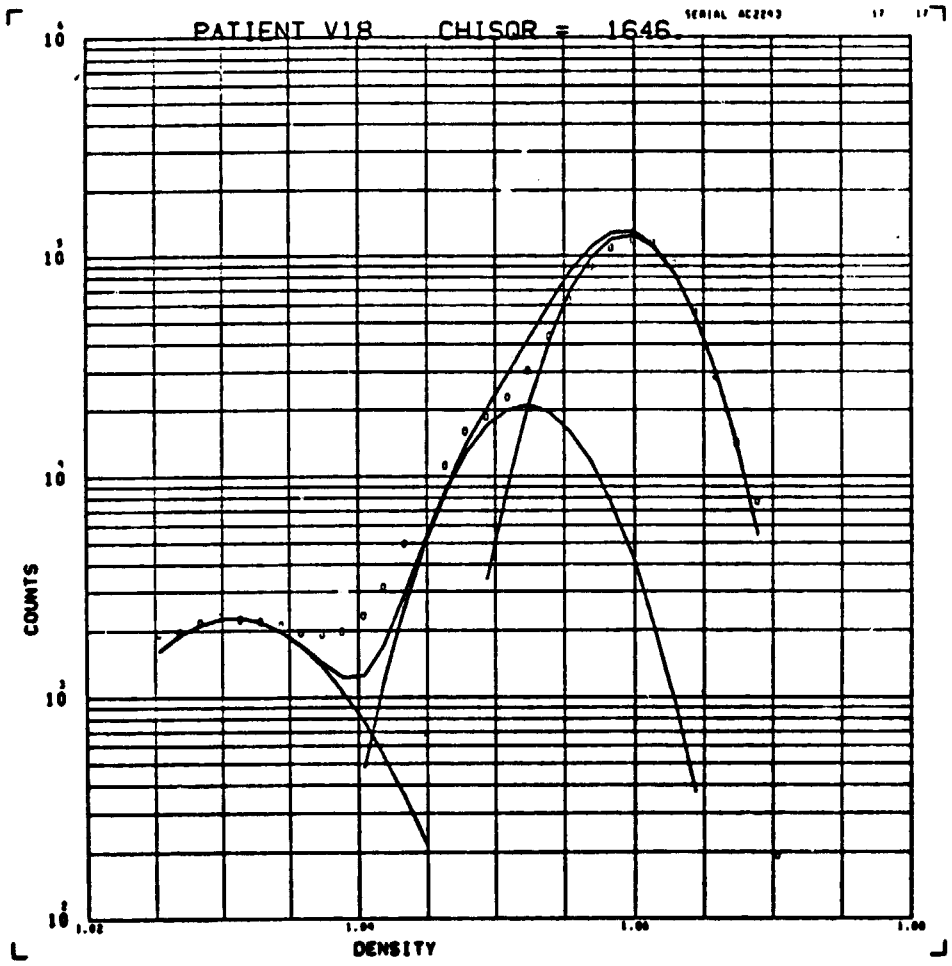
PATIENT V18 CHISQR = 1646.
COUNTS
DENSITY

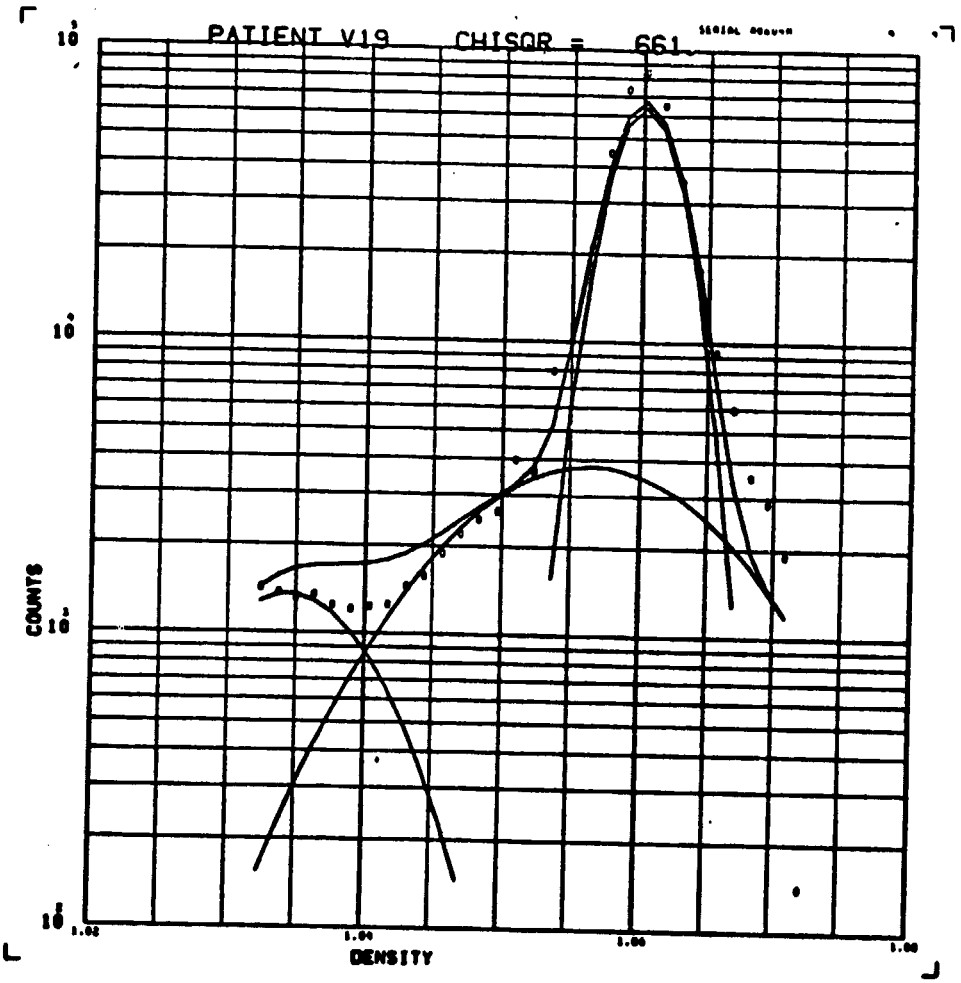
PATIENT V19 CHISQR = 661.
COUNTS
DENSITY

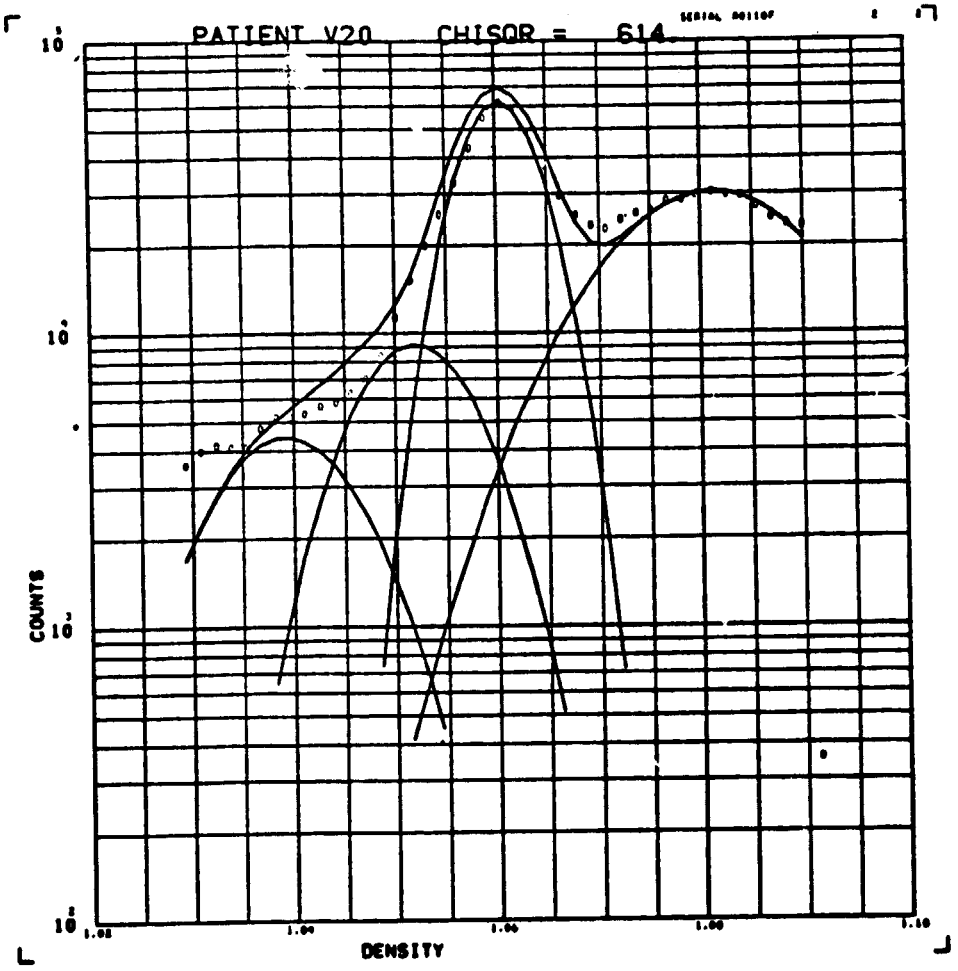
PATIENT V20 CHISQR = 614.
COUNTS
DENSITY

SUMMARY OF LITERARY REVIEW OF DENSITY GRADIENT STUDIES

Reference	Species	Strain	Tissue	Method	Results	Comments
D.T.Y. Yu, J.B. Peter H.E. Paulus K.M. Nils Clinical Immunology & Immunopathology 2: 333-342 (1974)	Human		Blood Lymph Nodes, Thoracic Duct Lymphocytes Tonsils Thymus	Discontinuous Ficoll Gradient (Equil)	B-cells predominate in light density fractions while T-cells predominate in heavy density fractions	
D.T. Yu P.J. Clements J.B. Peter J. Levy H.E. Paulus & E.V. Barnett Arthritis & Rheumatism 17 :37-45 (1974)	Human		Blood	Discontinuous Ficoll Gradient (Equil)	Azathioprine therapy in rheumatic patients was not found to alter the T-B proportions in the blood and did not change the density distribution.	
R.S. Geha F.S. Rosen E. Merler Nature, 248: 426-428 (1974)	Human		Tonsil	Discontinuous BSA gradient (Equilib?)	Pure populations of T&B cells obtained by gradient and rosette techniques. Pure B cells shown to be unresponsive to PHA.	
R.S. Geha J.G. Gatien R. Parkman J.D. Crain F.S. Rosen & E. Merler Clinical Immunology & Immunopathology. 2:404-415 (1974)	Human		Bone Marrow	Discontinuous BSA gradient (Equilib?)	Top of gradient rich in cells with high rate of DNA synthesis and ability to produce colony forming units. Middle of gradient cells have strongest response to allo-antigens. Bottom of gradient was rich in B-cells.	

SUMMARY OF LITERARY REVIEW OF DENISTY GRADIENT STUDIES (CONT)

Reference	Species	Strain	Tissue	Method	Results	Comments
R.S. Geha E. Schneeberger E. Merler F.S. Rosen New England J. Medicine, 291: 1-6 (1974)	Human	Blood	Blood	Discontinuous BSA density gradient (Equilib?)	Studied patients with "acquired" agammaglobulinemia. Found that all cells in the bottom 1/3 of gradient (10-15% of total) were absent in people who lack B-lymphocytes.	
M.I. Abdou & M.L. Abdou Clin. Exp. Immunol. 13: 45-54 (1973)	Human	Blood Bone Marrow	Blood Bone Marrow	Sucrose-plasma linear density gradient (velocity sedimentation)	Cells separated into two fractions. Upper fraction enriched in small lymphocytes. Lower fraction enriched in granulocytes and leucocyte precursors.	
S.S. Frøland J.B. Natvig & G. Husby Scand. J. Immunol. 2:67-73 (1973)	Human		Synovial Fluid	Ficoll-isopaque one step gradient	Separation of lymphocytes from synovial fluid in patients with rheumatoid arthritis.	
R.S. Geha F. S. Rosen E. Merler J. Clin. Invest. 52: 1726-1734 (1973)	Human	B	Blood	BSA Density Gradient (Equilib?)	3 subpopulations obtained 1st: Top 1/3 of gradient rich in cells with high rate of spontaneous DNA synthesis & colony forming units. 2nd: Rich in T-cells (middle 1/3 of gradient) 3rd: Rich in B-cells (bottom 1/3)	

SUMMARY OF LITERARY REVIEW OF DENSITY GRADIENT STUDIES (CONT)

Reference	Species	Strain	Tissue	Method	Results	Comments
D.T.Y. Yu J.B. Peter J.A. Stratton H.E. Paulus & H.I. Machleder Clinical Immunology & Immunopathology 1:456-462 (1973)	Human		Blood, Thoracic Duct Lympho- cytes	Discontinuous Ficoll gradient (Equilib)	In blood & lymph, lympho- cytes showed a decrease in number and a shift to lower density during pro- longed thoracic duct drainage. This suggests that high density lympho- cytes normally recirculate and that low density lymphocytes have prolifer- ated in response to the depletion.	
D.T.Y. Yu J.B. Peter H.E. Paulus, & H.I. Machleder J. Immunology 110:1615-1622 (1973)	Human		Thoracic Duct Lympho- cytes	Discontinuous Ficoll density gradient (Equilib.)	Separated lymphocytes into subpopulations which differed in morphology, basal unstimulated ^{3}H-TdR incorporation and response to stimulation by PHA and PMW.	
T.G. Pretlow II & D.E. Luberoff Immunology 24: 85-92 (1973)	Human		Blood	Isopycnic and programmed rate zonal centrifuga- tion	Effective and rapid means for separation of lympho- cytes and granulocytes from blood.	
L.K. Everson D.N. Buell & G.N. Rogentine J. Exp. Med. 137: 343-358 (1973)	Human		Lymphoid Cell Lines	Velocity Sedimen- tation	Separation of cells into G, S, & G_2 phase of reproductive cycle.	

SUMMARY OF LITERARY REVIEW OF DENSITY GRADIENT STUDIES (CONT)

Reference	Species	Strain	Tissue	Method	Results	Comments
T.G. Pretlow II, D.E. Luberoff & L. J. Hamilton P.C. Weinberger W.A. Maddox & J.R. Durant Cancer 31: 1120-6 (1973)	Human		Spleen (Hodgkin's Disease)	Isokinetic Gradient of Ficoll	Separation of Lymphocytes from solid tumors.	
D. Algom & M. Richter Laboratory Investigation 29: 587-594 (1973)	Human		Blood	Discontinuous BSA Gradient (Equiliib?)	Cells separated into fractions and response to various mitogens measured. In chronic lymphocytic leukemia and acquired hypogammablobulinemic patients, only the light fractions responding to various mitogens.	
N.F. Mendes M.E.A. Tolnai, N.P.A. Silveira R.B. Gilbertsen & R.S. Metzgar J. Immunol. 111: 860-867 (1973)	Human		Blood	Ficoll-hypaque 2 step gradient	Specific depletion of E-rosette forming cells (T-cells) or EAC rosette forming (B-cells) from a mixture of the two.	
R.S. Geha E. Schneeberger F.S. Rosen & E. Merler J. Exp. Medicine 138:1230-1247 (1973)	Human		Blood & Tonsil	Discontinuous BSA gradients (Equilib?)	Relatively pure populations of T- & B-cells were obtained. Proposed that human T-cells secrete a soluble product which, in combination with the antigen, triggers the B-cell into division and antibody secretion.	

SUMMARY OF LITERARY REVIEW OF DENSITY GRADIENT STUDIES (CONT)

Reference	Species	Strain	Tissue	Method	Results	Comments
J. M. Minderhoud & J. K. Smith Clin Exp Immunol 10: 571-579 (1972)	Human		Blood	Discontinuous Ficoll gradient (Equilib)	Lymphocytes fractionated and mixed with macrophages. Lymphocytes between 1.075 & 1.090 produced greatest effect on macrophage electrophoretic mobility.	
E. Mercer & M. Silberschmidt Immunology 22: 821-831 (1972)	Human		Tonsil	Discontinuous BSA gradient (Equilib?)	Dense Cells were found to specifically take up antigen.	
C.S. August E. Merler P.O. Lucas & C.A. Janeway Cell Immunol 1: 603-618 (1970)	Human		Thymus & Tonsil	BSA density gradient (Equilib?)	Lymphocytes separated into at least 3 populations. The first contained large and medium size lymphoblasts with spontaneous mitotic activity. Second population was 95% small lymphocytes which responded to PHA, tetanus toxoid and allogenic cells. The third contained more dense, small lymphocytes which responded poorly to mitogens.	

SUMMARY OF LITERARY REVIEW OF DENSITY GRADIENT STUDIES (CONT)

Reference	Species	Strain	Tissue	Method	Results	Comments
B. F. Argyris Transplantation 17:387-391 (1974)	Mouse	C57BL/6	Spleen	Discontinuous BSA gradient (Equilib?)	Gradient gives sub-population of cells (θ Positive) of medium density enriched in graft vs. host activity	Also evidence for light density rosette forming θ positive population.
W.C. Wallen J.H. Dean & D.O. Lucas Cell Immunol. 6: 110-122 (1973)	Mouse	CD-1	Spleen	Discontinuous BSA gradient (Equilib?)	Spleen cells separated into 6 fractions. Cells from each fraction cultured with several general mitogens and with a specific antigen PPD. The cultures were then assayed for mitogenesis and interferon production. Interferon producing cells were a different population than the cells undergoing a DNA synthetic response.	Results suggest a 2-cell requirement for interferon production in response to mitogens or PPD. Also, results suggest interferon producers are not a thymus dependent lymphocyte population.
A. H. Greenberg European J. Immunol. 3: 793-797 (1973)	Mouse	C3H DBA/2	Spleen	Linear Ficoll gradient velocity sedimentation	Sedimentation provides a simple, reproducible m method for fractionating lymphocytes from lymphoblasts. The T-lymphoblast was found to be an important cytotoxic cell in the early immune response to allo-antigen. At a later time, in the immune response, the small lymphocyte was shown to be the predominant cytotoxic cell.	

SUMMARY OF LITERARY REVIEW OF DENSITY GRADIENT STUDIES (CONT)

Reference	Species	Strain	Tissue	Method	Results	Comments
J. Marbrook & J. S. Haskill Cell Immunol. 2: 1-9 (1973)	Mouse	CBA	Spleen	Velocity sedimentation and linear BSA gradient (Equilib?)	Partially purified populations of cells were produced by density gradient. Several fractions were shown to contain precursors of plaque-forming cells.	
J.G. Zettergren D.E. Luberoff & T.G. Pretlow II J. Immunol. 111: 836-840 (1973)	Mouse	C3H BALB/c C57BL DBA	Hepatoma Melanoma Glioma	Linear Ficoll gradient (Equilib?) Velocity Sedimentation	Developed method for separating lymphocytes for solid tumors. Glass bead and velocity sedimentation gave lymphocytes of 58.4 to 95.2% purity. Adding isopycnic centrifugation gave 76.3 to 96.8% purity	
D.M. Vasudevan K.T. Brunner & J.C. Cerottini Brit J. Cancer 28: Suppl I, 35-36 (1973)	Mouse	C57BL	Spleen	Linear BSA gradient (Equilib?)	Lymphocytes of less than 1.08 g/cc were found to contain the cytotoxic cells. Elimination of heavier, irrelevant cells increased cytotoxic effect.	
F. Dumont & D. Sabolovic Biomedicine 19: 257-260 (1973)	Mouse	Swiss/B CBA	Thymus	Discontinuous BSA gradient (Equilib)	Hydracortisone-resistant thymocyte subpopulation separated into 4fractions. Electrophoretic mobility increased with density. Low density cells have high spontaneous DNA synthesis, but respond less to PHA than the densest cells.	

SUMMARY OF LITERARY REVIEW OF DENSITY GRADIENT STUDIES (CONT)

Reference	Species	Strain	Tissue	Method	Results	Comments
K. Shortman W.J. Byrd J.-C. Cerottini & K.T. Brunner Cell Immunol 6: 25-40 (1973)	Mouse	CBA/H	Spleen Thymus	Linear BSA gradient (Equilib?)	In the spleen, dense T-cells respond to PHA far more than light T-cells. In the thymus, only light cells respond to PHA or PWM. Dense cells were unresponsive.	In the spleen, dense T-cells were non-adherent in column separations. Light cells were adherent.
M.O. El-Arini & D. Osoba J. Exp. Medicine 137:821-837 (1973)	Mouse	C57BL/6J DBA/2J C3H/HeJ	Bone Marrow Spleen	Linear Ficoll density gradient (Equilib?)	Progenitors of T-cells are lighter in density than T-cells.	
S. Konda E. Stockert & R.T. Smith Cell. Immunol. 7: 275-289 (1973)	Mouse	CBA, A/J, C57BL/6 AKR	Thymus	Discontinous BSA gradient (Equilib?)	Two subpopulations identified by density and antigen patterns. Major subpopulation consisted of small lymphoid cells, is 80-90% of total cells, high density and rich in Θ, TL, G, X, LY-A, LY-B and LY-C, but little cr No. H-2. The minor subpopulation was low density, large lymphoid cells, comprised 10-15% of total cells and was relatively rich in H-2, but low in the above-mentioned antigens.	

SUMMARY OF LITERARY REVIEW OF DENSITY GRADIENT STUDIES (CONT)

Reference	Species	Strain	Tissue	Method	Results	Comments
R.S. Geha F.S. Rosen & E. Merler J. Clinical Investigation 52: 1726-1734 (1973)	Human		Blood	Discontinuous BSA gradient (Equilib?)	Normal lymphocytes are separated into three sub-populations by density gradient technique 1) Top 1/3 of gradient is rich in cells characterized by a high spontaneous rate of DNA synthesis, 2) middle 1/3 is rich in T-cells. Bottom 1/2 is rich in B-cells. Several patients with X-linked agammaglobu-linema were found to be totally deficient in B-lymphocytes.	
H. Von Boehmer & K. Shortman J. Immunological Methods 2:293-301 (1973)	Mouse	CBA/H Wehi	Spleen Thymus	Linear BSA gradient (Equilib?)	A low ionic strength buffer causes damaged cells to aggregate and adhere to cotton wo l columns much more than viable cells. This is considered a simpler method of elimina-ting nonviable cells than the density gradient method.	
J. D. Stobo & W. E. Paul J. Immunology 110: 362-375 (1973)	Mouse	BALB/C AKR	Bone Marrow Spleen Lymph Node	Discontinuous BSA gradient (Equilib?)	Spleen cells separated by gradient. Fractions displayed both increased and diminished PHA:CON A stimulation ratio. Least dense cells had diminished PHA:CON A ratio.	

SUMMARY OF LITERARY REVIEW OF DENSITY GRADIENT STUDIES (CONT)

Reference	Species	Strain	Tissue	Method	Results	Comments
B.F. Argyris A. Cooney & H. Haritou Cell Immunol 5: 264-279 (1972)	Mouse	C57BL/6 C3H/4e AKR	Spleen	Discontinuous BSA gradient (Equilib)	The Light density fractions are enriched in plaque forming (antibody forming) cells and rosette forming (T) cells. The bone marrow derived (B) cells in the bottom part of the gradient seem to be antibody forming precursor cells.	
S. Konda Y. Nakad & R. T. Smith J. Exp Med = 136:1461-1477 (1972)	Mouse	CBA A/J C57BL/6	Thymus Spleen	Discontinuous BSA gradient (Equilib?)	A minor low density population was derived by gradient centrifugation. This population was found necessary for graph vs. host reaction.	
K. Shortman M. Williams & P. Adams J. Immunological Methods 1: 273-287 (1972)	Mouse	CBA	Lymph Node Spleen	Linear BSA Gradient (Equilib?) Velocity Sedimentation	Velocity sedimentation useful for eliminating very fine and very coarse cell debris, density sedimentation useful for eliminating damaged cells (at pH 5.1) or damaged cells and erythroid cells (at pH 7.2).	

SUMMARY OF LITERARY REVIEW OF DENSITY GRADIENT STUDIES (CONT)

Reference	Species	Strain	Tissue	Method	Results	Comments
R. Burleson & R.H. Levey Cell Immunol 4: 305-315 (1972)	Mouse	C57BL6/J	Spleen Lymph Node Bone Marrow	Discontinuous BSA gradient (Equilib?)	Large, less dense cells (80% of total cells) were inert in graft vs. host rxn. Small dense cells active in G.V.H. Bone marrow is domicile of small, long-lived thymus derived lymphocytes.	
E.R. Suter H. Probst & P. Dukor European J. Immunol. 2: 189-190 (1972)	Mouse	C3H/f	Lymph Node Spleen	Discontinuous BSA gradient (Equilib?)	Rosettes formed by complement receptor lymphocytes with sensitized erythrocytes were purified by density gradient sedimentation. Complement receptor lymphocytes are ultrastructurally very uniform, small lymphocytes.	
K. Shortman K.T. Brunner J.-C Cerottini J. Exp. Medicine 135:1375-1391 (1972)	Mice	C57BL/6 CBA	Spleen Thymus	Linear BSA gradient (Equilib?)	Density gradient used to study development of cytotoxic lymphocytes, separate and characterize their progenitors and determine their relationships to subpopulations of T-cells.	
J. Mitchell Immunology 22: 231-245 (1972)	Mouse	CBA	Spleen	2-Step BSA gradient	Used gradient to separate live cells from dead cells.	

SUMMARY OF LITERARY REVIEW OF DENSITY GRADIENT STUDIES (CONT)

Reference	Species	Strain	Tissue	Method	Results	Comments
K. Shortman W. Byrd M. Williams K.T. Brunner & J.-C. Cerottini Aust. J. Exp. Biol. Med. Sci. 50:323-336 (1972)	Mouse	CBA/H C57BL/6	Blood Spleen Thymus	Linear BSA gradient (Equilib?)	Cells adherent to glass bead columns are light density, non-adherent cells, are dense; antibody forming cells and cytotoxic lymphocytes were predominantly light adherent cells.	
R.H. Levey & R. Burleson Cell Immunol. 4: 316-332 (1972)	Mouse	C57BL6/J	Thymocytes	Discontinuous BSA gradients (Equilib?)	Identification and recovery of an immunocompetent subpopulation of mouse thymocytes.	
Levy & Burleson Cell Immunol 4: 333-340 (1972)	Mouse	C57BL6/J	Thymocytes	Discontinuous BSA gradients (Equilib?)	Density gradient separation shown depletion of immunocompetent cell populations of the thymus by anti-lymphocyte serum. Compares normal neonatal w/als treated neonatal.	
J. W. Dyminski & B. F. Argyris Cell Immunol 5: 561-564 (1972)	Mouse	C31T/H_eJ AKR C56BL/6J	Lymph Node & Bone Marrow	Discontinuous BSA gradients (Equilib?)	Confirmation of Thymus-bone marrow cooperation during <u>in vitro</u> sensitization to transplantation antigens.	Previous work used D.G. to obtain subpopulations participating in <u>in vitro</u> sensitization Ag's
M. Williams & K.Shortman Aust. J. Exp. Biol. Med. Sci. 50: 133-151 (1972)	Mouse	CBA/H	Spleen & Thymus	Linear BSA & Ficoll gradients (Equilib?)	Determination of the effect of pH on the buoyant density of lymphocytes and erythrocytes.	

SUMMARY OF LITERARY REVIEW OF DENSITY GRADIENT STUDIES (CONT)

Reference	Species	Strain	Tissue	Method	Results	Comments
L. LaFleur R.G. Miller & R.A. Phillips J. Expt. Med. 135: 1363-1374 (1972)	Mouse	C3H/H_eJO$_{ci}$ C57BL/ 6JO$_{ci}$	Bone Marrow & Thymus	Velocity Sedimentation	Physical characterization of precursors of B-cells.	
T.G. Pretlow & N. Pushpara J. Immunology 22: 87-91 (1972)	Mouse	C57B	Peri-toneal Cells	Ficoll Linear Density Gradient rate-zonal centrifugation	Developed method to separate lymphocytes from peritoneal cells.	
M.J. Stevart T.G. Pretlow & R. Hiramoto Am. J. Pathology 68: 163-177 (1972)	Mouse	BALB/C	Plasma-cytoma Tumor	Isopycnic & Isokinetic Ficoll linear gradients (Equilib?)	Separation of malignant cells from benign cells.	
K. Shortman J.-C. Cerottini & K.T. Brunner Eur. J. Immunol. 2: 313-319 (1972)	Mouse	CBA	Spleen & Thymus	Linear BSA gradient (Equilib?)	Separation of subpopulations of T & B lymphocytes. 1) Minor population of thymus cells with high H-2 & low Θ corticosteroid resistant, low density 2) B&T cells have overlapping distributions, but some regions enriched for T or B 3) Different mouse strains had different T&B distributions 4) EAch antigenic type of lymphocyte had density heterogeneity. 5) Density distribution of cells in spleen & thymus similar. 6) High H2 low Θ starts in thymus, goes to peripheral circulation high Θ, low H-2 stays in thymus.	

SUMMARY OF LITERARY REVIEW OF DENSITY GRADIENT STUDIES (CONT)

Reference	Species	Strain	Tissue	Method	Results	Comments
J.S. Haskil & J. Marbrook Cell Immunol. 3: 448-460 (1972)	Mouse	CBA	Spleen & Thymus	BSA Gradient (Equilib?) and velocity sedimentation	Separation of rosette-forming cells into sub-populations possessing distinct immunological functions. Investigated interrelationships between these sub-populations.	
H. Von Boehmer K. Shortman & P. Adams J. Exp. Medicine 136:1648-1660 (1972)	Mouse	CBA/H C57BL	Bone Marrow Spleen Thymus	Linear BSA gradient (Equilib?)	Spleen cells fractionated on gradient. Activity of each fraction as a target in the mixed lymphocyte reaction was measured.	By using bone marrow and thymus, it was found that only B-cells act as targets.
J.W. Dyminski & B.F. Argyris Cell Immunol. 5: 280-287 (1972)	Mouse	C57BL/6J C3H/HeJ	Lymph node & bone marrow	Discontinuous BSA gradient (Equilib?)	Five subpopulations of lymph node cells obtained. Light & medium fractions needed for in vitro sensitization to alloantigens. Five sub-populations of bone marrow cells obtained. Only top two fractions required for in vitro sensitization.	
L. LaFleur, B.J. Underdown R.G. Miller & R.A. Phillips Ser. Haemat. 5: 50-63 (1972)	Mouse	BDF1	Bone marrow Spleen Thymus	Velocity sedimentation	Precursors of B-cells are distinct from hemopoetic stem cells, but may be derived from the stem cells.	

SUMMARY OF LITERARY REVIEW OF DENSITY GRADIENT STUDIES (CONT)

Reference	Species	Strain	Tissue	Method	Results	Comments
H.C. Miller & G. Cudkowicz Science 171: 913-915 (1971)	Mouse	C3H C57BL/10	Bone marrow	Discontinuous BSA gradient (Equilib?)	Bone marrow cells capable of generating IgG or IgM were separated by density gradient centrifugation. IgM producers denser than IgG producers.	
J. Pelet K.T. Brunner A.A. Nordin & J.-C. Cerottini Eur. J. Immunol. 1: 238-242 (1971)	Mouse	C57BL/6	Spleen	Discontinuous BSA gradient (Equilib?)	Alloantibody plaque-forming cells are found predominantly in low densities. Cytotoxic lymphocytes are found mainly in the medium and high densities.	
K. Shortman & J. Palmer Cell Immunol. 2: 399-410 (1971)	Mouse	CBA C57B	Peritoneal exudate cells Spleen	Linear BSA gradient (Equilib?)	Shows that light, adherent radiation resistant "accessory" cell needed for in vitro response of mouse lymphocytes to sheep erythrocytes is a macrophage.	
K. Shortman J. Cell. Physiol. 77:319-330 (1971)	Mouse	BALB C	Spleen Thoracic duct Lymphocytes Thymus	Linear BSA gradient (Equilib?)	Thymus has more dense cells than spleen or thoracic duct. Large lymphocytes generally less dense than small lymphocytes.	

SUMMARY OF LITERARY REVIEW OF DENSITY GRADIENT STUDIES (CONT)

Reference	Species	Strain	Tissue	Method	Results	Comments
L.I. Johnson Proc. Soc. Exp. Biol. & Med. 136: 1277-1283 (1971)	Mouse Rat	CF1 Charles River	Bone marrow	Linear sucrose-serum gradient (velocity sedimentation)	Four major fractions recovered from gradient. Three fractions 99% pure lymphocytes. High reproducibility of purity and yield.	
T. Takiguchi W.H. Adler & R.T. Smith Cell Immunol. 2: 373-380 (1971)	Mouse	CBA DBA/2	Bone marrow Spleen Thymus	Discontinuous BSA gradient (Equilib?)	A low density thymus cell population was found to be the cooperative "helper" cell involved in the response to sheep RBC antigenic challenge. This population consists of 30% small lymphocytes and 70% large lymphoid cells and blasts.	
T. Takiguchi ACTA HAEMATOLOGICA JAPONICA 34: 396-410 (1971)	Mouse	CBA	Spleen Thymus	Discontinuous BSA gradient (Equilib?)	Density gradient used to study thymectomized mice. Spleen cells normal, but decreased in PHA responsiveness. Dense cells particularly reduced in PHA responsiveness. In the thymus, light cells were PHA responsive, low O, and high spontaneous DNA synthesis.	
R.M. Gorczynski R.G. Miller & R.A. Phillips Immunology 19: 817-829 (1970)	Mouse Rat	C3H/HeJ C3H/HeO$_{ci}$ C57BL/6J Fisher 344	Spleen	Linear Ficoll gradient (Equilib?)	Antibody forming cells band in a single peak at 1.070 g/cc.	

SUMMARY OF LITERARY REVIEW OF DENSITY GRADIENT STUDIES (CONT)

Reference	Species	Strain	Tissue	Method	Results	Comments
W. H. Adler D. Peavy & R.T. Smith Cell Immunol. 1: 78-91 (1970)	Mouse	BALB/C	Spleeen	Discontinuous BSA gradient (Equilib?)	Effect of various mitogens on spleen cell subpopulations was determined. Cooperation between popu- was suggested in some cases.	
R.I. Mishell R.W. Dutton & D.J. Raidt Cell Immunol. 1: 175-181 (1970)	Mouse	C57BL/6 DBA/2	Spleen	Discontinuous BSA gradient (Equilib?)	Density gradient separated spleen cell subpopulations were found to cooperate in the immune response.	
C. Bianco R. Patrick & V. Nussenveig 702-719 (1970)	Human		Blood	Discontinuous BSA gradient (Equilib)	Complement receptor lympho- cytes (b cells) are in significantly higher pro- portion in the upper layers of the gradient.	
M.G. Mage W.H. Evans & E.A. Peterson Proc. Soc. Expt. Biol. & Med. 127: 478-481 (1968)	Mouse	BALB/C	Spleen	Discontinuous sucrose gradient (velocity sedimentation at 1-G)	18 fold enrichment of antibody plaque-forming cells by sedimentation at 1-G.	

SUMMARY OF LITERARY REVIEW OF DENSITY GRADIENT STUDIES (CONT)

Reference	Species	Strain	Tissue	Method	Results	Comments
Y. Kinoshita S. Kimura M. Fukamizu T. Nagasawa Exp. Cell. Res. 86: 136-142(1974)	Rat	Wistar	Thymus	Discontinuous gum acacia gradient (Equilib?)	Three kinds of lymphocyte populations were found. Surface antigens of the different populations were found to differ from each other.	
W.E. Bowers J. Cell Biology 59: 177-184 (1973)	Rat	HO	Thoracic Duct Lympho-cytes	Zonal centrifuga-tion (velocity) and isopycnic density centrifugation	Developed method of separating thoracic duct lymphocytes according to size. Showed lysosomes and large amount of cathespin D present, mainly in small lymphocytes.	
C.M. Newlin Cell Immunol. 8: 198-208 (1973)	Rat	BH BN DA	Blood	Discontinuous BSA gradient (Equilib)	Lymphocytes separated into subpopulations. All sub-populations respond euqlly to alloantigens. Cells of intermediate density re-spond to PHA at concentra-tions equal to that for unfractionated cells. Low and high density cells respond poorly to PHA, but when mixed show enhanced response.	
J.J. Miller, III K. Shortman & P. Byrt J. Immunol. 108: 1591-1595 (1972)	Rat	Lewis	Lymph node	Linear BSA gradient (Equilib?)	Lymph node lymphocytes labeled with ^{3}H-TdR with or without immune stimulus. With immune stimulus, the proportion of light cells (<1.07 g/cc) was greater than without stimulus.	

SUMMARY OF LITERARY REVIEW OF DENSITY GRADIENT STUDIES (CONT)

Reference	Species	Strain	Tissue	Method	Results	Comments
A.Y.S. Wu & B.H. Waksman Cell Immunol. 3: 516-528 (1972)	Rat	Lewis	Lymph node and thymus	Discontinuous BSA gradients (Equilib?)	Separation of rat thymic subpopulations.	
Y. Kinoshita & S. Kimura Exp. Cell Res. 68: 471-476	Rat	Wistar	Thymus	Density gradient (Equilib?)	Antisera prepared against dense thymocytes enhanced tumor growth remarkably.	
N. Kraft K. Shortman & J. Marchalonis Immunology 20: 919-930 (1971)	Rat Toad	Lewis Bufo Marinus	Blood Spleen	Linear BSA gradient (Equilib?)	Gradient used to study antibody forming cells in rat and toad. In the toad, a definite sequence of density peaks appeared progressively during the response to antigen. In the rat, cells making various antibody classes gave different density profiles and could be partially separated from each other.	
A.C. Aisenberg & C. Murray J. Immunol. 107: 284-288 (1971)	Rat	Fischer	Spleen Thymus Thoracic Duct Cells	Discontinuous BSA gradient (Equilib?)	Separation achieved between antibody producing cells and small lymphoid cells. Thymocytes can be distinguished from thoracic duct lymphocytes. Rat thymocytes are smaller and denser than thoracic duct cells.	

SUMMARY OF LITERARY REVIEW OF DENSITY GRADIENT STUDIES

Reference	Species	Strain	Tissue	Method	Results	Comments
N. Kraft & R. Wistar Aust. J. Exp. Med. Sci. 49: 11-20-(1971)	Rat Mouse	Lewis CBA	Blood Lymph Node Spleen Thoracic Duct Lympho-cytes	Linear BSA gradient (Equilib?)	IgM producing cells from rat spleen found mainly at densities of 1.0547-1.0558 and 1.0636-1.0649.	
J.S. Haskill D.G. Legge & K. Shortman J. Immunol. 102: 703-712 (1969)	Rat	Wistar	Blood Lymph Nodes Spleen Thoracic Duct Lympho-cytes	Linear BSA gradient (Equilib?)	A circulating antibody forming population of cells was enriched 100 times by density gradient techniques.	Evidence presented for distinct stages rather than a con-tinuum in the development of the antibody-forming cell.
P. Tamminen A. Toivanen & P. Toivanen Europ. J. Immunol. 3, 521-523 (1973)	Chicken	White Leghorn Line P	Thymus	Discontinuous BSA gradient (Equilib?)	Enriched antibody forming capacity in low density cells. Graft vs host reaction found in high density cells. 4-1/2 week old chickens do not show this separation, while 10-week olds do.	
E. Pick European J. Immunol. 3: 317-319 (1973)	Guinea Pig		Lymph Node	Discontinuous BSA gradient (Equilib)	Macrophage migration inhibitory factor pro-duction limited to lymphocytes of low density.	

SUMMARY OF LITERARY REVIEW OF DENSITY GRADIENT STUDIES (CONT)

Reference	Species	Strain	Tissue	Method	Results	Comments
O. Rudzik & J. Bienenstock Lab. Invest. 30: 260-266 (1974)	Rabbit	New Zealand White	Gut Mucosa	Two step BSA gradient (Equilib?)	Developed method for isolation of lymphocytes from gut mucosa.	
N. Kraft & K. Shortman J. Cell. Biology 52: 438-452 (1972)	Toad	B. Marinus	Blood Spleen	Linear BSA gradient (Equilib?) Sedimentation velocity	Differentiation of antibody forming cells (AFC) followed by density and size. Antibody formers were purified 17-fold by density and 140-fold by velocity sedimentation.	Results suggest AFC starts as a large, light, dividing "blast" cell and becomes identical to a small lymphocyte in size density and morphologic appearance.

BIBLIOGRAPHY

1. Chiba, S, T. Yamanaka, T. Nakao. Detection of Cell-mediated Immunity to Measles Virus with ^{51}Cr Release Assay in Patients with Natural Measles. Tohoku Journal of Experimental Medicine, Vol. 112, pp 285-288. 1974.

2. Hall, JG, B. Morris, G. D. Moreno and M. C. Bessis. Journal of Experimental Medicine, Vol. 125 #1, pp 91-110. January 1967.

3. Hilal, SK, D. G. Mosser, M. K. Loken and R. W. Johnson. A New Technique for High-resolution Density Gradient-separation of Bone Marrow Cells. Annals of the New York Academy of Science, Vol. 144, pp 661-76. 1964.

4. Haskill, JS, D. G. Legge and K. Shortman. Density Distribution Analysis of Cells Forming 19S Hemolytic Antibody in the Rat. Journal of Immunology Vol. 102, pp 703-712. 1969.

5. Kelton, AA. Fractionation of Human Peripheral Blood Lymphocytes on a Ficoll Density Gradient. Doctoral Dissertation. UCLA. 1969.

6. Williams, N., M. A. S. Moore, K. Shortman, L. Condon, B. Pike, and G.J.V. Nossal. Density Separation and Characterization of Human Blood Leucocytes, Including T and B Lymphocytes. Australian Journal of Experimental Biology and Medicine, Vol. 52, Part 3, pp 491-503. 1974.

7. Kelton, AA, M. B. Lawton, and J. L. Sever. The Density Distribution of Peripheral Lymphocytes from Patients with Multiple Sclerosis. Submitted for publication.

8. Diem, K. and C. Lentner. Editors "Scientific Tables", Seventh Edition, Ciba-Geigy, Ltd. Basle Publisher. 1970.

9. Hald, A. "Statistical Theory with Engineering Applications", pp 153-158. John Wiley and Sons, Inc., Publishers. 1952.

10. Bevington, P. R. "Data Reduction and Error Analysis for the Physical Sciences". McGraw-Hill Book Company, Publishers. 1969.

11. Türk, W. Klinische Untersuchungen Über Das Verhalten Des Blutes Bei Akuten Infektionskrankheiten, Braumüller, Vienna. 1898.

12. Litwins, J. and S. Lebowitz. Abnormal Lymphocytes ("Virocytes") in Virus Diseases Other Than Infectious Mononucleosis. Acta Haematologica, 5, pp. 223-231. 1915.

13. Downey, H. and C. A. McKinlay. Acute Lymphadenosis Compared with Acute Leukemia. Arch. Int. Med. 32, pp. 81-112. 1923.

14. Wood, T. A. and E. P. Frenkel. The Atypical Lymphocyte. American Journal of Medicine, 42, pp. 923-936. June 1967.

15. Benjamin, B. and S. M. Ward. Leukocytic Response to Measles. American Journal of Diseases of Children, Vol. 44, Number 5, pp. 921-63. Nov. 1932.

16. Rebuck, JW. Infectious Mononucleosis II Blood, Bone Marrow, Lymph Nodes. Staff Meet. Bull., Hosp. U. Minn, Vol. 13, p. 342. 1942.

17. Sramkova, L, D. Stanislav and D. Cermakova. Activation of Lymphocytes in Peripheral Blood in Parainfectious Encephalitis Associated with Exanthema. Scandinavian Journal of Infectious Diseases, Vol. 6, pp. 23-27. 1974.

18. Michalowski, H and W. Plenert. Studien Zur Differenzierung der Lymphozyten des Peripheren Blutes im Kindesalter II Bacterielle und Virus-Infectionen. Folia Haematol, Vol. 85, pp 227-235. 1966.

19. Heyn, RM, D. G. Tubergen, and N. T. Althouse. Lymphocyte Size Distribution. American Journal of Diseases of Children, Vol. 125, pp. 789-793. June 1973.

20. Kelton, AA, L. F. Brown, B. J. O'Loughlin. The Lymphocyte Specific Gravity Distribution in Radiation Therapy. MDAC PAPER WD 1954. May 1972.

21. Niklasson, PM and R. C. Williams, Jr. Studies of Peripheral Blood T and B Lymphocytes in Acute Infections. Infection and Immunity, Vol. 9, pp. 2-7. 1974.

22. Riethmüller, G, E. P. Rieber and D. Riethmüller. Untersuchungen Zur H Heterogenität Humaner Lymphocyten: Trennung Peripherer Lymphocyten im Albumindichtegradienten und Untersuching der Einzelen Zellpopulationen auf Ihre Proliferative Reaktion in Vitro Klinische Wochenschrift, Vol. 48, Number 22, pp. 1343-1349. 1970.

23. Geha, RS, J. G. Gatien, R. Parkman, J. D. Crain, F. S. Rosen, and E. Merler. Discontinuous Density Gradient Analysis of Human Bone Marrow: Presence of Alloantigen-Responsive, PHA-unresponsive Cells in Normal Bone Marrow; Absence of B-Lymphocytes in the Bone Marrow of Patients with X-linked Agammaglobulinemia. Clinical Immunology and Immunopathology, Vol. 2, pp 404-415. 1974.

24. Yu, DTY, JB Peter, HE Paulus, and KM Nies. Human Lymphocyte Subpopulations Study of T and B Cells and Their Density Distribution. Clinical Immunology and Immunopathology, Vol. 2, pp. 333-342. 1974.

25. Wheelock, EF and ST Toy. Participation of Lymphocytes in Viral Infections. Advances in Immunology, Vol. 16, pp. 123-184. 1973.

26. Jack, I and Grutzner, J. Cellular Viraemia in Babies Infected with Rubella Virus Before Birth. British Medical Journal. Vol. 1, pp. 289-292. 1969.

27. Horta-Barbosa, L, R Hamilton, B Wittig, DA Fuccillo and JL Sever. Subacute Sclerosing Panencephalitis: Isolation of Suppressed Measles Virus from Lymph Node Biopsies. Science, Vol. 173, pp. 840-841. 1971.

28. T Yamauchi. Private Communication.

29. Papp, K. Fixation du Virus Morbilleux Aux Leucocytes du Sang des la Periode D'Incubation de la Maladie. Bulletin de L'Academie de Medicine, Vol. 117, pp. 46-51. Jan 1937.

30. Denman, AM, B. Rager-Zisman, TC Merigan and DAJ Tyrrell. Replication or Inactivation of Different Viruses by Human Lymphocyte Preparations. Infection and Immunity, Vol. 9, pp. 373-376. 1974.

31. Bloom, BR, L. Jiminez and PI Marcus. A Plaque Assay for Enumerating Antigen Sensitive cells in Delayed-type Hypersensitivity. Journal of Experimental Medicine, Vol. 132, pp. 16-30. 1970.

32. Wallen, WC, JH Dean and DO Lucas. Interferon and the Cellular Immune Response: Separation of Interferon-producing Cells from DNA-Synthetic Cells. Cellular Immunology, Vol. 6, pp. 110-122. 1973.

33. Dent, PB and RPB Larke. Viral Infection and Immunity. Medical Clinics of North America, Vol. 56, pp. 353-370. 1972.

34. Shortman, K, KT Brunner, and J-C Cerottini. Separation of Stages in the Development of the "T" Cells Involved in Cell-mediated Immunity. Journal of Experimental Medicine, Vol. 135, pp. 1375-91. 1972.

35. Greenberg, AH. Fractionation of Cytotoxic T-lymphoblasts on Ficoll Gradients by Velocity Sedimentation. European Journal of Immunology, Vol. 3, pp. 793-797. 1973.

36. Vasudevan, DM, KT Brunner and J-C Cerottini. Increased Cytolytic Effect of Immune Lymphocytes in a Syngeneic Tumor System Following Simple Purification Procedures. British Journal of Cancer, Vol. 28, Suppl. I, pp. 35-36. 1973.

37. Pelet, J, KT Brunner, AA Nordin, and J-C Cerottini. The Relative Distribution of Cytotoxic Lymphocytes and of Alloantibody-Forming Cells in Albumin Density Gradients. European Journal of Immunology, Vol. 1, pp. 238-242, 1971.

38. Landy, M, RP Sanderson, MT Bernstein, and AL Jackson. Antibody Production by Leucocytes in Peripheral Blood. Nature, Vol. 204, pp. 1320-1321. December 1964.

39. Hurley, JV. "Acute Inflammation". pp. 125-135. The Williams and Wilkins Company, Publishers, Baltimore. 1972.

40. Ellis, ST and JL Gowans. The Role of Lymphocytes in Antibody Formation. Proceedings of the Royal Society of London, Part B, Vol. 183, pp. 125-139. 1973.

41. Adler, WH, D. Peavy and RT Smith. The Effect of PHA, PPD, Allogeneic Cells and Sheep Erythrocytes on Albumin Gradient-Fractionated Mouse Spleen Cell Populations. Cellular Immunology, Vol. 1, pp. 78-91. 1970.

42. Gorczynski, RM, RG Miller and RA Phillips. Homogeneity of Antibody-producting Cells as Analyzed by Their Buoyant Density in Gradients of Ficoll. Immunology, Vol. 19, pp. 817-829. 1970.

43. Pick, E. Localization of Lymphocytes Producing Macrophage Migration Inhibitory Factor in Albumin Density Gradients. European Journal of Immunology, Vol. 3, pp 317-319. 1973.

44. Tardieu, M and F Daguillard. Fractionated T-Lymphocytes Can Inhibit Mitogenic Responses through Dialyzable Factors. Cellular Immunology, Vol 19, pp. 148-150. 1975.

45. Dawkins, RL and PJ Zilko. Separation of Cells Involved in Phytohaemagglutinin-Induced Mitogenesis and Cytotoxicity. Nature, Vol. 254, pp. 144-145. 1975.

46. Mawas, C, M Sasportes, D Charmot, Y Christen, and J Dausset. Cell-mediated Lympholysis in Vitro. Clinical and Experimental Immunology, Vol. 20, pp 83-92. 1975.

47. Dyminski, JW and BR Argyris. In Vitro Sensitization to Transplantation Antigens IV Density Gradient Centrifugation of Sensitized Cells and Sensitization of Density Gradient-fractionated Cells. Cellular Immunology, Vol. 5, pp. 280-287. 1972.

48. Wisloff, F, SS Froland and TE Michaelsen. Characterization of Subpopulations of Human Lymphoid Cells Participating in Phytohemagglutinin and Concanavalin A-induced Cytotoxicity. International Archives of Allergy, Vol. 47, pp. 488-497. 1974.

49. Zisman, B and AM Denman. Inactivation of Myxoviruses by Lymphoid Cells. Journal of General Virology, Vol. 20, pp. 211-233. 1973.

50. Fauci, AS and DC Dale. The Effect of Hydrocortisone on the Kinetics of Normal Human Lymphocytes. Blood, Vol. 46, pp. 235-243. 1975.

51. Kissling, M, B Speck and H Goselink. Effects of Hydrocortisone on Lymphocytes Stimulated by Phytohaemagglutinin and Pokeweed Mitogen. Vox Sanguin, Vol. 23, pp. 344-349. 1972.

52. Famaey, J-P and MW Whitehouse. Interactions Between Non-steroidal Anti-inflammatory Drugs and Biological Membranes. Biochemical Pharmacology, Vol. 22, pp. 2707-2717. 1973.

53. Matejkova, E. The Effects of Combined Administration of Cytembena and Cyclophosphamide on the Blood Count and Morphology of Nucleoli in Peripheral-Blood Lymphocytes in Patients with Malignant Tumors. Neoplasma, Vol. 22, pp. 45-54. 1975.

54. Mottironi, VD and PI Terasaki. "Lymphocytotoxins in Disease I. Infectious Mononucleosis, Rubella, and Measles", pp 301-308. Histocompatibility Testing. Williams and Wilkins Co., Publisher. 1970.

55. Kreisler, MJ, AA Hirata and PI Terasaki. Cytotoxins in Disease III Antibodies Against Lymphocytes Produced by Vaccination. Transplantation, Vol. 10, pp 411-415. 1970.

56. White, G, SA Armentrout and S Van Den Noort. Purification of a Lymphotoxic Factor from Multiple Sclerosis Serum. Neurology, Vol. 24, pp. 384-385. 1974. And private Communication.

57. Zucker, RM and B Cassen. Effect of Chemotherapy with Cyclophosphamide on the Buoyant Density Separation and Volume Distributions of Lymphocytes in Chronic Lymphocytic Leukemia and Lymphosarcoma. Jounral of the National Cancer Institute, Vol. 52, pp. 1691-1697. June 1974.